AN ABSTRACT OF THE THESIS OF

Nasser Talebbeydokhti for the degree of Doctor of Philosophy

in Civil Engineering presented on July 27, 1984.

Title: Incipient Resuspension of Silt-Clay Deposits in

Oscillatory and Unidirectional Flows

Redacted for Privacy

Abstract Approved: _____

Peter C. Klingeman

Incipient motion of cohesive sediment and the role of flow

parameters were investigated for separate and combined unidirectional

and oscillatory flows. Sediment from Sturgeon Lake, mainly silt and

clay with organic matter, was used as bed material in recirculating

and wave flumes.

Bench-type experiments indicated that when the submerged sediment

was under no active hydraulic disturbances, it consolidated

substantially. The removal of fine sediment and organic matter from

the sediment surface caused greater consolidation of the remaining

coarse sediment.

The mechanism for incipient motion of cohesive sediment under the

action of flowing water was found to be complex. The top surface of

the fine-grained sediment exhibited a skin layer which governed the

the Incipient motion process. Formation of this layer was evidently caused by physicochemical bonding of sediment particles by organic matter and Iron In the sediment. When Induced shear stress exceeded that required to Initiate erosion, the bonded particles started to peel off, leaving pit marks and causing the development of streak lines. Suspension of sediment particles was a part of this process.

Incipient motion for unidirectional flow could be expressed In terms of the mean velocity and shear stress necessary to Initiate erosion of the cohesive sediment surface. Incipient motion for oscillatory flow could be expressed In terms of maximum orbital velocity and maximum shear stress. The results of the two sets of experiments could be used to speculate on the combined effects of oscillatory and unidirectional flows.

It was found for fine cohesive sediment that: (1) the principles governing Incipient motion under unidirectional flow are applicable for oscillatory flow; (2) the effects of combined unidirectional and oscillatory flows can be estimated from separate effects of each flow; (3) when Induced shear stress exceeds skin bonding strength, peeling off of the skin layer begins; (4) sediment consolidation has little effect on Incipient motion; (5) Incipient motion of the sediment bed occurs at lower shear stress and velocity under oscillatory flow than under unidirectional flow; (6) a bed with a rough surface Is more susceptible than a smooth bed to Incipient motion; and (7) bioturbation affects Incipient motion of fine-grained sediment.

INCIPIENT RESUSPENSION OF SILT-CLAY
DEPOSITS IN OSCILLATORY AND UNIDIRECTIONAL FLOWS

By

Nasser Talebbeydokhti

A THESIS

Submitted to

Oregon State University

In Partial Fulfillment of
the requirements for the
degree of

Doctor of Philosophy

Completed July 27, 1984

Commencement June 1985

APPROVED:

Redacted for Privacy

Professor of Civil Engineering in charge of major

Redacted for Privacy

head of department of Civil Engineering

Redacted for Privacy

Dean of Graduate School

Date thesis is presented_____July 27, 1984_____

Typed by Sue Reggiani for ____Nasser Talebbeydokhti____

TABLE OF CONTENTS

LIST OF FIGURES

LIST OF TABLES

LIST OF SYMBOLS

a   some reference height (y=a) above the bed

a   major ellipse semiaxis of particle movement

a_δ half of the orbital diameter = orbital amplitude

A   any properties of fluid produced due to wave action

b   minor ellipse semiaxis of particle movement

c   drag coefficient or friction factor of the unidirectional flow

C   sediment concentration

$\dfrac{dC}{dy}$ rate of change of sediment concentration in the vertical direction

C_a sediment concentration at reference height a above the bed

C_4 pressure coefficient

C_D drag coefficient

C_F form drag coefficient

C_L lift coefficient

C_M volume force coefficient

C_S surface drag coefficient

d   water depth

d   water depth, based on the still-water level

d_0 orbital diameter

D   particle grain size diameter

D_1 diameter of particle in plane bed

D_{50} particle size in a mixture of sizes such that 50 percent of all particles are smaller

D_{90} particle size in a mixture of sizes such that 90 percent of all particles are smaller

D_{mean} mean diameter of particles

D_S average diameter of eroded clay particles

f   Darcy-Weisbach friction coefficient

f'   friction factor acting on the plane bed surface

f'   coefficient associated with the kinematic wave pofile

f''   friction factor due to irregularities of the bed surface

f'''   friction factor due to granular materials

f_ω friction factor under oscillatory flow

$f(\alpha)$ stress coefficient (friction factor)

F_B buoyant force due to fluid displacement

F_D total drag force

$F_{D,F}$ form drag force

$F_{D,S}$ surface drag force

F_G gravity force due to the mass of the grain

F_I inertial force due to displaced fluid

F_L lift force due to vertical component of pressure differences

F_P pressure force due to instantaneous pressure gradients

F_{rr} resistance force due to rolling friction

F_v volume force

$F_{v,h}$ volume force due to the added hydrodynamic mass of the particles

$F_{v,p}$ volume force due to the pressure gradient

g   gravitational acceleration

H   wave height

K   Von Karman universal constant

K_S roughness coefficient

ℓ mixing length

L   wave length

M   dummy variable for other variables

$\dfrac{dp}{dx}$ streamwise pressure gradient in the channel

R_e Reynolds number for unidirectional flow

R_{e_*} dimensionless grain Reynolds number

RE   Reynolds number of oscillatory flow

R_h hydraulic radius

s   specific gravity

S   slope of the energy grade line

S_s inertial force coefficient

S_v shear strength of sediment

t   time

T   wave period

u   local fluid velocity in horizontal direction in unidirectional flow

$\dfrac{du}{dy}$ vertical variation of the horizontal velocity component

$\bar{u}$ average velocity in unidirectional flow

u' fluctuating turbulent velocity component in x direction

u_c critical velocity in unidirectional flow

u_{3c} critical velocity 3 cm above the bed

u_* shear velocity in unidirectional flow

u_{*c} critical shear velocity

U   near-bottom horitzontal component of velocity of water particle under wave

U_0 potential flow velocity of wave motion

$\bar{U}$ mass-transport velocity

U_m near-bottom maximum velocity under oscillatory flow

$\bar{U}_{max}$ maximum mass-transport velocity

v' fluctuating trubulent velocity component in y direction

V_g grain velocity

V_s settling velocity

W vertical component of velocity of water particles under waves

x horizontal coordinate in direction of wave propagation, with origin at wave crest

y distance from the bed to the water surface

y' zero depth of flow for rough boundary

z dummy variable

Z vertical coordinate measured from the still-water level positively upwards (at the bed, $Z = -d$)

α beach slope

α Goda's coefficient

α $\frac{1}{C^2}$ (c is friction factor)

α_1 packing factor (dimensionless)

α_2, α_3 dimensionless shape factors

β constant

β coefficient relating diffusion coefficient and eddy viscosity

β angle between resultant of viscous resistance forces and beach slope in radians

β' measure of viscous effect under a wave

γ specific weight of water

γ_s specific weight of sediment, $\gamma'_s = \gamma_s - \gamma = (\rho_s - \rho) g$

γ'_s submerged specific weight of sediment,

δ boundary layer thickness under unidirectional flow

δ_L boundary layer thickness under oscillatory flow

ε eddy viscosity

ε coefficient of rolling friction

ϵ characteristics dimension of grains equivalent to grain size diameter

ϵ_s diffusion coefficient

ζ verticle displacement of a water particle under a wave

η free surface elevation relative to the still-water level

Θ Shields entrainment function

Θ angle of internal friction

μ dynamic viscosity

ν fluid kinematic viscosity

ξ hortizontal displacement of a water particle under a wave

ρ fluid density

ρ_s sediment density

τ shear stress

τ_o boundary shear stress

τ'_o real bed shear stress acting on the plane bed surface

τ''_o shear stress due to irregularities of the bed surface

τ'''_o shear stress due to granular materials

$\bar{\tau}_o$ average bed shear stress

τ_{oc} critical bed shear stress

τ_m maximum bed shear stress under oscillatory flow

$\tau(\theta)$ shear stress in terms of stress coefficient

ϕ phase angle

ϕ angle of grain with bed

ω critical angular velocity,

$\boxed{}$ Yalin parameter

INCIPIENT RESUSPENSION OF SILT-CLAY DEPOSITS

IN OSCILLATORY AND UNIDIRECTIONAL FLOWS

I. INTRODUCTION

Research Need

An understanding of the processes of incipient motion, erosion, and deposition of fine-sized sediment in flowing water still is in its developing stage. Much progress has been achieved in recent years in the investigation of fundamental laws governing the transport of fine cohesive sediments. However, there has not been a comprehensive study of incipient motion of fine-sized cohesive bed sediment caused by waves, unidirectional flow, and the combined effect of waves and unidirectional flow.

Incipient motion is the starting point for erosion. The erosion of fine cohesive sediment is very important from an engineering standpoint. Major concerns include: (1) control of erosion and shoaling of such material in rivers, canals, harbors, estuaries, and navigable waterways; (2) control of erosion at lake and reservoir shorelines due to waves; (3) protection of the storage capacity and useful life of lakes and reservoirs; and (4) protection of coastlines against erosion.

The existing literature identifies major differences in the general features of sediment transport processes between

unidirectional flow and oscillatory flow. In particular, the
conditions governing incipient motion differ. Furthermore, the
condition of incipient motion is itself subjectively determined,
rather than by absolute criteria, leading to additional differences
among experimental findings for the two types of flow. Beyond these
difficulties, the bulk of literature about sediment transport due to
oscillatory flow is primarily based on sand particles, rather than
cohesive silt-clay sediment. There is very little literature
available that deals with both flow regimes as part of the same
research on sands and apparently no literature that does so for
silt-clay sediment.

As a result of these circumstances, there is a need for careful
systematic examination of the incipient motion of silt-clay deposits
under the separate and combined conditions of unidirectional and
oscillatory flow to fill in gaps of past research. Such
investigation is also needed so that the same consistent analysis is
applied to both flow regimes for a given sediment, to better treat
the subjectivity involved in defining incipient motion.

Purpose of Research

The research forming the basis of this dissertation has the
purpose of enlarging our understanding of the processes of sediment
erosion in flowing water. More specifically, the main purpose of
this dissertation is to investigate the incipient motion of fine
cohesive sediment due to wave action and unidirectional flow and the
possible combined effect of waves and unidirectional flow. Such

Investigation brings together considerations of the dynamic behavior of the fluid and the physical/chemical behavior of the sediment being dislodged from a nearly stable bed.

Research Objectives

There are three principal objectives of my dissertation research, in order to investigate my starting hypotheses. These are:

1. To determine the effects of the important flow parameters of unidirectional flow on the incipient motion of fine sediment and to derive quantitative relationships describing these effects. Some of the important variables involved are bed shear stress, initial sediment concentration, flow depth, and flow velocity near the bed;

2. To determine the effects of the important flow parameters of oscillatory flow on the incipient motion of fine sediment and to derive quantitative relationships describing these effects. Some of the variables involved are wave height and wave period, bed shear stress, flow depth, and flow velocity near the bed; and

3. To investigate the combined effects of unidirectional flow and oscillatory flow on incipient motion of fine sediments and their interaction to bring the fine sediment into motion.

The three main objectives are supported by four additional objectives. These are:

1. To investigate the effect of suspended sediment concentration on incipient motion of the bed under unidirectional flow;

2. To Investigate the effect of bed consolidation on Incipient
    motion of that bed under oscillatory flow;

3. To Investigate whether a bed consisting of fine-sized sedi-
    ment is more suspectible to incipient motion if it has a
    smooth surface or if it has a rough or duned surface, both
    for unidirectional and oscillatory flow; and

4. To formulate a model describing the incipient motion of
    fine-sized sediment in unidirectional flow and in
    oscillatory flow.

In each case. results from this research are compared with
results obtained by other investigators who have studied incipient
motion of sediment.

Starting Hypotheses

Two main hypotheses are involved in this research. The first
hypothesis is that the incipient motion of silt-clay sediment under
oscillatory flow can be determined and described in a manner similar
to that used for unidirectional flow. It has been demonstrated that
for non-cohesive sediment particles, such as sand, the principles
governing the incipient motion under unidirectional flow can be
applied under oscillatory flow. However, because of sediment
cohesion and the unsteady nature of oscillatory flow, it has not yet
been shown that such application is also valid for silt-clay sediment
beds.

My second hypothesis, as initially conceived, was that the
combined effects of unidirectional flow and oscillatory flow on

incipient motion were additive and could be treated by linearly summing the separate effects. As the review of literature progressed, however, it became evident that a more fundamental hypothesis was needed to better address limitations identified from the literature. Furthermore, it became clear that the available laboratory apparatus would limit certain aspects of experimentation. Therefore, the revised second hypothesis is that from consistent measurements of the separate effects of unidirectional flow and oscillatory flow on the incipient motion of a silt-clay sediment bed, it is possible to reasonably estimate the effects of combined unidirectional and oscillatory flows on the incipient motion of such cohesive sediment.

The hypotheses are tested by a detailed literature review followed by a combination of field observations, laboratory experiments, and analysis of published data. The field observations involve a silt-clay sediment that is later used for laboratory work. Separate laboratory experiments are conducted for unidirectional flows and oscillatory flows. From available theory and data for non-cohesive sediment under separate and combined unidirectional and oscillatory flows, an estimate of incipient motion behavior is made for cohesive sediment. This is compared with estimates from my own experimental results. Finally, an attempt is made to experimentally determine the combined effects of the two flow regimes on incipient motion of silt-clay sediment.

Research Scope and Approach

This research is directed towards understanding the mechanism of incipient motion of fine cohesive bed sediment in terms of flow variables. Because the behavior of fine sediment is influenced both by flow variables and by physical/chemical parameters, a specific fine sediment is used in a water of known quality so that the physical/chemical properties of the sediment suspension can be kept constant and the incipient motion of the sediment can be related directly to identifiable flow variables. The incipient motion of fine cohesive sediment subject to unidirectional flow of the overlying water is determined in terms of the water depth, velocity, shear stress, and the suspended sediment concentration. The incipient motion of fine cohesive sediment subject to oscillatory wave flow conditions in the overlying water is determined in terms of wave parameters, shear stress and maximum horizontal velocity at the bed, orbital diameter of particles at the bed, and suspended sediment concentration. The incipient motion of fine cohesive sediment due to the combined effect of oscillatory and unidirectional flow is determined by summing the conditions resulting from the separate oscillatory and unidirectional flows. For all three of these cases, incipient motion is also determined by visually observing the changes in the bed surface.

The research is restricted to the incipient motion of fine-sized cohesive sediment that was previously deposited naturally from a water-sediment suspension and is subsequently subjected to shear

stresses caused by increased fluid motion. Because of the complexity
of natural environments, systematic investigation of a prototype
water body is supplemented with investigation made under simpler
controlled laboratory conditions that generally match the essential
features of the prototype setting.

The prototype study of sediment and water characteristics for a
natural waterbody, as well as its hydrodynamic characteristics, is
conducted in Sturgeon Lake. This lake is located within Sauvie
Island and is subject to the flows and tides of the Willamette and
Columbia Rivers. This investigation gives insights to aid in
understanding the relevant natural processes. Laboratory
experimental work is conducted in two flumes, one with a flap-type
wave board to cause oscillatory flow and the other with a
recirculating pump to cause unidirectional flow. The bed material
tested in the flumes, is also typical of Sturgeon Lake bed material
and contains approximately 78 percent silt and 20 percent clay, with
less than 2 percent fine sand. Water at several different depths is
used with fixed sediment bed surfaces in each flume. The wave
parameters and unidirectional flow rates are gradually varied through
a series of test runs. At each new condition, velocity, shear
stress, suspended sediment concentration, and incipient motion
features are observed and recorded.

As rationale for the above-described approach, it is noted that
hydraulic engineering research to understand a physical process
generally utilizes one or more of several techniques. These include

analytical techniques, mathematical models, computer models, physical models, and flume studies. In the study of sediment resuspension involving complex flow variables, such as wave flow and unidirectional flow, the complexity of the problem is increased due to the behavior of fine cohesive sediment. The analytical tools are not yet readily available to describe the phenomena and processes in mathematical or computer-model format. This complexity also inhibits true physical modeling in the sense of scaling all of the relevant variables. Therefore, for complex hydraulic problems such as the transport of fine cohesive sediment, quasi-scale-model flume studies are widely used as tools for understanding these phenomena.

Organization of Dissertation

The following chapters of this dissertation each deal with a specific aspect of the incipient motion of fine cohesive sediment. Chapter II consists of a review of the literature pertaining to the incipient motion of fine cohesive sediment due to unidirectional flow and oscillatory flow. The governing laws and the similarities and differences of sediment transport between these types of flow are discussed. Properties of fine cohesive sediment are discussed. The experimental materials and methods used in past investigations are also discussed in detail. Chapter III contains relevant aspects of my prototype study of fine-grained sediment behavior at Sturgeon Lake. It encompasses lake hydrodynamics, sediment sources and transport, and sediment characteristics. These are all important to the development of a process model for sediment transport that can be

tested under more controlled laboratory conditions. Chapter IV presents experimental materials and methods that I used for conducting the laboratory investigation. The apparatus used, equipment design, sediment and water characteristics, bed preparation, and experimental procedures are all described. Chapter V presents the reults and initial analyses of my laboratory experiments. It includes the incipient motion of fine sediment in oscillatory flow and unidirectional flow utilizing velocity, bed shear stress. suspended sediment concentration, and subjective determinations made by visual observation. A synopsis of experimental runs is also provided. Chapter VI presents a more detailed analysis of my experimental results. The results are discussed in conjunction with theory and the literature. Chapter VII concludes the investigation by summarizing the results obtained and drawing conclusions on their relation to the initial working hypotheses. Further research needs are also identified to achieve a better theoretical understanding of incipient motion of fine cohesive sediment.

II. LITERATURE REVIEW

Basic Aspects of Suspended Sediment Transport

Terminology

Sediment movement occurs in various forms. Based on the transport mechanisms involved, the total sediment transport load of a stream can be divided into bed load and suspended load. Based on the sources of sediment that is being transported, the total sediment transport load of a stream can be divided into bed material load (bed sediment load) and wash load. The wash load consists of small-sized sediment that is not found in appreciable amounts within the streambed but which instead enters the channel with storm runoff and is washed on through the stream as part of the suspended load. The bed material, when disturbed by strong flows, may be transported both as bed load and as suspended load.

To better define and differentiate suspended load from bed load, it is convenient to describe the motion of sediment particles caused by flowing water over a flat bed. At very low velocities no sediment particle will move; at somewhat higher velocities, some individual sediment particles will roll and slide along the bed; at still higher velocities, some sediment particles will also make short bounces or jumps away fom the bed, either staying within the body of water for a short instant of time, or returning to the bed again; if the flow velocities continue to increase, the rolling, sliding, bouncing and jumping by sediment particles will become more intense frequently and some of the smaller particles will be swept up into the body of water

and kept in suspension for great lengths of time, due to the flow turbulence. The sediment transport occurring in this illustration is called bed material transport. Part of the bed material load is carried in suspension and is called suspended load; part of the bed material load is moved on or near the bed in almost continuous contact (contact load) or by bouncing (saltation load) and is called bed load.

Processes Affecting Small Particles

The smaller sediment particles are most likely to be moved by a fluid while in suspension. Three physical processes are recognized as responsible for the transport of small particles: Brownian diffusion (thermal effects), fluid shear (flow effects), and differential settling (gravity effects). The particle size distribution of a suspension has an important bearing on the relative significance of these three processes.

Brownian or molecular diffusion is a random motion of small particles brought about by thermal effects. The driving force for this transport is a function of the absolute temperature. The kinetic energy of water molecules is transferred to small sediment particles during the continuous bombardment of these particles by the surrounding water molecules. Transport by Brownian diffusion depends on these thermal effects only and is independent of such factors as fluid flow and gravity forces (O'Melia, 1980).

The second process affecting the transport of small particles is fluid shear, either turbulent or laminar. Velocity differences or gradients occur in all real flowing fluids. Hence, particles that

follow the motion of the suspending fluid will travel at different velocities. The fluid and particle velocity gradients can produce interparticle contacts among particles suspended in the fluid. Particle transport in this case depends upon the mean velocity gradient.

The third process involved is gravity, which produces vertical transport of particles and depends upon the buoyant weight of these particles compared to gravitational attraction.

Small particles are also subject to coagulation and flocculation. This occurs when particles come close enough that they can form some type of interparticle contact or bond. All three processes noted above can bring particles close together or cause their collision. The basic developments describing coagulation in aquatic systems were presented long ago (e.g., Smoluchowski, 1917). Over time, such analysis has shifted from single-size mixtures to heterodisperse suspensions (O'Mella, 1980).

Steady State Suspended Sediment Transport

According to Graf (1971), the suspension phenomenon was poorly understood until the 1930's. Later, it was realized that turbulence and its associated consequences are important to the suspension process. Turbulence might be loosely defined as an irregular or random component of motion that, under certain conditions, becomes superimposed on the mean or overall motion of a fluid when that fluid flows past a solid surface or past an adjacent stream of the same fluid with a different velocity. One of the most significant

features of turbulence is the transport of such things as momentum, heat, solutes, or suspended matter across planes parallel to the mean flow direction by the random motions of fluid masses back and forth across these planes.

The distribution and quantitative determination of the vertical suspended matter under steady-state and under non-steady-state conditions are of great importance. Here, the discussion includes only the steady-state vertical distribution of suspended matter. The interested reader can refer to sediment transport textbooks such as Graf (1971) for more detailed information about non-steady-state conditions.

Many models have been presented to describe the suspension phenomenon. For example, a diffusion-dispersion model has been proposed which is based on the principle of conservation of mass, whereby equilibrium exists between the rate of change of a fluid property (such as its mass of sediment) in a control volume (region in space) and the net rate at which the property leaves or enters the control volume (i.e., the rate of change of a property due to diffusion).

Theoretical Approach

Suspended grains are held up above the stream bed by the turbulent motion of the fluid. The particle weight is therefore supported by the fluid. When the vertical component of turbulence is about equal to the settling velocity of the grain, the grain remains suspended in the body of water.

For grains of uniform size, the settling velocity or rate of downward movement of grains is given by V_s. If these grains move

downward from a region in the fluid having a concentration, C, the rate of settling per unit volume is equal to the product of settling velocity and concentration V_sC. We can make the assumption that the upward vertical diffusion of particles will follow a Fickian diffusion law, like many other diffusion processes:

$$\text{rate of turbulent diffusion (per unit volume)} = \varepsilon_s \left(\frac{dC}{dy}\right)$$

where ε_s is a diffusion coefficient, which should be constant in a field of homogenous isotropic turbulence of any particular type and strength, and $\frac{dC}{dy}$ is the rate of change of sediment concentration in the vertical direction, y. Assuming a steady state and equating the two rates gives a formula for the vertical distribution of the concentration of suspended particles:

$$V_sC + \varepsilon_s \left(\frac{dC}{dy}\right) = 0 \tag{1}$$

The diffusion coefficient is assumed proportional to the kinematic eddy viscosity.

Suspension in a Shear Flow

In a shear flow, turbulence is not isotropic the strength of the upward velocity components is the same as that of the downward components except perhaps at large distances from the bed. It is expected that the diffusion coefficient will vary in the vertical (y) direction. Therefore, an expression is needed that tells how the diffusion coefficient varies with y, before equation (1) can be used to predict how the sediment concentration varies with y.

To find such an expression, we assume the sediment diffusion coefficient to be proportional to the eddy viscosity, ϵ, given by

$$\tau = \rho\epsilon \frac{du}{dy} = \mu\frac{du}{dy} \qquad (2)$$

where τ = shear stress;

ρ = fluid density;

u = local velocity in the horizontal direction;

$\frac{du}{dy}$ = vertical variation of the horizontal velocity component; and

μ = dynamic viscosity of the fluid, $=\rho\epsilon$.

Assuming that the diffusion coefficient and eddy viscosity can be related by a coefficient β :

$$\epsilon_s = \beta\epsilon$$

gives

$$\tau = \frac{\epsilon_s\rho}{\beta} \frac{du}{dy}$$

where the coefficient β is expected to be close to one. In a uniform open channel flow, τ must vary linearly with y. This can be expressed in terms of the boundary shear stress τ_0 and the water depth d as

$$\tau = \tau_0 \ (1-y/d) \qquad (3)$$

Therefore,

$$\epsilon_s = \beta \frac{\tau_0}{\rho} (1-y/d)/(du/dy) \qquad (4)$$

Introducing the shear velocity, u_* , where;

$$u_* = \sqrt{\tau_0/\rho} \qquad (5)$$

gives

$$\epsilon_s = \beta u_*^2 (1-y/d)/(du/dy) \qquad (6)$$

Using the law of the wall

$$du/dy = 1/K \ u_*/y \qquad (7)$$

where K is the Von Karman universal constant, having a mean value of 0.4 for clear fluids, we have

$$\epsilon_s = \beta u_*(1-y/d)/(du/dy) \tag{8}$$

Combining 1 and 8 gives

$$\frac{dC}{C} = \frac{-V_s dy}{\beta K u_*(1-y/d)y} \tag{9}$$

which may be integrated to give the equation first described by Rouse (1937):

$$\ln C = \frac{V_s}{\beta K u_*} \int_d^a \frac{dy}{(1-y/d)y} \tag{10}$$

and

$$\frac{C}{C_a} = [\frac{d-y}{y} \cdot \frac{a}{d-a}]^z \tag{11}$$

where $z = \dfrac{V_s}{\beta K u_*}$;

   C = sediment concentration at height y above the bed;

   C_a = sediment concentration at reference height a above the

      bed; and

   a = some reference height (y=a) above the bed.

The above equation applies to sediment grains with a settling velocity V_s and gives their concentration C at any height y above the bed relative to their concentration C_a at some arbitrarily chosen level y = a (generally chosen to be close to the bed).

Incipient Motion of Cohesionless Sediment

   Incipient motion is the beginning of movement of individual particles or flocs of particles from an erodible bed. Some approaches to the analysis of particle stability for non-cohesive sediment include:

   1. dimensional analysis;

2. static equilibrium of acting forces;

3. dynamic equilibrium of acting forces;

4. statistical methods; or

5. combinations of the above.

Many investigators are pioneers in the study of incipient motion of sediment. These include Fortier and Scobey (1926), Shields (1936), White (1940), Einstein (1942), Gessler (1965), Neill (1967, 1968), Paintal (1971), and many others.

The best known treatise on initial bed grain stability is that by Shields (1936). Physical arguments were used to combine the parameters of interest into several non-dimensional relationships. These parameters include particle diameter D, sediment density ρ, fluid kinematic viscosity ν, fluid shear stress τ, and gravitational acceleration g. They are combined in terms of the following functional relations:

$$\theta = \frac{\tau_0}{(\rho_s-\rho)gD} = \frac{\rho u_*^2}{(\rho_s-\rho)gD} = f(\frac{u_*D}{\nu} \text{ and } D/g) \qquad (12)$$

where θ = Shields entrainment function;

δ = thickness of the viscous sublayer given by $\delta=\frac{10\nu}{u_*}$; and

$\frac{u_*D}{\nu} = R_{e_*}$, the dimensionless grain Reynolds number.

Figure 1 shows the Shields threshold curve. Many investigators have used Shields empirical equation and have plotted their data on his diagram. It shows considerable scatter. One of the main reasons for this data scatter stems from the difficulty encountered in consistently defining critical flow conditions (Task Committee, 1966). Difficulties arise because there is no single flow at which bed particles of a given size are suddenly placed in motion. The
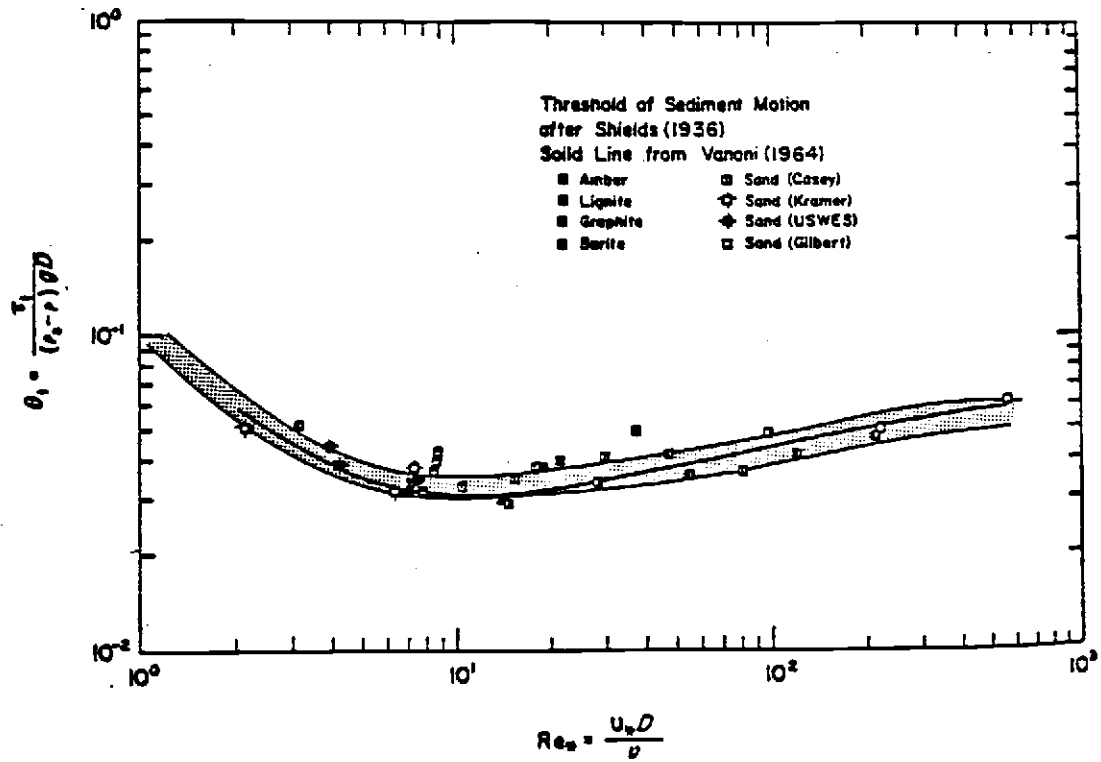
Figure 1.   The Shields Threshold Curve
(Source: Miller et al., 1977)

initiation of bed movement occurs gradually over a wide range of average bed shear stress as the flow velocity increases. Another source of data scatter in the Shields diagram results from the influence of flow turbulence. The turbulent structure close to the bed is only similar in terms of such parameters as average bed shear stress, provided that the flow boundary conditions remain similar. However, as soon as the boundary conditions are changed, the structure of the boundary region turbulence also changes and no longer shows similarity with respect to the average critical shear stress values derived from the Shields curve.

Miller et al. (1977) presented a comprehensive review of threshold of non-cohesive sediment motion under unidirectional currents. Using data from open channel flumes with parallel sidewalls where flows were uniform and steady over flat beds of unigranular, rounded sediments, they applied various existing empirical curves to predict the threshold. They presented a modified Shields-type threshold diagram, reproduced here as Figure 2. Even with carefully selected data, Miller et al. found considerable scatter. They mentioned two important sources for this scatter:

1. the manner in which the various investigators defined the threshold condition; and

2. Flow turbulence producing natural variability from causes such as: experimental apparatus; variation in grain size distribution; and grain shape

The subjective nature of defining the threshold condition is apparent by studying the criteria of different investigators.
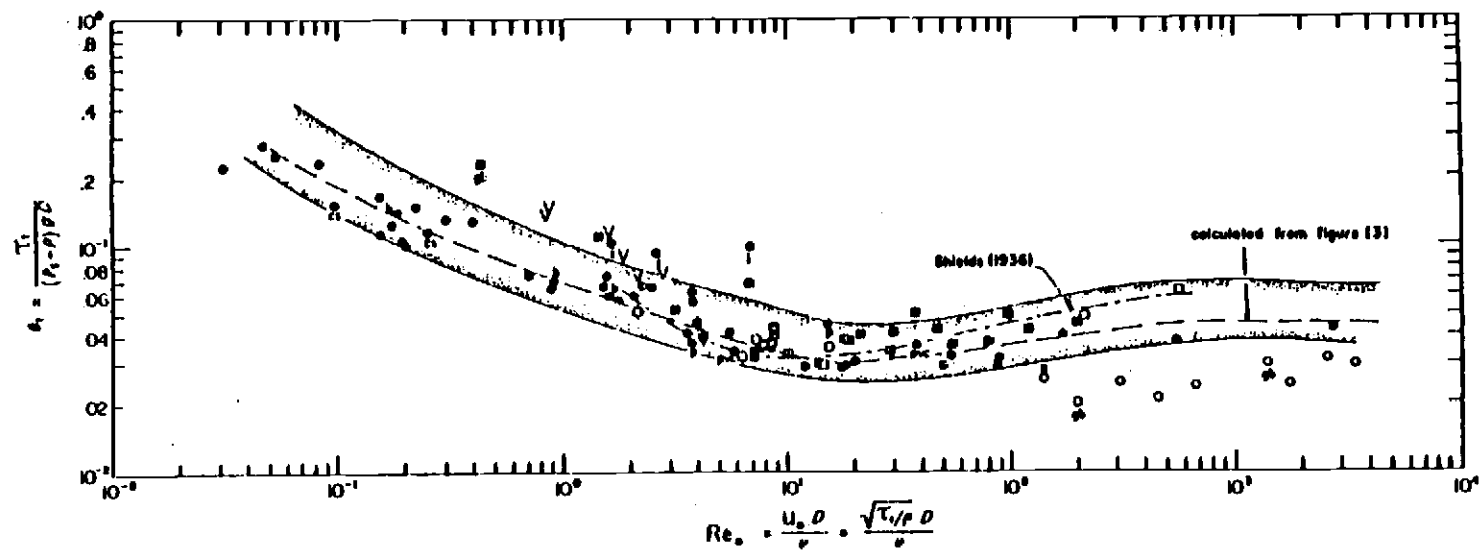
Figure 2.   Shields Curve as Modified by Miller et al. (1977)

Shields (1936) based his threshold criterion on the measurement of a "small degree" of sediment transport. He then extrapolated the transport curve backward to zero transport and determined the flow condition at that point. The incipient motion has been defined by others as a weak movement (i.e., Kramer, 1935), as general bed movement (i.e., Chepil, 1959), as the condition for a single stone to be first displaced (i.e., Neill, 1967), and as scattered particle movement (i.e., Rathburn and Guy, 1967).

Some investigators replaced the band shown in the Shields diagram by a single line for quantitative convenience; it now is most often shown in that way (Vanoni, 1964).

Yalin (1972) proposed the combination of $\theta + R_{e_*}$ in a manner so as to eliminate u_* and retain only properties of the fluid and grains in the abscissa. The resulting Yalin parameter, Ξ, is

$$\Xi = \frac{R_{e_*}^2}{\theta} = \frac{(\rho_s - \rho) g D^3}{\rho v^2} \tag{13}$$

A log plot of the Shields entrainment function versus the Yalin parameter is shown in Figure 3. This curve has the same general shape as the Shields curve but has the advantage that $\sqrt{\Xi}$ can be calculated from known fluid and grain properties. Thus, the threshold can be determined directly without any iterative processes. The Yalin scheme of Figure 3 is the most useful general plot available for sediment threshold.

Another frequently used curve in threshold-of-motion studies is that of Hjulstrom (1935, 1939). This is presented as Figure 4 and shows critical velocity versus grain diameter. Graf (1971) gives an excellent review of this type of curve. Other widely used curves
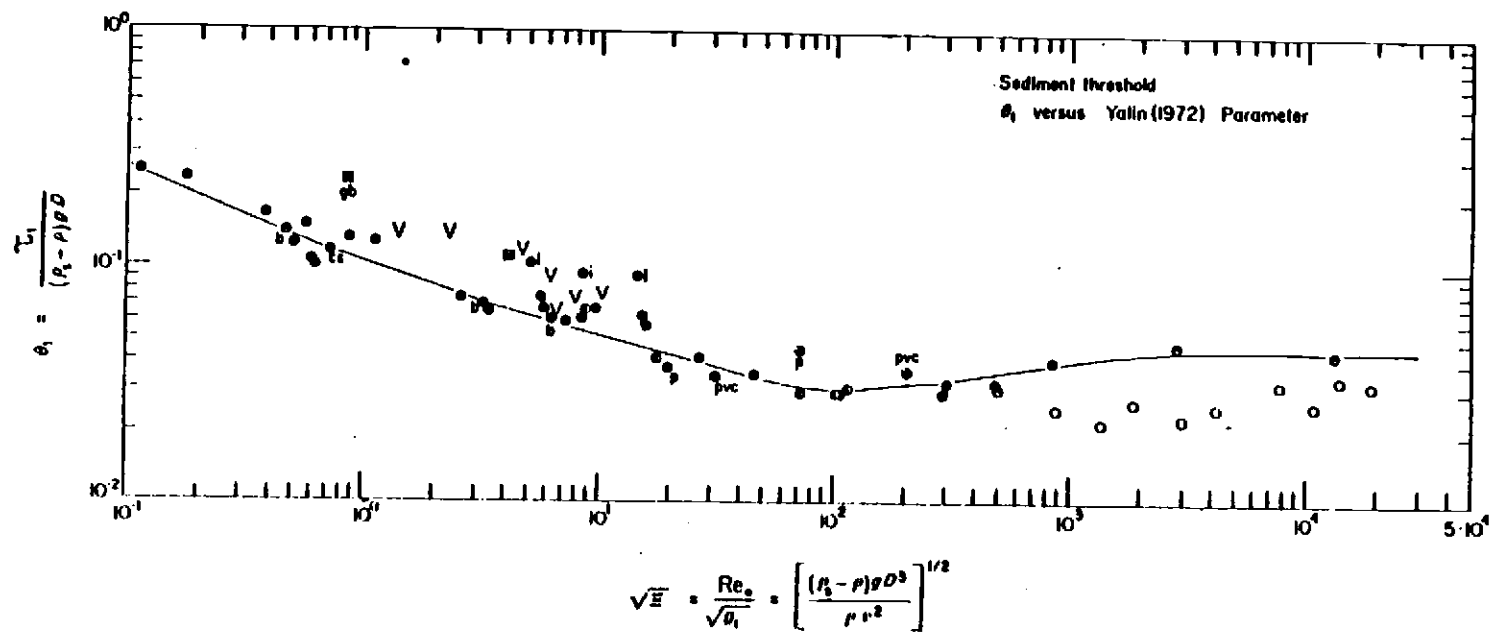
Figure 3. The Shields Entrainment Function Versus the
Yalin parameter (Source: Miller et al., 1977)
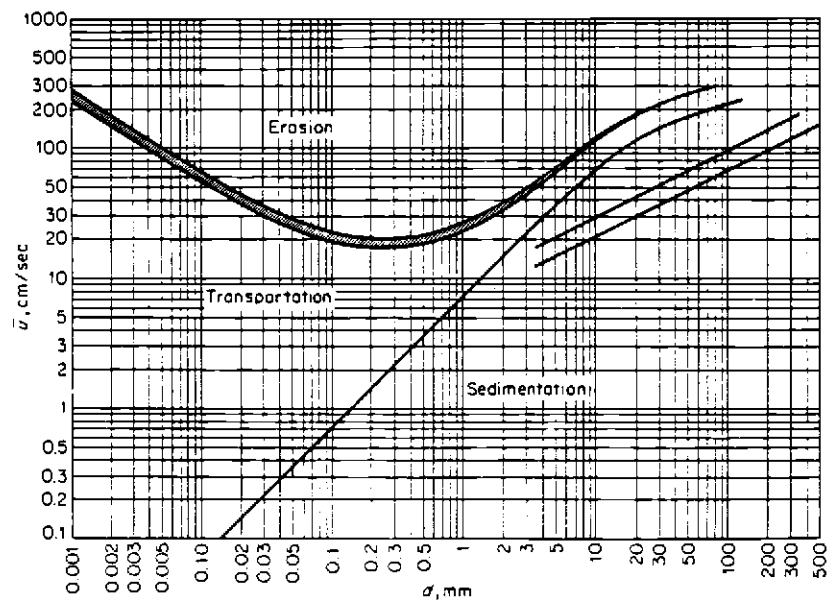
Figure 4. Hjulstrom's Curve of Critical Velocity for
Incipient Motion Versus Grain Size Diameter
(Source: Hjulstrom, 1935)

Include those of of Bagnold (1963), Sundborg (1956), and Lane (1955), which are presented in Figures 5 through 7.

The classicial work by Fortier and Scobey (1926) on permissible canal velocity is still the basis for canal design by many engineers. Critical velocities are given in tabular form for a variety of earth materials subject to clear water scour and scour when a suspension is present.

The Task Committee (1966) states that according to Shields, White, Einstein and Barbarossa, and Sundborg, the critical shear stress for a given sediment is larger when the bed is dune-covered than when it is flat, because form drag is added to skin friction resistance and increases the flow depth of a given discharge (and hence the calculated shear stress). Conversely, critical velocities for duned beds are smaller than for flat ones.

Yang (1973) stated that the unit stream power is the dominant factor in the determination of total sediment concentration. He criticized the use of the Shields diagram. His stream power equation is derived from basic concepts of fluid mechanics and boundary layer theory and is supported with 153 sets of data for incipient motion.

As shown by the foregoing review, study of incipient motion of cohesionless sediment has been pursued in great depth for several decades. The remaining unknown theoretical aspects are continuing to be explored. For more information on this matter, the interested reader may refer to many published textbooks and recent journals on the field of sediment transport.
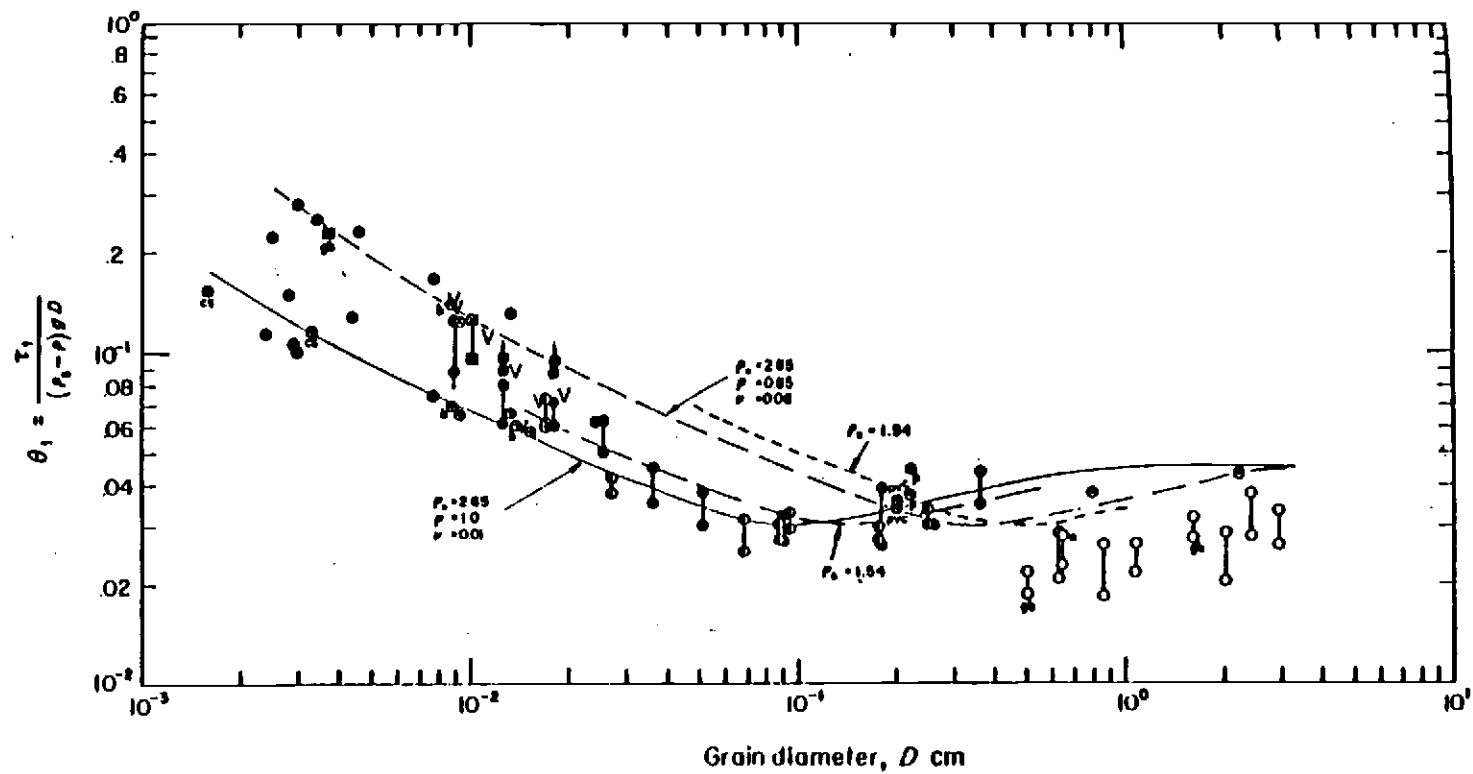
Figure 5.   The Shields Threshold Criterion Versus the Grain Diameter
With Bagnold's Data   (Source: Miller et al., 1977)
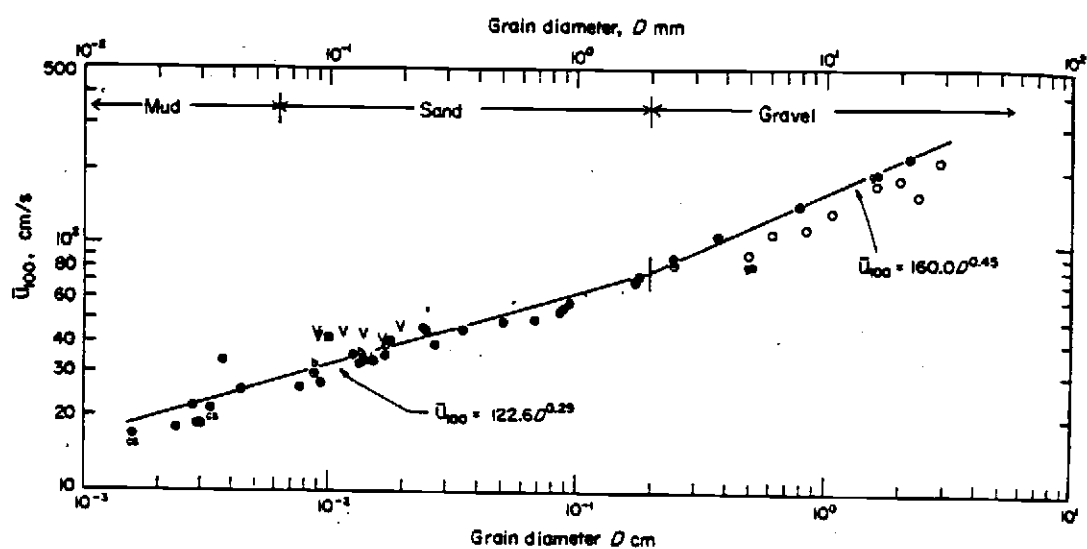
Figure 6. Modified Sundborg Curve of Flow Velocity Versus Grain Diameter (Source: Miller et al. 1977)
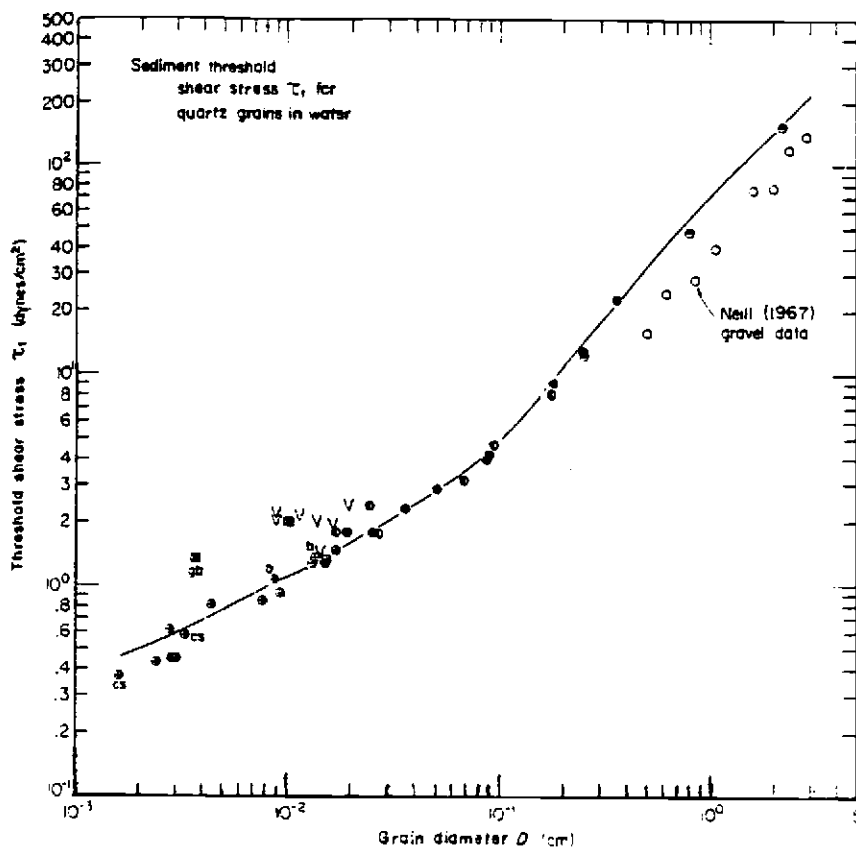
Figure 7. Modified Lane Curve of Shear Stress Versus
Grain Diameter (Source: Miller et al, 1977)

Properties of Fine-Grained Cohesive Sediment

In general, the term clay implies a natural, earthy, fine-grained material which develops plasticity when mixed with a limited amount of water. Clays are composed of silica, alumina, and water, frequently with appreciable quantities of iron, alkalies, and alkaline earths. A size of 2 microns (μ) is frequently used to separate clay-mineral from larger and non-clay-mineral components of natural materials.

Fine cohesive sediment particles have large specific surface areas (surface area per unit weight) in comparison with bigger cohesionless particles such as sand. As a consequence of large specific surface areas, the physicochemical forces acting on the fine particle surfaces are larger than the gravitational forces. This is in contrast with the behavior of cohesionless sediment particles, where gravitational forces are more important.

Factors controlling the properties of fine cohesive sediments include clay-mineral composition, non-clay-mineral composition, organic matter, exchangeable ions, soluble salts, texture, and forces that bind the particles together in clay materials. These forces are: attraction of masses of particles to each other, intermolecular forces, electrostatic forces, and the binding action of absorbed polar molecules (Grim, 1968). As a result, any classification of a fine sediment in terms of one of these factors alone is not sufficient to describe all the properties of the sediment. The most common method of classification used by engineers and geologists is based on particle size. Although by no means completely descriptive,

It is adequate for a preliminary or a general description. In general, particles in the silt and clay size range are expected to exhibit cohesion, with the degree of cohesion depending upon other factors, such as on the type of the sedimentary material.

Structure of Clay Material

The lattices of most clay minerals are based upon two structural units. One unit consists of two sheets of closely packed oxygen or hydroxyl atoms in which aluminum, iron, or magnesium atoms are embedded in octahedrical coordination. These metal atoms are equidistant from six oxygen or hydroxyl atoms. The other common unit consists of a sheet built of silica tetrahedra in which a silicon atom is equidistant from four oxygen or hydroxyl ions arranged in the form of tetrahedron. The above two units combine to give several types of clay minerals, such as kaolinite, halloysite, montmorillonite, illite, chlorite and vermiculite. Of these, the three most common types are described below.

Kaolinite

The kaolinite structural unit is composed of a silica tetrahedral sheet and a single alumina octahedral sheet combined in a unit so that the tips of the silica tetrahedrons and one of the layers of the octahedral sheet form a common layer. Because the individual units are nearly neutral electrically, it is difficult for water molecules or cations to penetrate between the units. Kaolinit particles have plate-like forms with well-defined hexagonal boundaries. Kaolinite has a low liquid limit and low activity.

Montmorillonite

The montmorillonite structural unit is made up of two tetrahedral layers with their tips pointing towards each other and with an octahedral sheet in between. The oxygen atoms of the tetrahedral tips are shared with the oxygen atoms of the octahedral layer, so that the three layers form a single structural unit. The unit assumes a net negative charge, which results in the attraction of exchangeable cations between the units. Water molecules can penetrate between the units, in addition to exchangeable cations, leading to the well-known swelling characteristics of montmorillonite. It has high activity and a high liquid limit.

Illite

The illite structure is similar to that of montmorillonite, except that there is a significantly greater substitution for silicon by lower valence cations, especially aluminum. This substitution leaves a net negative charge deficiency within the structural lattice that is considerably greater than montmorillonite. The layers are bonded together by potassium ions, which are just the right size to fit into the hexagonal holes of the silica sheet. The potassium ions appear to act as a bridge binding the units together so that they do not expand in the presence of water. Illite has properties intermediate between kaolinite and montmorillonite with respect to activites.

Table 1 which is extracted from Kandiah (1974) reveals basic characteristics of some clay minerals.

Table 1. Basic Characteristics of Some Clay Minerals
(From Kohnke, Source Kandiah, 1974)

| | Two layer clays, 1:1, 'diphormic' | Three layer clays, 2:1, 'triphormic' | |
		Expanding lattice	Nonexpanding lattice
Group members	Equidimensional kaolinite, dickite, Elongate halloysite	Equidimensional montmorillonite, beidellite, vermiculite Elongate nontronite, hectorite, saponite	Equidimensional illite, biotite, muscovite
Structure	Rigid lattice one tetranadral layer for each octanedral layer	Lattice expanding and contracting with water content, sheets made up of one catahedral layer with a tetranedral layer on both sides	Rigid lattice sheets made up of one octahedral layer with a tetrahedral layer on both sides. K bonds sheets together
Swelling and shrinking	Very little	Much	illite litte Micas none
SiO_2/R_2O_3	1.9 - 2.1	4.0 - 6.0	2.1 - 3.2
Isomorphic substitution	None	Al for Si; Mg, Fe, Mn, Ti for Al; Li for Mg	Al for si
Specific surface	25 - 50 m^2/g	Around 750 m^2/g	75 - 125 m^2/g
Cation exchange capacity	5 - 10 meq/100 g	80 - 120 meq/100 g	20 - 30 meq/100 g
Adsorptive capacity for inorganic and organic ions, water, gases	Small	Large	Intermediate
Stability of H (Al) clay in aqueous sollution	Low	Great	Intermediate
Heat of wetting	1 - 2 cal/g	10 - 20 cal/g	Around 4 cal/g
C axis basal spacing	7.2 $\overset{o}{A}$	17 $\overset{o}{A}$	10 $\overset{o}{A}$
Temperature of first endothermic depression	$600^\circ C$	$100 - 200^\circ C$	$50 - 100^\circ C$

Physicochemical Properties of Clays

The following properties of the clay particles are important in
engineering applications to predict the clay behavior.

Specific Surface Area

The clay particles in general experience a tremendous increase in
the amount of surface area and in specific surface (area per unit
volume or weight) when divided into smaller particles. The small
particle size and platy shape of a clay particle are the causes of
its large specific surface area. The activity of clay and its many
colloidal properties are related to these large specific surface
areas.

Surface Charge Density

Substitution of one ion for another in the clay lattice and
imperfections at the lattice edges lead to negative electric charges
on clay particles. Surface charge density is defined as the amount
of negative charge per unit surface area. Surface charge density is
important because it determines the ion exchange capacity and the
magnitude of the electrical forces in the clay-water system.

Hydration

Clay particles are surrounded by layers of absorbed water
molecules. These water molecules are considered part of the clay
surface when the behavior of clays is considered. Plasticity,
compaction, interparticle bonding, and water movement are all
influenced by the water layers.

Plasticity

Plasticity is the ability of a material to change shape

continuously under the influence of an applied stress and to retain
the new shape after removal of the stress. Fine sediment exhibits
plastic behavior. The range of water content over which sediment
particles exhibit plastic behavior is defined as that between the
plastic limit and liquid limit. The differences between the liquid
limit and plastic limit is defined as the plasticity index. The
activity of a soil is defined as the ratio of the plasticity index to
the percent of clay-sized particles.

Swelling

Swelling is defined as expansion of clays in polar liquids to a
volume many times that in a clay state. Montmorillonite clays have
the most swelling of all types of clays. The forces that cause
swelling in montmorillonite clay are due to the hydration of
exchangeable cations. The amount of swelling depends upon the clay
minerals and their arrangement or orientation in the clay soil, as
well as upon physicochemical factors such as valance of exchangeable
cations, pore water, salt concentration, and cementing bonds between
clay particles.

Thixotropy

Thixotropy is defined as a process of softening caused by
remolding followed by a time-dependent return to the original harder
state. Thixotropic behavior depends on the balance of forces acting
between particles.

Cation Exchange Capacity

Clay minerals have the important property of absorbing certain
cations and anions and retaining these in an exchangeable state,

i.e., these ions are exchangeable for other cations and anions by application of such ions in water solution. The cation exchange capacity (CEC) is measured in terms of milliequivalents per gram or per 100 grams at neutral pH (pH=7). In a fine cohesive sediment the CEC is largely restricted to the clay size fraction. It is independent of the ambient medium. The CEC of a mineral strongly depends on its chemical pretreatment. Particle size and temperature also affect the CEC. Materials such as iron oxide and sulfur compounds tend to cover the sites to be occupied by exchangeable ions and thereby reduce the CEC.

Interparticle Forces

Two types of interparticle forces are important in flocculation: Van der Waals forces and electric surface forces.

Van der Waals Forces: Van der Waal's forces between particles are always attractive and are independent of the electrolyte. The total attractive force between the particles is the sum of the forces between all atom parts. The magnitude of this total force depends on the size and shape of the particles. These forces are strong at short range, being related inversely with the seventh power of separation for small spheres and with the square or cube of the distance for parallel plates.

Electric Surface Forces: Many attractive and strongly repulsive forces are generated by electric charges on the particles. These charges are caused by imperfections within the interior of the crystal lattice, which may give a net negative or net positive lattice charge and preferential absorption of certain specific ions

on the particle surface. The magnitude of the total charge on a particle depends upon the type of absorbing material as well as on the availability of certain ions in the matter.

The Electric Double Layer

Any charged particle in an ion-containing water will attract ions of opposite charges (counter-ions) to compensate its own electric charge. The counter-ions tend to deffuse over the particle surface because of their thermal activity. Such diffusion takes place from a zone of high ionic concentration to one of lower ionic concentration. Therefore, a clay particle will be surrounded on either side by a diffused layer of counter-ions, whose positions will be determined by the balance between their electrostatic attraction and thermal activity. This layer is called "electric double layer" and the particles together are electrically neutral. This layer significantly determines the properties of clays in suspension.

Flocculation

Flocculation, or aggregation of fine sediment particles, is a well-known phenomenon in saline water. But flocculation can also take place in fresh tap water. Flocculation of fine sediment particles occurs as a result of cohesion between particles coming together, i.e., particle collision. Particle collisions are caused by Brownian motion of suspended particles, by the differential settling velocities of suspended particles, and by the shear flow (Krone, 1962). Net cohesion results from the predominance of

<u>Past Experiments Involving Unidirectional Flow</u>

<u>Critical Condition for Fine-grained Sediment</u>

Water flowing over a bed of sediment exerts forces on the
grains that tend to move or entrain them. When the hydrodynamic
forces acting on a grain of sediment or on aggregate particles of a
cohesive sediment has reached a value that, if increased even
slightly, will put the grain or aggregate into motion, critical or
threshold conditions are said to have been reached. The
corresponding values of the bed shear stress, stage of a stream,
stream discharge, and mean velocity, are all said to be the critical
or threshold values.

Analysis of the initiation of motion for coarse (non-cohesive)
sediment generally has been made by considering the forces involved
and equating the moments of gravity and drag forces. Lift forces
have often been neglected without proper justification (Task
Committee, 1966).

Sediment composed of or containing significant fractions of
fine-grained material in the silt and clay sizes has greater
resistance to entrainment in the flow than does coarser sediment
consisting only of sand. The high critical velocity of fine-grained
sediment is ascribed to cohesion that acts in conjunction with the
weight of the sediment to inhibit entrainment.

The oldest information on this subject was obtained by
engineers through experience in design and operation of canals. One
such example is Fortier and Scobey (1926). This type of information
is useful, even though it does not clarify the mechanisms of the

entrainment process for fine sediment.

Sundborg (1956) suggested that the cohesive force for a grain resisting entrainment is proportional to the shearing strength of the sediment. His formula for the critical shear stress at the bed, applied to a cohesive sediment in a hortizontal bed, is:

$$\tau_{0_c} = \alpha_1 \alpha_2 (\gamma_s - \gamma) 2D_s + \tan \theta_i + \alpha_3 S_v \qquad (14)$$

where τ_{0_c} = critical shear stress;

α_1 = packing factor (dimensionless);

α_2, α_3 = dimensionless shape factors;

γ_s = specific weight of sediment;

γ = specific weight of water;

D_s = average diameter of eroded clay particle;

θ_i = angle of internal friction; and

S_v = shear strength of sediment.

He argued that first term of equation 14 is negligible in comparison to the second term. If this is true, then $\tau_{0_c} = \alpha_3 S_v$, i.e., critical shear stress is proportional to shear strength.

The Task Committee (1966) did a comprehensive review of the literature up to 1966. A brief summary of that review follows. The Task Committee stated that since 1956 the critical shear stress for cohesive sediment has been correlated with (1) shear stress, (2) plasticity index, and (3) percent of weight of clay or silt and clay. In comparison of four experiments in which critical shear stress was measured, the results varied 200-fold in shear stresses. Whether this is a true variation or is caused by errors due to

differences in technique can not be evaluated. However, it does suggest that the resistence to erosion of cohesive sediment varies greatly. The committee concluded that shear strength, plasticity index, and perhaps clay content, all have an important bearing on cohesive erosion, and also that the chemical environmental factors should be considered.

Dunn (1959), Smerdon and Beasley (1961), and Flaxman (1963) studied the initiation of fine-grained sediment and presented rlationships for critical shear stress against plasticity index, percent clay and unconfined compressive strength, respectively. Flaxman suggested that tractive power was a better measure of effective erosion forces.

Abdel-Rahman (1964) studied erosion resistance of a clay sediment (median size = 0.009 mm, 22 to 25 percent by weight was finer than 0.002 mm and 90 to 96 percent was finer than 0.2 mm) with a plasticity index of 23. He presented the mean erosion depth as a function of time, as is shown here in Figure 8. The author indicated that as the bed eroded, hydrodynamic roughness tended to increase and that the erosion process was related to the swelling of clay; when erosion ceased, the bed surface was observed to be covered by a thin layer of sticky material. The work of Abdel-Rahman also indicates that erosion will occur over a range of fluid shear stresses and sediment properties, if given sufficient time. This result indicates that there is no critical shear stress for clays in the sense that one exists for non-cohesive sediment.

Parthenaides (1962) conducted flume experiments with San
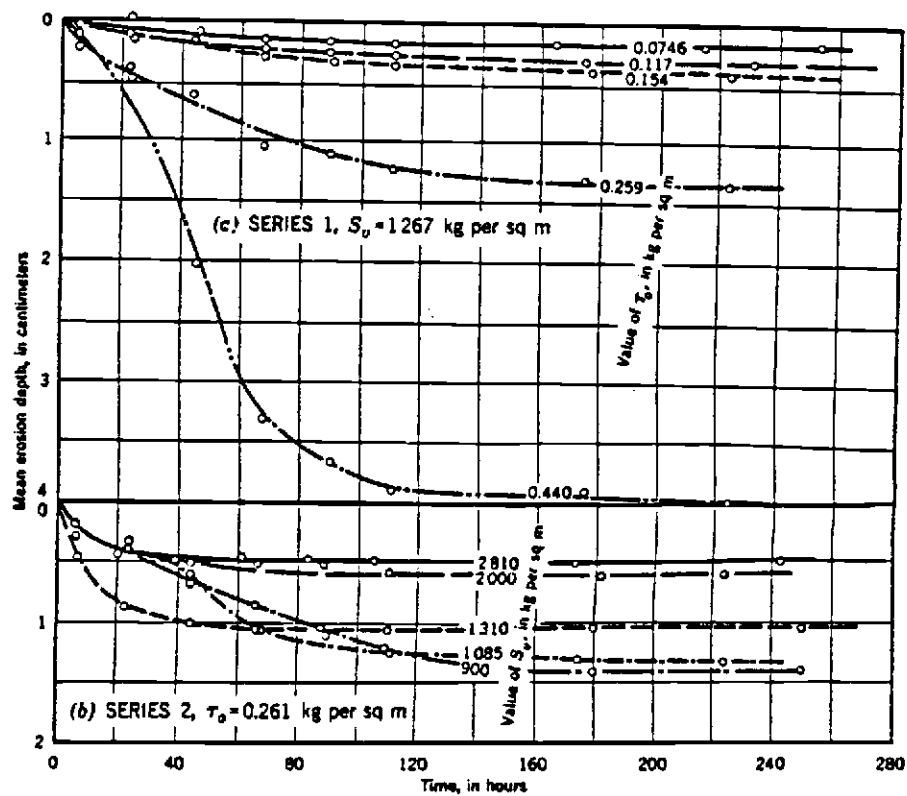
Figure 8.   Mean Erosion Depth Versus Time For a Clay Soil
(Source: Abdel-Rahmann, 1964)

Francisco Bay mud using salt water with ocean salinity. Sixty percent by weight of his sediment was finer than 2_μ; a trace of very fine sand was also present. Pathenaides found that the critical shear stress was independent of the Vane shear strength. He stated that the critical shear stress depends on the bond strength of clay flocs but does not depend on the degree of consolidation.

Kamphius and Hall (1983) observed that in the majority of their test runs, the appearance of small pit marks over the entire surface of the soil indicated initiation of erosion. They stated that these marks enlarge with time, creating deeper, large-diameter holes which cause additional turbulence. This turbulence is caused by an increase in the local shear stress at the bed, resulting in an increased erosion rate. Kamphius and Hall also determined the critical velocity, u_c, at which material begins to move using

$$\frac{u_c}{u_{*_c}} = \frac{1}{K} \ln\left(\frac{9 u_{*_c} y}{\nu}\right) \qquad (15)$$

where u_{*_c} = critical shear velocity; and

$\frac{u_{*_c} y}{\nu}$ = critical shear Reynolds number.

Also, by plotting critical boundary shear stress, τ_{o_c}, versus the critical velocity they found that

$$\tau_{o_c} = 2.93 \, u_{3c}^{1.75} \qquad (16)$$

where u_{3c} = critical velocity 3 cm above the bed; and

$$\tau_{o_c} = \rho u_{*_c}^2$$

In summary, to determine the incipient motion of fine-grained sediment particles, it is necessary to determine the velocity and/or shear stress. The suspended sediment concentration is also of interest to indicate that incipient motion has begun.

Analysis Methods

The following sections briefly describe the methods past investigators used to measure or calculate velocity, shear stress, and suspended sediment concentration.

Velocity Determination

In the study of sediment particle suspended under unidirectional flow, obtaining the velocity distribution near the bed and above the sediment-water interface is essential. Many investigators in laboratory studies of sediment suspension measured the velocity using different types of available instruments. Theoretical derivations of velocity were performed by most investigators to verify or validify the measured velocities or to provide values in cases where it was practically impossible to obtain measurements in the very small boundary layer. Velocity measurement techniques are summarized later in this chapter, both for unidirectional flow and oscillatory flow. Velocity computation techniques for unidirectional flow are briefly described below. Both theoretical and empricial equations are used to describe the velocity.

Most textbooks in fluid mechanics and hydraulics cover the Prandtl-Karman basic logarithmic velocity equation. A brief discussion of the velocity equation and its applicability is instructive here also. The original Prandtl-Karman logarithmic equation for hydraulically smooth and rough flow is given as:

a) smooth flow $\quad\quad \dfrac{\bar{u}}{u_*} = 5.75 \log_{10} \dfrac{u_* y}{\nu} + 5.5$ $\quad\quad\quad$ (17)

b) rough flow $\quad\quad \dfrac{\bar{u}}{u_*} = 5.75 \log_{10} \dfrac{y}{K_s} + 8.5$ $\quad\quad\quad$ (18)

where $\bar{u}$ = average velocity; and

$\quad$ K_s = roughness coefficient.

Sternberg (1968) used the logarithmic velocity profile for hydraulically smooth flow to determine the velocity at any height above the bed. He found out the same equation as 17. Smooth flow means that the thickness of the laminar sublayer existing adjacent to bed is large enough to cover all boundary roughness elements; thus, the bed irregularities do not influence the flow beyond that of a perfectly smooth boundary.

Coleman (1981) discussed the accepted form of the law of the wall and of the velocity defect law, which contained so-called wake flow terms, in addition to remarks about the original Prandtl-Karman form. These wake flow terms account for the deviation of the velocity defect law from the logarithmic form in the outer part of the boundary layer of an open channel flow. Coleman also stated that the roughness coefficient does not

decrease with an increase in suspended sediment concentration, as others has assumed; the roughness coefficient is not dependent on sediment concentration. Kamphius and Hall (1983) found the measured velocity distribution to be logarithmic within 50 mm of the bed and the flow was found to be hydraulically smooth.

Shear Stress Determination

The fluid flow parameter most closely related to the degree of bottom sediment motion is the boundary shear stress. Therefore, determination of time-average boundary shear stress is an integral part of the studies where the initiation of motion or sediment transport is involved (Nece and Smith, 1970).

The intensity of fluid shear will vary as a linear function of normal distance from the free (air-water) surface. The corresponding shear stress equation can be given as:

$$\tau = \gamma(d-y)S \tag{19}$$

where S = slope of the energy grade line and all other terms are as previously defined.

Hence, the bottom shear stress becomes:

$$\tau_0 = \gamma \cdot R \cdot S = \gamma \cdot d \cdot S. \tag{20}$$

combining these expressions:

$$\tau = \tau_0(1-y/d) \tag{3}$$

This shear stress can be obtained directly or indirectly from the known flow conditions.

Direct Measurement: To directly measure the boundary shear
drag, techniques used generally consist of isolating a certain
length of channel from the remaining channel. The isolated segment
is independently supported on the same line and grade as the
remaining channel but with a small gap between the two. Ghosh and
Roy (1970) used this techniques (which was originally employed by
Bagnold) and suspended the channel segment by a three-point
suspension. They found that for a smooth rectangular channel
lining, the maximum shear intensity occurs at the free surface and
at the bed centerline; for an artifically roughened lining it
occurs at some distance from the top and bed centerline toward the
corner. They also mentioned that total boundary drag per unit
length of channel in direct and indirect measurement are in good
agreement but that the stress distribution varies.

Nece and Smith (1970) stated that direct shear stress
measurement is impractical in large river and marine environments.

The advantage of the direct measurement is that it involves no
assumptions regarding the nature of the velocity distribution.
Disadvantages are that 1) it is difficult to measure such a small
force, and 2) the measurement is restricted to a predetermined
fixed point or channel segment, thus preventing exploration of the
actual distribution of shear-stress over the whole walled
parameter.

Indirect Measurement of Shear Stress: Indirect measurements of
shear stress can be obtained by means of several techniques. These
include use of momentum analysis, heat transfer similarity, the

logarithmic velocity profile, and the apparent shear stress. A variety of instruments have been used to make these determinations, including miniature current meters, the Preston Tube, hot-film anemometers, and others. The actual techniques are summarized later in this chapter, both for unidirectional and oscillatory flow. The analysis techniques are briefly summarized here.

The momentum analysis technique can be applied to fully developed flow in a straight parallel channel, where a simple momentum balance yields

$$\overline{\tau}_o = R_h \; dp/dx \tag{21}$$

where $\overline{\tau}_o$ = the mean of the bottom shear stress, τ_o, around the perimeter of the channel;

R_h = hydraulic radius; and

$\frac{dP}{dx}$ = streamwise pressure gradient in the channel.

Major difficulties are involved with the estimation of shear stress from measurement of the pressure gradient. But, if adequate care is taken with the experiment, the methods provides satisfactory results.

In using the heat transfer similarity method for boundary-layer flow along a surface, it is assumed that the velocity field is independent of the temperature field, provided that the temperature difference between the surface and the free stream is small. The rate of heat transfer by forced convection will depend on the wall

variables. Use of a calibrated heated element device for a given situation then allows shear stress to be deduced from measurement of the heat transfer and temperature differences between the surface and the free stream. This technique is applicable only within the viscous sublayer.

The logarithmic velocity profile method can be used in a pipe or channel where wall shear stress is already known. From available data the shear velocity u_* and the function $(u/u_*)[\frac{u_* y}{\nu}]$ can be determined. For any other related situation, from a measurement of the fluid velocity at a point the shear velocity and shear stress can then be found. The velocity measurement points used for calculation should be within the zone where the logarithmic profile is applicable (i.e., the zone where the law of the wall is valid).

If the apparent (Reynolds) shear stress could be measured at two elevations near the bottom in a turbulent boundary layer, an extrapolation based on an assumed linear variation of the shear stress would yield the apparent shear stress.

$$\tau = -\rho\overline{u'v'} \qquad\qquad (22)$$

where u' and v' are fluctuating turbulent velocity components in the x and y directions, respectively, which can be measured and $\overline{u'v'}$ is the time-averaged product of fluctuating values.

Empirical Derivation Involving Friction Factor: One approach to determine the shear stress indirectly involves evaluation of the

boundary friction factor and roughness coefficient. The Task
Committee (1963A), in its friction factor determination for open
channels, concluded that there is a great utility in expressing
resistance in terms of the Darcy-Weisback friction coefficient.

Blinco and Parthenaides (1971) calculated bed shear stress using
the Darcy-Weisbach friction factor:

$$\tau_o = \frac{f}{8} \rho \bar{u}^2 \qquad (23)$$

where f = Darcy-Weisbach friction coefficient. The friction factor
can be evaluated from the Moody diagram by use of the Reynolds
number and relative roughness, which are expressed by

$$\text{Reynolds number} = Re = \frac{4R_h \bar{u}}{\nu} \qquad (24)$$

$$\text{Relative roughness} = \frac{K_s}{4R_h} \qquad (25)$$

where K = average particle roughness coefficient.
For a rough boundary, an apparent origin for the elevation y, can
be obtained from the universal logarithmic velocity equation by
introducing y = y' =

$$\frac{\bar{u}}{u_*} = \frac{2 \cdot 3}{K} \log \frac{y'}{K_s} + \beta \qquad (26)$$

where y' = zero depth of flow for rough boundary, Blinco and
Parthenaides used y' = 0.27 K, where K is the Von Karman universal
constant.

They also mentioned that Einstein and El-Samni used $y' = 0.2$ K and Goma and Gellon used $y' = 0.23$ K.

Statistical Study of Shear Stress: Many investigators have used the Nikuradse sand grain roughness in shear stress and sediment transport studies. Nikuradse used sand to roughen the inside of pipes having various diameters, thus giving several relative roughnesses, and assumed that the height of roughness which interferred with the pipe flow was equal to the diameter of the sand grains used. Currently, sediment transport investigators assume that the roughness coefficent used in the friction relation can be replaced by the grain diameter. Thus, $K_s = D$.
Dimensional analysis of the relative roughness by Kamphius (1974) gave:

$$\frac{K_s}{D} = \phi(\frac{d}{D} , \frac{u_* K_s}{\nu})$$

(27)

where all terms are as previously defined.
Kamphius also used the logarithmic velocity distribution for turbulent flow assuming K = 0.4 for clear water.

Yalin and Russell (1977) concluded that for a natural channel bottom the particle roughness coefficient, K_s , could be replaced by approximately twice the magnitude of the D_{90} particle (that particle size in a mixture of sizes such that 90 percent of all particles are smaller) under certain conditions. These where d/D_{90} is large enough to warrant discussing the resistance of the total bed (grains and bedforms) rather than only resistance of individual particles.

This conclusion by Yalin and Russel is in contradiction to the assumption that $K_s = D_{90}$ which has been used by the majority of researchers.

Blinco and Simons (1973) reviewed the statistical approaches to the study of shear stress and summarized the available literature. They stated that many investigators have reported both experimental and analytical studies to determine the statistical characteristics of the instantaneous hydrodynamic forces. These studies indicate that the hydrodynamic forces at the boundary can be approximated by a Gaussian distribution function. Blinco and Simons used a hot-film anemometer to measure the local boundary shear stress in a smooth open channel and concluded that the flush-mounted hot-film sensor is capable of measuring the turbulent boundary shear stress in a hydrodynamically smooth flow and that the probability density function of the shear stress is positively skewed.

Suspended Sediment Concentration

In the study of sediment suspension, a turbulence-related sediment transfer mechanism exists; e.g., turbulent velocity fluctuation is responsible for keeping some particles in suspension. Turbulence is the commonly observed irregular motion of a flowing fluid. It results from eddies that are swirling in an irregular manner as they are carried along by the flow. New eddies are formed by the shearing action of the fluid while eddies already in existence are being dissipated into heat by viscous friction. The Task Committee (1963C) study of suspension of sediment recognized the importance of turbulence and the need for suitable differential

equations to describe suspended sediment and its distribution in a turbulent flow.

Some of the basic aspects of suspended sediment transport and variations in the suspension concentration were discussed earlier in this chapter. A few investigators have looked more closely at the suspension behavior near the boundary layer.

Coleman (1969) studied sediment suspension and supported the observations of Richardson (1937) and Vanoni (1946) that near the channel bed the suspended sediment concentration is inversely proportional to the distance from the boundary, whereas farther from the boundary in the open stream the concentration varies in a different exponential manner. Coleman stated that sediment suspension took place in both an inner regime near the bed and an outer regime in the free stream but that the patterns for the two regimes are different. A straight line fitted the concentration versus depth data on semi-log paper for the outer regime and indicated an exponential variation of concentration with distance from the bed; the portion of the profile near the bed (in the inner regime) showed a characteristic deviation from a straight line.

General Review of Erosion Studies

In the past, erosion and deposition of fine sediments were studied by means of 1) laboratory flume research and 2) by correlations of maximum channel velocity or competent bottom velocity or bottom drag (tractive) force with soil characteristics such as mean grain diameter, void ratio, Atterberg limits, and shear strength.

The U.S. Bureau of Reclamation (1953) compared maximum tractive force with plasticity index and mean grain size. The correlations were poor, with wide scattering. This was particularily true for the correlation with the mean grain size.

Kuiti and Yen (1976) stated that in the case of fine sediments, two important parameters beside those describing the erosion and deposition of coarse sediment should be studied. The first involves clay characteristics and deals with the physicochemical behavior of the sediment. The percentage of clay minerals and type of clay should be determined. These give the sediment its cation exchange capacity and, as a result, cause various physicochemical effects. The second parameter involves the composition of the sediment mixture. From this the relative importance of the gravitational forces in comparison to physicochemical forces of sediment mixtures may be expressable by use of the mean diameter of the clay-silt-sand mixture.

Krone (1957) studied silt transport utilizing radioisotopes. For investigating the scour and erosion of the silt bed subject to unidirectional flow, he started with low velocity. Krone then measured velocities and suspended sediment concentrations while progressively increasing the velocity. The observed changes allowed him to define the scour and erosion of silt particles. For investigating the deposition, he progressively decreased velocity while measuring velocity and suspended sediment concentration. He also conducted experiments to evaluate alternate deposition and scour. In all studies, velocity was used as the criterion for

defining erosion or deposition of fine sediment.

Partheniades (1962, 1972) has extensively studied the erosion and deposition of fine sediments and gives a comprehensive review of earlier work on the subject. He states that the typical assumption of macroscopic shear strength as a unique correlation parameter for erodibility is false and erroneous.

Parthenaides (1962) studied the erosion and depositional properties of cohesive sediments under unidirectional flow in a flume with recirculating water at ocean salinity. His results show that the erosion rates were independent of the bed shear strength and of the suspended sediment concentration, but that they depend strongly on the shear stress exerted by the fluid, increasing very rapidly after a critical shear stress value had been reached. Also, he found the minimum shear stress for initiation of erosion to be independent of the shear strength of the bed. Cementing agents dissolved in the water, as well as suspended sand, were found to cause significant changes in the properties of the bed surface. Parthenaides concluded that the mechanism of failure of a cohesive soil under the erosive action of flowing water is drastically different from the mechanism of mass shear failure due to external forces.

Parthenaides showed that a knowledge of bed erosion rates, settling velocities and structure of the turbulence controlling the diffusion process in the immediate neighborhood of the bed, is required in order to solve fine sediment problems for the simplest one-dimensional case.

Examination of the laboratory studies by Partheniades shows the disadvantage of the arbitrary and subjective nature of the criterion for establishing critical shear stress. The studies are also limited by use of a single type of clay mineral and a single method of exerting forces on the bed. Also, the water content at compaction and the clay fabric were not treated as variables in his studies.

The experiments by Abdel-Rhaman (1964) in an open flume revealed that bed scouring eventually terminates with time. The maximum depth of scour and the roughness of the resulting eroded bed increased with increasing applied bed shear stress. These also increased with decreasing shear strength of the bed.

Grissinger (1966) found that the soil erodibility, in terms of measured erosion rates, decreased with increasing particle orientation, with increasing clay content and with increasing cation exchange capacity of the clay portion of the sediment. Here, Grissinger's particle orientation refers the compaction condition and his findings imply that soils compacted to a particular dry density from an initial drier-than-optimum moisture content are expected to be more susceptible to erosion than soils compacted to the same dry density from an initial wetter-than-optimum moisture content. Grissinger also found that the resistance to erosion increases slightly with increasing bulk density of the soil.

Slaking of the soil is an important physical phenomenon contributing to soil erosion. It amounts to a gradual soil deterioration into flakes which can easily be transported by the flow.

Another factor which has been investigated is the effect of antecedent moisture content on soil erosion rates. There seems to be an optimum antecedent moisture at which the erosion rates are minimum, whereas for antecedent conditions above or below the optimum, the resistence to erosion decreases and the rate of erosion increases.

Temperature is another soil erosion parameter that has been studied. A significant increase of erosion rate with increase of temperature has been reported (Kandiah, 1974). A marked thixotropic effect with time observed, with the erosion rates decreasing by as much as ten percent from the initial rates after four hours of aging of the sample (Parthenlades, 1962).

Past Experiments Involving Oscillatory Flow

Overview of Types of Research on Sediment Transport Under Oscillatory Flow

The accelerated rate of erosion of the earth's beaches and shoaling in tidal estuaries, lakes and rivers has resulted in a high level of interest in the last few decades by many investigators in Europe, the United States, Japan and Australia to study sediment transport phenomena under wave action. The most quantitative approach to such studies has been through laboratory experimentation. Depending on the investigator's preferences and concerns, subjectivity in defining conditions, selected problem topic, and availability of technology and equipment, many different approaches have been used to attempt to realistically simulate

prototype conditions In the laboratory. Also, many different types of materials, particle sizes and densities have been studied.

Major advancement in the study of sediment suspensions under wave action started by the work of Bagnold (1946) in England. He simulated the oscillatory motion under laboratory conditions by oscillating a section of bed in pendulum form in still water. The type of apparatus, materials and results of his research are presented later in this chapter.

A few years later in Berkeley, California, suspension experiments under oscillatory flow began under direction of H.A. Einstein. Several researchers, such as Li (1954), Manohar (1955), Kalkanis (1957, 1964), Abou-Seida (1964), Carstens and Neilson (1967), and Das (1971) experimented with sediment suspension and waves by oscillating the bed in still water, rather than using the pendulum approach of Bagnold. They were generally trying to determine whether or not the principles of sediment transport studies under unidirectional flow were also applicable under oscillatory flow. Their studies and results are discussed in following parts of this chapter.

Vincent (1958) and some others criticized the use of an oscillating bed with still water in laboratory studies of sediment suspension under waves. Vincent used a wave flume with a fixed bed section and oscillated water with a flap-type or piston wave maker. Wave flumes have also been used in studies by Scott (1954), Ippen and Eagleson (1955), Alishahi and Krone (1964), Yalin and Russell (1966), Bhattacharya (1971), Mogridge and Kamphius (1972), Kobune

(1978), and Dingler (1979). Their studies and results are discussed later in this chapter.

Other types of apparatus have been used. Water tunnels were used by Carstens and Neilson (1967), Rance and Warren (1968), Riedel (1972), Mogridge and Kamphius (1972), Kamphuis (1975), Nakato et al. (1977), Jonsson and Carlson (1976), and Lofquist (1978). Lofquist criticized the use of a wave flume used to oscillate a section of bed with still water or to oscillate water with a fixed bed. An oscillating block of water was used by Silvester (1970) and Mogridge (1970) in their research. Chan et al. (1972) conducted studies of sediment suspension under waves by use of a horizontal tube subjected to an oscillatory liquid flow.

Other investigators, such as Davies and Wilkinson (1978) and Dyer (1980), have conducted field studies of the sediment motion at the sediment bed under waves. Several others have summarized and analyzed the published data. These include Jonsson (1963), Silvester and Mogridge (1970), Komar and Miller (1973), Wang and Liang (1975), Nielsen (1979) and Hallermeier (1980).

Several factors contribute to the complexity of sediment suspension under waves and to the complexity of studies of this phenomenon. Nakato et al (1977) identified the following difficulties:

1. The fluid motion is unsteady, non-uniform, and at least two-dimensional;

2. the fluid has two surface interfaces, one with air and one with sediment;

3. the interactions between the fluid and solid particles
    are complex; and

4. the presence of a solid can alter the characteristics of
    the flow field.

Table 2 identifies several of the above-mentioned investigators
who have studied sediment suspension under oscillatory flow,
together with the type of equipment used and the range of particle
sizes and particle densities studied. The studies, equipment, and
results are discussed later in this chapter.

Beyond the difficulties just mentioned, it is clear that many
types of waves can create oscillatory flow and affect sediment
transport. Therefore, the next section gives a brief review of the
motion of water due to waves, in order to provide a general
background for discussion to follow.

Motion of Water for Oscillatory Flow

Surface waves in water produce an oscillatory motion throughout
the water depth. The oscillatory motion can be analyzed by solution
of the equations of fluid motion. These equations, together with
the boundary conditions that they are required to meet, are used to
address the problem of describing wave motion.

Before solving the problem of wave motion characteristics, it is
apppropriate to define the wave system and some of the terminology
which will be used. For this purpose, the general case of linear
wave theory will be used. This is also referred to as
small-amplitude wave theory, and Airy wave theory. Figure 9 gives a
definition sketch for the general form of a linear wave system.

TABLE 2. Summary of Types of Apparatus and Sediments Used by Various Investigators in Sediment Study Under Oscillatory Flow

Investigator and Year	Type of Apparatus	Particle Size µm	Particle Density gram/cm^{3}
Bagnold (1946)	oscillating bed	90 - 2,500	1.5 - 7.6
Scott (1954)	wave flume	---	---
Li (1954)	oscillating bed	274 - 13,800	2.65
Manohar (1955)	oscillating bed	147 - 3,170	1.05 - 2.65
Ippen and Eagleson (1955)	wave flume	2,000 - 6,000	2.65
Vincent (1958)	wave flume	100 - 1,200	1.38 - 2.65
Eagleson and Dean (1961)	wave flume	2,000 - 6,000	2.65
Kalkanis (1957, 1964)	oscillating plate	580 - 2,620	2.65
Abou-Seida (1963)	oscillating plate	145 - 300	---
Alishahi and Krone (1964)	flume with wind-wave	more than half clay rest in silt range	---
Carstens and Nielson (1967)	oscillating water tunnel	4,000 - 48,000	---
Cartens and Nielson (1969)	oscillating water tunnel	190 - 585	2.6
Mogridge (1970)	water blocks	239	2.65
Bhattacharya (1971)	wave flume	210	2.65
Das (1972)	swing flume	589 - 701	1.13
Chan et al. (1972)	oscillating horizontal tube	100 - 1,100	1.05 - 5.1
Riedel (1972)	oscillatory water tunnel	369 - 50,000	---
Mogridge and Kamphius (1973)	wave flume and oscillatory water tunnel	360 - 1,540	1.05 - 2.38
Kamphius (1975)	oscillatory water tunnel	500 - 46,000	2.65
Jonsson and Carlson (1976)	oscillatory water tunnel	---	---
Nakato et al. (1977)	oscillatory water tunnel	sand	---
Lofquist (1978)	oscillatory water tunnel	180 - 550	---
Davies and Wilkinson (1978)	in-situ at sea	sand	---
Dingler (1979)	wave flume	177 - 1,454	2.65
Dyer (1980)	in-situ at sea	sand	---
Vongvisess-emjai (1984)	oscillating bed, wave flume and wave tunnel	medium sand	2.65
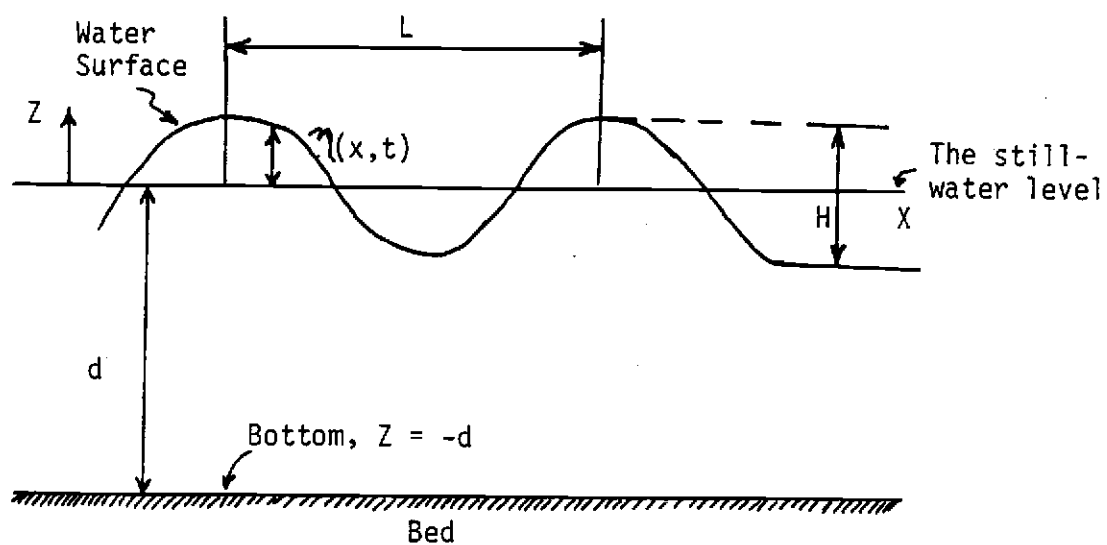
Figure 9. Definition Sketch for General Form of a Linear Wave System

The differential equation to be satisfied in the region from the wave water surface to the bed is the Continuity equation (Laplace equation). This can be given as:

$$\frac{\partial^2 \phi}{\partial x^2} + \frac{\partial^2 \phi}{\partial z^2} = 0 \qquad (28)$$

This equation is subject to the boundary conditions for the bottom and for the water surface boundary. The boundary condition to be satisfied on the fixed bottom is given as:

$$W = -\frac{\partial \phi}{\partial z} = 0 \text{ at } z = -d \qquad (29)$$

where W = vertical component of velocity of water particle under wave; and

Z = vertical coordinate measured from the still-water level positively upwards (at the bed, Z = -d);

The boundary condition to be satisfied at the oscillating water surface is given as:

$$\frac{\partial \eta}{\partial t} + \frac{\partial \phi}{\partial x} \frac{\partial \eta}{\partial x} - \frac{\partial \phi}{\partial z} = 0 \text{ at } z = \eta \qquad (30)$$

$$\frac{\partial \phi}{\partial t} + 1/2 \left[\left(\frac{\partial \phi}{\partial x}\right)^2 + \left(\frac{\partial \phi}{\partial z}\right)^2 \right] + g\eta = f(t) \text{ at } z = \eta \qquad (31)$$

Where $\eta(x,t)$ is the free surface elevation relative to the still water level and is positive upward.

Linear waves are waves of small amplitude compared to wave

length and water depth. For linear waves, the free-surface boundary conditions given above can be reduced to

$$\frac{\partial \phi}{\partial z} - \frac{\partial \eta}{\partial t} = 0 \text{ at } z = 0 \tag{32}$$

$$\frac{\partial \phi}{\partial t} + g\eta = 0 \text{ at } z = 0 \tag{33}$$

These may be combined to give:

$$\frac{\partial^2 \phi}{\partial t^2} + g\frac{\partial \phi}{\partial z} = 0 \text{ at } z = 0 \tag{34}$$

or

$$\eta = \frac{1}{g} \left(\frac{\partial \phi}{\partial t}\right)_{z=0} \tag{35}$$

The velocity has been predicted as a function of the wave height, wave period, and water depth by many investigators. Linear wave theory, through the use of potential velocity, provides one simple and almost accurate approach to predict the velocity. The velocity potential for a linear wave traveling in the positive X direction in an inviscid fluid can be expressed as:

$$\phi = \frac{gH}{2\omega} \frac{\cosh (2\pi(d+z)/L)}{\cosh\frac{2\pi d}{L}} \sin \left(\frac{2\pi X}{L} - \frac{2\pi t}{T}\right) \tag{36}$$

where ω = angular velocity, $\frac{2\pi}{T}$;

L = wave length;

X = horizontal coordinate in direction of wave propagation;

t = time; and

T = wave period.

By virtue of the definition of the velocity potential, the horizontal and vertical components of local fluid velocity may be obtained by the appropriate differentiation of potential flow velocity. This differentiation of the potential velocity equation with respect to X and Z gives the horizontal and vertical components of velocity under a wave, respectively. These equations can be given as:

$$U = -\frac{\partial \phi}{\partial x} = \frac{\pi H \cosh (2\pi(z + d)/L)}{T \sinh 2\pi d/L} \cos (\frac{2\pi x}{T} - \frac{2\pi t}{T}) \qquad (37)$$

$$W = -\frac{\partial \phi}{\partial z} = -\frac{\pi H \sinh (2\pi(d + z)/L)}{T \sinh 2\pi d/L} \sin (\frac{2\pi x}{L} - \frac{2\pi t}{T}) \qquad (38)$$

Where U = horizontal component of velocity of water particle under wave; and

H = wave height.

These equations express the velocity components due to the waves at the water surface or at any depth Z.

A fluid particle under oscillatory flow will occupy a certain position in space (X, Z) only instantaneously. Furthermore, as it moves away from (X, Z) its velocity continuously changes. The horizontal and vertical displacements of the water particle from its mean position below the surface of the water are given, respectively, by:

$$\xi = -\frac{1}{2} H \frac{\cosh (2\pi(d + z)/L)}{\sinh 2\pi d/L} \cos 2\pi(x/L - t/T) \qquad (39)$$

and

$$\zeta = +\frac{1}{2} H \frac{\sinh (2\pi(d + z)/L)}{\sinh 2\pi d/L} \sin 2\pi(x/L - t/T) \qquad (40)$$

Where ξ = horizontal displacement of a water particle under a wave; and

ζ = vertical displacement of a water particle under a wave. From these equations, it can be shown that the semi- orbital amplitudes in the horizontal and vertical direction for the motion of the particle below the water surface are given, respectively, by:

$$a = \frac{1}{2} H \frac{\cosh (2\pi(z + d)/L)}{\sinh 2\pi d/L} \qquad (41)$$

$$b = \frac{1}{2} H \frac{\sinh (2\pi(d + z)/L)}{\sinh 2\pi d/L} \qquad (42)$$

Where a = major ellipse semiaxis of particle movement; and

b = minor ellipse semiaxis of particle movement.

The particle paths, therefore, are generally elliptical in shape. The specific form of the particle paths can easily be determined by examining the values of a and b for the particular shallow water, intermediate water, or deep water conditions that may prevail.

For shallow water cases, i.e., d/L < 1/20, the maximum horizontal displacement is constant from the water surface to the

bottom. The maximum vertical displacement, on the other hand, varies from zero at the bottom to the wave amplitude at the surface. The water particles have an elliptical motion which becomes flatter and flatter with increasing distance below the water surface. The horizontal velocity component is nearly constant from water surface to the bed. The vertical velocity component decreases from its maximum value at the water surface to zero at the bed. These features are shown in Figure 10(a).

For deep water cases, i.e., d/L > 1/2, the horizontal and vertical displacements both vary in a similar manner. The water particles have a circular motion at the water surface and the diameter of the circular motion decreases with increasing distance below the surface, until the horizontal and vertical displacements become almost three percent of surface values at $Z \simeq -L/2$ below the still-water level. The velocity components in the horizontal and vertical directions are equal at each point. They are maximum at the water surface and decrease approximately to zero at one-half wave length below the still-water level. These features are shown in Figure 10(c).

For intermediate cases, i.e., 1/20 < d/L < 1/2, the horizontal and vertical displacement can be obtained from equations 2.39 and 2.40. The forms of the particle orbits and variation of particle velocity amplitude with depth are intermediate between shallow and deep-water cases and are summarized in diagrammatic form in Figure 10(b).

The solution of the equations of motions for waves can be

(a) Shallow water

(b) Intermediate depth

(c) Deep water
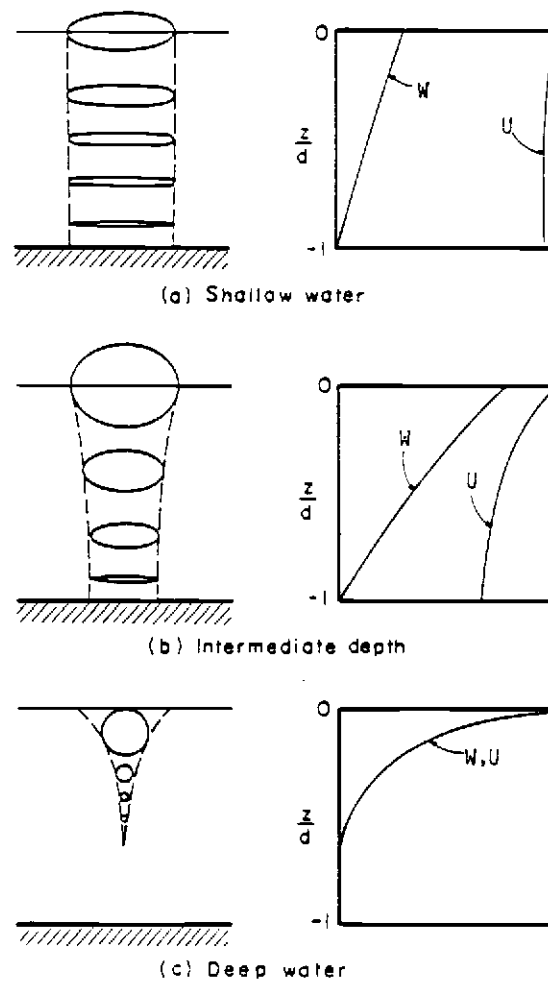
Figure 10. Variations of Particle Orbits and
Particle Velocities With Depth
(Source: Sarpkaya and Isaacson, 1981)

Improved over that based on linear wave theory. Inclusion of higher-order terms to fit various theories usually produces better agreement between theoretical and observed wave behavior. The higher-order theories can explain phenomena such as mass transport which can not be explained by linear wave theory. In a water wave, the particles of fluid possess, apart from their orbital motion, a steady second-order drift velocity. This drift velocity is usually called the mass transport velocity. With known wave height and wave period, the higher-order theories can provide more-accurate estimates of velocity and pressure fields due to waves than can linear theory.

Higher-order theories which are used to estimate the velocity and pressure fields due to waves include: Stoke's 2nd order, Stoke's 3rd order, Stoke's 4th order, Stoke's 5th order, stream function, and cnoidal theory. Investigators must define regions where various wave theories are valid. The U.S. Army Corps of Engineers (1977) presented a figure from LeMehaute to illustrate approximate limits of validity for several wave theories. This is reproduced as Figure 11. For given values of wave height, water depth and wave period, Figure 11 may be used as a guide in selecting an appropriate theory.

Solution of wave problems using linear wave theory involves the assumption of potential flow (no viscosity) and ignores the boundary layer which develops along the bed. Potential flow concepts (irrotational flow) can be applied fairly well to wave motion in the entire water body except to this very thin layer adjacent to solid boundaries. Near any solid boundaries, the viscous effects can not
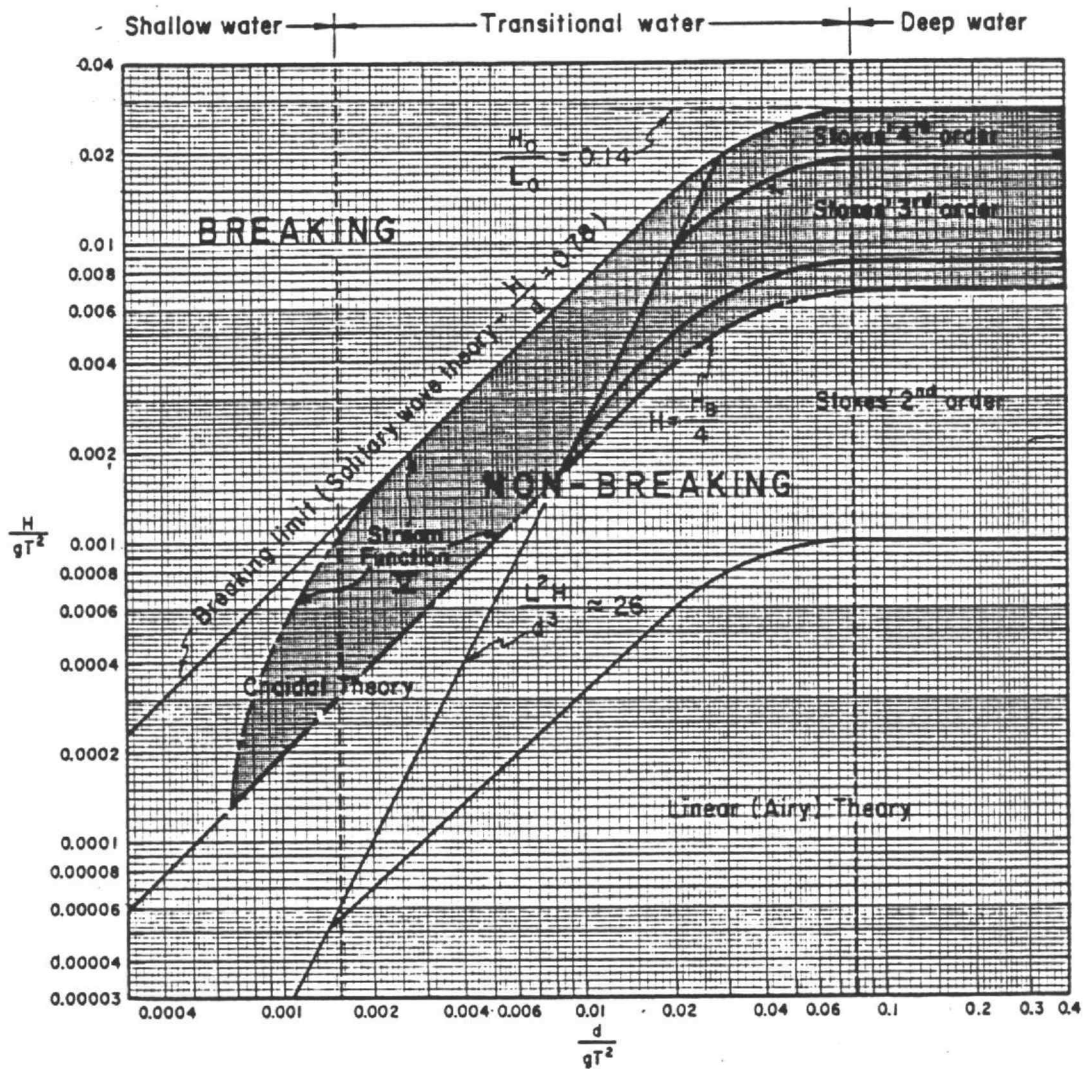
Figure 11.   Regions of Validity for Various Wave Theories,
              According to LeMehaute (Source: U.S. Corps of
              Engineers, 1977)

be neglected. Flow within the boundary layer is called boundary
layer flow.

The thin boundary layer plays a very important role in studying
the flow problem. Flow energy is dissipated in this layer, and
especially the skin friction is the direct effect of the presence of
this layer. The wave motion near the solid bottom has been found to
approximate very closely a simple harmonic motion (Li, 1954).
Therefore, application of linear wave theory to this layer will not
introduce major errors.

Progressive waves can be defined as waves in which successive
crests pass a fixed point while moving in one direction, in contrast
to standing waves and short-crested waves. A standing wave can be
defined as the superposition of two progressive waves of the same
amplitude and period traveling in opposite directions.
Short-crested waves can be defined as waves in which successive
crests pass a fixed point, but not at equal intervals. Linear wave
theory, which is strictly applicable to waves having a sinusoidal
shape and a very low steepness (small H/L ratio) can be applied to
progressive waves. In a progressive wave, by linear wave theory,
the particle orbits are as shown in Figure 12. Also shown are the
zones of potential flow and boundary layer flow. According to
Jonsson (1966) the amplitude of the horizontal displacement
component is slightly larger within the boundary layer than in the
zone immediately above, differing slightly from the situation shown
in Figure 10(b).
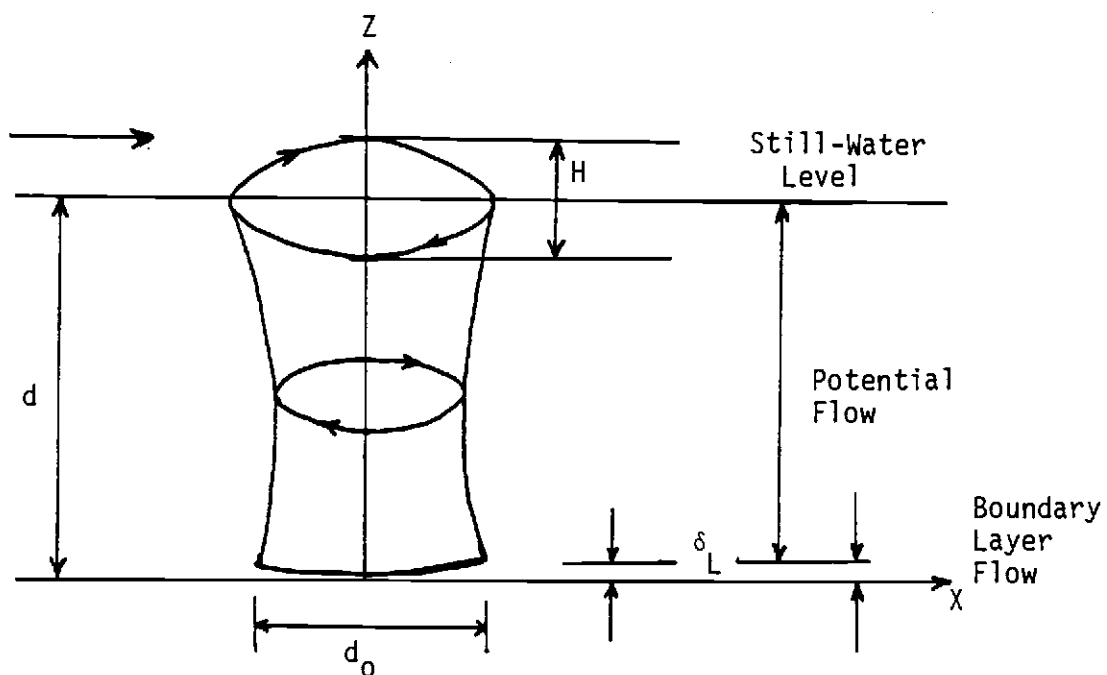
Figure 12. Wave Particle Motion at Different Levels
For Progressive Waves

For progressive (linear) waves, at the bottom boundary where d = -Z, the horizontal and vertical velocity components reduce to

$$U = \frac{\pi H}{T \sinh 2\pi d/L} \sin 2\pi(x/L - t/T) \tag{43}$$

$$W = 0 \tag{29}$$

The horizontal velocity component at the boundary (to-and-fro velocity) has a maximum value given by:

$$U_m = \frac{\pi H}{T \sinh 2\pi d/L} \tag{44}$$

This maximum velocity occurs twice during each wave period, once in the direction of wave advance under the wave crest and a second time in the opposite direction under the wave trough.

At the bottom boundary, the elliptical orbits flatten to a simple horizontal to-and-fro motion with a period equal to the period of the surface expression of the waves. The orbital diameter, d_o, of this motion, often called the total horizontal excursion distance of a water particle, is given by linear Airy wave theory as:

$$d_o = \frac{H}{\sinh 2\pi d/L} = \frac{U_m T}{\pi} \tag{45}$$

where d_o = orbital diameter of a wave.

Threshold of Sediment Movement Under Oscillatory Water Flow

Many researchers in recent years have studied waves and the interaction of waves and the bed, by means of laboratory flumes, physical models and field work. Most of these studies deal with wave behavior; some deal with the interaction of waves with the bed largely based on sand beds. Unfortunately, very few if any studies have been done with fine sediment (silt and clay) under wave action; in the course of this extensive literature, no references to such studies could be found. Fortunately, in recent years many researchers have devoted their time to understanding the behavior of cohesive (fine) sediment under unidirectional flow, mostly with salt water. Some of these results are helpful in better understanding the behavior or fine sediment under waves in fresh water.

In steady open-channel flow over a plane sediment bed, as soon as water starts flowing, hydrodynamic forces are exerted upon the solid particles of the bed. As flow intensities increase, the hydrodynamic forces increase. For a particular stationary bed, a condition is eventually reached at which particles in the bed are unable to resist the hydrodynamic forces and, thus, are first dislodged and eventually start to move.

The initial movement of the bed, frequently called the critical condition or initial motion, can be explained in several ways, according to Graf (1971). First, initial movement can be explained with critical velocity equations by considering the impact of the liquid on the particles. Second, the initial movement can be explained with critical shear stress equations by considering the

frictional drag of the flow on the particles. Third, explanation can be based on lift force criteria by considering the pressure differences due to the velocity gradient. Raudikivi (1976) and Yalin (1977), have extensively described the beginning of sediment motion, both theoretically and experimentally.

A critical velocity equation has been used to give a criterion for incipient motion by many investigators, most notably by Hjulstrom (1935), who developed a graph of critical average flow velocity against particle size.

Many investigators have questioned the validity of critical velocity equations as criteria for incipient motion and have instead proposed use of the bottom shear stress to establish a criterion for incipient motion. Lane (1953) presented his critical tractive force as function of grain diameter. Shields (1936) defined the incipient motion in terms of a dimensionless shear stress as function of Reynold's number. This was shown as equation 12. For incipient conditions, the dimensionless shear stress is based on the critical value of the boundary shear stress (i.e., $\tau_o \rightarrow \tau_{o_c}$).

Chien (1954) has compared many of the tractive force formulas. Figure 13 shows this comparision. As can be seen, agreements between the formulas is not good. As discussed by Graf (1971), such disagreement is due to: (1) the subjective nature of defining critical conditions; (2) the use of mean diameter, which does not correctly present the composition of a mixture; and (3) the effects of small particles hiding behind larger ones or acting as cementing agents.
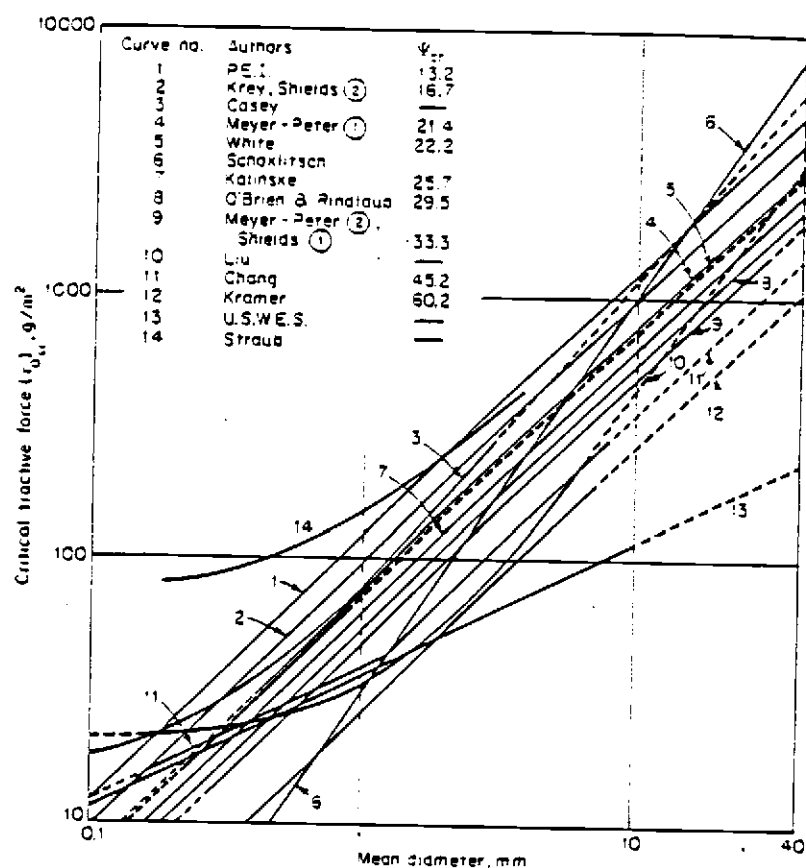
Figure 13. A Comparison of Relations for
Critical Shear Stress as Function
of Grain Diameter (Source: Chien, 1981)

To date no "critical lift" criteria has been presented which could be used as conveniently as, for example, the Shields diagram or Hjulström's diagram.

Suspension Under Oscillatory Flow

The sediment transport phenomena due to wave action that are considered in my research involve shear stress characteristics, velocity distributions, suspended sediment concentrations, initiation of motion, and erosion of sediments.

The threshold problem is the same as that in unidirectional flow, except that the peak velocities on grains will act only for a short time and the boundary layer problem is more involved. In unidirectional flow, the boundary layer is well developed, whereas under wave action in shoaling water, for example, the oscillatory boundary layer may be laminar, transitional or turbulent, depending on the relation between water depth and wave characteristics.

Less attention by other investigators has been given to the threshold of sediment movement under oscillatory water-wave motion than under unidirectional flow. This is in part due to the greater difficulty in obtaining satisfactory measurements with oscillatory flow and in part due to the more complex situation under wave motion where the currents are continuously varying and acceleration are important.

It is worth noting that many investigators, such as Manohar (1955), Eagleson and Dean (1959), Ippen and Eagleson (1955), Raudikivi (1976), have recognized that two types of grain motions will precede the formation of bed irregularites such as ripples.

They may be termed (1) initial movement and (2) general or established movement. This paper covers initial or threshold or incipient motion only.

The pioneering work in the area of sediment motion under wave action is that of Bagnold (1946), who used an oscillating section of bed through still water. The objectives of his experiments were to obtain quantitative data on (1) the size and character of the sand ripples made by waves, (2) the drag to which these ripples give rise, and (3) the minimum oscillating water motion required to initially disturb the sand.

At the University of California at Berkeley, Li (1954), Manohar (1955), Kalkanis (1957, 1964), Abou-Seida (1964) and Das (1971) used an oscillating bed through still water to study the sediment suspension by wave action. One common aim of their researches was to see if it is possible to use the same principles (approaches) of description and prediction of sediment transport with unidirectional flow for the description and prediction with wave flow. Einstein (1972) concluded that it became apparent that such similarity of approaches were quite feasible.

Many investigators such as Vincent (1958) assumed that turbulence has a considerable effect on solid particle transport, particularly near the bed. Einstein (1972) and others in Berkeley found and described that in unidirectional flow the turbulence which is responsible for the suspension can be described by the shear stress at the boundary, but in wave action it was not possible to find a useable expression for the shear stress because the boundary

layer was very thin. They concluded that it is impossible to derive the particle exchange in wave action from the momentum or vorticity exchange of the velocity distribution; instead they attacked the suspension problem in a strictly empirical way. Also they measured the suspended sediment concentration so as to be able to describe the sediment suspension under oscillatory flow.

Many other investigators such as Riedel (1972), Jonnson (1978), Dingler (1979), Nielsen (1979), Dyer (1980), and Vongvisessomjai (1984) tackled the problem of boundary layer flow and sediment suspension under wave flow. Their work will be discussed in detail later in this chapter.

Theoretical Model For Sediment Motion

Forces Acting on a Grain

Raudikivi (1976), Madsen (1976) and others mentioned that the analytical models of sediment motion under wave action are generally the same as for particle entrainment in steady flow. The only difference is that the equilibrium of forces is more complicated in a time-variable movement. It is helpful to briefly describe the forces that are involved in sediment motion under waves. Raudikivi (1976), Nielsen (1979), Eagelson and Dean (1959) and Manohar (1955), give detailed description of these forces.

The following forces are dominant on a grain of sediment in the bed:

1. gravity force due to the mass of the grain, F_G

$$F_G = \pi/6 \cdot D^3 \cdot \rho \cdot s \cdot g \qquad (46)$$

2. buoyant force due to fluid displacement, F_B

$$F_B = \frac{\pi}{6} D^3 \rho g \tag{47}$$

3. drag force due to fluid motion

    a. form drag force, $F_{D,F}$

$$F_{D,F} = C_F \frac{\rho}{2} \frac{\pi}{4} D^2 |U|U \tag{48}$$

    b. surface drag force, $F_{D,S}$

$$F_{D,S} = C_S \rho D^2 |U|U \tag{49}$$

    c. the total (combined) drag force, F_D

$$F_D = C_D \frac{\rho}{2} \frac{\pi}{4} D^2 |U|U \tag{50}$$

4. lift force due to vertical component of pressure differences, F_L

$$F_L = C_L \frac{\rho}{2} \frac{\pi}{4} D^2 U^2 \tag{51}$$

5. volume force due to pressure gradient and hydrodynamic mass of the particles, F_V

    a. volume force due to the pressure gradients of the flow, $F_{V,P}$

$$F_{V,P} = \rho \frac{\pi}{6} D^3 \frac{dU_0}{dt} \tag{52}$$

b. volume force due to the added hydrodynamic mass of

the particle, $F_{V,H}$

$$F_{V,H} = C_M \rho \frac{\pi}{6} D^3 \frac{dU_0}{dt} \tag{53}$$

c. volume force, F_V

$$F_V + F_{V,p} + F_{F,H} \tag{54}$$

6. pressure force due to instantaneous pressure gradients under

the wave, proportional to inertial force of displaced fluid, F_p

$$F_p = C_4 \frac{\pi D^3}{6} \rho \frac{dU_0}{dt} = M \frac{dU_0}{dt} \tag{55}$$

7. inertial force due to displaced fluid, F_I

$$F_I = \rho S_s \frac{\pi D^3}{6} \frac{dVg}{dt} \tag{56}$$

This force is equal and opposite to the resultant of all
external active forces on the particle.

8. Resistance force due to rolling friction, F_{rr}

$$F_{rr} = \varepsilon [(F_G - F_B) \cos\alpha - F_D \sin\beta - F_L] \frac{Vg}{Vs} \tag{57}$$

this force is proportional to the normal components of

gravity buoyance and fluid drag forces acting on the particle.

9. Reaction forces exist at each point of contact with the bed. The angle of these forces with respect to an axis normal to the bed is given by:

$$\tan\phi = \frac{\sqrt{3}}{2\sqrt{[(D/D_1)^2 + 2D/D_1 - 1/3]}}$$ (58)

where s = specific gravity;

C_F = form drag coefficient;

C_S = surface drag coefficient;

C_D = drag coefficient;

C_L = lift coefficient;

$U_0 = U_0 = \frac{wh}{2} \sin wt$, potential flow velocity of wave motion;

ω = angular velocity, $2\pi/T$;

C_M = volume force coefficient;

C_4 = pressure coefficient;

M = dummy variable for other variables as shown in the equation;

S_S = inertial force coefficient;

V_g = grain velocity;

ϕ = angle of reaction forces with respect to an axis normal to the bed;

D_1 = diameter of particle in plane bed;

ϵ = coefficient of rolling friction;

α = the beach slope; and

β = angle between resultant of viscous resistance forces and beach slope in radians.

and all other terms are as previously defined.

Nielsen (1979) assumes that the influence of lift forces on the initiation of motion is the same under waves as the steady flow and that the only difference the two types of flows is due to action of the volume forces which affect wave flow. Nielsen's work also shows that the effect of volume forces on the initiation of sediment motion under waves can be neglected, both for laminar and turbulent flow, except for experiments with very heavy materials supported on oscillating plates.

Eagleson and Dean (1959) and Raudikivi (1976) give the condition for incipient motion by taking moments about the points of contact of the bed particles. Also, they summed all forces parallel to the bottom to express the established sediment motion throughout the entire wave cycle.

Dimensional Analysis

Many investigators have used dimensional analysis to express the properties of interest in sediment suspension under wave action. Riedel (1972) expressed the shear stress at the bed using the dimensional analysis approach. Bhattrachya (1971) used dimensional analysis to find the diffusion coefficient in his study of sediment suspension due to wave action. Mogridge and Kamphius (1972) used

dimensional anlysls to describe the threshold of sediment movement under waves. Raudklvl (1976) used dimensional analysis to denote the velocity under the wave. Dingler (1979) used dimensional analysis to define the Incipient motion criteria.

Table 3 shows the parameters used by several Investigators for sediment transport studies under wave action. Many researchers used dimensional analysis to derive the Incipient motion condition. Any property, A, of the flow produced due to wave action, assuming no mass transport current, can be expressed as

$$A = f[\rho, \mu, \rho_s, K_s, D, H, T, d, g] \tag{59}$$

and all other forms are as already defined.

Here, time and the cartesian coordinate system are not Included. Dingler (1979) analyzed the flow property In the form of A, the Immersed weight of sediment transported rate per half wave cycle and obtained a non-dimensional functional relation which can be given as

$$A\rho^{1/2}/(\gamma_s D)^{3/2} = \phi(\rho\gamma_s' D^3/\mu^2, \gamma_s' T^2/\rho D, do/D, \frac{\rho_s}{\rho}) \tag{60}$$

where $\gamma_s' = (\rho_s - \rho)g = \gamma_s - \gamma$

and is the submerged specific weight of the sediment. He then mentioned that at the threshold of grain motion, the dependent variable Is equal to zero because grains are on the verge of moving. The non-dimensional variable ρ_s/ρ, which Is associated with the inertial force of the grains, Is not applicable here because the

Table 3. Parameters Used for Dimensional Analysis of
Sediment Transport Due to Waves

Investigator and Year	Parameters Used for Dimensional Analysis of Sediment Transport Due to Wave
Yalin & Russell (1966)	ρ, d, k, U_m, T, g
Rance & Warren (1968)	ρ, μ, ρ_s, D, H, T, g
Bhattarchya (1971)	K_s, y, H, T, g
Riedel (1972)	ρ, μ, K_s, D, H, T, x, z, t
Mogridge & Kamphius (1972)	ρ, μ, ρ_s, D, H, U_m, g
Dingler (1979)	ρ, μ, ρ_s, D, H, T, γ_s

Inertial force is zero at incipient motion. The non-dimensional relation thus becomes

$$0 = \phi(\rho\gamma_s'D^3/\mu^2, \gamma_s' \, T^2/\rho D, \, do/D) \tag{61}$$

or, rearranging, can be expressed as

$$\gamma_s' \, T^2/\rho D = \phi_1(\rho\gamma_s' \, D^3/\mu^2, \, do/D) \tag{62}$$

Taylor (1946) as a supplement to Bagnold's experimental observations, developed a non-dimensional relation for the threshold of grain motion for the case when grain diameter is smaller than the boundary layer thickness. This is shown in the following section. He also gives

$$T = d_0^{2/3} f \, (D) \tag{63}$$

This applies for the case of material of constant density in a fluid of constant density and viscosity. Taylor's theoretical analysis for incipient motion agreed well with empirical formula of Bagnold.

Empirical Approach

Bagnold (1946) developed an empirical formula for the critical water motion to first disturb a grain, based on the assumption that the bottom water oscillation is merely a simple harmonic function. The formula is based on the critical angular velocity resulting from oscillation of the fluid and can be written as:

$$\omega = 21.5 \; (\frac{do}{z})^{-0.75} (s-1)^{0.5} \; D^{0.325} \qquad (64)$$

Bagnold commented that an outstanding feature of the experiment was the absence of any sign of turbulence in the water, even at distances above the surface comparable with one grain diameter. Bagnold also noted several possible sources of error common to experiments of this type, including difficulties of consistently estimating "by eye" the point of incipient motion and the impossibility of using completely uniform material. Taylor, commenting on Bagnold's work, presented a theoretical derivation and arrived at a similar equation, although with slightly different exponents:

$$\omega = constant \; (\frac{do}{z})^{-2/3} [g(s-1)]^{5/9}(s-1)^{-1/4}D^{1/3} \qquad (65)$$

Silvester and Mogridge (1970) summarized the available empirical formulas derived for incipient motion of sand particles on a flat bed. They put them into a set of similar dimensionless forms. Table 4 shows these equations. Significant variations are evident in these

Table 4. Similar Dimensionless Forms of Empirical Equations for Incipient Motion of Sand Particles Under Oscillatory Flow (Source: Silvester and Mogridge, 1970)

Investigators	Flow Conditions	Dimensionless Equation
Bagnold[16]	laminar	$\dfrac{U_{max}}{(s-1)^{2/3}g^{2/3}D^{1/3}D^{0.1}T^{1/3}} = 3.18$
Bonnefille and Pernecker[17]	laminar	$\dfrac{U_{max}\nu^{1/6}}{(s-1)^{5/6}g^{5/6}D^{1/2}T^{1/2}} = 0.072$
Bonnefille and Pernecker[17]	turbulent	$\dfrac{U_{max}\nu^{19/30}}{(s-1)^{16/15}g^{16/15}D^{6/5}T^{1/2}} = 0.01$
Bonnefille and Pernecker[17]	modified	$\dfrac{U_{max}\nu^{5/18}}{(s-1)^{8/9}g^{8/9}D^{2/3}T^{1/2}} = 0.069$
Carstens et al[18][19][20]	turbulent	$\dfrac{U_{max}}{(s-1)^{1/2}g^{1/2}D^{1/2}} = 3.5$
Eagleson and Dean[21]	laminar	$\dfrac{U_{max}\nu^{1/2}}{(s-1)\,g\,D\,T^{1/2}} = 0.131$
Goddet[22]	turbulent	$\dfrac{U_{max}}{(s-1)^{2/3}g^{2/3}\nu^{1/24}D^{1/4}T^{3/8}} = 3.0$
Ishihara Sawaragi[23]	turbulent	$\dfrac{U_{max}}{g^{3/4}(s-1)^{3/4}D^{1/4}} = 0.093$
Manohar[24]	laminar	$\dfrac{U_{max}\nu^{1/3}}{(s-1)^{2/3}g^{2/3}D^{2/3}} = 0.159$
Manohar[24]	turbulent	$\dfrac{U_{max}}{(s-1)^{0.4}g^{0.4}D^{0.2}\nu^{0.2}} = 7.45$
Silvester and Mogridge[25]	flat bed	$\dfrac{U_{max}\nu^{1/18}}{(s-1)^{7/9}g^{7/9}D^{1/3}T^{1/2}} = 0.034$
Rance and Warren(26)	sand	$\dfrac{U_{max}}{(s-1)^{3/5}g^{3/5}D^{2/5}T^{1/5}} = 0.69$

formulas when put into a comparable form, in some cases amounting to several orders of magnitude..

Komar and Miller (1973) found that as the velocity of the to-and-fro water motion near the bottom under oscillatory waves is increased, there comes a stage when the water exerts a stress on the particles sufficient to cause them to move. They found that for grain diameters less than about 0.5 mm (medium sands and finer) the threshold is reached while the flow in the boundary layer is still laminar. This threshold is best related by the equation

$$\frac{\rho U m^2}{(\rho_s - \rho)gD} = 0.30 \ (d_0/D)^{\frac{1}{2}} \qquad\qquad (66)$$

where U_m is the near-bottom maximum orbital velocity of the wave motion.

For grains larger than 0.5 mm, the threshold occurs after the boundary layer has become turbulent. It is best predicted with an empirical curve relating d_0/D to $(\rho U_m)/[(\rho_s - \rho)gT)]$.

The above equations can be used for silts but not when any cohesive effects are involved.

Vincent (1958) provided a literature review of incipient motion of sediment due to oscillatory flow. This included the criteria used by different investigators for describing onset of motion. It also included the resultant initial velocities obtained, as shown in Table 5. The comparison shows some variation among the initial movement velocities. Vincent also showed the onset of grain movement in a graphical format, with grain size plotted versus wave period, as

Table 5. Resultant Incipient Velocities Summarized by
Vincent from Investigations by Others

Type of Material	Grain Diameter Microns	Sediment Density gram/cm^3	Resultant Incipient Velocity cm/sec
Sand	63	2.65	28.5
Sand	46	2.65	20.5
Sand	24	2.65	16.5
Pumice	160	1.38	11.0
Pumice	120	1.38	8.5
Pollopas (granulated plastic)	110	1.46	10.5
Pollopas	39	1.46	7.0

shown in Figure 14.

Davies and Wilkinson (1978), in their incipient motion study, used wave analysis, to draw two main conclusions: (1) for the sand ripples, there is an apparent doubling in the threshold value of the potential velocity for sediment motion on a flat bed, compared with motion on the crest of the sand ripple; and (2) there is not just a single value of potential velocity associated with the initiation of grain motion; rather, there is a wide range (transition) of values for which some but not all of the measured waves moved sediment particles.

Dingler (1979) determined the threshold relation for sand-size material under progressive gravity waves and found that the published results from oscillating bed experiments are applicable in progressive wave systems. For a fixed wave period and variable wave height he concluded that his experiment with progressive gravity wave and Bagnold's oscillating-bed experiments gave similar results. He also found that the threshold of quartz sand in a wave channel can be defined in terms of the wave period as:

$$T = 0.17 \ (d_0{}^2/D)^{1/3} \tag{67}$$

Chan et al. (1972), in their study of beds of dense particles in a horizontally oscillating fluid, observed that the threshold at which general surface motion of the particles occurs could be correlated as follows:

Sand n°1

Sand n°2

Sand n°3

Pumice n°1

Pollopas n°1
(Granulated plastic)

Pumice n°2

Pollopas n°2

ORBITAL DIAMETER, cm

20
18
16
14
12
10
9
8
7
6
5
4
3
2

Value of h

h cm = 60, circle

h cm = 30, full circle

h cm = 20, cross

h cm = 10, asterisk

Sable n°1 d $_{50}$ = 0.063

Sable n°2 d $_{50}$ = 0.046

Sable n°3 d $_{50}$ = 0.024

Ponce n°1 d $_{50}$ = 0.16 — Po

Ponce n°2 d $_{50}$ = 0.12

Pollopas 1 d $_{50}$ = 0.11 — Pa$_1$

Pollopas 2 d $_{50}$ = 0.039 — Pa$_2$

0,5   0,7   1   1,4   2   3   4   5   6   7   8   9

WAVE PERIOD, SECOND

Figure 14. Onset of Grain Movement as Summarized
by Vincent (Source: Vincent, 1958)

$$\frac{H_\omega^{1.5}}{2(\gamma g)^{0.75} d^{0.25}} = 0.37 \tag{68}$$

They also found that the transition from a dune-forming bed to a bed
in which the surface particles were in motion was found to occur when

$$\frac{H_\omega^{1.5}}{(\gamma g)^{0.5} d^{0.1} \nu^{0.2}} = 6.6 \tag{69}$$

Eagleson and Dean (1959) derived an expression for incipient
motion of sand in sea water. This can be given as:

$$D \sin (\alpha \pm 0.92) = 8.0 \times 10^{-6} \frac{f'}{\omega} \beta' \tag{70}$$

where f' = coefficient associated with the kinematic wave
properties; and

β' = measure of viscous effects under a wave.

They also presented a graphical form of the relation for incipient
motion.

Rance and Warren (1968) conducted experiments to determine the
threshold of movement of beach shingle stones under oscillatory wave
conditions. The results of their experiments make it possible to
determine the necessary wave conditions to induce motion in shingle
of a given size. Also, they pointed out that the rate at which work
is performed on a particle may be a more significant consideration
for incipient motion than is the maximum instantaneous acceleration
during an oscillatory cycle. This stems from consideration that,
regardless of the maximum acceleration, if sufficient work is done on

a particle in each cycle, the particle will simply rock up and fall
back into its original position.

The Shore Protection Manual of the U.S. Army Coastal Engineering
Research Center (1977) addresses incipient motion as follows:

> "Research has come to the agreement that the initiation
> of motion on a level bed of fine or medium sand requires
> less shear (lower velocities) than the initiation of motion
> on a level bed of silt or gravel. It is generally agreed
> that the critical entraining velocity for sands are less
> than one foot per second."

The manual uses the linear wave theory velocity components into a
dimensionless expression for velocity at the bed surface to determine
the point of incipient motion:

$$\frac{U_m T}{H} = \frac{\pi}{\sinh 2\pi d/L} \tag{71}$$

Several curves are presentd for use in determining U_m for given wave
characteristics. Figure 15 shows the minimum velocity for initiation
of motion in sands of different diameters. From this figure, it
appears that velocities on the order of 0.4 to 1.0 feet per second
may result in incipient motion. Inman (1957) studied the incipient
motion of sediment particles under waves and concluded that ripples
are always present whenever U_m is greater than
0.33 ft/s.

Dyer (1980) presents the results of an incipient motion study
conducted on the Coast of England. Underwater television cameras
were used to monitor the movement of sediment (medium sand) over a
tidal cycle. His findings are discussed later in this chapter.
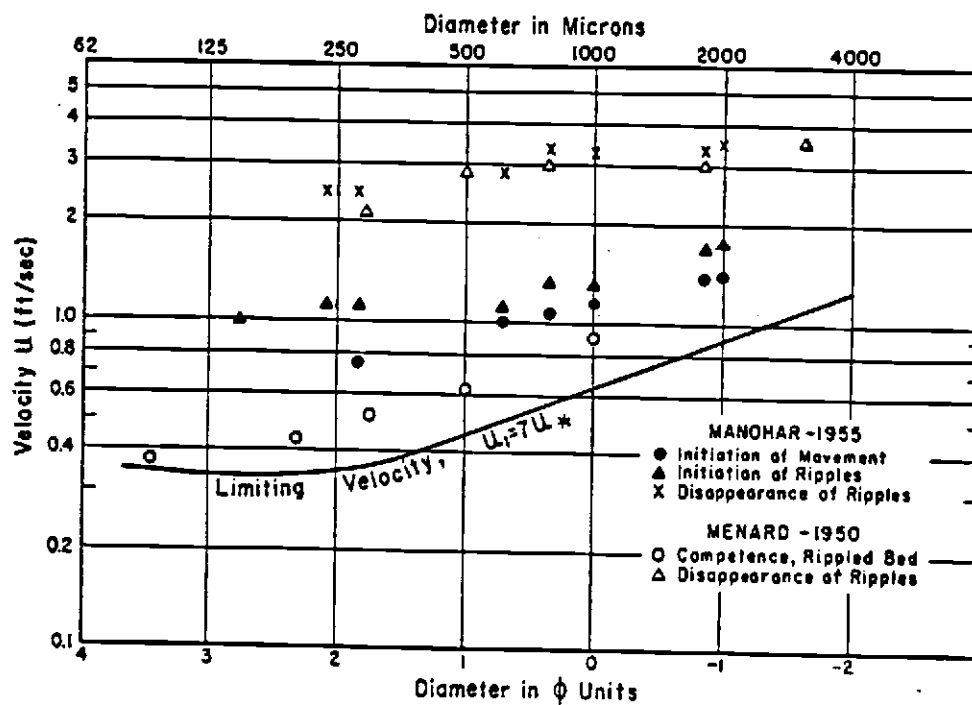
Figure 15. Incipient Motion Velocity Versus Particle Diameter
(Source: Inman, 1957)

Application of Shields Diagram in Incipient Motion Study

Shields (1936) presented an empirical relation for the threshold of grain motion due to unidirectional flow, as already discussed. Bagnold (1963) presented a simplified version of the Shields diagram for the threshold of quartz and other material of similar density. He mentioned that there is no theoretical or experimental justification for assuming that the effective threshold shear stress bears a relation to the orbital velocity near the bed for the case of oscillatory water motion, similar to that which the threshold shear stress bears to the velocity gradient in the steady flow case. He suggests that it is better to define the threshold of bed movement in terms of critical angular velocity in the dimensionless form

$$\frac{\omega}{(\rho_s-\rho)gD[(\rho_s-\rho)gD/\rho]^{\frac{1}{2}}} \tag{72}$$

than in terms of the critical bed shear stress in the dimensionless form $\theta = \dfrac{\tau_c}{(\rho_s-\rho)gD}$

Komar and Miller (1973) argue that the application of Shields function to define the theshold of sediment motion under oscillatory water waves can lead to a considerable error due to fundamental differences between the entrainment forces associated with an unsteady oscillatory flow and those associated with a steady undirectional flow. In support of their argument, they use that part of Bagnold's 1946 experimental data giving the initiation of sediment motion under oscillatory flows. These data exhibit considerable scatter when plotted in a diagram of sediment grain diameter versus a

modlied Shlelds parameter In the form:

$$\theta = \frac{\rho Um^2}{(\rho_s-\rho)gD} \qquad (73)$$

Madsen and Grant (1975) demonstrate that the scatter exhibited by Bagnold's data In the Komar and Miller diagram Is caused primarily because they used the maximum velocity on the shield criterion Instead of maximum shear stress. Later, Madsen and Grant (1975) and Komar and Miller (1975) mentioned that the data of Bagnold are In good agreement with the Shlelds function when plotted In a Shlelds diagram using the Shlelds parameter In the form

$$\frac{\tau_{om}}{(\rho_s-\rho)gD}$$

based on the maximum bottom shear stress under oscillatory flow, τ_{o_m}.

Figure 16, from Miller et al (1977), presents a comparison of Shlelds criterion under unidirectional flow and oscillatory flow.

Madsen and Grant (1975) applied the data of Manohar (1955) to the Shlelds diagram and found that It plotted somewhat above but not too far from the Shlelds function. They concluded that the Shlelds function, with all Its shortcomings, may serve as a relatively reliable and quite general criterion for the threshold of sediment movement under water waves. Nielsen (1979) also stated that Shlelds criterion for Inltlatlon of motion can be used.

Hallermeler (1980) presented a new calculation procedure for Inltlatlon of sand motion on a level bed In oscillatory flow, using a simplified Shlelds criterion adopted from steady flow.
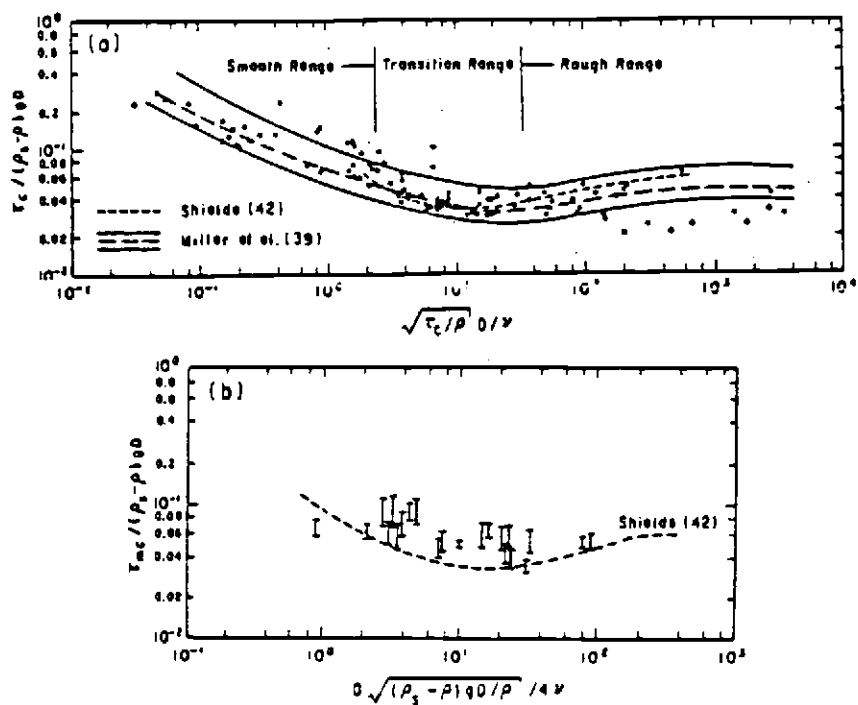
Figure 16. Comparison of Shields Criterion for Incipient Motion with Unidirectional Flow and Oscillatory Flow for Tests with Sand Grains (Source: Miller et al., 1977)

Criteria for the Onset of Movement

Due to the subjective nature of the point of incipient motion, it is necessary to summarize the criteria of incipient of motion used by different investigators. This is essential when comparing experimental results obtained by several different methods. Many investigators just visually observed the critical condition for threshold of sediment particles; some used photographic techniques, including recent use of high speed cine photography. Dye and other chemicals have been used to aid in visual observation. Bagnold (1946) and Manohar (1955) observed the oscillation characteristics of the plate carrying the test material to determine when the grains first started to move.

Eagleson et al. (1958) used the term "incipient sediment motion" to denote the condition when a given particle size on a given slope is on the point of movement due to the maximum instantaneous local velocity. It was assumed that the incipient motion occurs for given flow characteristics at that wave phase angle at which the hydrodynamic portion of moment is a maximum.

Eagleson and Dean (1959) experimentally defined incipient motion by gradually varing the local wave characteristics until stationary sediment particles tipped out of their individual bed depressions and oscillated within the troughs of the existing bed forms (i.e., in the trough of adjacent ripples). They correlated measurement of incipient motion with Reynold's number by means of a derived resistance coefficient.

Ippen and Eagleson (1955) in their study of sediment sorting by shoaling waves, presented a theoretical analysis which yields a

general functional equation for net particle velocity. They used
zero net motion as an indication of threshold condition. They
expressed the threshold motion in terms of the wave and particle
characteristics.

Madson and Grant (1975) defined the initiation of motion as
occuring when the bottom shear stress reaches a critical shear stress
value.

Lofquist (1978) stated that incipient motion occurs when as much
as 10 to 20 grain/cm^2 are in motion.

Dyer (1980) described the threshold of sediment movement based on
in-situ observation of the sea floor during a tidal cycle using a
television camera. Visual estimates of sediment movement were made
for 10-second intervals; these were then summed over one-minute
intervals, concurrently with velocity measurements, to obtain a
percentage frequency of sediment movement. The fluid velocity 100 cm
from the bed and the shear velocity at the bed, both varying with
time, were correlated with percentage of sediment moving. Dyer gave
the following sequence of events that occurred as flow velocity
increased above the threshold of motion, based on analysis of the
video-taped television information.
1. In the lee of the ripples, organic debris and shell fragments
begin intermittent, slow, random movements. This phase may well
indicate the onset of flow separation in the ripple lee.
2. Occasionally, small numbers of sand grains are pushed off the
ripple crests and cascade down the lee slope. These cascades often
occur at preferred locations. No movement of replacement grains up

the facing slope is observed, the result being a change in the location of the crest.

3. Bursts of movement carry a stream of sand grains over several ripple wave lengths as a fairly thin carpet 1-2 cm thick. These patches of movement are on the order of 10 cm wide and the duration of the bursts is about one second. The movements are intermittent in space and time, though they often seem to originate at bifurcation points on the ripple crest.

4. Bursts of movement become longer in duration, more frequent and wider.

5. Swirls occur, during which sand grains are picked up in a turbulent whirling fashion at least to the height of the camera (30 cm). Their duration is several seconds.

6. Suspension carpet. The whole bed becomes obscured by a zone of grains moving in suspension. The zone is about 10 cm thick. The upper surface of the carpet is fairly distinct, although it has a gradual rather than abrupt change in concentration. The upper surface has a billowing form not unlike clouds seen from above.

Kennedy and Falcon (1965) define the incipient motion of a flat bed as occurring when 10 percent of the sediment particles were in motion. Carstens et al (1969) also defined the initiation of motion as occurring when 10 percent of the grains are in motion.

Rance and Warren (1968) were not able to predict the threshold of movement of sediment in their oscillatory water tunnel. Instead they used a method analogous to the zero-transport approach to define incipient motion. They observed three distinct phases in bed

movement:

1. Initially, a broad band on flow conditions existed for which particles rocked to and fro without actually moving in position;

2. then, one or two particles would be dislodged and move a few grains downstream; and

3. finally, with a small increase in velocity and acceleration, many particles move. This observed condition was found to equate to the upper limit of the threshold for motion.

Kennedy and Falcon also noted that it is better, for visual determination, to fix the wave height and gradually decrease the wave period until the threshold was reached, rather than to alter the wave height.

Manohar (1955) defined initial movement at the situation "when only a few grains move". His results are from experience where the sand was oscillated. He also mentioned that initial motion took place in a laminar boundary layer and that general motion took place with turbulent boundary layer conditions.

Dingler (1979) defined the incipient motion by assuming a constant wave period of 2 to 10 seconds and measuring the wave height that caused incipient motion. His results correlate well with the data from the oscillating bed experiments of Bagnold (1946), suggesting that the oscillating bed technique satisfactorily reproduces wave bottom motions, at least for this set of conditions.

Sternberg (1971) investigated the incipient motion through observation, time-lapse photography and velocity measurement in the sea bed. From the data he estimated the mean bottom velocity at

100 cm above the bed, shear velocity, and Shields coefficient
associated with sediment movement. For comparison with velocities
causing incipient motion, he observed that general sediment motion
occurred for a mean velocity of 38.5 cm/sec measured 100 cm above the
bed and with grains 0.40 mm in diameter.

Velocity Determination: Supporting Evidence for Use of Linear Wave Theory Approximation

The velocity near the bed under oscillatory flow is a function of
the height and period of the wave and of the water depth. It is well
known that potential flow theory can be applied fairly well to the
entire surface wave motion except to a very thin layer adjacent to
the solid boundaries. There, viscous effects can not be neglected
compared with the inertia forces, no matter how small the viscosity
of the fluid.

This important layer near the boundary can be treated according to
boundary layer theory. For low Reynolds numbers, the boundary layer
will be laminar and the velocity distribution will be determined from
corresponding equations. For larger Reynolds numbers, a turbulent
boundary layer will occur together with a laminar sublayer
immediately adjacent to the bed. The velocity distribution is more
complex with a turbulent boundary layer.

It is common to use linear wave theory to predict the velocity
distribution in design waves even though it is known that actual
waves are quite irregular and their shape and kinematics may not
conform to the periodic theory. Bagnold (1946) and Li (1954) stated
that for waves in deep water and also for those shallow water waves

In which the wave height is small compared with the depth, the horizontal oscillations of the water near the bottom closely approximate simple harmonic motion. Li (1954) also stated that for this type of motion the stability of the laminar boundary layer and transition boundary layer from laminar to smooth turbulent flow are important in many aspects. One is the determination of sediment transport along the bottom, for which the existence of turbulence is a governing factor.

Collins (1963) indicated that he and others studying inception of motion of sediment and formation of ripples have noted that the turbulent boundary layer, after its formation, seems to remain as a local band near the bed, hardly spreading into the main body of the wave motion. He concluded that this observed phenomenon substantiates that the potential wave theory works well in practice for describing wave motion except close to the boundary layer.

Miller (1978) stated that for simple waves, such as generated in laboratory experiments, if the reflection coefficient is small, the linear or first-order theory of progressive surface waves developed by Airy in 1845 provides a satisfactory description of the wave motion with a minimum of mathematical complexity and a sufficient degree of mathematical precision.

Dingler (1979) calculated the near-bottom orbital diameter using the linear wave theory and stated that this can be measured by visually following suspended fine material during a wave period.

Raudkivi (1976) stated that the Airy theory yields results for velocity near the bed which are in good agreement with observation.

He also mentioned that these results neglect viscous effects and are, therefore, applicable only outside the bottom boundary layer. He further reported that it has been found by experiment that these calculated velocities in the boundary vicinity are, for engineering purposes, in reasonable agreement with observation. The major shortcoming of the theory is that it does not predict mass transport by waves. The Stokes wave theory predicts a mean mass transport velocity over a complete cycle.

Many investigators measured the velocity under the wave to obtain the velocity distribution. Unfortunately, there are many problems with measuring velocity under waves, partly because of usual low dynamic response to high-frequency fluctuations and also because much equipment is not very sensitive to low-speed steady flow. Goda (1964) measured the velocity under waves with a miniature propeller current meter and proposed a velocity equation under waves which overcomes the above difficulties. Goda's equation modifies the horizontal velocity given by Airy theory in order to correctly express the large velocity near the still water level. According to Dean (1974), the Goda equation gives as good a fit with measured velocities as does the Dean's stream function theory.

Kobune (1978) measured the velocity under waves in a wave flume with a propeller current meter and hot-film anemometer and obtained favorable results when compared with the predicted velocity using linear wave theory. He concluded that the Airy theory provides an excellent prediction of the mean velocity near the bed beneath the wave crest. He also mentioned that for periodic tests, where

frequent recalibration is not a problem, the maximum horizontal and vertical velocity can be measured accurately with a hot-film anemometer. The correlation between the maximum velocity measured with the hot-film anemometer and that measured with the propeller current meter was quite good.

Almost all of the investigators utilized the linear wave theory approach in the study of sediment suspension under oscillatory flow. The linear wave theory provides an accurate measure of velocity near the bed under oscillatory flow.

Mass Transport Velocity

In a water wave, the particles of fluid possess apart from their orbital motion, a steady second-order drift velocity. This drift velocity is usually called the mass transport velocity (Longuet-Higgens, 1953). Figure 17 shows the net drift as well as the vertical variation of the horizontal mass transport velocity due to a wave.

Silvester (1970) stated that water particles in the oscillatory flow usually do not follow an enclosed orbit predicted by linear wave theory; instead they advance a small amount during each cycle. This net advance, divided by the wave period, gives a calculated velocity similar to the drift velocity of Longuet-Higgens. This velocity can be defined theoretically for laminar boundary layer conditions and empirically for turbulent boundary layer conditions. Silvester also stated that velocity at the bed is in the direction of wave advance. He presented an equation for the theoretical mass transport velocity for laminar boundary layer and smooth bed. Mogridge (1970) gives
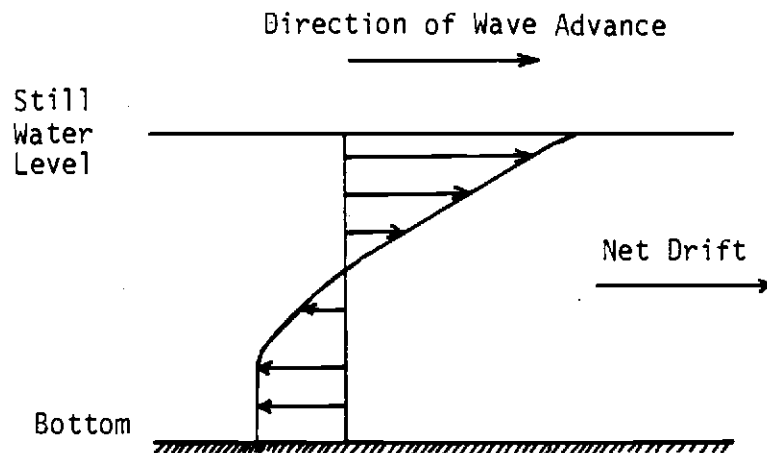
Figure 17. A Typical Mass Transport Velocity
            Distribution in a Wave Without Friction

horizontal and vertical components of velocity for the progressive

wave of finite amplitude which was first studied by Stokes in 1880.

The mass transport velocity due to Stokes is given by:

$$\bar{U} = \tfrac{1}{2} \frac{\pi^2}{T} \frac{H^2}{L} \frac{\cosh \frac{4\pi(y+d)}{L}}{\sinh^2 \frac{2\pi d}{L}} \tag{74}$$

where $\bar{U}$ = mass transport velocity; and other variables are as

described before. However, for a closed wave channel, the mass

transport velocity is given by:

$$\bar{U} = \tfrac{1}{2} \frac{\pi^2}{T} \frac{H^2}{L} \frac{\cosh \frac{4\pi(y+d)}{L} - (\frac{L}{4\pi d})\sinh \frac{2\pi d}{L}}{\sinh^2 \frac{2\pi d}{L}} \tag{75}$$

Longuet-Higgins (1953) gives the maximum mass transport velocity in

the boundary layer as:

$$\bar{U}_{max} = 1.376 \frac{\pi^2}{T} \frac{H^2}{L} \frac{1}{\sinh^2 \frac{2\pi d}{L}} \tag{76}$$

The above equation can be written as

$$\bar{U}_{max} = \frac{1.376T}{L} U_m^2 \tag{77}$$

where U_{max} = maximum value of the mass transport velocity

Mogridge (1970) stated that the equation of Longuet-Higgins has

been proven usable over the range of d/L up to 0.5 for calculations

in respect to sediment movement at the bed. Vincent (1958) also

measured the entrainment current in the immediate vicinity of the bed

and confirmed the Longuet-Higgins expression for mass transport velocity.

Collins (1963) gives the laminar boundary layer thickness and mass transport velocity under periodic gravity waves. From solution of Navier-Stokes equation, he derived a velocity equation which could be reduced to the form of Prandtl's boundary layer equation. Raudikivi (1976) used a mass transport velocity which was derived from the Stokes wave theory.

Shear Stress Determination

Water waves interact with the bottom of a sea or lake bed by drag and other processes. Surface waves provide an oscillatory flow above the bed which produces and maintains bed forms by local movement of sediment particles. The sediment particles are influenced by local tangential stresses caused by the flow. The local flow pattern is largely shaped by the pressure field around the bed form. This pressure field produces a distribution of normal stresses over the surface of the bed. The average bottom stress can be defined by dividing the horizontal component of tangential and normal forces acting on a large area of irregular shaped bed by the corresponding area. Manohar (1955) and Taylor (1946) assumed that initial motion of sediment in a laminar boundary layer is produced by the shear stress acting on the particle. Nece and Smith (1970) stated that in sediment transport studies it is the local boundary shear stress (skin friction) which must be determined and not the total boundary shear stress on the bed (skin friction plus the form drag of the non-uniform boundary).

Effects of Pressure Forces on Initiation of Motion

Sediment motion arises primarily as a result of the near-bed velocity field. However, the possible role of pressure gradients at the bed surface must also be considered. Davies and Wilkinson (1978) found that the pressure-induced forces on the surface grains are of little or no importance in the transport of coarse sands by waves. However, outside the breaker zone it appears that sediment movement by waves can be explained in terms of the near-bed velocity field alone.

Dingler (1979) concluded that due to the major difference between the flow fields caused by progressive waves and the flow field resulting from an oscillating bed, pressure gradients exist in the former case and are absent in the latter. He also concluded that similarities between the two methods suggest that the pressure field does not play an important role in the initiation of grain motion under either condition.

Sleath (1975) showed that when the roughness size is small compared with the thickness of the viscous boundary layer, the lift force is negligible compared with the drag except at very high value of $\frac{U_0}{(\omega v)^{\frac{1}{2}}}$. He also mentioned that for small roughness size, the shear stress is much larger than the pressure-induced stress on the bed. For particles whose size is large compared with the thickness of the viscous boundary layer, neither of above conclusions is true. Monahar (1955) also stated that it is safe to account for drag only, but mentioned that lift forces can not always be completely ignored.

Theoretical Derivation of Shear Stress

Flow resistance in steady unidirectional or oscillatory flow is due to the granular roughness (skin roughness), irregularities of the bed surface (form roughness), and foreign matter diffused into the body of the flow (from suspended matter). In general, the bed shear stress is defined as:

$$\tau_o = \tau'_o + \tau''_o + \tau'''_o \tag{78}$$

where τ'_o = real shear stress acting on the plane bed surface;

τ''_o = shear stress due to irregularities of the bed surface; and

τ'''_o = shear stress due to foreign matter.

The sum of shear stresses due to irregularities and foreign matter is called the apparent stress. In general, the bed friction factor can be defined similarly:

$$f = f' + f'' + f''' \tag{79}$$

where f' = friction factor acting on the plane bed surface (skin friction);

f'' = friction factor due to irregularities of the bed surface (form friction); and

f''' = friction factor due to foreign matter

For the case of a plane bed during the initiation of sediment transport, the apparent stresses are zero or neglibile; therefore, the total shear stress is equal to τ'_o, i.e., only skin friction is

Involved. For the case of an irregular bed, during and after the initiation of sediment transport but before stabilization of bed froms, the shear stress and friction factor are due to skin friction and form friction.

In oscillatory flow the same friction principle as for unidirectional flow can be applied. That means that in the case of a plane bed, the bed shear stress is equal to skin friction. For the case of an irregular bed, the shear stress is the sum of friction and form drag.

The shear stress at the bed in which the viscosity plays a predominant role has been found to be proportional to the rate of relative strain, that is, to the velocity gradient, du/dy, with a constant of proportionally, μ, defined as the coefficient of viscosity or dynamic viscosity. Thus, $\tau_o = \mu \dfrac{du}{dy}$.

The linearized equation of motion in the boundary layer for a fixed bed neglecting the non-linear inertia terms, pressure gradients and viscous effects in the x-direction can be given as

$$\frac{\partial U}{\partial t} = \nu \frac{\partial^2 U}{\partial z^2} \tag{80}$$

For the laminar case, the solution to the above equation yields (Lamb, 1932)

$$U = U_m [\sin \omega t - \exp(-\frac{\pi}{2} \frac{z}{\delta}) \sin (\omega t - \frac{\pi}{2} \frac{z}{\delta})] \tag{81}$$

with

$$\delta = \frac{\sqrt{\pi}}{4} \cdot \sqrt{\nu t} \tag{82}$$

substituting into $\tau_0 = \mu \frac{du}{dy}$ yields the shear stress distributions as

$$\frac{\tau_0}{\rho} = \frac{\pi}{\sqrt{2}} \frac{\nu U_m}{\delta} \exp(-\frac{\pi}{2} \frac{z}{\delta}) \cos (\omega t - \frac{\pi}{2} \frac{z}{\delta} - \frac{\pi}{4}) \qquad (83)$$

and at the bottom

$$\frac{\tau_{om}}{\rho} = \frac{\pi}{\sqrt{2}} \frac{\nu U_m}{\delta} \qquad (84)$$

substituting $U_m = \frac{\pi H}{T \sinh \frac{2\pi d}{L}}$ and $\delta = \frac{\sqrt{\pi}}{4} \sqrt{\nu t}$ into the above equation yields

$$\tau_{cm} = 1.41 \mu [\frac{\pi}{T\nu}]^{\frac{1}{2}} \frac{\pi H}{T} \frac{1}{\sinh^2 \frac{2\pi d}{L}} \qquad (85)$$

Assumptions made in deriving the shear stress equations are: (1) waves in generating area can be described as sinusoidal waves and (2) laminar shear conditions.

For boundary layer flow, it is common to relate the bottom shear stress to the near bottom velocity. This can be done through the following general relation:

$$\tau_0 = c\rho U|U| = c\rho U^2 \qquad (86)$$

Where C is friction factor or drag coefficient of the unidirectional flow.

Bagnold (1946) evaluated the maximum bed shear stress from the following equation:

$$\tau_m = \rho \sqrt{\omega \nu U_m}$$ (87)

where τ_m = maximum bed shear stress under oscillatory flow.

For laminar flow, the friction factor, f_ω can be obtained from

$$f_\omega = \frac{2\sqrt{\omega \nu}}{U_m} = \frac{2}{\sqrt{RE}}$$ (88)

where RE = wave Reynolds number = $\frac{U_m(U_m/\omega)}{\nu} = \frac{U_m a_\delta}{\nu} = \frac{U_m d_0}{2\nu}$

$\frac{U_m}{\omega} = \alpha_\delta = \frac{1}{2}d_0$; and

α_δ = half of orbital diameter.

Thus, for the laminar case, the maximum bed shear stress of Bagnold's equation can be written as:

$$\tau_m = \frac{1}{2} \rho f \omega U_m^2$$ (89)

Yalin and Russell (1966) presented a theoretical analysis of the shear stress acting on a horizontal rough bed due to wave motion of a real fluid. They express bed shear stress in terms of wave charactristics in a form that could be used for any instant during a wave period. They find that bed shear stress can be given as:

$$\tau_0 = \alpha \rho U^2 + \beta \gamma sd$$ (90)

where $\alpha = \frac{1}{c^2}$; and

$\beta = 0.04$

They stated that for a large wave period, the second part of the

equation can be ignored and for a small wave period the first part of the equation can be ignored.

Jonsson (1966) defined the maximum bed shear stress in the form of equation 89. He developed a diagram similar to the Stanton diagram for pipe flow relating friction factor to Reynolds number with different values of $\frac{\alpha_\delta}{K_s}$

Neilsen (1979) stated that the concentration of moving sediment close to the bed is most likely to be a function of the non-dimensional bed shear stress which was introduced by Shields. Neilsen's maximum shear stress can be given as:

$$\tau_m = \frac{1}{2} \rho f \omega (\alpha_\delta \omega)^2 \tag{91}$$

Outside the boundary layer the velocity can be related by:

$$U_0 = \alpha_\delta \omega \sin \omega t \tag{92}$$

and the shear stress by:

$$\tau = \tau_m (\sin(\omega t + \phi)) (\sin(\omega t + \phi)) \tag{93}$$

where ϕ = phase angle.

Jonsson (1978) found that the phase angle ϕ by which the shear stress leads the water velocity outside the boundary layer is $\frac{\pi}{4}$ in the laminar case and $\frac{\pi}{6}$ in the fully developed turbulent case.

Riedel (1972) used the same approach as proposed by Jonsson and modified the friction factor diagram. Kamphius (1975) used the same

type of equation to calculate the maximum shear stress at the bed.
Dingler (1979) used the same equation as Riedel to calculate the
shear stress under oscillatory flow. Lofquist (1978) measured
oscillatory drag on sand ripples and obtained bed surface profiles.
He called the friction factor a stress coefficient (f(θ)) and gave the
shear stress as

$$\tau(\theta) = \frac{1}{2} \rho f(\theta) U^2 \qquad (94)$$

He measured the friction factor in laboratory experiments with a
rippled bed and presented several curves of stress coefficient
(friction factor) as a function of phase angle water velocity, ripple
length and ratio of ripple length to half orbial diameter.

Theoretical derivation of shear stress for a turbulent boundary
layer with oscillatory flow can be obtained using the principles of
turbulent boundary layers in unidirectional flow. The major
limitation is the lack of knowledge concerning velocity profiles in
the oscillatory boundary layer. If the velocity profile is known,
the shear stress can be obtained by the mixing length approach, as
follows:

$$\tau = \rho \ell^2 \left(\frac{dU}{dy}\right)^2 \qquad (95)$$

where ℓ is the mixing length; for unidirectional flow, $\ell = ky$.
Riedel (1972) proposed that in oscillatory flow the mixing length is
a function of orbital diameter, roughness coefficient and height

above the bed. Measurement of turbulent velocity fluctuations and flow visualization of eddies formed around roughness elements could be used to postulate a mathematical form of the shear stress equation.

Vongvisessomjai (1984) used an oscillating bed, a wave flume, and a water tunnel to study oscillatory boundary layers and eddy viscosity. He developed an appropriate oscillatory velocity profile which was then used to determine the boundary layer thickness, the shear stress profile, the friction factor, and the eddy viscosity profile. He found that there are differences between an oscillating bed and oscillating fluid. This contradicts the old belief that these two flow situations are the same.

Flow Regime

Jonsson (1963, 1966) and Collins (1963) stated that natural oscillatory flow near the sea bed under a wave motion is always rough turbulent. According to Jonsson (1963) and Vincent (1957), turbulence near the bed can also be generated under laboratory conditions. Jonsson (1966) stated that in the laboratory, smooth turbulent flow will often be found near the bed.

The flow regime can be determined for smooth and rough beds by using the $\dfrac{U_m \delta_L}{\nu}$

or $\dfrac{U K_s}{\nu}$ parameters, respectively. Where δ_L = laminar boundary layer thickness = $\dfrac{\sqrt{\nu T}}{\pi}$.

In addition to use of these parameters, the type of near-bed flow regime can be determined by observation of dye streaks. Interpretation of dye streaks results is subjective.

Table 6 gives limiting values for laminar and turbulent flow regimes obtained by some investigators. Riedel (1972) mentioned that for the case of a rough bed, the parameter $\frac{UmKs}{\nu}$ is not realy suitable for defining the transition between flow regimes but probably has been used because shear velocity was not known. The roughness coefficient in this parameter is a function of the size of the bed particles as well as of the bed geometry (grain spacing, shape, and size distribution). Most investigators of sediment transport replaced the roughness coefficient with the grain size. Kamphius (1974) found that the roughness coefficient can be replaced by twice the grain size. Also, when the flow around the grain was turbulent, the depth of flow was very much greater than the grain size.

Madsen (1976) used the roughness coefficient as the grain diameter when the bed was smooth and flat. Riedel (1972) used the roughness coefficient as three times the grain size, in his bed shear measurements under waves and indicated that if different values of roughness coefficient are used, all of his curves regarding friction factor should be changed.

Based on dye streak observations, Bagnold reported that the boundary layer was laminar in all experiments even though quartz grains as large as 3 mm were used. Manohar (1955) also studied the threshold of grain motion using an oscillatory bed. Contrary to

Table 6. Limits of Flow Regimes for Smooth Beds
Given by Some Investigators

Investigator and Year	Upper Limit for Laminar Flow Regime		Lower Limit for Smooth Turbulent Flow Regime	
	$\dfrac{U_m{}^a\delta}{\nu}$	$\dfrac{U_m\delta L}{\nu}$	$\dfrac{U_m{}^a\delta}{\nu}$	$\dfrac{U_m{}^\delta L}{\nu}$
Li (1954)	1.6×10^5	565	---	---
Vincent (1958)	6.2×10^3	110	---	---
Collins (1963)	1.3×10^4	160	---	---
Kajiura (1968)	6.2×10^2	35	4.2×10^5	920
Riedel (1972)	10^4	142	6×10^5	1,100

Bagnold, he reported that the boundary layer becomes turbulent for grain sizes larger than 0.6 mm. His data show two trends; for a laminar boundary layer, his data parallel Bagnold's data, but are displaced toward larger critical velocity values for a given grain size; under turbulent boundary conditions, his data correlated well with the relation developed by Rance and Warren (1968) in a pulsating water tunnel. Also, he found that the initial and general motion of small sizes of sediment occur in a laminar boundary layer. He also stated that ripples were found when the boundry layer was turbulent.

According to the work carried out at Berkeley (Li, 1954; Kamphius, 1957; Manohar, 1955), the bed would be smooth, in the hydraulic sense of the word, if;

$$\frac{\delta_L}{\epsilon} > 30$$

and rough if:

$$\frac{\delta_L}{\epsilon} < 18.5$$

where δ_L = boundary layer thickness = $6.5 \ (\frac{\nu}{\omega})^{\frac{1}{2}}$ = $2.61\sqrt{\nu T}$

ϵ = characteristics dimension of a grain equivalent to grain size diameter.

Li (1954) studied the transition from laminar to turbulent boundary layer in an oscillatory flow for both smooth and rough boundaries. He found that over a smooth boundary, the critical Reynolds number at which the transition takes place is about equal to 800 and is constant. For a rough boundary, he found that the Reynolds number is constant for each roughness element. Wakes were obserbed to develop behind each roughness element for oscillatory flow over a rough bottom. The transition boundary layer that

developed was due to instability of the flow along these wakes.

Vincent (1958) used dye for studying the flow regime. He found that the streak of dye quickly spread for a turbulent boundary Layer situation and dispersed in gentle undulations for a laminar boundary layer. Also, he found that the flow was laminar for $\frac{U^{\delta}L}{\nu} < 160$. He also mentioned that the values obtained at Berkeley appear to exaggerate the importance of the laminar conditions.

Collins (1963) found that in laboratory wave studies the boundary layer flow is laminar. But he recognized that turbulence exists for most prototype boundary Layer cases. He also found values of critical Reynolds number for the start of turbulent when $\frac{U^{\delta}L}{\nu} \approx 160$. He further mentioned that the great difference between the Reynolds number for waves and Reynolds number for an oscillatory plate in still water is to be expected as proposed by Li since the inertia effects of two cases are completely different. The Reynolds number for waves is less than the Reynolds number which Li found with an oscillatory plate. Vincent obtained lower Reynolds numbers than Li. He defined turbulence by observing streaks of dye. He also stated that it is not easy to draw a sharp distinction between cases where the streak of dye spreads out (turbulent boundary layer), and where it disperses in gentle undulations (laminar boundary layer).

Jonsson (1966) used Reynolds number for identifying boundary layer flow regimes and to find the friction factor for each case. He presented a graph of $\frac{\hat{a}_{\delta}}{K_s}$ = versus Reynolds number to obtain the flow regime. This is given in Figure 18.

Riedel (1972) and Kamphius (1975) also studied the boundary layer
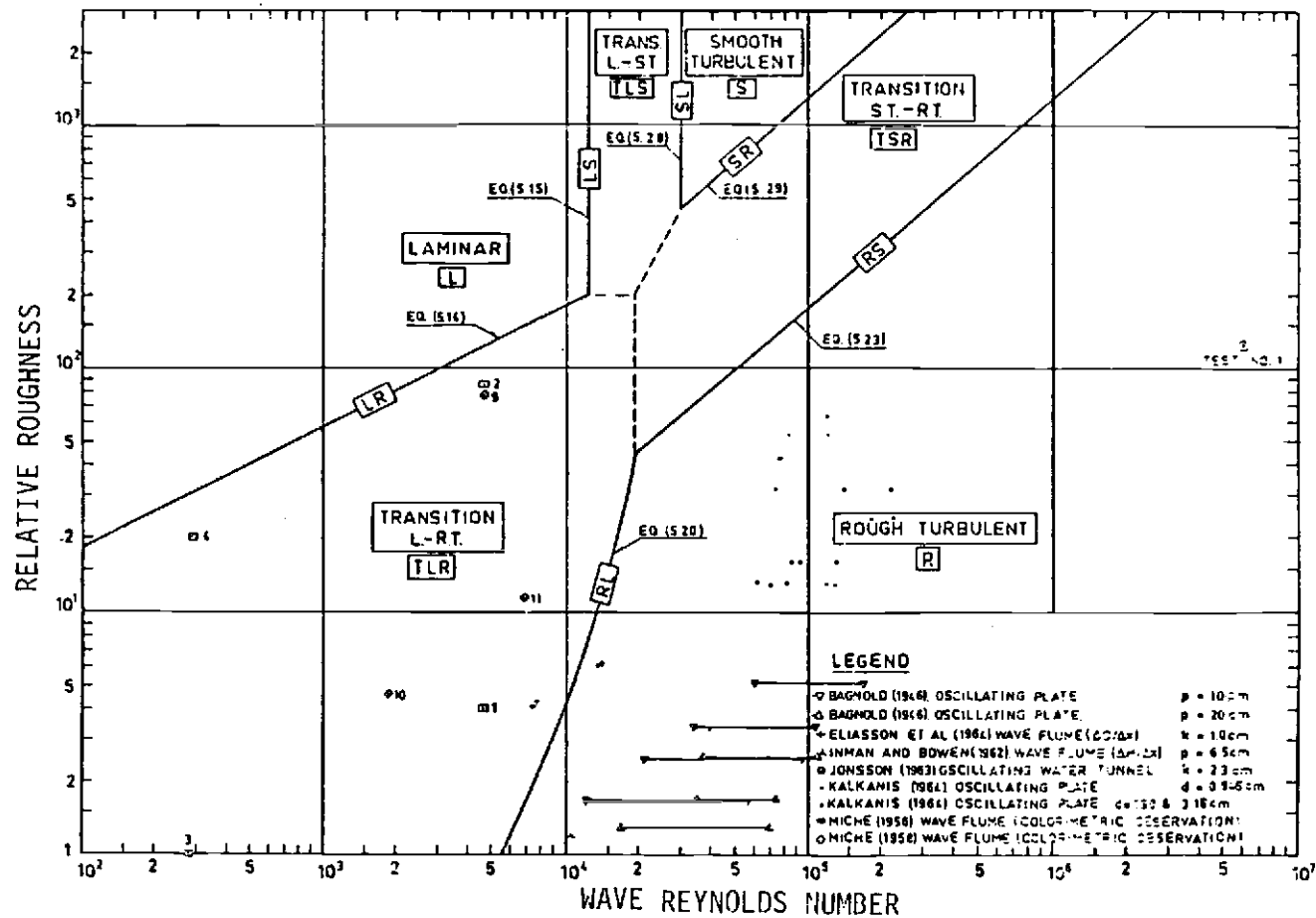
Figure 18.   Flow Regimes for Oscillatory Flow Over a Fixed Bed of Sediment
(Source: Jonsson, 1966)

flow regime and presented graphs of $^a\delta/K_s$ vs Reynolds Number.
Riedel's graph is given in Figure 19. The regions of laminar
transition (from laminar to smooth turbulent), and rough turbulent
boundary layer can be obtained from Riedel's graph. Kamphius found
the upper limit of the laminar range to be 10^4. Collins (1963) found
this upper limit to occur at a Reynolds number of 1.3×10^4. This
discrepency with Kamphius is due to observer interpretation of the
transition.

Chan et al. (1972) identified five different flow regimes which
are essentially similar to those observed by Bagnold (1946), Manohar
(1955) and Carstens et al. (1969). These regimes are: 1) stationary
bed; 2) incipient motion; 3) general surface motion; 4) mobile bed;
and 5) suspended bed. For the stationary bed regime, the sediment
particles were undisturbed by the motion of the fluid; the bed stayed
stationary. The stationary bed regime can be smooth or rough
depending on the Reynolds number. In the incipient motion regime,
sediment particles on the bed surface started to be moved to and fro.
Chan et al. stated that often a sediment particle would be dislodged
from one position and later anchor itself in an apparently more
stable position. The observations made for these two regimes suggest
that the boundary layers were laminar.

It is usually hard to identify the limits of the incipient motion
regime, because incipient motion is rather poorly defined. However,
Chan et al. reported that a gradual increase in amplitude or period
resulted in transition from occasional motion to the general surface
motion regime of the sediment particles. The surface particles were
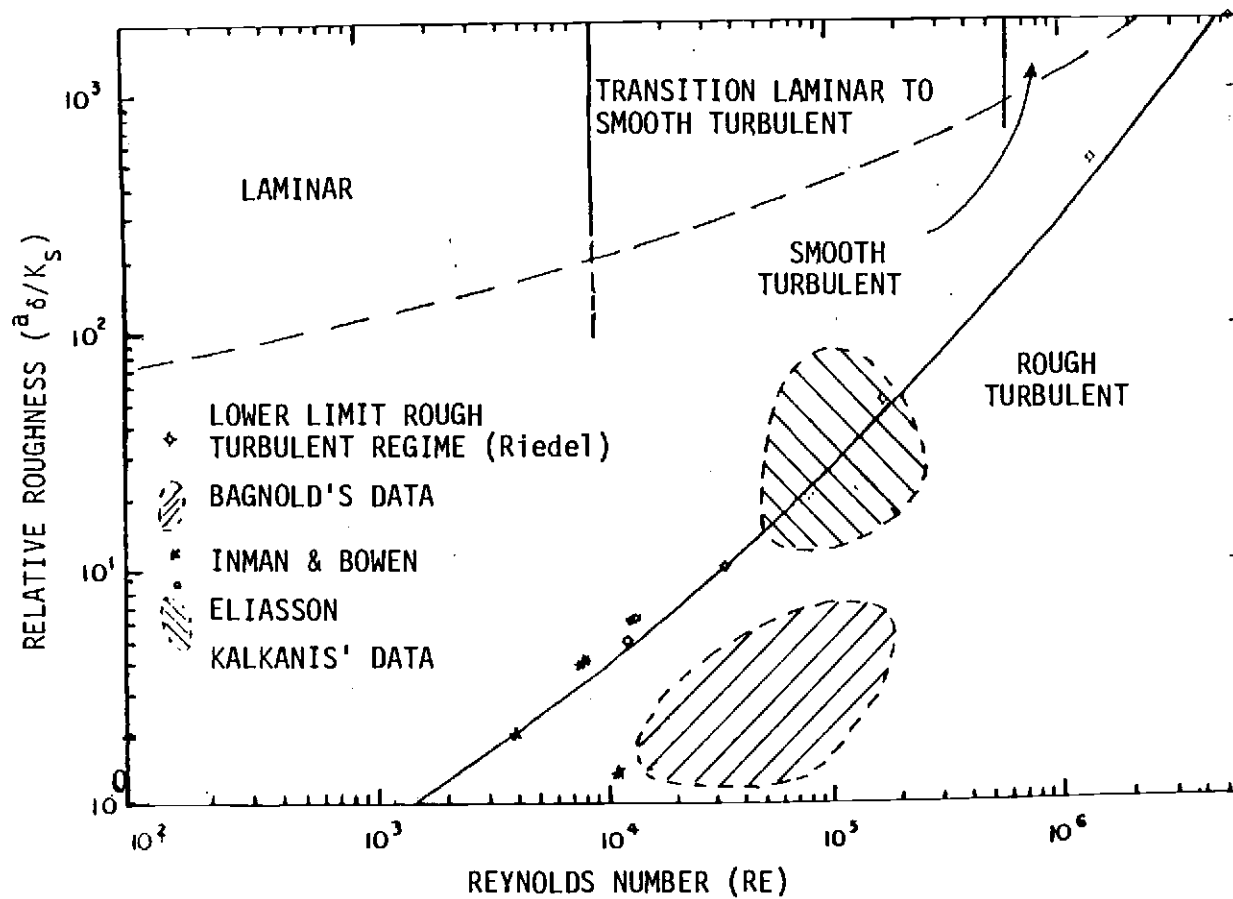
Figure 19. Flow Regimes for Oscillatory Flow (Source: Riedel, 1972)

set in motion at least during part of the oscillation cycle when the liquid velocity was high. At these conditions, ripples appeared in the bed surface after several minutes of oscillation and dune formation was observed. Bagnold (1946) defined two types of dune: rolling grain dunes and vortex dunes. Rolling grains dunes were observed at a relatively low velocity. The vortex dunes were formed when the slopes of the dunes were steep and the oscillation velocity was high. Bagnold (1946), Manohar (1955) and several other investigators have given the mode of particle motion and dune mechanism. Chan et al. (1972) mentioned that although the liquid flow in the boundary layer above the bed was turbulent, the moving body of the oscillating liquid remained laminar. Longuet-Higgins (1981) in their study of oscillating flow over steep sand ripples, assumed that the sand-water interface is fixed and that the effect of sand in suspension is, to a first approximation, negligible. They found that the calculated drag coefficients are in remarkably good agreement with the high values found experimentally. They also found that the total momentum per ripple wave length and the horizontal force on the bottom can be expressed very simply in terms of the shed vortices at any instant. The force consists of two parts: an added-mass term which dissipates no energy, and a vortex drag, which extracts energy from the oscillating flow.

According to Chan et al (1972), an increase of wave amplitude or frequency resulted in a mobile bed regime. This inhibited the further formation of stationary dunes. Either the bed surface broke into a series of ripples with suspended material moving to and fro

above them or the bed surface appeared flat, though in horizontal motion. In either case, the surface particles did not appear to settle completely at any point in the cycle.

At very high oscillation velocities, Chan et al. reported that particles from the entire bed were suspended and conditions were clearly turbulent throughout. This case was termed the suspended bed regime.

Friction-Factor-Determination

The classic procedure for obtaining wave friction factor is to measure directly the wave friction factor. Jonsson (1966) provides methods for measuring the wave friction factor. In general, the wave friction factor can be measured by energy loss, force or velocity. These three measurements can be schematically subdivided as:

1) energy loss

   a) direct measurement

   b) measurement of wave height attenuation

measurement of wave friction factor

2) force

   a) direct measurement

   b) measurement of the slope of mean water level

3) velocity

   a) equation of motion

   b) the law of wall

   c) velocity measurement at fixed level
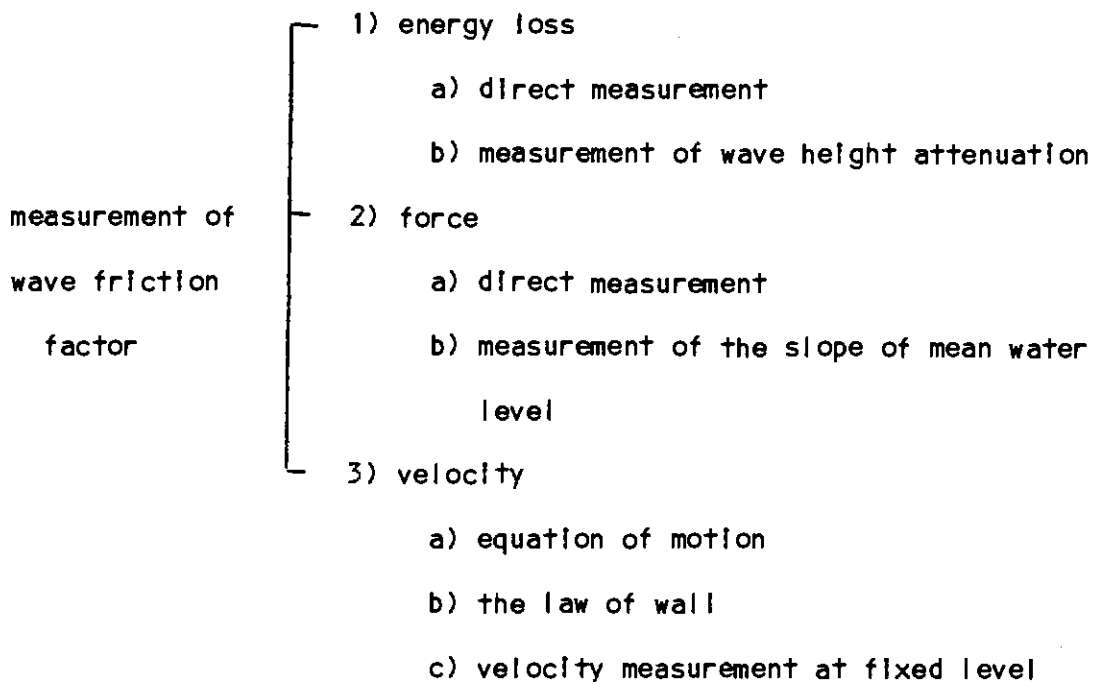
The measurement of the slope of mean water level does not provide good results. After knowing whether the flow regime is laminar or

turbulent, the friction factor can be obtained by using the appropriate equations or graphs.

Laminar Flow

In general, the friction factor is a function of the Reynolds number and the relative roughness of the boundary layer. This can be expressed as:

$$f_\omega = f(RE, \frac{a_\delta}{K_S})$$ (96)

where all terms are as previously defined.

Jonsson (1966) gives a theoretical expression for friction factor based on the maximum shear stress under oscillatory boundary layers:

$$f_\omega = \frac{2}{\sqrt{RE}}$$

He presented a graph of wave friction factor against Reynolds number. This is given in Figure 20. This also can be derived from solution of linearized equations of motion. Excellent agreement of experimental data with this calculation was observed by Riedel (1972). Kamphius stated that Jonsson's expression is not valid for Reynolds numbers greater than 10^4. However, Jonsson mentioned that others had proposed that smooth turbulence starts at a Reynolds number of 1.26×10^4 or larger. For example, Collins (1963) gave a Reynolds number of 1.28×10^4, Li (1954) gave a Reynolds number of 1.60×10^5, whereas Vincent (1958) reported a value of 6.2×10^3. It can be seen there was general agreement between different investgators. In contrast to Jonsson's expession, Neilsen (1979) expressed the laminar case as:

$$f_\omega = 2\sqrt{\frac{\nu}{a_\delta^2 \omega}}$$ (97)
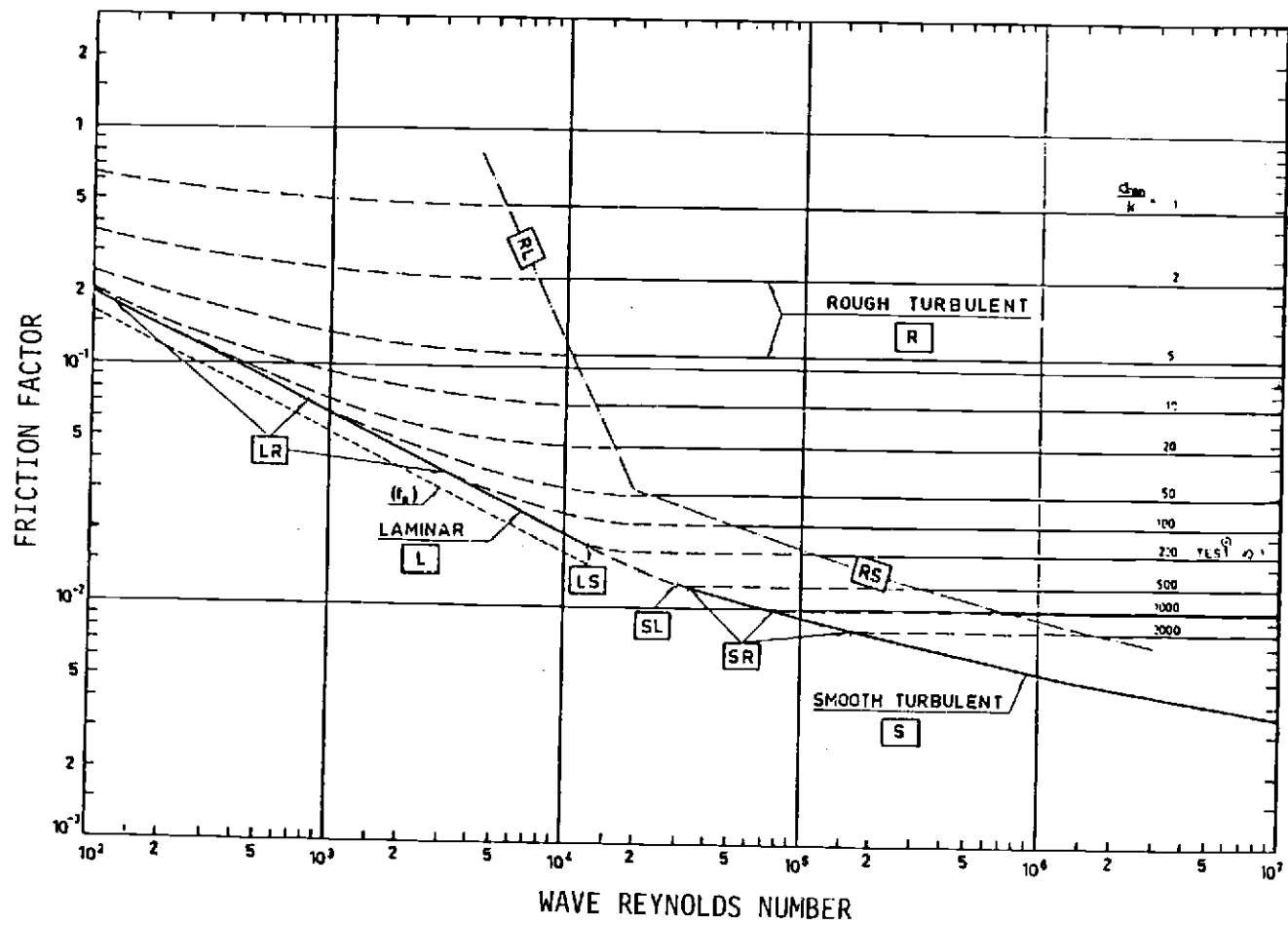
Figure 20.   Wave Friction Factor for Oscillatory Flow   (Source: Jonsson, 1966)

Turbulent Flow

In the case of a turbulent boundary layer the friction factor is independent of the wave Reynolds number and is thus a function of the relative roughness of the boundary layer only, i.e.

$$f_\omega = f(\frac{a_\delta}{K_s}) \tag{98}$$

Kajiura (1968) developed a theoretical basis for the turbulent boundary layer. He assumed an average state of turbulence over the wave period and used the constants evaluated from unidirectional flow measurements. He divided the boundary layer into inner, overlap, and outer layers and obtained the friction factors. For a smooth boundary he gave

$$\frac{1}{8.1\sqrt{f_\omega}} + \log\frac{1}{\sqrt{f_\omega}} = -0.135 + \log\sqrt{RE} \tag{99}$$

For a rough bed, he gave

$$\frac{1}{4.05\sqrt{f_\omega}} + \log\frac{1}{4\sqrt{f_\omega}} = -0.254 + \log\frac{a_\delta}{K_s} \tag{100}$$

Jonsson (1963) presented a friction factor equation for rough surfaces based on measurement of velocity profiles. This can be given as:

$$\frac{1}{4\sqrt{f_\omega}} + \log\frac{1}{4\sqrt{f_\omega}} = -0.03 + \log\frac{a_\delta}{K_s} \tag{101}$$

He assumed that a logarithmic velocity profile existed near the wall which could be extended into the potential flow regime. Riedel (1972) used the same form of equation as Kajiura and Jonsson and applied his data with the least squares method and to obtain separate friction expressions, depending on the relative roughness of the boundary layer.

$$\text{For } \frac{a_\delta}{K_s} > 25 \quad \frac{1}{4.95\sqrt{f_\omega}} + \log\frac{1}{4\sqrt{f_\omega}} = 0.122 + \log\frac{a_\delta}{K_s} \tag{102}$$

$$\text{and for } \frac{a_\delta}{K_s} < 25 \quad f_\omega = 0.25\left(\frac{k_s}{a_\delta}\right)^{0.77} \tag{103}$$

$$\text{or } \frac{U_*^2}{U_m^2} = 0.125\left(\frac{k_s}{a_\delta}\right)^{0.77} \tag{104}$$

He presented a friction factor diagram in rough turbulent flow. This is given in Figure 21. He stated that the assumption of a logarithmic velocity profile at the instant of maximum free stream velocity is reasonable.

Nielsen (1979) used the Swarts' 1974 formula of friction factor:

$$f_\omega = \exp\left[5.213\left(\frac{K_s}{a_\delta}\right)^{0.194} - 5.977\right] \tag{105}$$

to calculate the bed shear stress.

Bagnold (1946) estimated a wave friction factor value of 0.28 for an extremely rough bed, where $\frac{a_\delta}{K_s} < 1.7$.

The limit between the smooth turbulent and rough turbulent transition regime was determined as $\frac{K_s}{\delta_L} = 0.287$ by Jonsson (1966).
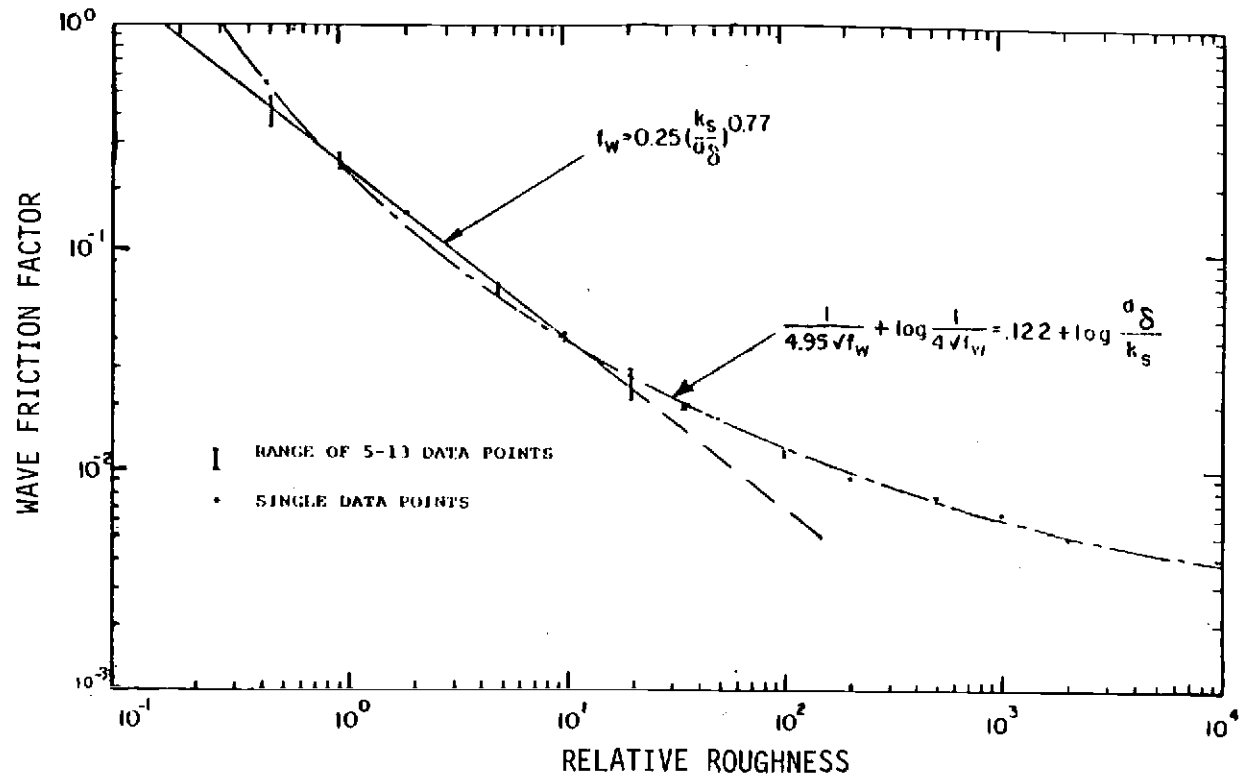
Figure 21. Wave Friction Factor in Rough Turbulent Regime
(Source: Riedel, 1972)

Riedel (1972) used the same approach as Jonsson (1966) and developed modified curves of the wave friction factor in general and the wave friction factor in a rough turbulent regime. He measured and calculated the shear stress on both smooth and sand roughened beds in an oscillating water tunnel. He found good agreement in the laminar range with the theoretical shear stress calculated from first order wave theory. However, in the turbulent flow regime, Riedel's experimental measurements of shear stress gave values 20 to 50 percent smaller than that predicted by Jonsson's expressions. Direct measurement of shear obtained from wave attenuation tests by Inman and Bowen (1962) gave results that were 20 percent higher than those from the Riedel data.

Boundary Layer Thickness

The thickness of the boundary layer affected by friction may be estimated. Einstein (1942) predicted this thickness as the distance, y, from the smooth bed to that point at which the friction-induced motion is reduced to 10 percent of its value at the bed. Li (1954) predicted the boundary layer thickness above an oscillatory plate in still water as extending to that point where the amplitude of the oscillating velocity has only 1 percent of that of the boundary. He gave this thickness as:

$$\delta_L = \frac{4.6}{(\omega/2\nu)^{\frac{1}{2}}} = 6.5\left(\frac{\nu}{\omega}\right)^{\frac{1}{2}} \tag{106}$$

Jonsson (1966) used dimensional analysis to determine the boundary layer thickness in terms of the half-orbital diameter for different flow regimes. His results can be given as:

Flow Regime	δ_L / α_δ
Laminar	$f(U_m a_\delta / \nu)$
Smooth Turbulent	$f(a_\delta / K_s)$
Rough Turbulent	$f(U_m a_\delta / \nu)$

He also mentioned that the boundary layer thickness for short waves is 1/100 of the water depth, or is the distance from the bed to the point where the velocity has increased sufficiently to equal the potential velocity under the wave. Figure 22 shows the typical velocity profile in and above the boundary layer thickness. Jonsson concluded that the boundary layer thickness with oscillatory flow is similar to the boundary layer thickness employed in steady flow over which the velocities deviate significantly from the free-stream velocity. He provided a graph which gives the wave boundary layer thickness for different flow regimes and as a function of roughness coefficient. This is given in Figure 23.

Dingler (1979) also provided an equation for the laminar sublayer thickness under oscillatory flow. His equation can be given as:

$$\delta_L = (\mu T / \rho \pi)^{\frac{1}{2}} \tag{107}$$
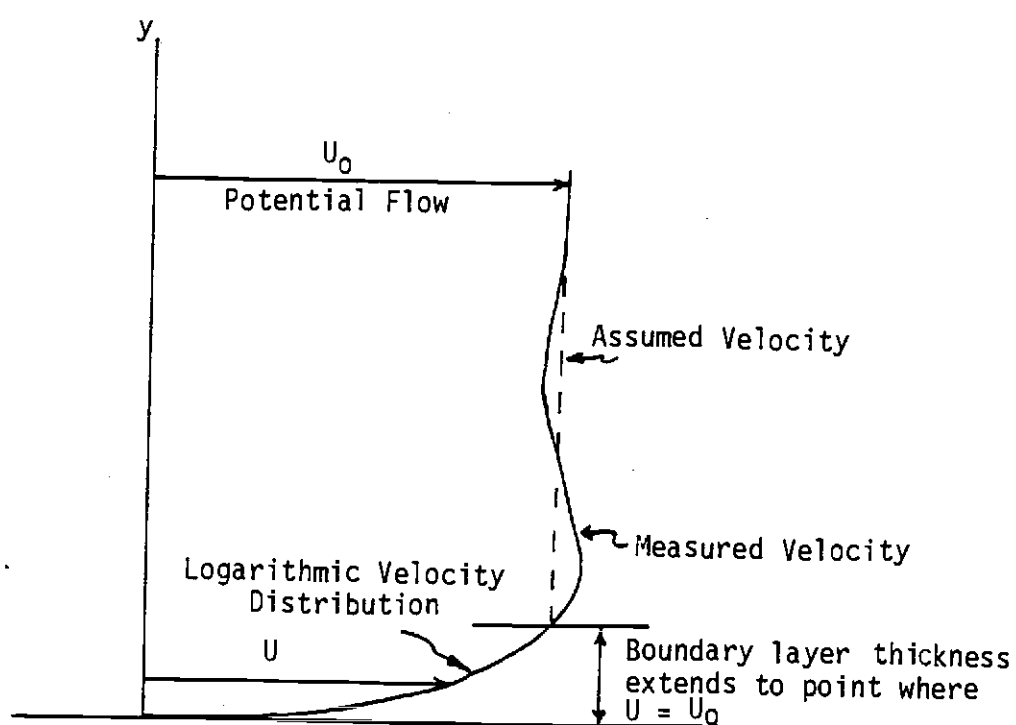
Figure 22. Typical Velocity Profile Near the Bed and
Boundary Layer Thickness Under Oscillatory Flow
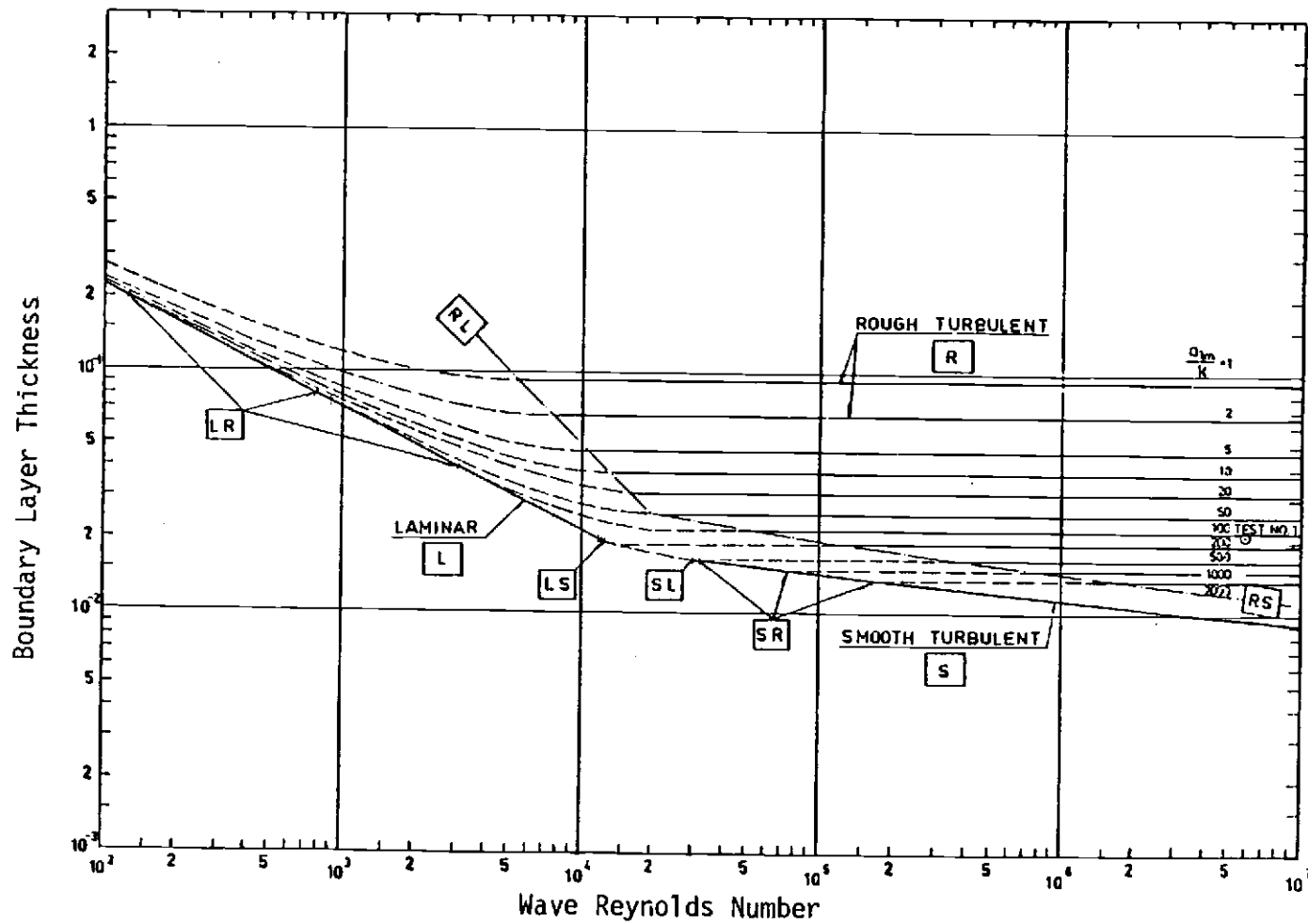
Figure 23. Wave Boundary Layer Thickness for Oscillatory Flow
(Source: Jonsson, 1966)

Similarities and Differences of Sediment Transport Between
Unidirectional and Oscillatory Flow

Beginning in the 1950's under the direction of Einstein, several
investigators in Berkeley conducted research in areas of sediment
transport by wave action. Their aim was to see if it is possible to
establish a general system approach for the description and
prediction of sediment transport by waves similar to that under
unidirectional flow. Einstein (1972) stated some of the principles
governing unidirectional flow as:

1) Sediment motion can be divided into bed-load motion (or
   surface creep) and suspension;

2) while moving as bed load, the particle weight is to a
   large part transmitted directly to the non-moving bed,
   not to the flow;

3) the rate of bed-load motion is defined by the equilibrium
   exchange of sediment between the bed-load and the non-moving
   bed;

4) this equilibrium gives a direct relationship between the
   sediment rate and the flow conditions near the bed,
   including the turbulence;

5) the flow condition near the bed can be predicted for a
   unidirectional boundary layer as a function of only the
   bed shear and the bed roughness;

6) the bed particles moving as bed load in the rather thin
   bed layer define a sediment concentration for this layer;

7) above the bed layer, bed particles move in suspension,
   i.e., continuously transmitting their weight to the

surrounding water; and

8) the distribution of the concentration in a suspension is
defined by the equation of equilibrium exchange of particles
through the various horizontal planes, with the bed-load
concentration in the bed layer as a boundary condition.

Einstein concluded that all of these eight principles for
unidirectional flow, except principle 5, are assumed (and seem) to
apply equally for the problem of sediment transport by wave action.
He stated that the basic variable describing a undirectional flow is
the rate of friction or of stress at the boundary. For wave motion
the basic condition is mainly an exchange between potential and
kinetic energy which may, in first approximation, be described as a
frictionless motion--it does not by itself define a shear stress at
the boundary. Also, movement of sediment by waves takes place in a
boundary layer that is developed at the bottom from the effects of
viscosity of the fluid.

Kalkanis (1957) showed that from the point view of the boundary
layer, the two cases of boundary layers in unidirectional and wave
action are exactly equivalent, even if there is a minor difference
with respect to the ability of the two cases to move sediment.

Chan et al. (1972) found that oscillatory flow was generally more
effective than steady flow in bringing about the threshold of
particle motion. However, oscillatory flow was somewhat less
effective in bringing about suspension. They also mentioned that
this is consistent with the well-known tendency for purely
oscillatory flows to remain laminar at velocities which, in steady
flow, would correspond to turbulent conditions.

Many investigators correlated physical characteristics of the grain with sediment initiation in unidirectional flow. Vincent (1958), in his study of sediment suspension under waves, indicated that it would be misleading to try to derive a relationship between the velocity at which the grains begins to move and the physical characteristics of the grains from a set of insufficiently complete results. There are many reasons, chiefly that it is very difficult to characterize a grain of material by its shape using a simple relationship and to characterize the influence of local turbulence on grain behavior.

Past Experiments Involving Combined Oscillatory and Unidirectional Flow

Unfortunately, there is limited information in the literature regarding suspension of fine sediment under the combined effects of wave and unidirectional flows, the theoretical relationship between flow variables and sediment parameters are not developed. Hence, the brief review of available literature must be based mostly on coarse (non-cohesive) sediment.

Nielsen (1979) observed that the majority of sand that is moved under waves alone and under waves with a current is moved in suspension. Primarily, the oscillatory motion is responsible for picking up the sand, after which the current is responsible for its transportation. This is consistant with the remarks of Chan et al. (1972) given in the preceding section. Nielsen also mentioned that the relative importance of the waves and the current to the

diffusivity of suspended sediment is at present unclear, as our knowledge is very limited regarding the boundary layer under a combination of waves and current. Very likely, the current is quite dominating in this respect as long as the waves are not breaking, whereas the influence is more equal in the surf zone. Nielsen also presented a model for the suspension of non-cohesive sediment under waves and currents.

Einstein (1972) mentioned that those particles moving with the water near the bed will follow the water in any direction in which it flows. If the water has, in addition to the wave motion, a small additional one-directional velocity (such as a littoral current caused by the angular incidence of the waves or a secondary circulation caused by the geometry of the beach), then one must expect a systematic transport of the moving sand particles in that direction.

Manohar (1955) found that the superposition of unidirectional flow did not markedly change the oscillatory condition necessary for initiation of sand motion. Vincent (1958) stated that the sand particles set in motion by the waves may be easily transported by even a very slight sea current. He also stated that the effect of the waves, when superimposed on the current, is either to considerably reduce the critical entrainment tractive force for the material or cause the grains to begin to move. Bijker and Vellingu (1976) also studied the sand transport by waves and currents. They concluded that if a uniform flow in the direction of wave propagation is superimposed on the wave movement, the direction of sand transport

Is not necessarily equal to a drift current direction. They also found that the sand transport direction equals the direction of the biggest orbital velocity.

Inman and Bowen (1962) conducted flume experiments on sand transport by waves and currents. They used a wave channel with a paddle-type wavemaker and superimosed the unidirectional flow. Their results showed that superposition of waves on currents of 2 cm/sec produced a two-fold increase in the sand transport for wave periods of both 1.4 and 2.0 seconds, but that faster currents of 4 and 6 cm/sec caused the discharge of sediment to decrease somewhat.

Rance and Warren (1968), in their sediment-wave study, found that the superimposing of a unidirectional flow (stream-type flow) did not markedly change the oscillatory current necessary for the initiation of movement.

It has been shown that when oscillatory flow superimposed on unidirectional flow, the mean velocity near a smooth bed are increased and the mean velocity near a rough bed reduced (Peregrine and Jonsson, 1983). Does the turbulent structure inside the boundary layer remain constant, does the direction of wave propagation change, how does the friction factor behave are many questions that further theoretical work could shed light on.

The assumption of simple linear summing of the results of the individual effects for combined effects look likes too simplistic inside the boundary layer. But, it could be used at some cases, such as; determination of whether oscillatory or unidirectional flow is responsible either for entrainment or transportation of sediment

particles.

It is evident that the interaction of oscillatory and unidirectional flows is a fundamental aspect of most coastal littoral and estuarine sediment transport. A physically-based prediction and consistent experimental results with physical insight are lacking. More theoretical and experimental work are needed.

For sediment in suspension, the turbulence and the current are two important factors. Measurements of turbulence with good spatial distribution under a combination of unidirectional and oscillatory flows are reported by Kemp and Simons (1982). Their interpretation of the measurements, as they apply to sediment transport, is repeated as follows:

"The entrainment of sediment under flat bed conditions can be related to the predicted instantaneous shear stress. However, although the entrainment of material from the bed can be considered to show a considerable increase under the combined action of waves and currents, the distribution of turbulence intensities suggests that the zone of diffusion would not increase. In fact, the results indicate a reduction in boundary layer thickness (when waves are added to a current.) One might expect, therefore, that there would be an increase in sediment concentration in the near bed region. In the light of Nielsen's (1979) observations, this distribution would change dramatically under spilling breakers, the material rapidly dispersing over the whole depth of flow.

"The greater turbulent stresses found when waves are superimposed on a current are likely to result in a considerable increase in sediment pickup from a rippled bed. While the increase in turbulence is limited to a region within 6 or 7 roughness heights of the bed with a tendency for this zone to decrease with wave height for a constant wave period, it is to be expected tht sediment brought into suspension by the nearbed vortex action will be diffused over the zone of the current-induced turbulence. This could result in significantly higher transport rates as long as the increased bed shear stress is not such as to prevent the formation of high bed ripples.

"In the case of waves alone, the shear stresses at the bed are of the same order as for combined wave and current flow, but the

vortex-dominated layer extends only approximately four roughness heights above the bed, and the only means of transporting sediment is by relatively weak wave-induced mean velocities. The limited thickness of the wave-induced vortex layer over a rippled bed has previously been noted by Tunstall and Inman (1975). This suggests that sediment would be concentrated in this near-bed layer."

Fredsoe (1984) studied the turbulent boundary layer in a combined wave-current flow field. He calculated the mean velocity profile in the combined wave-current motion by use of the depth-intergrated momentum equation. To do this, he assumed the vertical velocity distribution to be logarithmic inside as well as outside the wave boundary layer, but with different slopes. He also found that for the case of no mean current, the theoretical findings agreed well with the measured friction factor for both the rough bed case and the smooth bed case.

Experimental Materials and Methods of Past Investigators

Types of Experimental Apparatus With Oscillatory Flow

Many investigators have tried to reproduce prototype conditions in laboratory experiments to study sediment transport by wave action. The techniques used to reproduce prototype conditions are reviewed here and shortcomings and problems associated with each technique and apparatus are described.

The reproduction of incipient bed motion, ripple formation, dune development, and a final smooth bed have all been achieved with both oscillating water over a fixed bed and an oscillating bed under still water. It is preferable to conduct tests with full-scale amplitudes

of water motion, since it is impossible to scale down sediment sizes, unless pebble-sized prototype particles are being represented (Silvester, 1970). However, this is not always possible.

Silvester (1970) summarized the modeling of sediment motions offshore in great detail. Mogridge (1970) summarized the techniques for sediment modeling and the advantages and shortcomings of each technique. The variety of equipment available for use includes flumes, water tunnels, water blocks, wave basins, and other devices.

Flumes

Many investigators have used wave tanks or channels (flumes) with a paddle-type or piston-type wavemaker to oscillate the water. This includes Ippen and Eagleson (1955), Vincent (1958), Eagleson and Dean (1959), L'Hermitte (1961), Inman and Bowen (1962), Hom-ma et al. (1963), Alishahi and Krone (1964), Yalin and Russell (1966), Bhattacharya (1971), Mogridge and Kamphius (1972), and Dingler (1979). Figure 24A shows a typical wave flume. Chan et al. (1972) used a horizontal tube which was subjected to an oscillating liquid flow. Many investigators realized the difficulties associated with oscillating water in the flume so as to reproduce prototype conditions on a small scale. Longuet-Higgins (1953) mentioned that the transport of sediment in a flume occurs by mass-transport, which is "swiftly" established throughout the whole depth of water. In prototype situations, such as in oceans or lakes, it takes many days for this net motion to be converted or diffused from the bed or the surface to the interior of the liquid. This introduces errors when the distribution of sediment throughout the depth of the flume differs from that in the prototype situation. The mass-transport distribution

A. WAVE FLUME

Wave
Generator   Test Section   Sloping Beach

B. OSCILLATING BED

water

moving plate

C. OSCILLATING WATER TUNNEL

exhaust   air
valve   supply

air   air

water   water

Test   Section
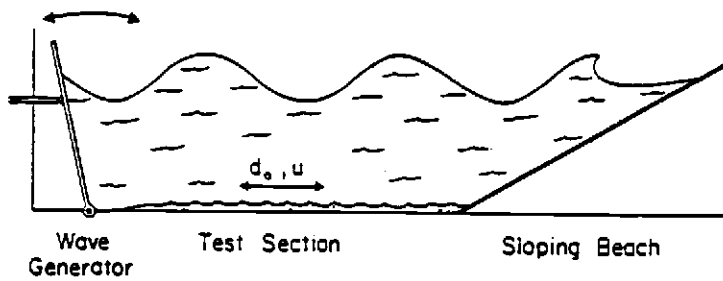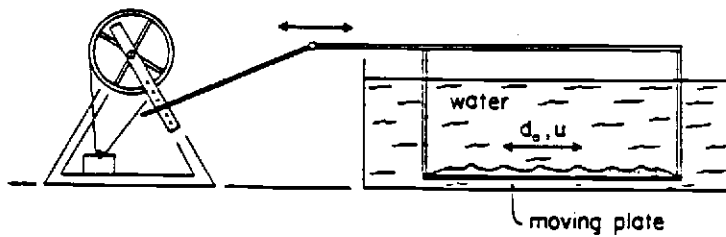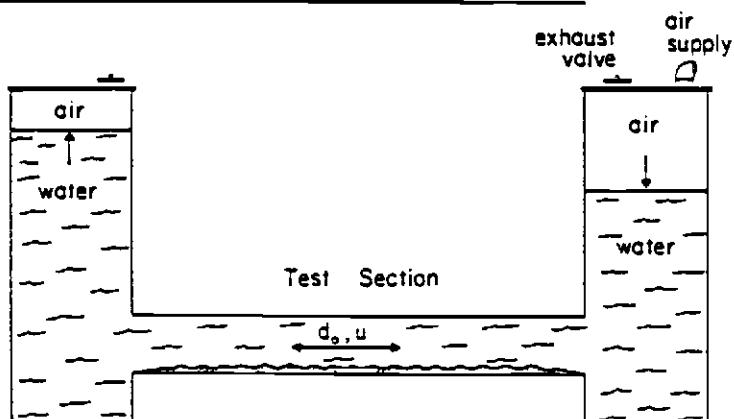
Figure 24.   Types of Laboratory Apparatus Used to Simulate Wave
Orbital Motion (Source: Miller, 1978)

also varies with bed roughness (Bagnold, 1946).

Mogridge (1970) also mentioned two particular problems with wave flumes. First, the velocity for incipient motion in a wave flume cannot be compared directly with the same velocity under prototype conditions, because the flume is associated with a boundary layer of different thickness. As the roughness cannot be reproduced, turbulence cannot be scaled down. Second, there is difficulty of eliminating reflection from both the wave-making machine and the artificial beach at the opposite end of the flume. Mogridge proposed either to oscillate the bed in still water or to oscillate the water in a conduit so as to overcome the above-mentioned difficulties.

Several investigators have employed oscillatory beds. Bagnold (1946) was the first to use an oscillating bed in still water to study sediment under wave action. His was a pendulating bed. At Berkeley, Li (1954), Manohar (1955), Abou Seida (1964), and Kalkanis (1957, 1964) employed a horizontal plain bed which was oscillated harmonically in still water with amplitudes and periods appropriate to prototype water waves. Figure 24B shows a typical oscillating bed. Das (1971) used a swinging flume oscillated by a driving mechanism. In this case, near-bottom conditions very similar to the prototype can be obtained in the laboratory and the scale effects of sediment size, boundary layer, bed roughness, and so on can be overcome.

Mogridge (1970) stated that it is unlikely that the laboratory turbulence structure is similar to that in the prototype. He stated

that the relative velocities of the fluid acting on a sediment particle are, in theory, identical for the cases of an oscillating bed and an oscillating fluid; this means that the drag and lift forces due to the Magnus effect are the same. The Magnus effect due to rotation of a sediment particle in a uniform flow causes an increase of velocity above the particle and a decrease of velocity below it. Therefore, a pressure difference exists and a lift is applied to the particle.

Vincent (1958) questioned the validity of the oscillating bed tests. He mentioned several differences in characteristics between the laboratory oscillating bed or wave flume and the prototype situation. These include entrainment currents (mass transport currents), acceleration of fluid particles, pressure fluctuations in the immediate vicinity of the sea bed, development of turbulence, and so on. He also stated that the greatest difference between the critical Reynolds number for waves and for an oscillating plate in still water is that the inertial effects in the two cases are different; for example, the critical Reynolds number for a progressive wave is lower.

L'Hermitte (1961) also criticized the oscillating bed tests because of the acceleration effects on the sand particles, but mentioned that the accelerations involved are small compared with those due to gravity, and are 90 degrees out of phase with the major entrainment forces. He also has questioned the inertia effects of sand particle on the bed. These could be small at the stage of incipient motion but could become significant as accelerations

Increased. However, the similarity of dimensionless parameters used
by Carstens and Neilson (1967) and Manohar (1955) indicates that the
motions are not dissimilar, unless some compensatory influences have
operated (Silvester, 1970).

Silvester (1970) pointed out that at the threshold of sand
movement and rolling-grain ripple formation, the forces on the
particles are similar to those in wave flumes. However, as the
velocities increase so do the rotational speeds of the eddies. He
suggested that the Magnus effect be examined for sand particles and
water masses for the two different modes of generation. Figure 25,
which is taken from Silvester (1970), shows the forces on rotating
masses from oscillatory flows produced by oscillating the bed and by
oscillating the water. Silvester concluded that for the oscillating
bed, vortices tend to move away from the bed and sand grains remain
suspended longer; for the oscillating water, the reverse is the
case.

Water Tunnels

Water tunnels are a recent development in sediment transport
studies with wave action. The water periodically flows to and fro
through a small rectangular conduit, as shown in Figure 24C.
Silvester (1970) describes several different types of water tunnels
used in Denmark, England, the United States, and Australia. Jonsson
(1963), Dedow (1966), Carstens and Neilson (1967), Rance and Warren
(1968), Carstens et al. (1969), Riedel (1972), Mogridge and Kamphius
(1972), Kamphius (1975), Jonsson and Carlson (1976), Nakato et al.
(1977), Lofquist (1978), and Vongvisessomjai (1984) all used
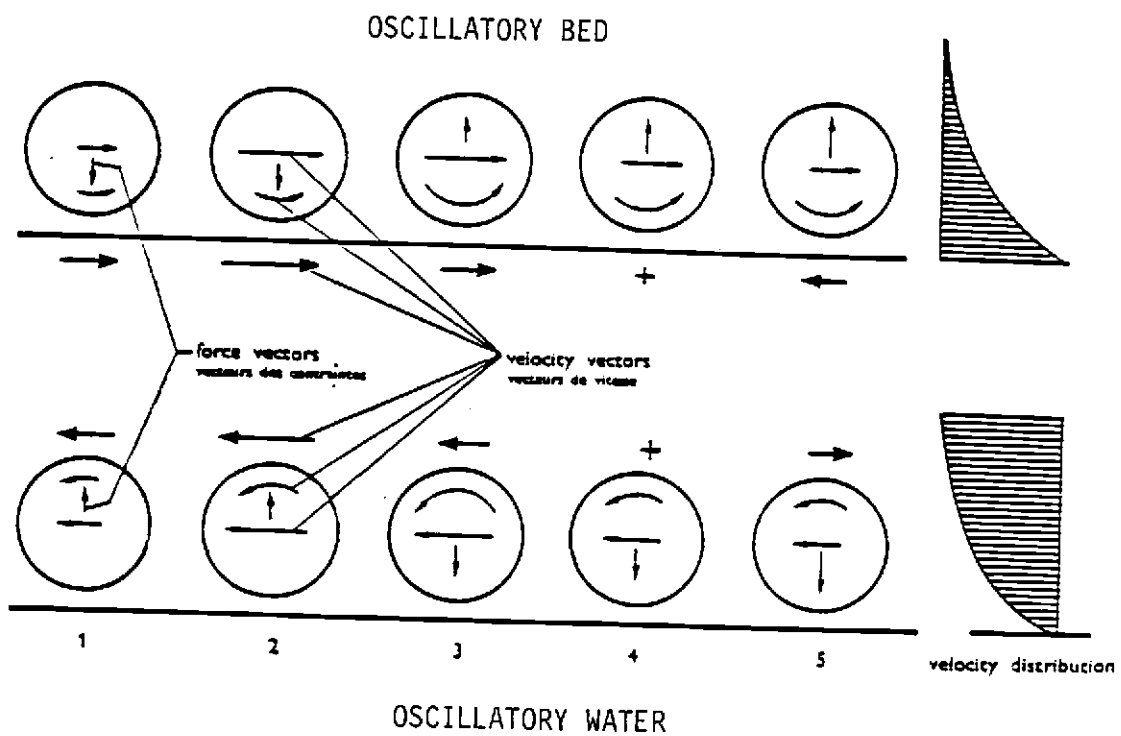
Figure 25.   Forces on Rotating Waves Under Oscillatory Flow
(Source: Silvester, 1970)

oscillating water tunnels to overcome the difficulties associated with oscillating beds and oscillating water. Mogridge (1970) states some problems and limitations associated with use of water tunnels to represent prototype conditions. This includes eddy formation in the bends that are difficult to eliminate completely and which could be carried into the test section of the conduit. The occurrence of any such eddies would initiate unnatural turbulence of the bed. Also, there is a problem due to boundary layer effects from the walls and ceiling of the tunnel. These, in turn, affect the macro-turbulence in the vicinity of the bed. Such distortion increases as velocity is increased, but should not greatly alter conditions for incipient motion, or even for the first stage of dune formation (Silvester, 1970).

Chan et al. (1972) carried out an experiment using a variation of the water tunnel involving a small pipe 5.08 cm in internal diameter which contained a bed of dense particles and was subjected to an oscillatory liquid flow. They studied the effect of varying the liquid density, particle size, and amplitude, and frequency of oscillation.

Water Blocks

To permit reasonable development of macro-turbulence, a more economical approach may be to create a block of water which can be oscillated over a fixed bed. Silvester (1970) suggested a simple method of oscillating a block of water over a tidal bed to accurately reproduce the conditions of the oscillatory fluid motion at the bed beneath a wave train. Mogridge (1970) described this

technique in detail. It involves an inverted box that is driven

back and forth over the stationary flume floor. This technique has

the advantage of reproducing prototype conditions in full scale in

the laboratory with a relatively large working volume of fluid and

sediment to eliminate boundary effects and to be completely

versatile. Some problems could arise due to edge effects from

having a short sediment bed. The system can only be used for

orbital amplitudes of 2.5 ft or less, according to Riedel (1972).

Unfortunately, to the best of my knowledge no studies have been

reported which make use of water blocks.

Wave Basins

Wave basins are often used to study littoral processes.

According to Silvester (1970), a major benefit to studying sediment

transport due to waves in a basin is that the combined action of

waves and currents can be ascertained. Unfortunately, no reports of

such experiments could be found. Wave basins do not represent the

actual wave behavior of the prototype.

In-situ Measurements and Observations

Several investigators have studied sediment transport phenomena

in the sea. Dyer (1980) used underwater television to study

incipient motion, ripple formation and related processes. Others

have used SCUBA and other diving equipment, often recording their

observations using still or moving-picture cameras.

Materials Used

Several types of materials have been used for the laboratory study of sediment transport under oscillatory flow. These include: quartz, coal, steel, glass, plastic pellets, limestone chips, concrete tubes, polystyrene, granulated pumice, pollopas, bakelite, perspex cubes, cane sugar, glass beads, and hematite (iron ore).

These materials have a variety of different sizes and densities. Table 2.2 (presented earlier) includes the range of particle sizes and their densities. Particle sizes ranged from 0.09 mm to 48 mm, which includes very fine sand to coarse gravel. Densities ranged from 1.05 gram/cm^3 to 7.6 gram/cm^3. Most investigators used quartz particles in the sand sizes. Unfortunately, no investigators (to the best of my knowledge) used very fine materials in silt and clay sizes.

Velocity Measurement Techniques

In order to understand the mechanics of the interaction between the wave-induced velocity and the bed, a thorough knowledge of both velocity profiles within the boundary layer and shear stress at the bed is needed. Accurate measurements of the water particle velocities in wave motion are difficult to make. Also, standard methods of measuring velocity in unidirectional flow are often not suitable for use with oscillatory flow where small velocities occur and the flow direction reverses. Kalkanis (1957) gave a brief summary of velocity measurement techniques and the problems associated with each technique. The main techniques are dicussed here.

Pitot Tubes

Pitot tubes normally give a useful output for unidirecional flows above one ft/sec but are not suitable for oscillatory flows due to their slow response to rapid fluctuations. Several investigators, such as Kalkanis (1957, 1964), Parathenlades (1962), Ippen and Drinker (1962), Hwang and Laursen (1963), and Ghosh and Roy (1970), used a specially designed pair of pitot tubes to measure the velocity and shear stress. However, only maximum velocity could be reliably determined with the pitot tubes.

Miniature Propeller Current Meter

Miniature propeller current meters are useful to measure velocities in steady or slowly varying flows due to wind, open channel flow, flow in ducts, or tidal flow. However, Kobune (1978) mentioned that there is a difficulty in using them in waves, especially in laboratory wave tanks, because of their slow dynamic response to high frequency fluctuations. In addition, they are usually not very sensitive to low speed.

Jonsson (1963), Goda (1964), Nece and Smith (1970) and Kobune (1978) measured the velocity under oscillatory flow utilizing miniature propeller current meters. To overcome measurement difficulties with a propeller current meter, Goda proposed an empirical formula to use for estimating the horizontal velocity beneath the wave crests.

Dyer (1980) used four Braystoke rotor flow meters spaced at logarithmically increasing heights up to 2m above the sea bed on a bottom-mounted frame. The frame also held two electromagnetic flow

meters, each measuring the instantaneous vertical and horizontal components of the flow. The analyzed data allowed him to obtain turbulence characteristics near the sea bed.

Propeller current meters usually are provided with calibration curves by the manufacturers. But in most cases, it is advisable to calibrate the current meter for conditions matching the experimental tests. Problems sometimes arise, depending on linear or non-linear behavior. Some other problems, such as insulation failure and severe abrasion of the meter, are associated with use of this equipment.

Photographic Methods with Hydrogen Bubbles

The water particle motion can be visualized and measured with tracers, such as naturally buoyant particles or hydrogen bubbles. The particle velocities in the wave can be measured with the aid of a high speed movie camera. Grass (1970) reported that he obtained accurate results using hydrogen bubbles. However, Riedel (1972) experimented with and rejected the use of the hydrogen bubble flow visualization technique. He used electrolysis to generate a sheet of hydrogen bubbles at a platinum wire suspended in the flow; from analysis of the motion of bubble sheets he mentioned it was possible to obtain a time history of velocity profiles within the boundary layer. However, Riedel discussed three main drawbacks for his rejection of this method: (1) water impurity resulting from foreign organic material; (2) bubble rise velocities; and (3) practical maximum measureable velocity of about one ft/sec.

Hot-Film and Hot-Wire Anemometers

Hot-film and hot-wire anemometry is based on the cooling of the sensor by the moving fluid. The total amount of heat transferred depends on the flow velocity, the difference in temperature between the wire and the fluid, the physical properties of the fluid, and the dimensions and physical properties of the wire. The wire is cooled by heat conduction, free and forced convection, and heat radiation. In general, the effects of radiation and free convection are neglected. The conversion of the anemometer output into velocities requires an equation relating fluid velocities to electric current or potential and to the resistance characteristics of the sensor. Such relationships have been derived on the basis of theoretical and experimental studies of the convective heat transfer from a heated cylinder in a moving fluid. The values of some parameters in equations can be determined by calibrating the hot-film anemometer against some known velocity. Accurate results could be obtained if the tedious calibration procedures are followed successfully.

Hot-film and hot-wire anemometers are common instruments for the measurement of turbulence in air and water flows. Many investigators used this technique to measure the velocities. Blinco and Parthenaides (1970) described the hot-film and hot-wire veleocity measurement and calibration procedures. Raichlen (1967), Yucel and Graf (1973), and Blinco and Simons (1973) measred turbulence with hot-film anemometers in an open flume to obtain the wall shear stress.

When using hot film probes, it is essential that the water be kept deaerated and perfectly clear. Another problem with the instrumentation is cost. Kobune (1978) mentioned several other problems with using these probes for velocity measurement in oscillatory flow. They are the inability of the film sensor to detect the flow direction when the velocity vector is in the plane perpendicular to the hot film axis, the strong non-linearity in the correlation between the flow speed and the output voltage when the flow speed varies over a wide range, and film sensitivity to flows that are parallel to the film axis.

UltaSonic Doppler Current Meters and Laser Doppler Anemometers

Ultrasonic Doppler current meters have been used to measure the velocities in random waves. They can be operated in laboratory wave tanks and in the ocean. The laser Doppler anemometer is the only suitable velocity measuring device that can be used without being immersed in the flows. Riedel (1972) described the Greated's laser velocimeter and reported that it was a highly suitable instrument for laboratory study of waves.

Float Techniques

The float technique provides easy measurement of the surface velocity, but is unsuitable for mesurements near the bed or of the turbulance structure.

Prandtl Tube

The Prandtl tube is a modification of the pitot-static tube for velocity measurement. Some investigators such as Blinco and Partheniades (1971) have used the Prandtl tube to measure the local

time average flow velocity and have reported quite good results.

Heated Thermister

The heated thermister operates on the basis of supplying sufficient current to heat the probe tip to approximately 20^0C above ambient temperature in typical flows.

Heated thermisters have used by Caldwell and Chriss (1979) at the ocean floor to obtain the thickness of the viscous sublayer by measuring the velocity. They reported successful results from using this equipment. The sensory area of the themister used was about 0.02 centimeter, which did not disturb the flow pattern. The power dissipated in the thermister per unit change in temperature is related to the flow velocity. Current speed can be determined to within 0.1 cm/sec.

Shear Stress Measuring Techniques

Brown and Joubert (1969) outlined all the existing methods of wall shear stress measurement for unidirectional flow. Their outline is still valid today. Figure 26, shows a schematic diagram of the wall shear stress measurements taken from their publication.

Riedel (1972) stated that only direct shear stress measurements and wall similarity techniques, in particular the "velocity profile" and "Preston tube" methods have been used for boundary layers with oscillatory flows. However, Inman and Bowen (1962) and Trelear (Riedel, 1972) measured bed shear stress under waves by measurement of wave attenuation. Eliasson et al. (1964) determined bed shear stress by measurement of wave thrust, with results restricted to small-amplitude waves produced in a wave flume.

Wall Shear Stress Measurements

Momentum techniques

Direct measurement

Dye traces

Fully developed flow
in pipes and channels

Wall similarity
techniques

Momentum integral
methods

Velocity profiles

Heat transfer similarity

Similarity of flow about obstacles

Static pressure
holes

Boundary layer
fence

Preston Tube

Stanton tube and
razor blade technique

Figure 26.   Wall Shear Stress Measurements Methods
(Source: Brown & Joubert, 1969)

Direct Measurement Techniques

Riedel (1972) reviewed the methods of direct measurement of shear stress in detail and stated that these methods are independent of the flow phenomenon and, therefore, well suited to the study of wave boundary layers for which the turbulence structure is not yet understood.

Bagnold (1946) used an artificially rippled plate to obtain mean drag. Jonsson (1966) reanalyzed Bagnold's data in terms of maximum shear and equivalent sand roughness and found fair agreement.

Other investigators have used flat shear plates. Two types of such shear meters have bed used: the moment type and floating element device.

Eagleson (1962) and Iwagaki et al. (1965) used moment type shear meters. Their shear plates were suspended from above like a pendulum and the surfaces of the plates were flush with the bed of the wave flume. Forces on the plates caused them to deflect; the resulting movement were sensed at the upper ends of the support rods by shear-sensitive force balances or moment meters. Clyde and Chang (1969) used a dynomometer with strain gauges to measure the forces in the three coordinate directions to find the shear stress. Problems associated with these devices include secondary forces resulting from pressure gradients, possible flow under the plate, and inertial effects.

Floating-element shear meter devices have been used more commonly in unidirectional flow. Instruments of this type are supported from below by a leaf spring or similar system and their

movement under applied shear is recorded by a displacement transducer. Yalin and Russell (1966) used a plate with three thin legs to study long-period waves (2-20 minutes). The deflection of the plate under load was monitored by a displacement transducer. Bursal I (1967) employed a four-legged plate, its deflection was measured by a full strain gauge bridge. Some of the problems encountered include secondary forces and vertical loading.

Wall Similarity Techniques

It is possible to calculate shear stress from the boundary layer velocity profiles if it can be shown that a "law of the wall" concept exists similar to that for unidirectional flow. The methods used can be categorized as velocity profile and Preston tube methods.

Jonsson (1963), Kajiura (1968) and others used the velocity profile method to measure the bed shear stress. Blinco and Simons (1973) and Yucel and Graf (1973) used hot-film anemometers to get velocity profiles and calculate the instantaneous bed shear stress. The typical calculation method, following the example of Bagnold (1963), is to use data from two points of the vertical profile with the logarithmic velocity profile equation to solve for the shear velocity, from which the shear stress can be obtained using the definition equation for shear velocity.

A more direct measure of boundary shear stress can be made with a Preston tube. This device measures the pressure difference in the flow field adjacent to the boundary. This pressure difference gives a means of estimating local boundary shear stress. The technique is

based on the law-of-wall velocity for a turbulent boundary layer and has received extensive use in hydraulic laboratory studies as a means of measuring local boundary shear stress. Nece and Smith (1970) presented a detailed description of the use of a Preston tube in measuring boundary shear stress. They measured shear stress in conjunction with use of a miniature current meter to provide comparison between two techniques as independent indirect measurements.

Teleki and Anderson (1970) also used a Preston tube to measure the shear stress at the bed. They found that the use of a Preston tube is limited under oscillatory flow conditions although its simplicity of construction and applicability to both laminar and turbulent flows is appealing. Riedel (1972) mentioned that strong pressure gradients and rough boundaries under oscillatory flow restrict the use of the Preston tube.

Equipment and Procedure Used for Measuring Suspended Sediment Concentration Under Waves

A variety of equipment has been used in measuring the suspended sediment concentration under wave flow in laboratory experiments. Some of the earlier investigators used a siphon or piston-type suspended sediment sampler. Over time, improvements in sampling techniques and procedures have been made and more-sophisticated equipment has been developed. Included are an optical meter electrical resistor instrument, an electro-optical instrument, and use of the computer for data acquisition.

Parthenlades (1962) obtained suspended sediment samples using a 50 cc pipette with a broken tip to allow the entrance of coarse sediments. The reported sampling time was 40 seconds. The sample was transferred to an immersed 100 cc bottle. Then 10 to 50 cc of water filtered through an HA (0.45 micron) millipore membrane under vaccum, the residue was washed with 30 cc of distilled water and left overnight to dry in room temprature in dessicator containing silica gel. This was following by weighing of the sample.

Hom-ma and Horikawa (1962) and Hom-ma et al. (1963) used the photo-analyzer to measure the time variation of concentration and the mean concentration of suspended sediment over a wave period. Hattori (1969) used an electrical resistance instrument to count the number of sediment particles passing through a given cross section and from this calculated the suspended sediment concentration under a standing wave. Bhattacharya (1971) used an electro-optical instrument for in-situ measurement of sediment in suspension. Das (1971) developed an electro-optical meter for the in-situ measurement of the suspended particle concentration. Mehta and Parthenlades (1975) used a vacuum-filtration technique to determine the concentration. Instrumentation used by Nakato et al. (1977) included an optical type sediment concentration analyzer, a hot-wire anemometer, and IMB data acquisition and control system. Nielsen (1979) used a siphon type sediment sampler to measure the concentration. A bamboo sampler has been used in the open sea for measuring suspended sediment.

Types of Experimental Apparatus for Unidirectional Flow

A variety of experimental apparatus and techniques has been used to study sediment transport under unidirectional flow. Extensive reviews of the apparatus and techniques are reported elsewhere. Here, only an extremely brief summary is given.

Many different types of experimental apparatus have been used in the study of sediment suspension under unidirectional flow. These include:

Flumes

　Straight, Circular

Models

Pipes

Pinhole erosion devices

Submerged jet apparatus

Water tunnels

Rotating cylinders, disks, an impellers.

For fine-grained sediments, the test material is usually placed in the test section in one of three ways. These are: (1) placed undisturbed sediment; (2) sediment deposited onto the test surface from suspension; and (3) remolded sediment.

Beyond the velocity measurement techniques already described under oscillatory flow, water velocity by ultrasonic flow meter was measured by Schuster (1975). This meter uses two ultrasonic transceivers strapped to the outside of a pipe wall or submerged in an open channel. He described this technique and how to measure the velocity and discharge. He found the principle of ultrasonic

velocity measurement and equipment to be generally satisfactory.
Dracos (1980) made instantaneous velocity measurements by means of a
probe based on the principle of the Prandlt tube. Griffith and
Grimwood (1981) used an electomagnetic flow meter as a basic sensing
instrument to measure the turbulence.

Beyond the techniques mentioned for sampling suspended
concentration under waves, for unidirectional flows pump systems
have been used to obtain time-integrated samples and in-situ
collecting traps have been used to obtain instantaneous bulk water
samples. Indirect measurements have also been made that relate
turbidity to light attenuation. Ward and Chikwanha (1980) discussed
these techniques and mentioned that reduction in the intensity of a
light beam has the advantage of working satisfactorily over the
range of silt and coarse clay sizes, giving reasonable accuracy for
large and small concentrations. Conventionally, suspended sediment
sampling has required laboratory analysis involving evaporation and
weighing or filtration and weighing. These methods are
time-consuming and subject to errors. All methods must be
indiviually calibrated.

III. FIELD STUDY OF TRANSPORT-SEDIMENTATION-RESUSPENSION CYCLE
FOR FINE-GRAINED SEDIMENT

Selection of Field Site and Study Approach

The first experimental phase of this dissertation research, after literature review, involved gaining insights to suspension and transport processes under natural circumstances. A complex natural hydraulic environment was studied: a tidally influenced lake fed by and draining into two large rivers and subject to wind-generated waves. The field study site selected was Sturgeon Lake, Oregon. This setting provided opportunity to observe sediment deposition and resuspension due to both unidirectional and oscillatory flow. The sediment involved was predominately silt-size material with some clay and a small amount of sand and organic matter.

A program to investigate sediment transport processes was developed for this dissertation concurrently with a broader shoaling investigation of Sturgeon Lake. For purposes of the dissertation, the deposition, resuspension and transportation of fine-size sediment was analyzed using a variety of computational and sampling techniques. Extensive work was conducted at the lake and in the surrounding rivers over an eight-month period.

This chapter summarizes those aspects of the field study relevant to sediment resuspension. The experimental techniques were generally of a conventional nature and thus are described only rather briefly. For full details of the study, the reader is referred to two co-authored technical reports that resulted from the shoaling study and that contain extensive information of interest

but not essential to the further development of this dissertation. These reports are (1) Physical, Chemical and Biological Description of Sturgeon Lake (Klingeman et al., 1982a) and (2) Sturgeon Lake Problem Diagnosis, Options for Restoration, and Recommendations (Klingeman et al., 1982b).

The Shoaling Problem at Sturgeon Lake

The Sturgeon Lake study was initiated to investigate the probable cause of shoaling and massive siltation in the lake and to determine how to solve the siltation problem. During the past four decades, Sturgeon Lake has become an off-channel sedimentation basin for the Willamette and Columbia Rivers. Diking, dredge spoil disposal, blocking of creeks, and upriver reservoir flood control operations have contributed to this change. Sediment-laden river water fills the lake due to each big storm or snowmelt runoff. Water depths in the lake increase by more than 3 meters (10 feet) feet at such times. Siltation and shoaling results. As river and lake levels drop, wind-waves keep the system stirred up and cause currents that, together with tidal action, distribute sediment and organic matter throughout the lake. When the lake becomes quite shallow in late summer, with an average depth of 0.5 m (1.5 ft), wind-generated waves are the main cause of sediment resuspension. Tidal currents permit sediment redistribution in the lake at such times.

Characteristics of Sturgeon Lake

Physical and Hydrological Setting

Sturgeon Lake is a large, shallow, mud-bottomed lake within Sauvie Island. The Island is located at the confluence of the Willamette and Columbia Rivers. The mouth of the Willamette River divides into two channels around the island, with the longer one known as Multnomah Channel.

Over the years, diking projects on Sauvie Island and dredging along the Columbia River have almost completely enclosed and isolated Sturgeon Lake from the surrounding rivers. Today, the only significant water entry to and discharge from the lake is through the Gilbert River, which connects the lake with Multnomah Channel.

There are two seasons for major streamflow: winter and late spring. These result from winter rains and spring snowmelt. Reservoir flood control modifies the natural pattern. Lowest discharges in the Columbia River near Sturgeon Lake under natural conditions occur in late autumn. Reservoir flow augmentation releases have altered this pattern somewhat.

Sturgeon Lake and the adjacent Columbia and Willamette Rivers are tidally influenced by the Pacific Ocean at most times of the year. The tidal range in the rivers near Sturgeon Lake is typically on the order of 0.6-1.0 m (2-3 ft.) when river discharges are low or moderate. It becomes imperceptible when river discharges are large.

Hydrodynamics of Sturgeon Lake

Water motion in Sturgeon Lake is of great importance to describe the sediment processes in the lake. Three basic phenomena affect the water motion: 1) runoff inflow, 2) tides, and 3) wind-waves. The effects on water motion differ, as noted in the following paragraphs. Two other potential phenomena, Coriolis accelerations and water stratification, were determined to be insignificant.

Runoff Inflow

The only significant water entry to and discharge from the lake is through the Gilbert River. Because the Gilbert River connects the lake to Multnomah channel and thus to the Willamette and Columbia Rivers, the flow variation in the Gilbert River is governed by the seasonal flow patterns in the Willamette and Columbia Rivers. Therefore, Sturgeon Lake is strongly influenced by runoff inflow through the Gilbert River during two seasons: winter and late spring. The winter peak discharges are usually less severe than those in late spring.

The flow into and out of Sturgeon Lake through Gilbert River occurs at two locations, due to a breach of the river bank. Figure 27 shows the general nature of this flow during ebb and flood tides. The same pattern applies for the rising and falling stages of the Willamette and Columbia Rivers, except that considerable overtopping also occurs at low banks of the Gilbert River and facilitates the filling and draining of the lake at highest stages.

OREGON

LOCATION MAP

N

FLOOD TIDE

The Wash

Gilbert
River

North
Sturgeon Lake

South
Sturgeon
Lake

Lake Neck
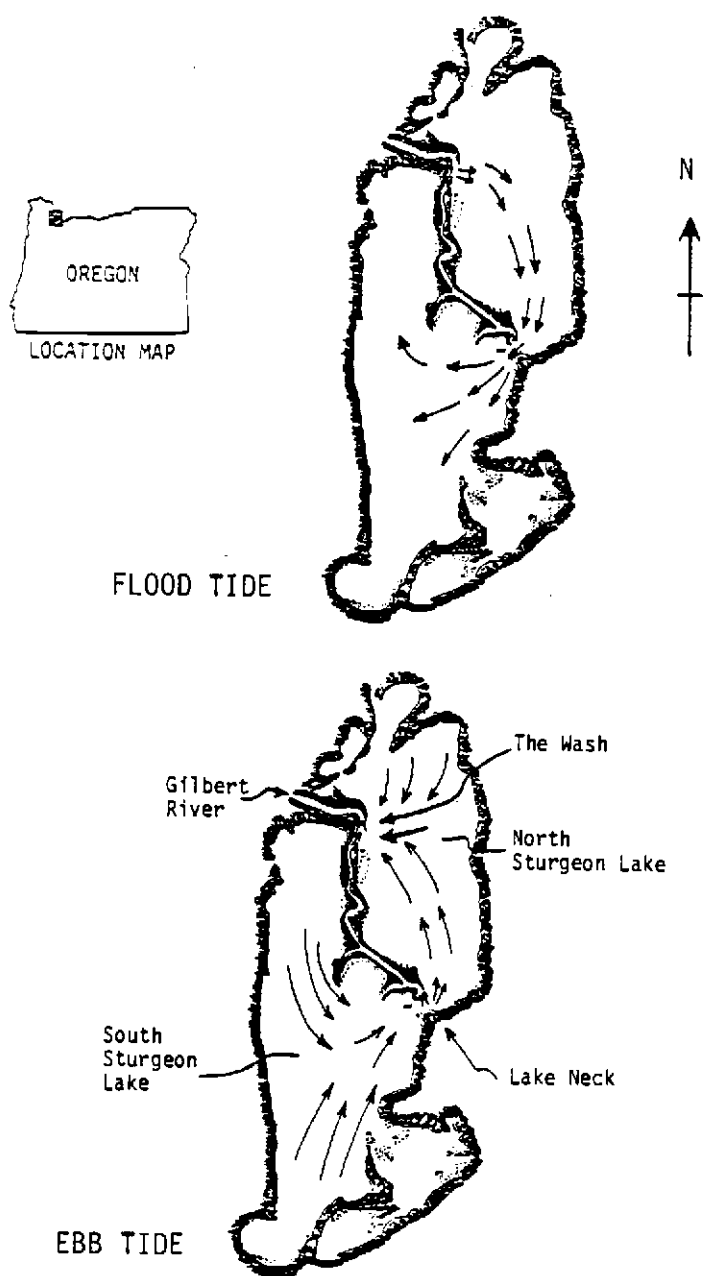
EBB TIDE

Figure 27.   Flow Into and Out of Sturgeon Lake Through
Gilbert River During Flood and Ebb Tides

<u>Tides</u>

Sturgeon Lake is subject to twice-daily high and low tides that vary in vertical range. This tidal action diminishes as it moves through the Gilbert River after passing through the Multnomah Channel, Willamette and Columbia Rivers from the Pacific Ocean. The tidal range of the lake is typically on the order of 0.1 - 0.2 m (0.3 - 0.6 ft) when river discharges are low or moderate and the corresponding mean lake level is on the order of 5 feet, msl. For brief periods of the year when river discharges are large, the tidal influences are markedly diminished and may become imperceptible at stages above 15 feet, msl.

<u>Wind-Waves</u>

Two dominant patterns were observed for wind direction at Sturgeon Lake. Strong winds blew from the south to the north in winter and from the north to the south in the summer. These winds readily generated waves in the lake because of the appreciable lake length (fetch) in the direction of the prevailing wind. The waves were frequently 0.5 feet in height and occasionally were almost one-foot high with some partial breaking of crests.

Wind on a shallow body of water not only produces waves, but also induces a drag which moves the surface water in the direction of the wind. The effects of such motion are transmitted downward through the water column to the lake bed.

During summer months, when Sturgeon Lake is very shallow, wind-waves have the greatest effect on mixing the water. Wave

action in shallow areas of the lake was found to be an important agent in the resuspension of bottom sediments. Tidal currents, which by themselves may not have the strength to suspend the sediments, are then able to transport the wave-suspended sediment to deeper parts of the lake.

Winds are also capable of producing a superelevation of water level in the downwind end of a fetch, which in turn produces a counter circulation of water. Such circulation and the waves induced by the wind increase the intensity of the mixing. These events may have occurred in Sturgeon Lake, although verifying data are lacking.

Lake Water Residence Time

A "residence" or "turnover" time for water in Sturgeon Lake can be estimated. One method for defining and estimating this term is to compare the volume of water contained in a lake with the volume of inflow or outflow over some time period. For Sturgeon Lake, the time of year selected has an extreme effect on water volume of the lake. Hence, residence time is a highly variable quantity in the lake.

The calculated late-summer residence time for water in Sturgeon Lake is about two days. This is based on typical conditions: a lake level of 5 feet, msl, a corresponding water volume of about 2,900 acre/feet and average tidal fluctuations of about 0.4 feet in the lake. Such conditions cause a twice-daily exchange of 760 acre-feet of water through the Gilbert River.

A typical winter between-storm residence time for water in

Sturgeon Lake is about four days. This is based on a lake level of 10 feet, msl, a corresponding volume of about 19,000 acre-feet, and a tidal fluctuation of about 0.5 feet in the lake which twice-daily exchanges about 2,400 acre-feet of water through the Gilbert River.

If the lake level rises to 14 feet, msl, due to winter storm runoff, the lake volume will be doubled (i.e., the inflow will match the initial contents). Since tidal effects are minimal at such times, lake residence time depends on duration of storm runoff and typically is about one week. Larger storm runoff or snowmelt runoff will lead to longer residence times for water in Sturgeon Lake.

The calculated residence times--two to four days for lake water at most times of year--are quite short. But in spite of this, it is doubtful if all of the water in the lake actually exchanges within this interval. More likely, the tides have a plunger-like effect on the water on Sturgeon Lake, rather than causing complete mixing (see Figure 27). Rising tides probably push the existing lake water away from Gilbert River. The added water results in a rise of lake level. Falling tides cause the lake level to drop and allow similar volumes of water to drain back out through Gilbert River. The outgoing water probably is a limited mixture of the recently added river water with lake water from North Sturgeon Lake. The mixing is unlikely to be very complete. Subsequent tides will bring back into the lake some of the same water that just left the lake but did not get beyond the Gilbert River mouth before the tidal reversal occurred. Meanwhile, mixing of North Sturgeon Lake and South Surgeon Lake water occurs due to flows through the lake neck. The

combined result is that water In North Sturgeon Lake probably does have a short residence time of a few tidal cycles but water In South Sturgeon Lake probably Includes particles that remain In the lake for several weeks or even for a full season.

This variable residence time for water In different parts of the lake Is quite significant to suspended sediment transport. Some suspended solids are likely to have long actual residence times. This Is largely due to the single Input-output point for lake water exchange. In a through-flow system, water exchange would be more effective.

Water Circulation

Water circulation In Sturgeon Lake Is due to several factors: tidal currents, filling and draining of storm runoff and snowmelt runoff, and wind-stress currents. The points of river Inflow and outflow to the lake also affect water circulation.

The circulation patterns In Sturgeon Lake were observed by releasing floats at many locations and mapping their movement. This was done at various phases of tidal cycles. The floats were weighted at the bottom of vertical submerged dowels, so that water current rather than wind would determine the direction of float movement.

At The Wash (see Figure 27) during flood tide, river Inflow to the lake tends to move south, due to Its momentum upon leaving the river channel. On ebb, water moves to The Wash from all directions but a stronger current frequently moves counterclockwise along the north edge of North Sturgeon Lake (evident on aerial photographs

when wind stirs up sediment). At the lake neck, flood tide from the Gilbert River often turns into North Sturgeon Lake rather than South Sturgeon Lake. Water often seems to move through the neck between the north and south parts of the lake without regard to the presence of the river there.

Sources of Sediment Input

The major external sources of sediment input to Sturgeon Lake under present conditions of river regulation are identified as:

1. Columbia and Willamette Rivers during high runoff and storms;

2. Bank and bed erosion of the Gilbert River;

3. Local soil erosion from land areas surrounding Sturgeon Lake;

In addition, there are sources within the lake boundaries. These include:

1. Shoreline erosion of Sturgeon Lake;

2. Sediment input to the main compartments of Sturgeon Lake from small isolated and semi-isolated lake areas; and

3. Redistribution of sediment within Sturgeon Lake.

Lake Water Quality

The water quality of Sturgeon Lake generally reflects conditions
in the Columbia and Willamette Rivers. Numerical values for
conserved properties (such as total dissolved solids) vary according
to the mixing of these river flows in Multnomah Channel and Gilbert
River. Numerical values for other parameters, especially
non-conservative parameters such as dissolved oxygen, water
temperature, and pH, may be greatly affected by the internal
"sources" and "sinks" within the lake, and thus may differ from
baseline values observed in the adjacent rivers.

Sturgeon Lake turbidity and suspended solids concentrations are
generally high, due to resuspension of bottom sediment (an internal
source). Secchi depths (depths of visibility in water) are
generally less than 0.5 m (1.5 feet), again indicative of high
turbidity from resuspended sediment. Although about 20-25 percent
of total suspended solids are volatile, indicating suspended organic
matter from internal sources, most of the suspended solids are
inorganic solids (e.g., small silt and clay) that originate from
riverine sources, prior to lake deposition and resuspension.

During most of the year, the levels of lake organic matter are
more than twice the levels in the nearby rivers. Probable internal
sources of organic matter include algal growth and die-out,
shoreline vegetative matter, and wastes from water birds, fish and
cattle.

Dissolved oxygen levels remain near saturation throughout the
water column. The pH of the water is generally in the near-normal

range of 7-8. The observed conductivity and dissolved-ion values are low and are typical of dilute fresh waters. Alkalinity and hardness are also in the range typical of relatively soft, low-alkalinity waters of the region.

The observed biological oxygen demand of lake water is low but indicative of some input of organic matter. The observed chemical oxygen demand of lake water is sufficient to suggest that much of the organic matter in the water column is a refractory form (e.g., humic substances).

Concentrations of total phosphorus and orthophosphorus are indicative of a moderate level of enrichment of lake water. Total phosphorus concentrations are generally below the limit indicative of highly eutrophic conditions. Observed nitrogen levels also appear to indicate a moderate enrichment of lake water.

Sediment Characteristics

Island Morphology and Soil Characteristics

Sauvie Island originated from alluvial deposits from the Columbia and Willamette Rivers. Natural ground elevations (excluding dikes) near Sturgeon Lake generally vary between 5 and 15 feet, msl. Soils in the Sauvie Island area are similar to those in the Willamette Valley floodplain. They are predominantly deep, silty, moderately dark, somewhat acid soils, commonly found in poorly drained areas. The soils are typically several feet deep.

Physical Characteristics of Suspended Sediment

Suspended sediment in river and lake water was routinely monitored on the basis of Secchi disk reading, turbidity meter reading, and (occasionally) photometer reading. Water samples of 1-liter size were also routinely collected and analyzed to determine the concentration of suspended sediment, as given by the non-volatile part of total suspended solids present. Larger suspended sediment samples were periodically collected in 20-liter containers to provide enough material for determining the particle sizes present and their relative proportions.

The principal results of these analyses are presented in Table 7 and complete results are given in Appendix N, Part 1 in Klingeman et al. (1982a). It can be seen that the suspended sediment carried in Multnomah Channel during winter runoff includes a little fine sand and about 25 percent clay, in addition to the predominating silt fraction. Most of the silt is fine-sized. Sturgeon Lake suspended sediment, in contrast, is about 50 percent clay, with fine silt comprising most of the remainder. Gilbert River suspended sediment has varying combinations of the lake and channel suspension characteristics.

Physical Characteristics of Lake Bed Sediment

Lake bed sediment samples were collected throughout the north and south portions of Sturgeon Lake for the analysis of particle size distributions. Bed material samples were also collected from

Table 7. Particle Size Distributions for Suspended Sediment in Sturgeon Lake and Nearby Rivers

Sampling Location and Date		Concentration mg/l	Particle Size Distribution, Percent[1]				
			Sand	Silt			Clay
				Coarse	Medium	Fine	
South Sturgeon Lake @ Staff Gage							
@ water surface	8/19/81	--	0	1	0	33	36
" " "	10/16/81	--	0	1	2	37	60
" " "	12/8/81	21.0	3	2	8	17	70
" " "	1/19/52	--	2	3	1	41	53
@ 2 m depth	2/23/82	18.8	1	0	3	36	60
@ 1 ft. above bed	"	20.6	2	0	3	32	63
@ water surface	3/11/82	28.6	0	0	3	81	16
North Sturgeon Lake @ Staff Gage							
@ water surface	11/21/81	--	1	1	12	43	43
" " "	12/4/81	--	4	4	3	44	47
" " "	12/8/81	56.4	1	0	2	36	61
@ 2 m depth	2/23/81	62.8	0	1	1	37	61
@ 1 ft. above bed	"	65.1	0	1	2	59	38
" " " "	3/2/81	65.1	1	2	1	48	48
@ water surface	3/11/82	18.6	0	1	5	66	28
Gilbert River							
@ mouth @ 1 m above bed	2/19/81	46.0	9	3	16	63	9
@ Wash " " " " "	2/27/81	--	10	4	11	69	6
@ Wash @ water surface	12/4/81	--	2	1	7	43	47
" " " " "	12/8/81	73.2	0	3	10	37	50
" " @ water Surface	2/23/82	55.6	1	1	2	64	33
" " @ mid-depth	"	61.4	0	2	0	47	51
" " @ 1 ft. above bed	"	64.0	0	1	0	34	65
" " @ 0.5 ft. " "	"	69.1	1	3	11	43	42
" " @ water surface	"	12.2	0	1	3	59	37
Multnomah Channel Upstream of Gilbert River							
@ water surface	12/8/81	93.6	2	3	17	38	40
@ 2 m above bed	2/19/81	43.6	7	4	12	61	16
@ water surface	2/15/82	--	2	11	13	50	24
" " "	3/11/82	13.6	2	1	19	60	18

[1] Sand: larger than 0.062 mm
Silt: coarse (0.062-0.031 mm), medium (0.031-0.016 mm), fine (0.016-0.002 mm)
Clay: smaller than 0.002 mm

the Gilbert River, Multnomah Channel, Willamette River, and Columbia River for comparative information on particle size distributions.

Table 8 summarizes the particle size distribution data for sediment found in the bed of Sturgeon Lake and nearby river beds. Figure 28 shows the particle size distributions for the bed sediment of Sturgeon Lake. Detailed results are presented in Appendix N, part 2 in Klingeman, et al. (1982a). Additional data on volatile solids and moisture content are included in Appendix O in Klingeman et al. (1982a) for a few lake bed samples.

The data show that the bed is predomiantly silt. In some areas, the clay content may each 25 to 35 percent. Where the currents are strong, the sand content may reach 25 to 30 percent. The bed of Gilbert River consists almost exclusively of fine sand, except near the mouth where some medium and coarse sand also occur. The Multnomah Channel bed consists of medium and fine sand. The Willamette River bed upstream of Multnomah Channel consists of fine sand and silt in roughly equal proportions. This difference from Multnomah Channel may be due to greater water depths where tidal currents may inhibit the net downstream transport of bed material. The bed of the Columbia River upstream of the Willamette is variable due to the flow variability caused by two channels and an island. Fine sand and silt predominate, based on local sampling. The bed of the Columbia River opposite Sturgeon Lake near Diary Creek and Reeder Beach is much coarser, consisting of gravel and all sizes of sand.

Sturgeon Lake bed sediment samples have moisture contents

Table 8.   Particle Size Distributions for Lake and
River Bed Sediments

Sampling Location	Particle Size Distribution, Percent[1]			Volatile Solids Present, %
	Sand	Silt	Clay	
Sturgeon Lake				
South, @ staff gage	0	75	25	3.7
" , between floats 3 and 5	26	52	22	3.3
" , @ float 11	0	66	34	5.5/4.8
" , @ float 9	3	61	36	5.0
At lake neck (float 18)	30	47	23	3.5
North, @ staff gage	10	60	30	4.0/3.4
" , @ northeast corner	1	68	31	3.3
Gilbert River				
@ lake neck staff gage (mid channel)	55	27	18	4.2/6.1
0.5 mi. upstream of The Wash (mid channel)	95	*	*	
Downstream of The Wash (near right bank)	64	*	*	
" " " " (mid channel)	96	*	*	
0.7 mi. upstream of mouth (mid channel)	92	*	*	
@ mouth (near left bank)	92/66	*	*	
" " (mid channel)	52/78	*	*	
" " (near right bank)	53	*	*	
Multnomah Channel				
Upstream of Gilbert River (mid channel)	100	0	0	
@ Bybee House (mid channel)	99	*	*	
Willamette River				
Upstream of Multnomah Channel (mid channel)	51	47	2	
Columbia River				
Upstream of Willamette River (mid channel	99	1	0	
" " " " (near Hayden Island)	39	60	1	
" " " " (edge of main channel)	96	4	0	
@ Dairy Creek (on beach)	99	*	*	
" " " (150 ft. from beach)	99	*	*	
" " " (400 ft. " ")	94	*	*	
" " " (600 ft. " ")	100	0	0	
" " " (900 ft. " ")	100	0	0	
@ Reeder Beach (off navigation pile 28)	100	0	0	

[1] Sand: Larger than 0.062 mm
Silt: between 0.062 and 0.002 mm
Clay: smaller than 0.002 mm

* Insufficient fines for hydrometer test
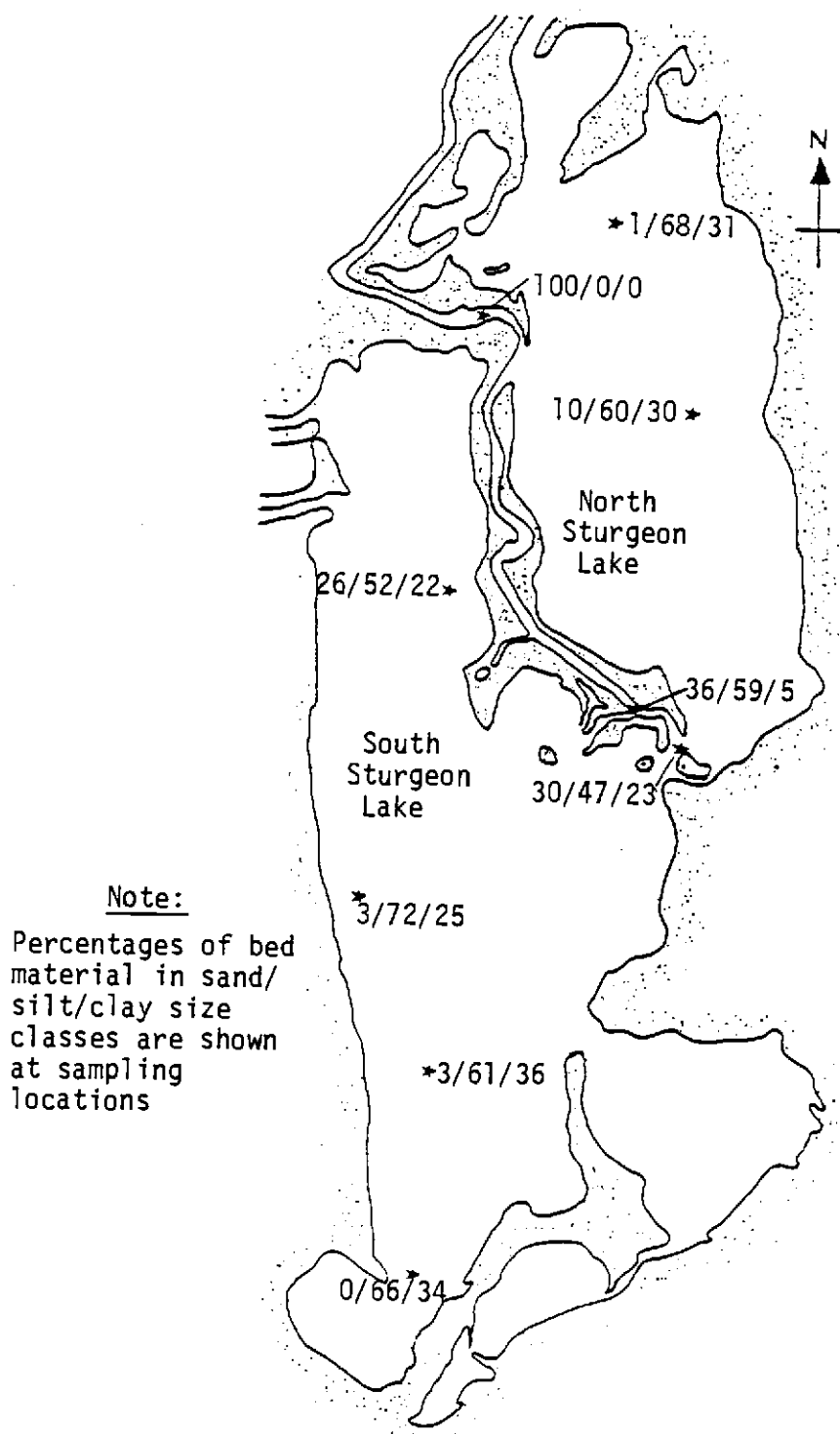
Figure 28. Bed Material Particle Size Characteristics
For Sturgeon Lake

ranging from 35 to 59 percent by weight. These large values are
indicative of poor consolidation. This observation is consistent
with the premise that wave action in the lake greatly disturbs the
bottom sediment.

Sturgeon Lake bed sediment samples contain 3 to 6 percent
volatile solids. These moderate values are indicative of
accumulative debris from algae and other organisms that grow in and
settle out from the enriched lake water. No pieces of roots,
plants, other macro-scale organic matter were noted in these
samples.

Observed Winter Sedimentation Rates

Experiments were conducted in Sturgeon Lake to determine the
upper limiting rate of sedimentation during winter storm runoff and
the size characteristics of depositing material. Buckets were
placed in different parts of the lake for various periods of time.
Sediment could readily settle into the buckets. However, the bucket
walls protected the settled material so that it was not likely to be
scoured and resuspended by the lake currents or by fish.

Table 9 summarizes the data on particle size distributions and
volatile solids. The complete data are given in Appendix N, Part 3
in Klingeman et al. (1982a). It can be seen from Table 9 that fine
and medium silt predominated in the fresh deposits. Some sand and
clay was also present.

Of particular interest is the comparison of these results with
the composition of suspended sediment (see Table 7) and of the lake
bed sediment (see Table 8). The overlying water may contain about

Table 9. Particle Size Distributions for Freshly Deposited
Suspended Sediment in Sturgeon Lake

| Bucket Location | Residence Period | Particle Size Distribution, Percent[1] | | | | | Volatile Solids Present in Silt and Clay % |
| | | Sand | Silt | | | Clay | |
			Coarse	Medium	Fine		
North Sturgeon Lake							
@ staff gage	12/4/81-1/19/82	15	19	31	20	15	4.3
@ staff gage	1/19/82-3/24/82	4	4	47	35	10	4.8
@ staff gage	2/13/82-3/24/82	5	4	21	57	13	7.3
Between floats 12 & 13	2/9/82-3/24/82	1	6	31	53	9	7.7
South Sturgeon Lake							
@ water level recorder	12/4/81-2/9/82	1	1	20	61	17	6.2
@ float 4	2/9/82-3/24/82	5	0	33	53	9	7.0
@ float 11	2/9/82-3/24/82	1	1	17	71	10	7.8
@ water level recorder	2/13/82-3/24/82						
high-well bucket		2	2	32	58	6	8.6
low-wall bucket		4	1	35	53	7	8.4

[1] Sand: larger than 0.062 mm
Silt: coarse (0.062-0.031 mm), medium (0.031-0.016 mm), fine (0.016-0.002 mm)
Clay: smaller than 0.002 mm

50 percent clay and the lake bed may contain 25 percent clay, but the fresh winter deposits at these same locations only contain about 10 percent clay. The implication is that the clay carried in suspension with winter runoff tends to remain in suspension (rather than settle out) because of turbulence caused by the high velocities and large volumes of water exchanged into and out of the lake. Yet, clay must settle out in some parts of the lake at some seasons, followed by its redistribution and mixing with other bed sediment due to wind-wave agitation and tidal currents.

Chemical Characteristics of Lake Bed Sediment

Chemical analyses were made of lake bed sediment from several sampling locations in North and South Sturgeon Lake and from the lake end of Gilbert River. These analyses included sulfide and seven metal ions: iron (Fe), manganese (Mn), lead (Pb), zinc (Zn), copper (Cu), cadmium (Cd), and mercury (Hg). These can be toxic to aquatic organisms or have other adverse effects if present in high concentrations. The data obtained are summarized in Appendix O in Klingeman, et al. (1982a).

Measurable levels of sulfides averaged 60 micrograms per gram (μg/g) of sediment, dry weight. This is a clear indication of anaerobic conditions in the bottom sediment and of subsequent sulfate reduction. (The measured concentrations may be typical of anaerobic lake sediments but are much lower than for estuarine sediments where sulfate is much more available.)

The average numerical values obtained for the seven metal ions, expressed as concentrations in μg/g, were: Fe, 20,000; Mn, 370; Pb,

26; Zn, 130; Cu, 30; Cd, 1; and Hg, 170 µg/g. None of these
concentrations is large enough to cause concern regarding toxicity
to aquatic organisms. The concentrations of heavy metals (cadmium,
copper, lead, zinc, mercury) are higher than would be expected for
clean sediment but are much below those levels to be expected for
highly contaminated sediment.

Bottom Sediment Turnover and Consolidation

The relatively flat lake bottom and the fairly uniform
size-distribution of lake sediment are indicative of a well-mixed
sedimentation environment. Bottom sediment is consistently
dominated by the silt size range throughout the lake, except for
locally coarser sediment near the Gilbert River. There are no lake
zones dominated by clay-size bottom sediment. Hence, no "quiet"
zones of the lake are indicated where enhanced sedimentation occurs.

Wind-wave agitation of bottom sediment, coupled with
wind-generated and tide-generated currents, is a major process in
keeping the lake bed unconsolidated. Fish, benthic (bottom)
organisms, and boat traffic also contribute to the turnover of
bottom sediment and inhibit its consolidation. The fine particle
size of this sediment is another factor contributing to slow
consolidation.

The input of a relatively large amount of organic matter to the
lake from aquatic and terrestrial plants and animals results in a
high percentage of organic matter accumulating in bottom sediment.
This organic matter inhibits consolidation of bottom sediment.

The consolidation and density of lake bed sediment are not

uniform through the lake. Sediment which is seasonally exposed to
air along the lake margin tends to be denser than sediment in
continually-submerged portions of the lake. (Gravitational drainage
of water from the exposed sediment and subsequent shrinkage of the
sediment upon drying lead to its consolidation). Exceptions occur
in deeper drainage features of the lake near present or historical
rivers and creeks, where bed sediment may be coarser (e.g., off Coon
Point, a long finger of land in the southeast part of South Sturgeon
Lake, where there once was a creek channel before diking occurred).

As sediment accumulates on the lake bed over the years, the
added weight of new material should help consolidate the underlying
material. However, for the continually submerged finer-sized
sediment containing organic matter that is found in Sturgeon Lake,
consolidation occurs very slowly over many years. Only limited
vertical consolidation was evidenced in the top four feet of the
lake bed sediment, which was sampled at several locations.

Insights Gained From Sturgeon Lake Study

The Sturgeon Lake field study involved a setting with a variety
of flow conditions that influenced the transport of fine-grained
sediment. The general features of pertinent natural sediment
transport processes could be distinguished or speculated upon. Even
though highly complex, these processes appeared to be explorable by
means of simplified experiments conducted under controlled
laboratory conditions, so that elements of the processes might be
quantified.

The processes of silt-clay transport, sedimentation and

resuspension in Sturgeon Lake were observed to be subject to several conditions. These include tidally-induced currents, wind-wave agitation and flow, runoff inflow, benthic organisms, scour from fish, and physical and chemical effects of the water and sediment.

Reduced flushing of the lake in recent decades has allowed much of the incoming suspended sediment to be retained. The relatively flat lake bottom and the fine-sized particles comprising the lake sediment demonstrate the effects of having a well-mixed sedimentation environment. Bottom sediment was consistently dominated by the silt -clay sizes. This suggests that considerable resuspension and redeposition occurred throughout the system due to wind-wave and tidally induced flows. Both oscillatory and unidirectional flow were clearly involved. The inorganic sediment particles were well-mixed with organic matter and were not well consolidated. This too is indicative of a state of frequent disturbance of the bottom sediment.

Tidal fluctuations in the lake, especially during times of the year when lake and river levels were low, caused considerable tidally-induced water inflow and outflow. This caused much mixing and exchange of river and lake water. Because river sediment concentrations were low, this offered opportunities for seasonal export of sediment from the lake because of the significant disturbance of the lake bed by wind and tides.

During high flow periods, the tidal effects diminished, and river runoff contributed major water and sediment inputs to Sturgeon Lake. Most of this sediment deposited within the lake system,

resulting in a seasonal net import of sediment to the lake. When the river levels later dropped, the tidal effect and wind agitation were again enhanced and particles were susceptible to resuspension and transport out of the lake system.

Wind blowing across Sturgeon Lake created waves which agitated shallow sediment deposits. The disturbed material was resuspended and transported about the lake by tidal and wind-induced currents. Some of the material was carried out of the lake in this manner.

Wind-wave agitation of bottom sediment, coupled with wind-generated and tide-generated currents, was observed to be a major process in keeping the lake bed unconsolidated. Fish, benthic organisms, and boat traffic also contributed to the turnover of bottom sediment and inhibited its consolidation.

The degree of consolidation and the density of lake bed sediment were not found to be uniform throughout the lake. Sediment which was seasonally exposed to air along the lake shoreline tended to be denser than sediment in continually-submerged portions of the lake.

The input of a relatively large amount of organic matter to the lake from aquatic and terrestrial plants and animals resulted in high percentage of organic matter accumulating in bottom sediment. This organic matter inhibited consolidation of bottom sediment.

Sturgeon Lake turbidity and suspended solids concentrations were generally quite high for a lake and were more indicative of river levels. However, these high sediment levels in the lake were primarily influenced by resuspension of bottom sediment rather than riverine sediment input.

Regarding the physicochemical influences that might affect silt-clay transport, several features were noted. Dissolved oxygen levels remained near saturation through the water column. The pH of the water was generally in the near-normal range of 7-8. Conductivity and dissolved-ion values were typical of dilute fresh waters. Alkalinity and hardness of the lake waters were also in the range typical of the relatively soft, low-alkalinity waters of the Pacific Northwest. Measurable levels of sulfides in bottom sediment was a clear indication of anaerobic conditions and subsequent sulfate reduction.

The year-around high turbidity of the lake water has greatly limited light penetration of the lake and has thus inhibited the growth of rooted aquatic plants in water more than several inches deep. Because rooted plants help to stabilize the sediment bed, the limited aquatic plant life at Sturgeon Lake indicate a lack of such bed stabilization.

The high amount of fine organic matter in Sturgeon Lake, both in suspension and in solution, was due to algal growth and die-out, shoreline vegetative matter, and wastes from water birds, fish and cattle. The organic matter incorported in the bed material tended to make it be less dense and less consolidated.

Entrainment of fine-grained sediments in Sturgeon Lake appeared to occur due to flow-induced shear stress at the sediment-water interface in excess of the inter-particle cohesive force of the surficial sediment. Suspended sediment particles in the water column appeared to exist as individual or bonded particles of

various sizes, depending on the hydrodynamic, chemical, and biological conditions during the entrainment process. Entrainment occurred primarily as a surface phenomenon, except when boat propellors or fish movement caused localized erosion and scour of the bed. Hydrodynamic forces were assumed to act within the relatively thin bottom boundary layer and to play a predominant role in causing entrainment of sediment. The entrainment process was assumed to also depend on properties of sediment and properties of interstitial and overlying water.

Thus, a general understanding was gained of the transport, deposition, and resuspension processes for silt-clay sediment in a shallow-water environment where oscillatory and unidirectional flows occurred, both separately and together. From these insights, simplified oscillatory and unidirectional flow conditions could be identified for followup detailed laboratory investigation to simulate the wind-wave, tidally-induced, and storm-runoff conditions of a natural environment. Also, a given sediment was available to use having known properties and for which prototype observations were available for incipient motion, resuspension, transport, and deposition.

IV. LABORATORY EXPERIMENTATION METHODS

A series of experiments were conducted on incipient motion of naturally deposited fine-sized sediment from Sturgeon Lake. Tests were performed during 1983 using two flumes in the Oregon State University Hydraulics Laboratory: one with a flap-type wave board and one with a throughflow or recirculating system. The physical and chemical characteristics of fine-sized sediment were previously determined. Density and consolidation characteristics of the fine-sized sediment were determined with a bench type laboratory experiment.

Apparatus and Techniques

Apparatus for Oscillatory Wave Flow

Flume

Tests were conducted in a horizontal 40 ft long, 2 ft wide, 2.2 ft deep wave flume constructed with clear plexiglass sidewalls and supported by an aluminum framework. The waves were generated by a hinged flap-type wave maker driven by a 1/3 horsepower electric motor with a speed control. The stroke and speed of the wave board were adjustable to produce the desired incident wave height and wave period.

By means of a false floor elsewhere, drop section 9 ft long was created in the flume bed a distance of 9 feet downstream from the wave board. This was used for placement of sediment and served as the test section. Plexiglass on both sides of the flume permitted

visual observations, and the recording and photographing of changes in the waves and sediment at the test section. Two point gages of 0.001 ft accuracy were mounted on a carriage travelling on the edges of the flume and were used for bed profile measurements. A simulated shoreline with flexible mats and other wave-dissipating material was placed at the end of the flume to minimize the reflected wave and to reduce the time required for the wave tank to come to rest between tests. The experimental apparatus is shown in Figure 29.

Sonic Wave Profiler

A sonic wave profiler was used in conjunction with a Hewlett-Packard strip chart recorder to measure and record wave heights. The profiler was placed in the center of the test section to measure the wave height and wave period.

Velocity-Measurement Device

A Nover Nixon Streamflow Probe 403 Propeller Current Meter was used to obtain a continuous measurement of the fluctuating velocity. Propeller current meters are commonly used for the measurement of quasi-steady flows such as open channel flow. The propeller diameter was 0.47 inches (1-2 cm). It is composed of fine blades mounted on a hard stainless steel spindle. Both ends of the spindle are fine burnished conical pivots which turn in framed jewels. The propeller was mounted on a thin tube attached to a support frame. An insulted gold wire in the head of the slim tube, terminates 0.1 mm from the blade tips. When the propeller revolves, the passage of a blade past the tip of the gold wire slightly varies the measurable

Wave Board

Test Section

Shore
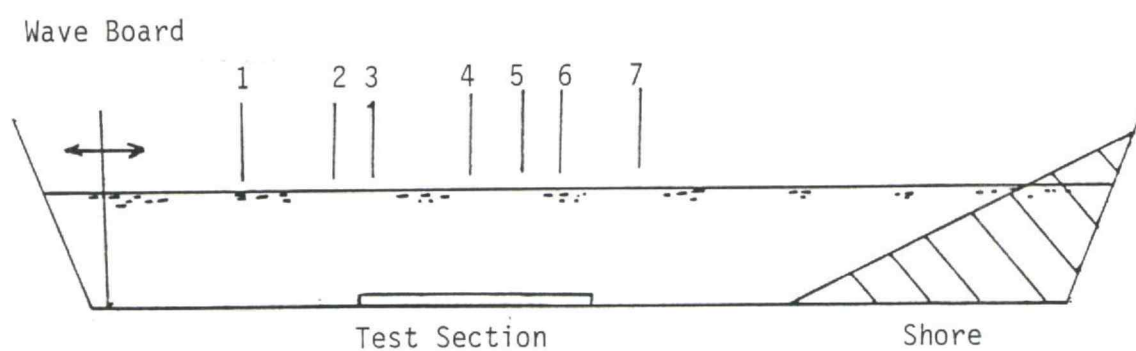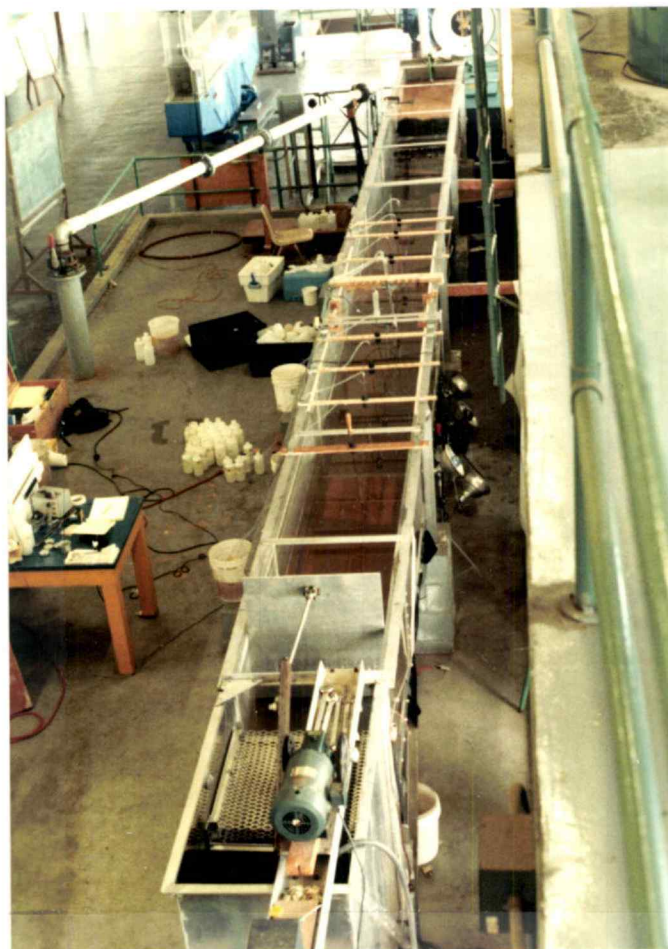
Figure 29.   Wave Flume System Used For Oscillatory Flow

Impedance between the tip and the blade. The variation of the
Impedance is amplified and generates an electric pulse.

Suspended Sediment Sampling

Individual suspended sediment samplers were installed at 200,
300, 360, 520, 580, and 625 cm from the wave board. In addition, a
multiple vertical suspended sediment sampler was installed 470 cm
from the wave board with eight taps position from near the bed to
near the water surface, respectively.

Apparatus for Unidirectional Flow

Flume

The unidirectional flume was rectangular, with a cross section
1.5 ft wide and 2 ft deep and 26 ft long. It was constructed of
plexiglass and aluminum and could be tilted. The hydraulic system
control consisted of a water storage tank, pumps, head tank, head
gate, flume, tailgate and tail tank. The flume could be used with a
recirculating pump or as a throughflow system. The recirculating
pump was more convenient but the throughflow system gave larger
discharges. Depth of water in the flume was controlled by the tail
gate and the pump discharge valve for the recirculating setup and by
the tail gate and pump speed for the throughflow setup. Discharge
was determined by use of a differential pressure menometer and
orifice plate, after first using a volumetric tank to obtain the
calibration curve.

The flume floor contained a drop section 7.6 ft long that was
located at a distance of 6 feet downstream from the head gate. This
was used for placement of sediment and served as the test section.

Plexiglass on both sides of the flume permitted visual observations and the recording and photographing of changes in the test section. A point gage of 0.001 ft accuracy was mounted on a carriage travelling on the edges of the flume and were used for bed and water profile measurements.

The entire flume system was mounted on a horizontal pivot, allowing the slope to be adjusted by means of jacks. A Venturi meter was installed in the pipe at the exit to measure discharge. The experimental apparatus is shown in Figure 30.

Velocity Measurement Devices

The Nover Nixon Streamflow Probe 403 propeller current meter was used to measure water velocity.

Shear-Plate

A shear plate was installed in the middle of the test section, with sediment on top of the shear plate. Complete discussion of the design and construction of the shear plate is given in the equipment design section.

Suspended-Sediment-Sampling

Individual suspended sediment samplers were installed at 130, 180, 260, 300, 380, 520, and 630 cm from the head gate. In addition, a multiple vertical suspended sediment sampler was installed 332 cm from the head gate with eight taps position from near the bed to near the water surface.

Bench-Type-Experiments

A series of bench-type experiments was conducted to study the density and consolidation characteristics of the sediment from
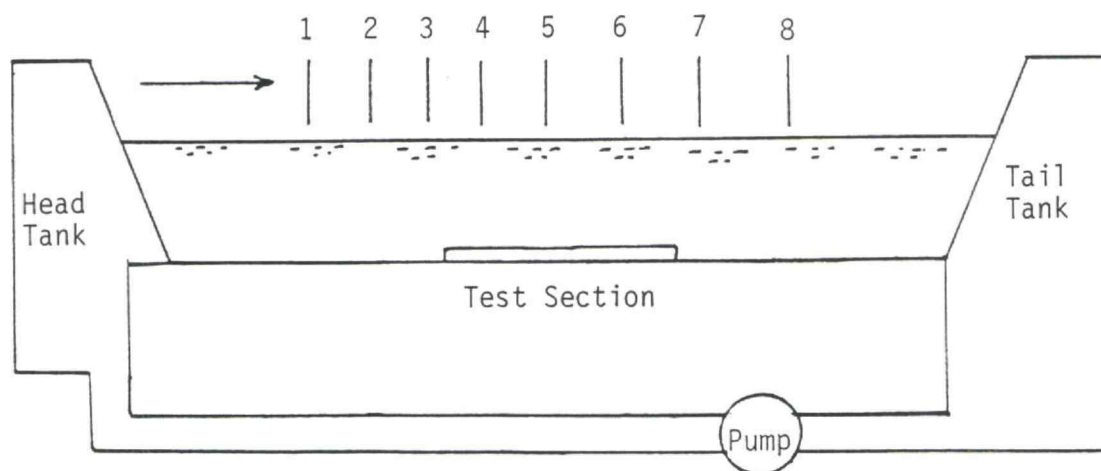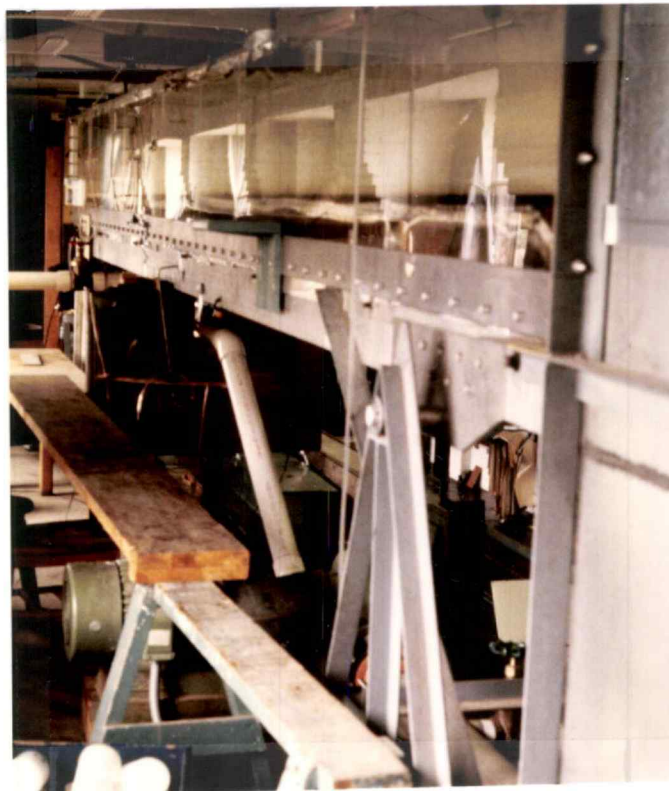
Figure 30.   Flume System Used For Unidirectional
Flow Experiments

Sturgeon Lake that was used in the flume experiments. These characteristics were determined under water and for sediment exposed to air. Containers of several sizes were used: one-liter and two-liter graduated cylinders and long columns. Long-column settling was done using clear plastic tubes 4 ft long and 0.46 ft diameter.

Equipment Design

Shear Plate

A shear plate was designed and constructed to measure the shear stress at the bed. This shear plate was only used in the recirculating flume for unidirectional flow.

The shear plate consisted of a 6 in. x 6 in. square plate 1/8-in. thick supported at its corners by four aluminum legs which are 1/16-in. thick, and 1/2 in. wide and 3 in. high. These legs were fastened to a 1/4-in. aluminum base plate and hinged to the shear plate. This plate and its support system were mounted inside an outer box so that in the equilibrium position there is a gap of approximately 1 mm at each side through which the plate can deflect. The shear plate is shown in Figure 31.

Strain gauges (type SR-4) mounted in pairs on the upstream support legs sensed any deflection of the shear plate. One gauge of each pair measured tensile stresses and the other measured compressive stresses when a shear force was applied to the plate. An insulating rubber coat protected the strain gauge wiring. A portable digital strain indicator Daytronic Model 870 was used to
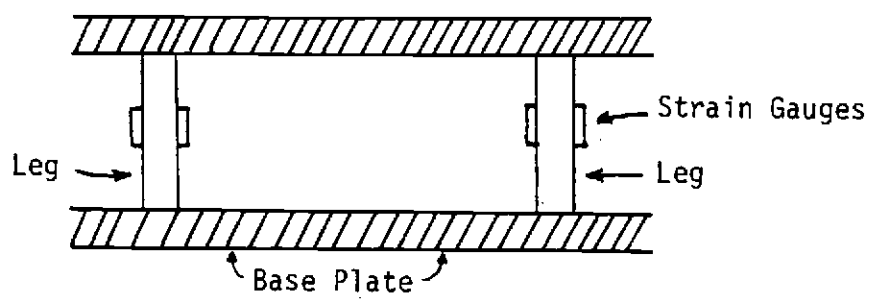
Figure 31.   Shear Plate Assembly

measure the strain directly; output also went to a Hewlett-Packard strip chart recorder.

Static calibrations were performed using the pully system shown in Figure 32. The calibration was done with and without a weight sitting on the shear plate. Duplicate pans allowed for alternate. positive and negative loading. The strain-gauges were sensitive to a 0.5 gm increment of load. A typical calibration curve is given in Figure 33.

The shear plate was installed in the floor of the recirculating flume. It was position in the middle of the test section, both laterally and longitudinally.

Limitation of Shear Plate

Design and construction of the shear plate was accomplished with no major difficulties or problems. The calibration of the shear plate with and without an added weight on the sensitive shear plate was then accomplished. Unfortunately, the problems arose during experimental tests. These included:

1. The end pressure force correction tended to be large, in many instances larger than the shear itself; therefore, the errors in the shear measurement also became large (as also observed by Riedel, 1972).

2. The gap between the shear plate and the outer box tended to become clogged with a white deposit, presumed to be aluminum oxide resulting from corrosion of the aluminum components.

3. The adjustment mechanism for alignment and clearance between the shear plate and the surrounding box was not very satisfactory for fine adjustments.
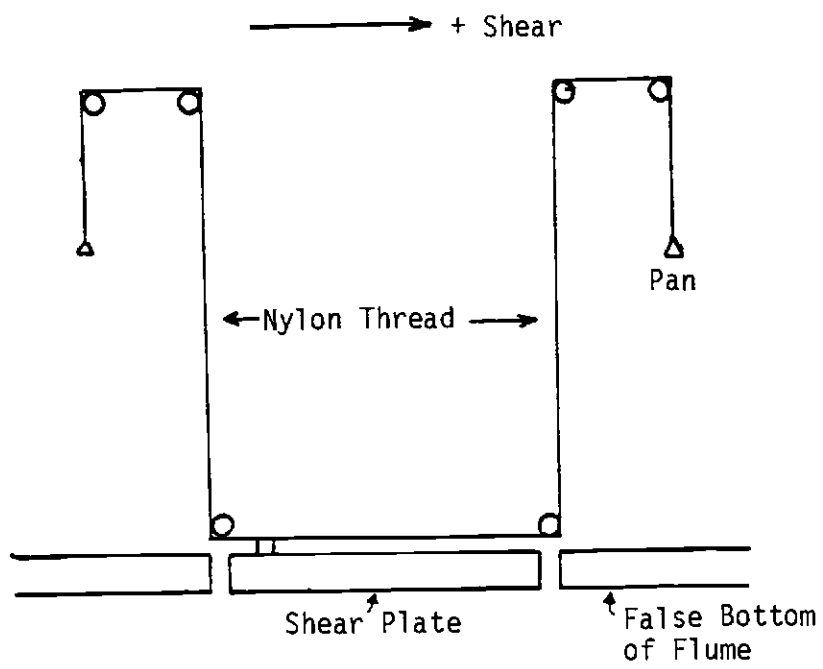
Figure 32. Shear Plate Calibration System
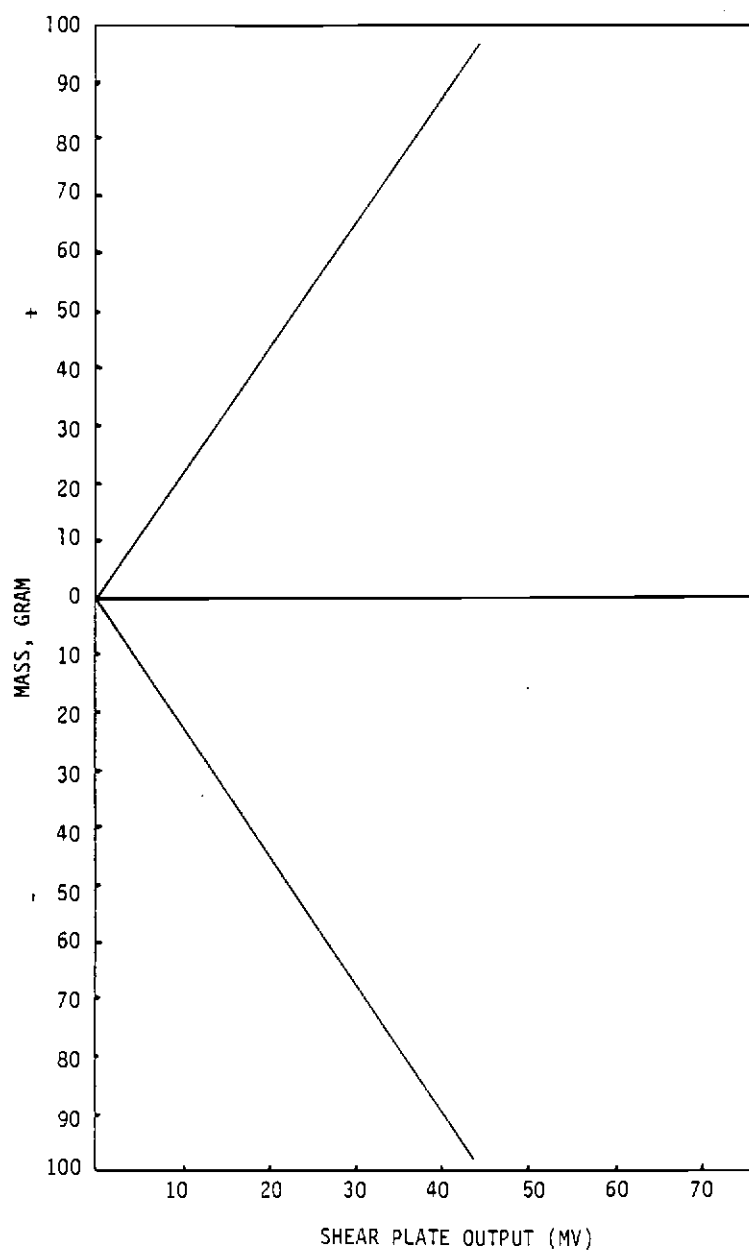
Figure 33. Shear Plate Calibration Curve

4. Flow under the plate, possibly secondary currents under the shear plate, occasionally caused major problems.

5. Vibrations from the flume pump affected the sensitive shear plate and were difficult to minimize.

6. To reach a given test water depth without disturbing the sediment bed surface at the start of a test, the water level in the flume was slowly raised to above the desired depth at near-zero velocity and then was lowered to the desired depth by lowering the tailgate. This procedure caused sporadic variations in shear plate output.

7. Vertical loading and movement of this load on the shear plate was another source of errors.

Unfortunately, the many sources of possible errors caused the shear plate to operate erratically. During a typical run, the shear stress fluctuated from positive to negative or vice versa. Due to the lack of special equipment, no attempt was made to rebuild the shear plate to correct all of the problems. For future research it is recommended that : (1) a brass base plate be used instead of aluminum, (2) end pressure and other possible secondary forces be minimized; (3) good alignment and fine adjustments be made between shear plate and surrounding plate, (4) flow under the plate be eliminated, (5) pump vibration and water depth variation be minimized, and (6) vertical loading and possible movement of sediment be taken into account.

Suspended-Sediment Sampler

For suspended sediment sampling, a simple siphon-type sampler

was designed and constructed. The single suspended sediment
samplers were constructed of L-shaped brass tubing connected to
plastic tubing with a clamp valve at the discharge end of the
plastic tubing. The multiple vertical suspended sampler was
assembled using several L shape glass tubes, each connected to
plastic tubing which had a clamp valve. The samplers withdrew water
by a siphoning action which was started by use of a suction bulb.
The suspended sediment samplers, mounted to the top of the flume,
could be lowered or raised. For each sampler, the intake elevation
over the bed surface and also the horizontal position relative to
the head gate or wave board were measured.

The Bed Material

The bed material consisted of a brownish inorganic silt and
clays with some fine sand. The sediment also included 5.4 percent
organic matter. This sediment was collected from the central part
of South Sturgeon Lake. This was very representative of the
hydraulically-active sediment bed over widespread parts of the lake.
Using the Unified soil classification system, the sediment is
designated as MH and OH. The principal clay mineral present is
illite (chloritic integrade).

The grain size distribution of the sediment was determined by
sieving and hydrometer tests. The following results were obtained:

Fine sand: about 1.5 percent by weight

silt: (between 2 and 75 microns) about 80 percent by weight

clay: (less than 2 microns) about 18.5 percent by weight

uniformity coefficient $(D_{60}/D_{10}) = 15$

When the uniformity coefficient is greater than 10, the material is considered to be well graded. Figure 34 shows the grain size distribution curve for the sediment used in the experiments.

The Atterberg limits were determined for the sediment, using standard soil mechanics methods. The following results were obtained:

liquid limit - 55%

plastic limit - 40%

plasticity index - 15%

water content - 65%

Chemical characteristics of the sediment were determined in the laboratory by use of standard environmental engineering methods. The following results were obtained:

cation exchange capacity = 34 meq/100 gram

total iron (Fe) = 22.8 mg/gram of dry weight

magnesium (Mn) = .425 mg/gram of dry weight

sulfide (s) = 0.057 mg/gram of dry weight

Clay mineralogy was determined in the Oregon State University Soil Sciences Laboratory. The following information about the methods and results was provided. All sediment samples were dispersed in a dilute (1 g/9 liters) solution of cold sodium carbonate. The less-than-2 micron (μ) clay fraction was separated from the sample by a combination of wet selving and gravity sedimentation. Samples of the clay suspensions were Mg- or K-saturated by three washings with normal chloride solutions followed by three washings with distilled water. Slides for X-ray
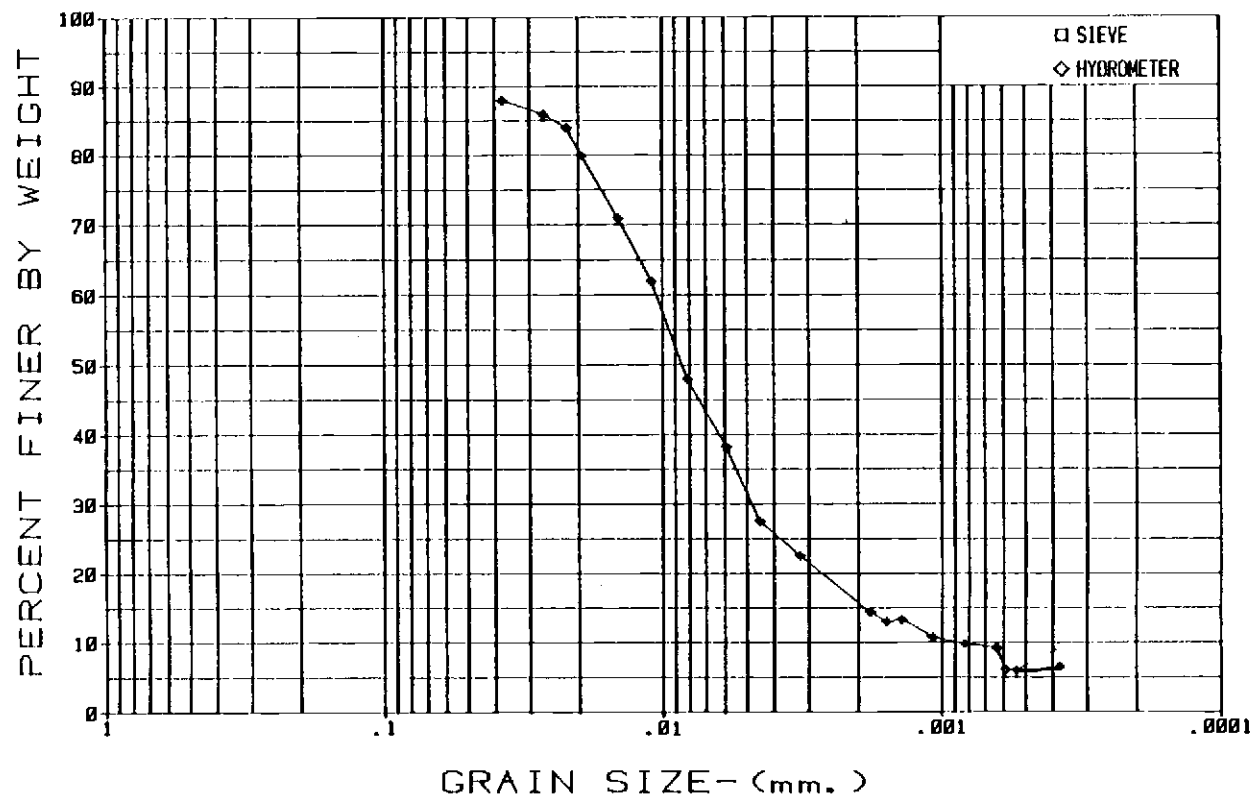
Figure 34.   Grain Size Distribution for Flume Sediment

diffraction were prepared by the paste method and identified according to established criteria. X-ray diffraction was performed on a Philllips Norelco X-ray Diffractometer. CuKα radiation was used with the generator operating at 35 kilowatts and 25 milliamps. The detector was a scintillation tube fitted with a focusing monochrometer.

X-ray diffraction showed that the clay minerals consisted of chloritic integrade and dehydrated halloysite with some indication of smectite. Figure 35 shows the x-ray diffraction pattern for Sturgeon Lake sediment.

Test Water Characteristics

Filtered river water was used in the flume experiments. Water temperature and pH were kept as constant as practical during experimental runs. Some of the common chemical characteristics of water, according to the staff at the City of Corvallis Water Treatment Plant, are:

pH = 7.2

Hardness = 30.0 mg/l

Alkalinity = 24.0 mg/ll

Average turbidity = 0.07 NTU

Total solids = 79 mg/l

Iron = 0.05 mg/l

Manganese = <0.01 mg/l

Specific conductors = 85 μmho/cm

Calcium = 11 mg/l

Sodium = 6.9 mg/l
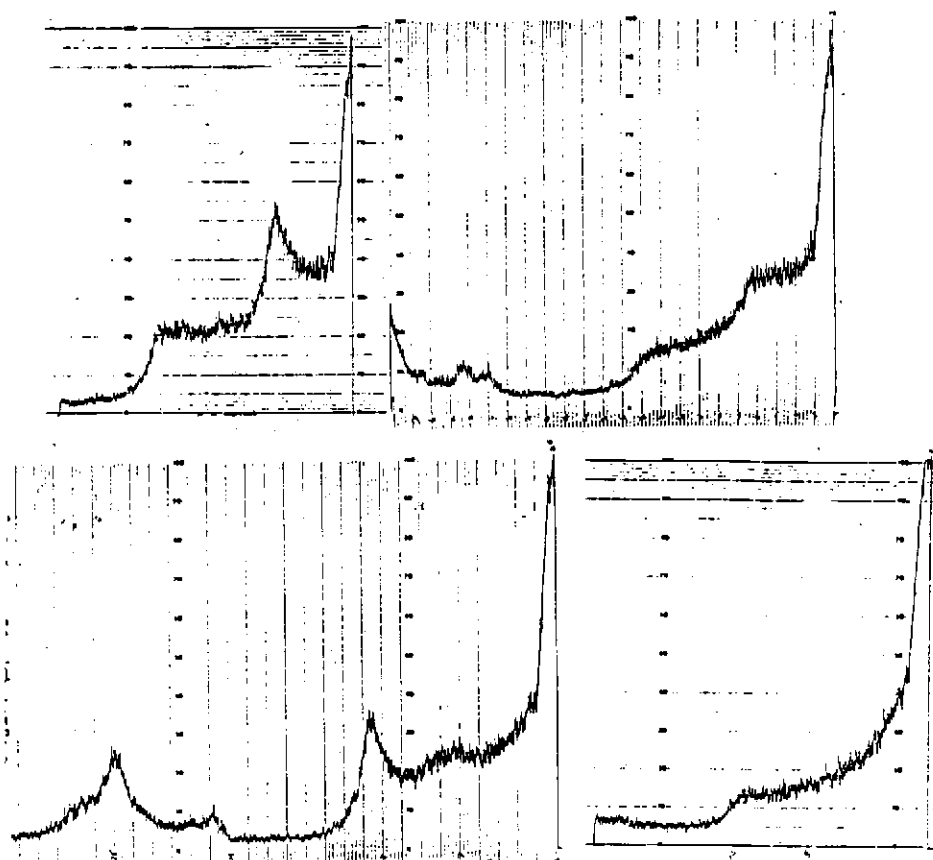
Figure 35. X-Ray Diffraction Pattern For Sturgeon Lake Sediment

Sediment Bed-Preparation in Flumes

Special attention was given to placement of sediment in the two laboratory flumes, to represent as closely as possible the prototype conditions. The steps in preparation for the experiments included the following:

1. The recirculating flume was filled with filtered river water to an average depth of 6 inches. The wave flume was filled to a depth of 12 inches.

2. Two temporary partitions were installed near both ends of the sediment test section. These were spaced 7.6 feet apart for the recirculating flume and 9 feet apart for the wave flume.

3. The Sturgeon Lake sediment was well mixed with water. A quantity of the resultant wet slurry sufficient to give at least a 4-cm deposit between the particles was added to the flumes. The sediment was allowed to settle naturally to simulate natural deposition in the lake. The end partitions were water-tight to prevent any loss of sediment out of the test section.

4. The partitions were carefully removed when the water between them was clear of fine particles, after approximately one week. The bed was kept submerged at all times.

5. The bed surfce was surveyed to determine its elevation and the presence of any bed forms, using two point gages in the wave flume and one point gage in the unidirectional flume.

Experimental Procedures

Wave Flume

Test Procedures

Procedures for the experimental runs included the following:

1. The current meter, sonic wave profiler, and supended sediment samplers were installed at designated locations (see Figure 4.1).

2. Filtered river water was added to increase the depth to the final test depth above the bed surface. The water depth was then kept constant for each run.

3. The bed surface was photographed from above before the start of and at the end of each experimental run.

4. The wave-making stroke and speed were set at the desired test position.

5. The wave profiler was started and wave records were collected continuously for at least 3 minutes.

6. Depending on the duration of the run (approximately 1/2 to 1 hour) wave records were obtained periodically for at least 2 minutes to monitor the wave characteristics.

7. The water and air temperature and the water pH were recorded.

8. Vertical profiles of the horizontal water velocity were recorded periodically at several lateral positions along a cross section including the flume centerline.

9. Photographs were taken through the side of the flume at the test section for recording the wave profile and any possible changes

in the bed surface or water column above it.

10. Observations were made and recorded of any visual perceptible changes in the bed surface and of the time when the changes occurred; this was done during the entire experimental run.

11. Water samples were taken before the start of the experiment and at intervals of several minutes during early parts of the run and then every 1/2 hour for the rest of the run. At sampling points 1 through 7 (as shown in Figure 4.1). These samples were subjected to turbidity and suspended sediment concentration measurements and organic content determination.

12. The wave height and wave period were measured to compare to the recorded wave determined by the sonic wave profiler. Also, the particle back-and-forth movement on the bed was observed and measured.

13. The time of incipient motion and possible erosion and deposition patterns were recorded.

14. When there were no visually perceptible changes in water turbidity and in the shape of the test bed, the run was terminated and a new run started with increasing wave-board speed. If still no changes took place, a new wave-board stroke was set with a lower speed and the speed was progressively increased until changes took place.

15. To determine the effect on incipient motion due to a naturally compacting sediment bed, the test section was left to naturally settle under 1 foot of water depth for 91 days. Steps 2 through 13 were then repeated.

Measurements and Calculations

The following measurements and calculations were made for preliminary analysis of the data:

1. For each run, the average values of wave height and wave period were obtained from wave profile records.

2. Water samples were subjected to turbidity measurement on the same day as sampling, by use of a model 2100 A Hach turbidity meter. Also, water samples were initially subjected to suspended sediment concentration measurement by the filtration technique and organic content was determined by combustion. After a few samples had been collected, the turbidity data were related to suspension concentration by regression analysis. Once this was available, for the rest of the runs only turbidity were measured, the suspension concentration being obtained from the graph of turbidity versus concentration. Nevertheless, during experimental runs, occasional samples were subjected to concentration measurement to prevent any possible errors.

3. The velocity measured by the miniature current meter was analyzed. An average maximum velocity for each experimental run was obtained by summing the maximum velocity at each wave period divided by the number of wave periods.

4. The horizontal component of the local fluid velocity was calculated by using linear wave theory for various values of z and t during the passage of wave. This was done by using equations 37 and 44.

5. Wave length was also calculated by using linear wave theory

methods. The calculated wave length was compared with measured ones for agreement.

6. The shear stress at the bed was calculated for each run from the shear stress equation 85 and from Jonsson's emprical equation 89.

7. The orbital diameter, was calculated from linear wave theory approximation, using equation 45. The orbital diameter was also measured by visually observing the particle movement along the bed.

Recirculating Flume

Test Procedures

Procedures for the experimental runs included the following:

1. The current meter and suspended sediment samplers were installed at the designated locations (see Figure 30).

2. The bed surface was photographed from above before the start of and at the end of each experimental run.

3. The pump was set at fixed speed and discharge valve opening. Water depth and water velocity were then controlled by means of the tailgate opening.

4. Several minutes were allowed for water to reach equilibrium at the desired depth; then the water depth was recorded.

5. Vertical profiles of the horizontal water velocity were recorded periodically at several lateral positions along a cross section.

6. The shear stress at the bed was recorded continuously on the chart recorder.

7. The water and air temperature and the water pH were

recorded.

8. Water samples were taken at regular intervals at points 1 through 7 (shown in Figure 30).

9. Observations were made and recorded of any visual perceptible changes in the bed surface and of the time when the changes occurred; this was done during the entire experiment.

10. Surface water velocity was measured by floating materials as a quick check of flow conditions.

11. Photographs were taken during the run to record any possible changes that took place.

12. The time of incipient motion and possible erosion and deposition patterns were recorded.

13. When there were no visually perceptible changes in water turbidity and in the shape of the test bed, the water velocity was increased and steps 3 through 12 were then repeated.

14. The downstream half of the test section was formed into dune shapes and steps 3 through 13 were repeated.

15. The slope of the flume was increased and steps 3 through 14 were repeated.

Measurement and Calculation

The following measurements and calculations were made for preliminary analysis of the data.

1. Discharge was determined by use of the calibrated orifice meter, through measurement of the differential pressure manometer in inches of mercury.

2. Velocity at a point was measured by use of the miniature

current meter and the mean velocity was obtained by dividing the discharge by the cross-sectional area of the flow.

3.   Shear stress was measured by use of the shear plate.

4.   Shear stress at the bed was calculated by using equations 2, 10, and 23.

5.   Water samples were handled in the same manner as done for those collected in the wave flume.

Bench-Type-Experiments

Eight 1-liter cylinders were used to study sediment consolidation under water and the corresponding density changes. One 3-ft long cylinder was used to study sediment consolidation and corresponding density changes for a deeper deposit. Two 2-liter cylinders were used to study the effects on consolidation of washing away the fine-sized suspended matter from the disturbed upper zone of a settled slurry. A bucket was used to study consolidation of air-exposed sediment.

Procedures for the experiments included the following steps for the eight 1-liter graduated cylinders:

1.   The mixed slurry sediment and lake water was poured into graduated cylinders, which were then shaken a few times before being allowed to settle.

2.   The volume of sediment and the sediment depth in each column was measured every minute for the first hour and then every hour for the next five hours. Thereafter, it was measured at convenient times for up to 5 months.

3.   The sediment in each graduated cylinder was subjected to

density measurement. This was done by subjecting the cylinders to different test periods, at the end of which the density of the entire sample was obtained by measuring the sample volume, disposing of the supernatant water, and oven-drying and weighing the sample.

For the 3-foot long cylinder:

1. The mixed slurry of sediment and lake water was poured into the long settling column and additional lake water was added and stirred into the slurry.

2. The volume of sediment and the sediment depth in each column was measured every minute for the first hour and then every hour for the next five hours. Thereafter, it was measured at convenient times for up to 5 months.

3. The sediment was extracted from the long settling column at several different heights and subjected to density measurement.

For the two 2-liter graduated cylinders:

1. The mixed slurry of sediment and lake water was poured into two 2-liter graduated cylinders. The cylinders were shaken a few times before being allowed to settle.

2. 500 ml of the lake water were added to each cylinder, with moderate agitation from the pouring action to disturb the top sediment particles in the graduated cylinders.

3. 10 minutes were allowed for settling after this disturbance for the first two tests and 2 1/2 minutes allowed for the remaining tests with each cylinder for a total of seven tests.

4. After each settling interval, the top 500 ml of the suspended materials were collected by suction.

5. The removed suspension was subjected to concentration and volatile solid measurements.

6. The volume of the sediment and height of the sediment remaining in the cylinder were recorded periodically for several days to observe consolidation.

For the bucket:

1. A known amount of well-mixed sediment from the lake was placed directly in the bucket and initially submerged by a few centimeters of Sturgeon Lake water.

2. The bucket was allowed to sit in the air for several weeks to dry out.

3. The sediment height and volume were measured after the sediment had dried.

V. PRESENTATION AND ANALYSIS OF EXPERIMENTAL RESULTS

Experiments With Oscillatory Flow

Outline of Experimental Runs

A total of 67 experimental runs were made. These can be divided into three separate categories of experiments. Table 10 shows the detailed data for each of the experimental runs.

The first set of runs (runs 1 through 34) involved study of the incipient motion of the freshly deposited sediment bed at fixed water depth for different wave parameters, i.e., wave height and wave period. Wave height and wave period and resultant maximum water velocity at the bed and maximum shear stress were regulated by changing the stroke and speed of the wave board. This category of runs covered the full range of wave heights and wave periods practical in the flume. Water concentrations were measured at fixed locations at frequent intervals. The test section consisted of 3 feet of irregular rough bed followed by 6 feet of smooth bed surface. This condition also attempted to determine the incipient motion of the bed sediments on a rough bed in comparison to a smooth bed surface.

The second category contained runs 35 through 62. This series of experiments started 71 days after the last experiment of category 1 (run 34). It was intended to determine: (1) the effects of consolidation (natural densificiation due to expulsion of water with time) of the same bed as previously tested on incipient motion under

Table 10. Synopsis of Experimental Runs With Oscillatory Flows

Run	Time of run hr. min. sec.	State of Sediment Bed Fresh Compacted	Water Depth cm	Wave Height cm	Wave Period Second	Fluid Tap Water / Chemical Added	Bed Flat / Rough	Maximum Velocity at the bed cm/sec	Orbital Diameter cm	Maximum Shear Stress dyne/cm²	Maximum Suspended Sediment Concentration mg/l	Type of Flow	Water Temperature °C	pH
1a	00 02 30	x	30.48	1.07	4.65	x	x x	2.97	0.50*	.36	-	Laminar	17.6	6.55
1b	00 06 00	x	30.48	2.26	2.25	x	x x	5.91	0.50*	1.02	-	"	17.6	6.55
2	00 06 00	x	30.48	2.79	1.45	x	x x	6.38	0.50*	1.37	6.4	"	17.6	6.55
3	00 20 00	x	30.48	4.47	1.09	x	x x	8.28	0.50*	2.05	7.4	"	17.6	6.55
4a	00 01 00	x	30.48	5.28	0.97	x	x x	8.45	--	2.22	--	"	17.5	6.05
4b	01 07 30	x	30.48	5.69	0.91	x	x x	8.21	2.00*	2.23	8.2	"	17.5	6.05
5	03 00 00	x	30.48	6.05	0.86	x	x x	7.88	2.00*	1.19	4.4	"	17.9	6.05
6	11 05 00	x	30.48	6.60	0.77	x	x x	6.62	1.62	1.95	3.6	"	18.1	6.24
7	08 01 00	x	30.48	7.32	0.76	x	x x	6.98	1.69	2.06	2.6	"	17.8	6.35
8	04 27 00	x	30.48	8.13	0.73	x	x x	6.84	1.59	2.10	2.3	"	16.3	6.35
9	00 01 00	x	30.48	9.55	0.81	x	x x	10.72	2.76	3.11	2.3	"	16.3	6.35
10	03 09 00	x	30.48	7.32	1.01	x	x x	12.40	3.99	3.22	13.4	"	16.7	6.30
11	02 45 00	x	30.48	8.84	0.95	x	x x	13.73	4.15	3.67	6.6	"	17.2	6.45
12	01 21 00	x	30.48	11.38	0.87	x	x x	15.01	4.16	4.18	4.4	"	17.2	6.45
13	00 44 00	x	30.48	10.97	0.81	x	x x	12.31	3.17	3.56	4.4	"	17.3	6.45
14	00 16 00	x	30.48	12.40	0.74	x	x x	10.58	2.49	3.20	4.0	"	17.3	6.45
15	00 33 00	x	30.48	8.13	1.06	x	x x	14.59	4.92	3.67	9.6	"	17.3	6.45
16	00 29 00	x	30.48	12.60	0.95	x	x x	19.56	5.91	5.20	14.6	"	17.5	6.45
17	02 39 00	x	30.48	13.41	0.83	x	x x	16.20	4.28	4.60	12.4	"	17.5	6.55
18	11 52 00	x	30.48	13.41	0.82	x	x x	15.64	3.98	4.49	17.6	"	18.3	6.61
19	01 01 00	x	30.48	11.18	1.09	x	x x	20.69	7.18	5.03	6.1	"	18.9	6.35
20	00 39 00	x	30.48	13.41	0.97	x	x x	21.46	6.63	5.53	13.6	"	18.9	6.35
21	00 52 00	x	30.48	15.24	0.86	x	x x	19.87	5.44	5.44	10.4	"	18.9	6.35
22	00 15 00	x	30.48	13.82	1.02	x	x x	23.72	7.70	5.97	8.2	"	18.9	6.45
23	01 14 00	x	30.48	15.85	0.90	x	x x	22.32	6.39	5.99	30.6	"	18.8	6.55
24	01 52 00	x	30.48	14.22	1.06	x	x x	25.54	8.62	6.30	19.8	"	19.0	6.45
25	01 06 00	x	30.48	15.44	0.92	x	x x	22.79	6.24	6.24	30.8	"	16.4	6.40
26	00 16 00	x	30.48	12.19	0.84	x	x x	14.91	3.99	4.27	25.9	Trans.Laminar to smooth tur	16.4	6.40
27	00 14 00	x	30.48	14.63	1.10	x	x x	27.33	9.57	6.84	27.8	Laminar	16.4	6.40
28	-01 05 00	x	30.48	16.46	0.97	x	x x	26.33	8.13	7.04	22.3	"	16.2	6.35
29	00 24 00	x	30.48	13.21	0.79	x	x x	14.04	3.53	4.15	15.4	T-L to ST	16.1	6.45
30	00 07 00	x	30.48	8.94	0.70	x	x x	6.49	1.45	2.04	10.8	Laminar	16.2	6.25
31	00 11 00	x	30.48	8.33	0.66	x	x x	4.61	0.97	1.49	8.6	"	16.2	6.25
32	00 13 00	x	30.48	7.72	0.62	x	x x	3.33	0.66	1.11	9.0	"	16.2	6.25
33	00 09 00	x	30.48	6.50	0.52	x	x x	0.88	0.15	0.32	8.6	T-L to ST	16.3	6.15
34a	00 02 00	x	10.48	1.83	0.73	x	x x	1.54	0.36	0.47	8.6	"	16.4	6.25
34b	00 01 00	x	30.48	2.03	0.66	x	x x	1.13	0.24	0.17	--	"	16.4	6.25
34c	00 01 30	x	30.48	2.24	0.49	x	x x	0.16	0.02	0.066	--	"	16.4	6.25
34d	00 07 30	x	30.48	2.64	0.44	x	x x	0.07	0.01	0.028	--	"	16.4	6.25

(Wave Reflection = 3-5)   *Visually Measured

Table 10 Continued. Synopsis of Experimental Runs With Oscillatory Flows

Run	Time of run hr.	min.	sec.	State of Sediment Bed Fresh	Compacted	Water Depth cm	Wave Height cm	Wave Period Second	Fluid Tap Water	Chemical Added	Bed Flat	Rough	Maximum Velocity at the bed cm/sec	Orbital Diameter cm	Maximum Shear Stress dyne/cm²	Maximum Suspended Sediment Concentration mg/l	Type of Flow	Water Temperature °C	pH
35	00	34	00		X	30.48	7.54	1.37	X		X	X	16.68	2.00*	3.53	4.4	Laminar	20.9	6.40
36	01	00	00		X	30.48	14.22	0.84	X		X	X	17.52	4.68	4.73	9.6	"	21.1	6.0
37	00	25	00		X	30.48	12.80	0.75	X		X	X	11.67	2.79	3.33	10.8	"	21.2	6.0
38	00	44	00		X	30.48	13.18	0.69	X		X	X	8.93	1.96	2.66	4.0	"	21.2	6.0
39	07	12	00		X	30.48	12.98	1.01	X		X	X	21.96	7.06	5.39	12.8	"	21.4	6.10
40	00	29	00		X	30.48	14.50	0.95	X		X	X	22.53	6.81	5.70	7.0	"	20.9	6.20
41	00	32	00		X	30.48	?18.24	0.80	X		X	X	19.94	5.08	5.52	12.0	"	20.9	6.20
42	01	27	00		X	30.48	17.63	0.90	X		X	X	24.99	7.16	6.52	11.6	"	20.9	6.35
43	02	24	00		X	30.48	18.14	0.83	X		X	X	21.75	5.75	5.91	13.6	"	20.8	6.50
44	00	35	00		X	30.48	18.97	0.94	X		X	X	28.93	8.66	7.41	10.4	T-L to ST	20.8	6.50
45	00	17	00		X	30.48	20.50	0.83	X		X	X	24.58	6.49	6.71	11.6	Laminar	20.8	6.50
46	06	16	00		X	30.48	20.24	1.02	X		X	X	34.70	11.27	8.53	26.2	T-L to ST	20.3	6.55
47	00	04	00		X	22.86	21.83	2.00	X		X	X	5.52	3.51	0.97	18.0	Laminar	20.7	6.5?
48	00	06	00		X	22.86	3.10	1.25	X		X	X	8.01	3.19	1.78	6.4	"	20.7	6.50
49	00	19	00		X	22.86	6.43	0.80	X		X	X	11.01	2.80	3.06	6.4	"	20.7	6.50
50	00	09	00		X	22.86	7.65	0.73	X		X	X	10.95	2.54	3.19	..	"	20.7	6.50
51	00	33	00		X	22.86	10.01	0.78	X		X	X	16.37	4.06	4.61	9.2	"	20.7	6.50
52	00	18	00		X	22.86	12.50	0.80	X		X	X	21.42	5.45	5.96	7.8	"	20.8	6.45
53	00	04	00		X	22.86	14.96	0.74	X		X	X	20.20	4.76	5.84	..	"	20.8	6.45
54	00	26	00		X	22.86	14.02	0.88	X		X	X	27.63	7.74	7.33	9.6	T-L to ST	20.8	6.45
55	00	09	00		X	38.10	6.40	1.38	X		X	X	11.82	5.19	2.50	10.0	Laminar	20.8	6.45
56	00	05	00		X	38.10	14.15	0.96	X		X	X	16.34	4.99	2.34	10.0	T-L to ST	20.8	6.45
57	00	09	00		X	38.10	15.06	0.78	X		X	X	9.51	2.36	2.68	8.2	Laminar	20.8	6.45
58	00	19	00		X	38.10	20.35	0.86	X		X	X	17.89	4.90	4.82	11.6	"	20.4	6.40
59	00	10	00		X	38.10	26.34	0.94	X		X	X	29.05	8.69	7.49	10.0	T-L to ST	20.4	6.40
60	00	19	00		X	38.10	21.08	1.15	X		X	X	32.68	11.96	7.61	14.6	"	20.4	6.40
61	03	06	00		X	38.10	22.96	1.10	X		X	X	33.59	11.76	8.01	18.4	"	20.1	6.40
62	00	29	00		X	38.10	28.45	1.11	X		X	X	42.03	14.85	9.97	25.2	"	20.4	6.40
63	00	13	00		X	30.48	7.32	0.76	X	X	X	X	7.88	4.23	2.06	20.6	Laminar	22.1	..
64	01	42	00		X	30.48	11.18	1.09	X	X	X	X	20.69	7.18	5.03	24.0	"	22.1	..
65	00	19	00		X	30.48	15.24	0.96	X	X	X	X	19.87	5.44	5.44	35.8	"	22.4	..
66	00	08	00		X	30.48	12.80	0.97	X	X	X	X	20.47	6.32	3.42	12.0	"	22.4	..
67	04	51	00		X	30.48	14.63	1.10	X	X	X	X	27.33	9.57	6.84	50.2	"	22.4	..

†Wave Reflection = 3-5%   *Visually Measured

oscillatory flow; (2) whether the erosion patterns developed in the same way as happened in category 1 tests; and (3) the effect of variable water depth on incipient motion of bed sediment under oscillatory flow.

The third category contained runs 63 through 67. The same bed was used as for category 2 runs, except that 800 grams of granulated sodium hexametaphosphate dispersive agent was added to the water column to determine the incipient motion of bed sediment with a dispersive agent under oscillatory flow conditions.

Results of First Category of Runs (Runs 1-34)

As already mentioned, this category of runs attempted to determine the incipient motion of bed sediment in terms of shear stress, velocity, orbital diameter, and suspended sediment concentration under oscillatory flow.

1. Emergence of Bugs and Worms -- Runs 1 and 2

Run 1 consisted of two phases. In phase 1a, the shear stress was too small to disturb any of the bed surface; no changes were noticeable to the naked eye. A 2-mm paper wad was placed on the smooth bed surface and its movements observed. It was noticed that the spitball moved in a pivoting manner rather than by sliding.

In phase 1b the water velocity at the bed was increased by changing the wave board speed. During this phase, bugs and worms which lived in the sediment emerged. The maximum velocity and maximum shear stress at the bed at which bugs and worms first emerged were 5.9 cm/sec and 1.02 dyne/cm^2, respectively. The measured orbital diameter was recorded almost 0.5 cm. The suspended

sediment concentration did not change from the initial background condition.

Run 2 started after a short stop of the wave machine. When wave motion stopped the worms and bugs retracted into the sediment. At the restart of the wave machine at a higher speed, the benthic worms again reemerged. Again, the bed surface did not change its pattern in any way. No suspended sediment concentration changes took place.

2. Initiation of Motion in Rough Bed -- Runs 3-8

At the start of run 3, shortly after conclusion of run 2, the benthic worms reemerged. Few, if any, fine particles went into motion at the worm holes. The spitball at the middle of the smooth test section caused some minor resuspension of sediment. The significance of this run lies in the initiation of motion at the rough bed. Small clouds of sediment went into motion there as a result of the local peeling off of the sediment "skin" and formation of narrow grooves or pit marks and streaks on the bed surface. This condition was considered to represent incipient motion. The initial maximum values of velocity and shear stress at which incipient motion developed at the rough bed during the run were 8.3 cm/sec and 2.05 dyne/cm^2, respectively. The orbital diameter recorded almost 0.5 cm. The suspended sediment concentration changed from 5.1 mg/l to 7.4 mg/l at the bed as incipient motion developed. The organic content of suspended sediment was almost 34 percent.

In run 4, immediately following run 3, loose particles from the previous run reinitiated a motion similar to that of the previous

run. Loose particles from the rough bed and the spitball, over time, formed some sort of ripples.

Figure 36 shows the suspended sediment concentrations against time for runs 1 through 4. The results show that over time the suspended sediment concentration remained close to the background condition. At the end of run 4 no visible cloud of sediment was observed anywhere, thus confirming the results of the suspended sediment concentration plot.

After overnight settling, the water column was clear and the bed smooth-looking due to settlement of the small amount of suspended sediment from the day before. No ripple pattern was evident.

Run 5, with an increase in wave maker speed over run 4 showed only some sediment activities in the rough bed areas. Pit marks were evident at the rough bed area. No signs of pronounced ripple formation were observed anywhere.

In run 6, scour streaks were evident in the rough bed. Scour streaks looked like knife scratches approximately 1 cm to 5 cm long (most of them are less than 2 cm). Loose sediment particles in this run grouped into a ripple formation in the rough bed.

During runs 5 through 8, few pit marks on the smooth bed surface were apparently due to the benthic worm activities. During these runs, some loose sediment from both ends of the test section went into motion. The maximum velocity and shear stress associated with these sets of runs ranged from 6.6 to 8.5 cm/sec and 1.95 to 2.23 dyne/cm^2, respectively. Figures 37 and 38 show the suspended sediment concentrations against time for runs 5 and 6, and 7,
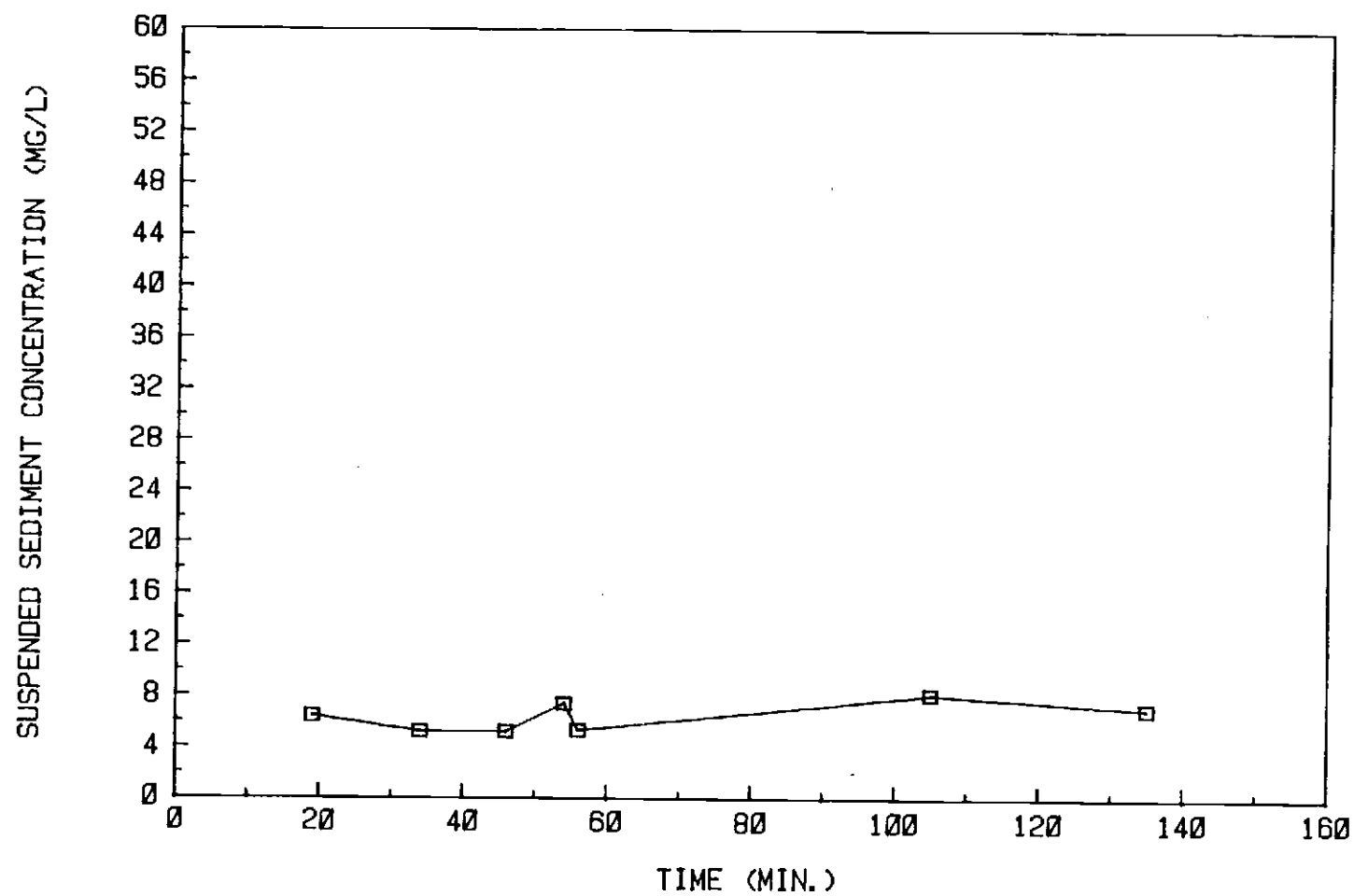
Figure 36. Suspended Sediment Concentrations For Runs 1 Through 4
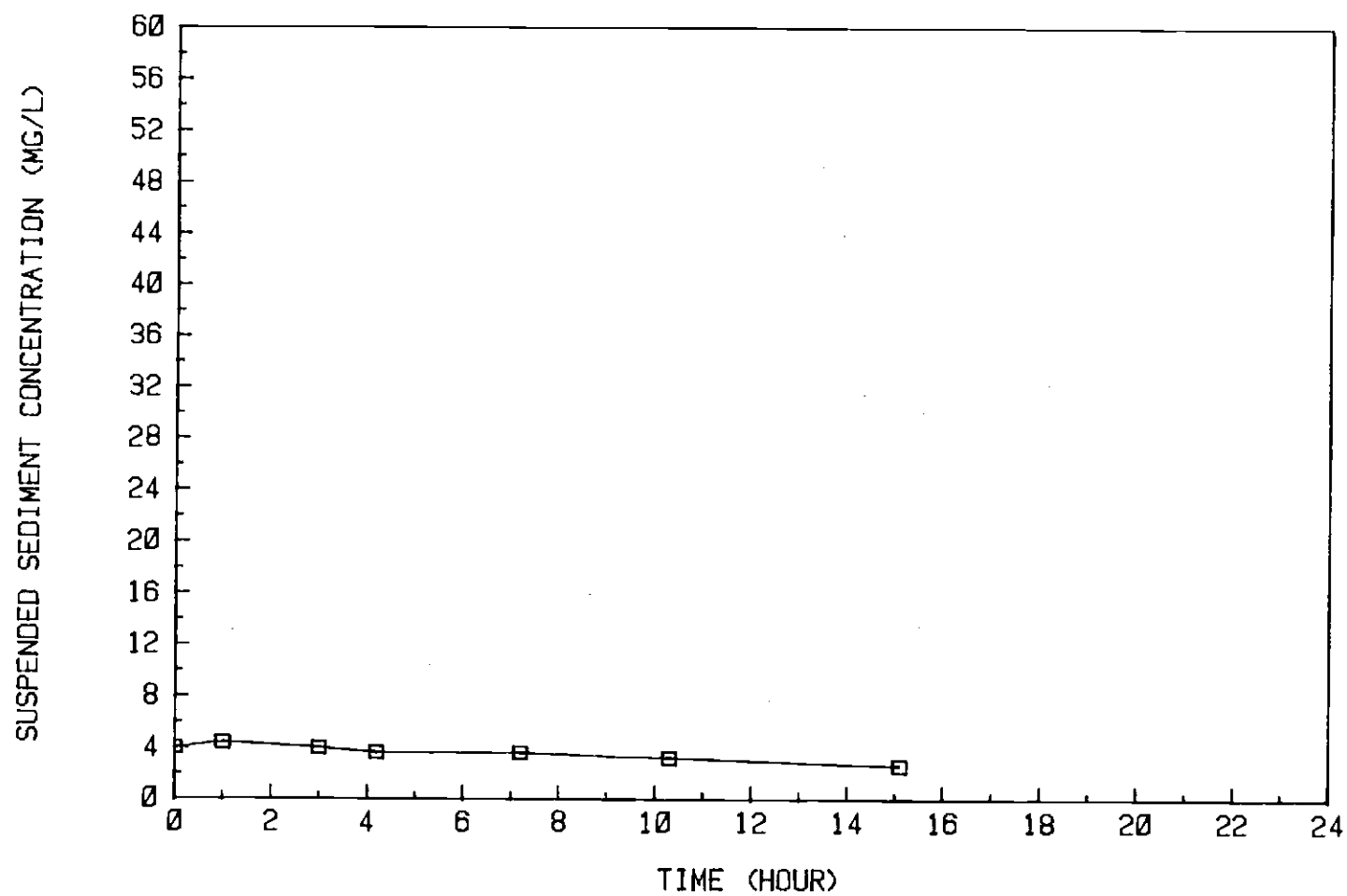
Figure 37.   Suspended Sediment Concentrations For Runs 5 and 6
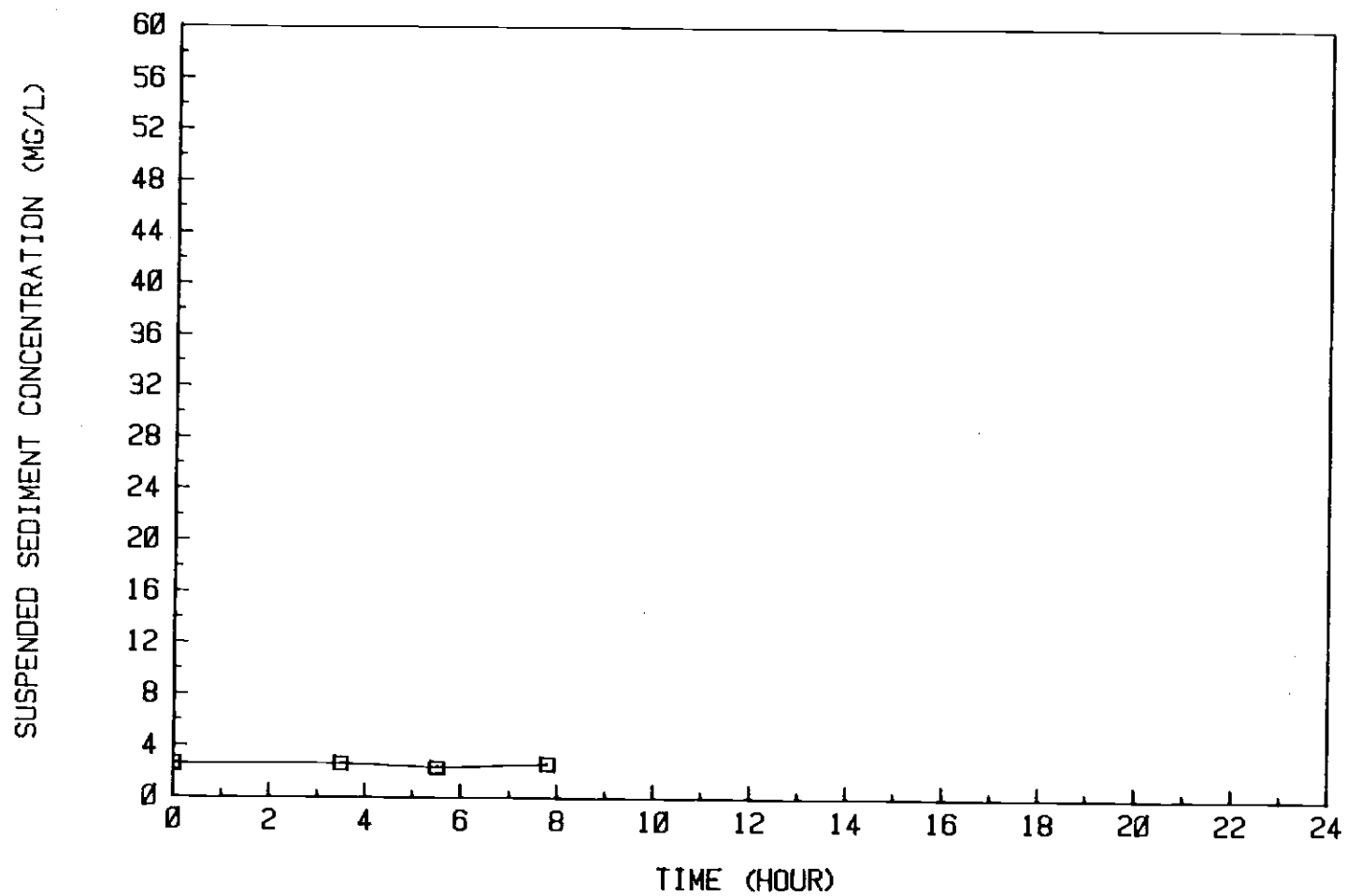
Figure 38. Suspended Sediment Concentrations for Run 7

respectively. The suspended sediment concentration data show a steady decrease in concentration due to a decrease in maximum water velocity at the bed. The suspended sediment organic matter increased from 45 percent to 63 percent for runs 5 through 8.

The following phenomena were observed during visual observation of the bed for runs 1 through 8:

a) The rough bed surface with fine irregularities and slight duned formation, seemed to scour faster than the smooth bed surface;

b) some particles were moved back and forth in a pivoting manner at the bed surface with some net transport in the downstream direction; and

c) loose particles were also picked up and put into suspension higher in the body of water.

3. Transition to Incipient Motion at Smooth Surface--Runs 9 and 10

For runs 9 and 10, the wave board stroke and wave machine speed changed to increase the shear stress at the bed. Suspension occurred at the downstream edge of the bed and at the rough bed. Scour streaks continued to grow in the rough bed and at the two ends of the test section. Scouring of 1 to 2 mm of the top surface of the rough bed started by peeling off the top layer which hereafter will be called the skin layer. The eroded skin layer material were subjected to organic content determination and found to contain 13 percent organic matters. By comparison, the bed material had

approximately 5 percent organic matter. The extra organic matter in the skin layer was thought to be added to the surface of the sediment bed from other sources, such as microbial activity, benthic organisms, and deposition of fine dust particles from the ambient air of the laboratory. The organic matter is believed to bond with clay and silt particles to form the skin layer. The skin layer is thus formed of fine dust, microbes, clay and fine silt particles. These particles were firmly bonded together; the shearing force of the water broke the weakest bond and started to peel off the pieces of bonded sediment.

Figure 39 shows the suspended sediment concentrations versus time for runs 8 through 10. It shows a sudden increase of concentration to 13 mg/l at the beginning of run 10 and a gradual decrease to 6 mg/l by the end of run 10. The maximum velocity and shear stress at the bed for run 10 were 12.4 cm/s and 3.22 dyne/cm^2, respectively. The orbital diameter at this run increased to 4 cm from about 2 cm for previous runs. The maximum recorded of organic content of the suspended sediment for these runs was 47 percent.

4. Incipient Motion at Smooth Bed Surface—Runs 11-21, 26, 29

Resuspension of the skin layer occurred rapidly at the start of run 11. Large bonded particles peeled off. Some of the particles were observed approximately 20 cm above the bed surface at 2 minutes after the start of the run, especially at the rough bed. At the smooth surface, especially at the places where some sort of irregularities due to worm activities or bed form existed, the skin started to peel off. It took a short amount of time (2 to 3
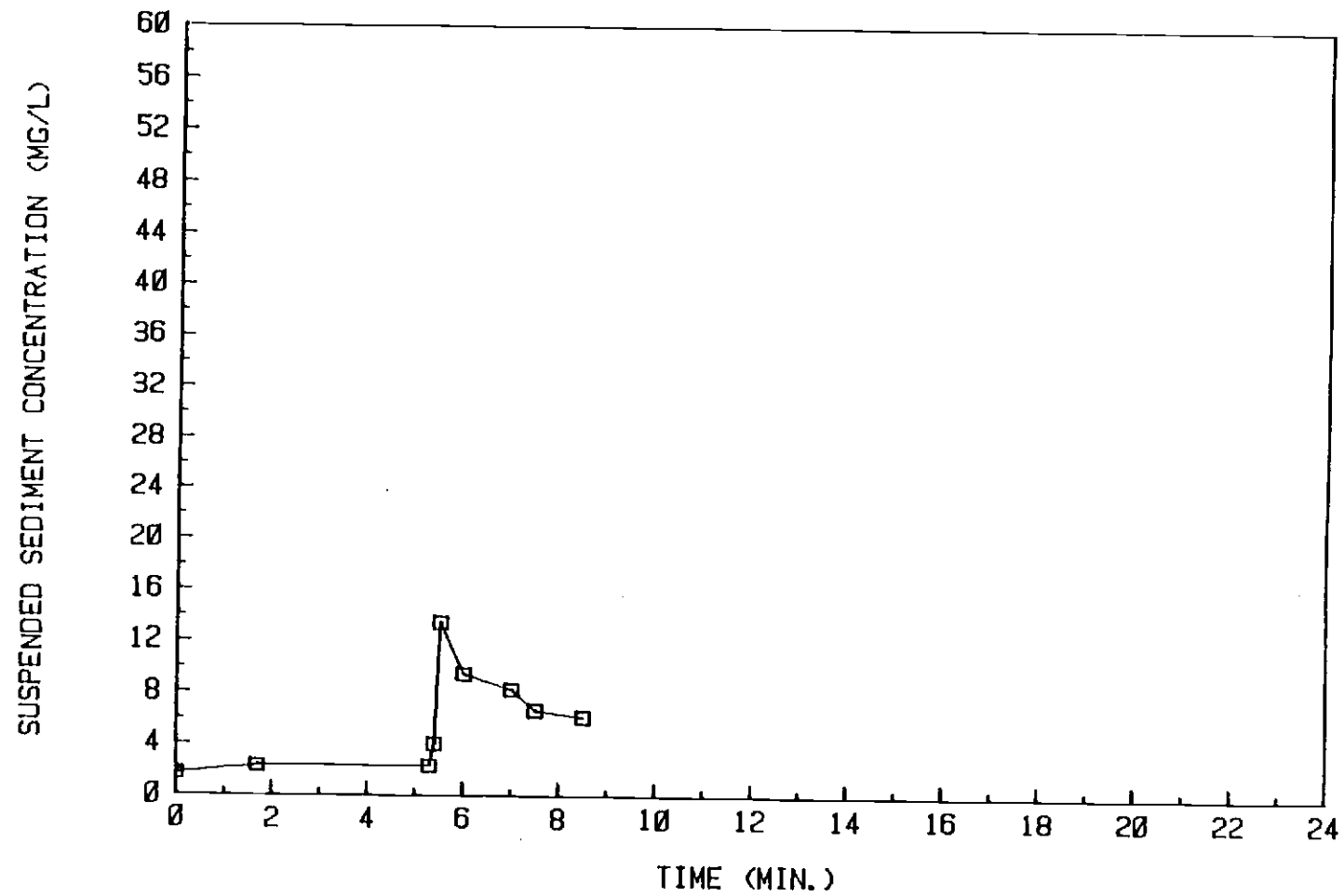
Figure 39.   Suspended Sediment Concentrations For Runs 8 Through 10

seconds) for the skin to be peeled off and start to be transported
downstream by a pivoting motion at the bed. It took a long time for
the bonded particles from the skin layer in the rough bed to
transport downstream by a pivoting motion. Therefore, deeper scour
streaks were observed in the rough bed. At the smooth bed, a short
period of time was required for bonded particles to move downstream
of the test section, except when they encountered any irregularities
on the bed surface. This caused resuspension of sediment into the
overlying water.

Three distinct types of sediment behavior were observed in the
deep scour streaks of the rough bed:

a) the top-skin layer bonded particles moved back and forth
   almost 2 cm;

b) fine silt particles moved back and forth about 5 mm; and

c) fine sand or coarse silt moved back and forth only
   1 mm or less.

Shear stress decreased for runs 13 and 14, and was not great
enough to initiate incipient motion of the smooth bed surface.

Runs 11, 12, 15 through 21, 26, and 29 are regarded as having
had incipient motion conditions for the smooth bed surface, even
though the maximum velocity at bed ranged from 13.7 cm/s to 21.5
cm/s and maximum shear stress at the bed ranged from 3.67 dyne/cm^2
to 5.53 dyne/cm^2. The orbital diameters ranged from 4.2 cm to 7.2
cm. These variations in velocity and shear stress for incipient
motion of fine sediment are mainly due to fine sediment
characteristics. Also, the following factors are responsible, to a

lesser degree:

    a)   The bed not being completely smooth;

    b)   Irregularities at the two ends of the test section;

    c)   benthic worms and bug activities;

    d)   wave board behavior; and

    e)   signal noises in recording wave parameters, caused by many factors such as cross wave formation, circulation, oscillation, reflected waves, and leekage around the wave board.

The following phenomena were observed during visual observation of runs 11 through 21, 26 and 29:

    a)   The skin layer started to peel off from the surface of the smooth bed;

    b)   some of the bonded particles (sediment, microbes and dust) suddenly went into motion upward as far as the water surface, traveled in a circular motion, and finally settled back to the bed surface;

    c)   the majority of the eroded bonded particles moved downstream by a pivoting motion;

    d)   the eroded bonded particles moving close to the bed, in route downstream, abraded any irregular or loose sediment particles on the bed and sent them into motion;

    e)   evidence of pit marks all over the bed surface indicated the start of incipient motion;

    f)   the peeling off of the skin layer and development of streaks was accelerated in the pit marks;

g) with time, the streaks in the smooth bed surface grew
    longer and wider, but not deeper;

h) existing streaks deepened in the rough bed;

i) individual particles traveled back and forth and some-
    times formed a ripple-like formation;

j) after removal of the skin layer, individual particles
    from the layer below the skin layer went into motion
    but, with time, a new skin layer formed and continued
    to peel off the same way as the top skin layer (but
    the bonded particles were not as big as for the original
    skin layer);

k) particles shreded from the surface layer when enough
    of the skin layer was in motion to tear away from the
    remaining surface layer;

l) deep scour streaks were observed at the end of the test
    section due to irregularities and roughness;

m) the individual silt and clay particles from the exposed
    layer which went into motion followed a circular motion.
    Particles near the water surface traveled upstream to the
    wave board and particles near the bed traveled downstream;
    and

n) the surface pattern of the bed consisted of pit marks, at
    both the smooth and rough surfaces and scour streaks at the
    rough surface and streaks at the smooth surface.

Figures 40, 41, and 42 show the suspended sediment
concentrations against time for runs 11 through 17, 18, and 19
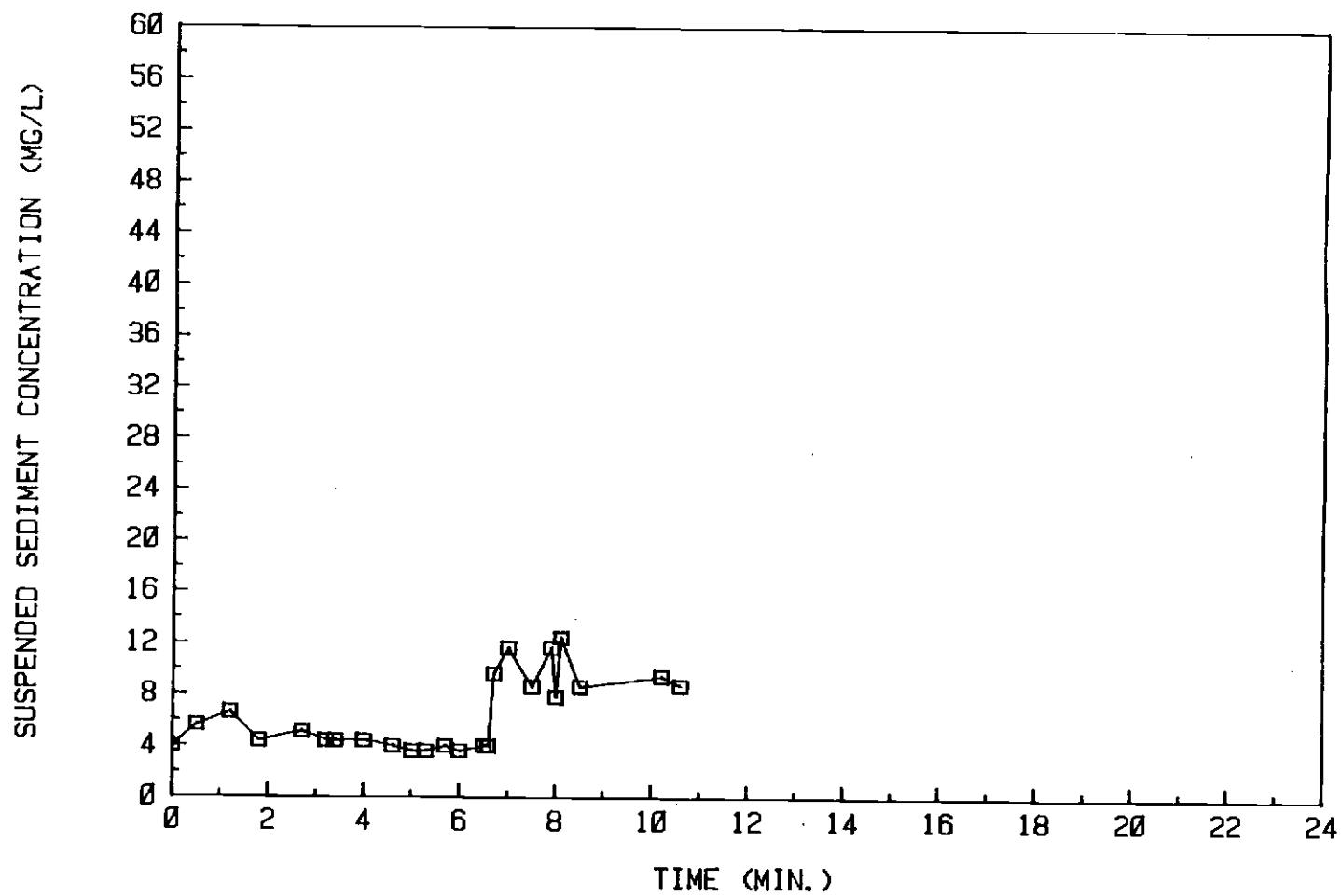
Figure 40. Suspended Sediment Concentrations For Runs 11 Through 17
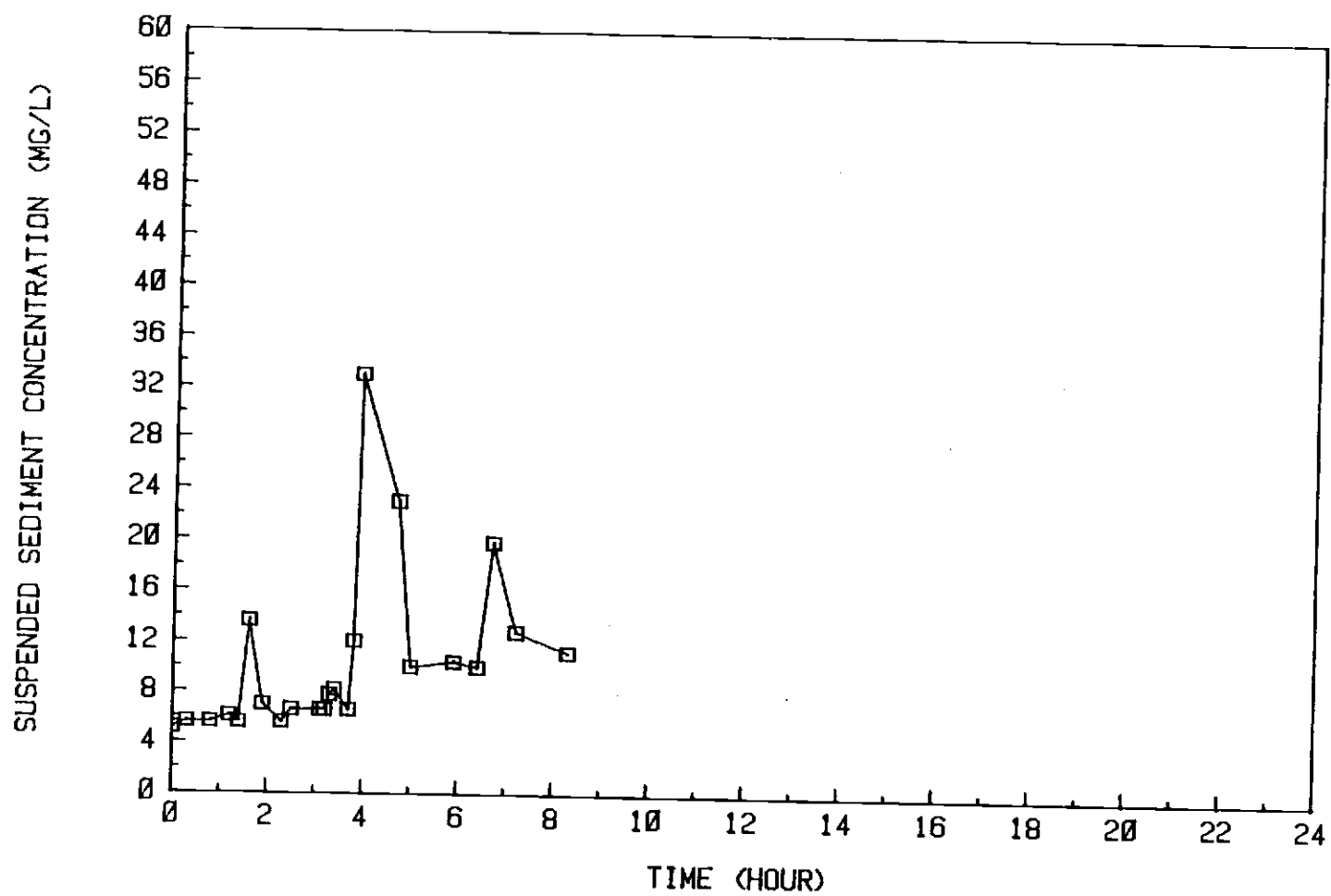
Figure 41.   Suspended Sediment Concentrations For Run 18
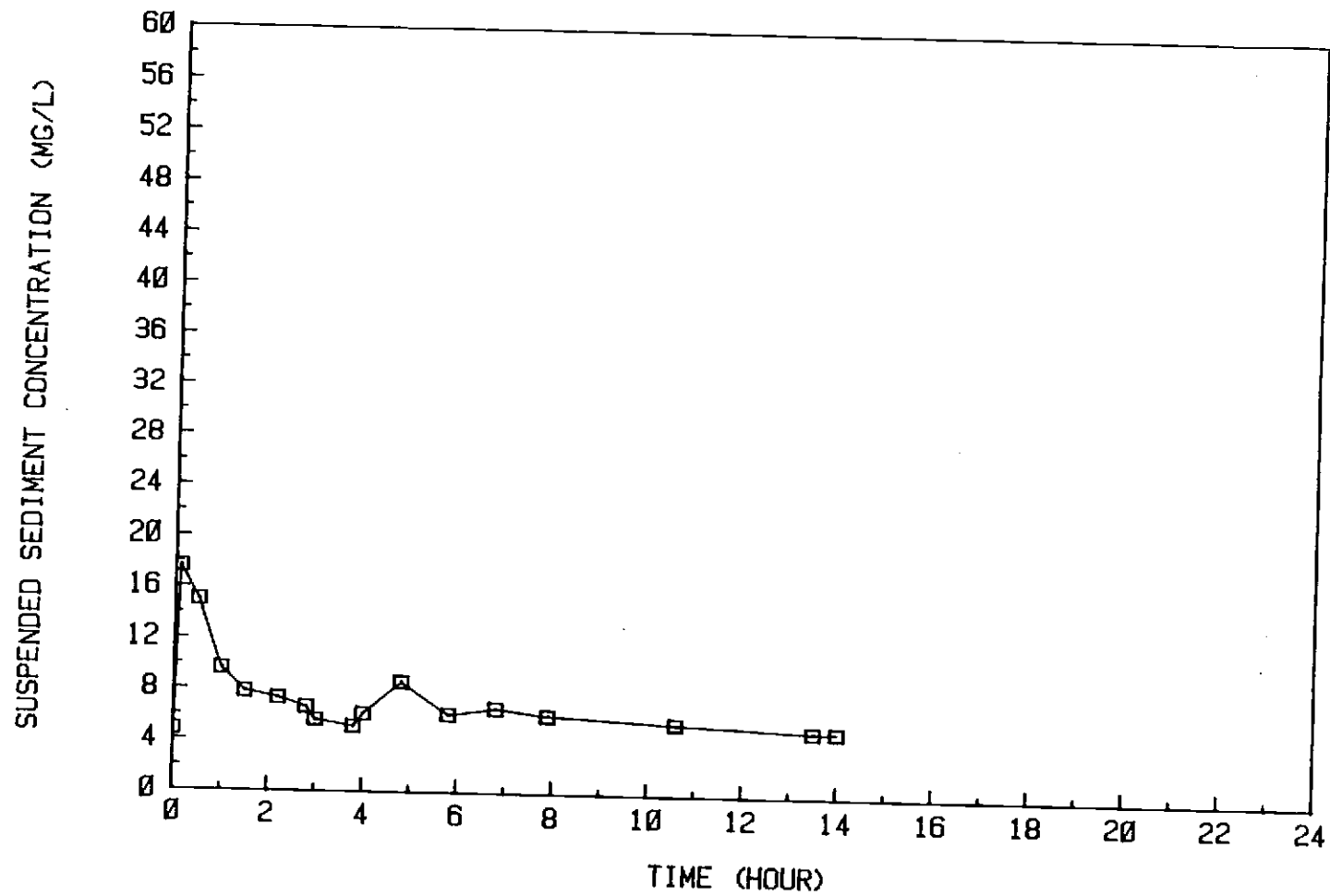
Figure 42.   Suspended Sediment Concentrations For Runs 19 Through 24

through 24 respectively. There are several peaks, especially at runs 15, 16, and 17. Run 18, the longest run, started with a concentration of about 5 mg/l and showed a sudden increase to 17.5 mg/l and then decreased and reached an equilibrium concentration of around 5 mg/l. Runs 20 and 21 also showed sudden increases in suspended sediment concentration. Organic content of the suspended sediment for these runs ranged from 14 to 50 percent.

5. Sediment Particles Motion--Runs 22-25, 27-28

For runs 22 through 25 and 27 through 28 the maximum velocity and shear stress at the bed ranged from 22.3 cm/sec to 27.3 cm/sec and from 5.97 dyne/cm to 7.04 dyne/cm , respectively. The orbital diameters ranged from 6.4 cm to 9.6 cm. The remaining old skin peeled off and streaks in the smooth surface grow longer and deeper. Large amounts of particles went into suspension. Large and deep scour streaks provided a source of sediment for further suspension. Peeling off of the new skin was observed at the rough bed and smooth bed surface, but the eroded new skin particles were not bonded as strongly as the original top skin layer. At the start of run 25, no old skin was evident anywhere. Individual particles grouped together to form ripple-like formations.

Figure 43 shows the concentrations of suspended sediment against time for runs 25 through 34. The suspended sediment concentration increased to 36 mg/l and then decreased with decreasing shear stress to about 9 mg/l. Suspended sediment concentration increased suddenly at the beginning of each run and then gradually decreased to an equilibrium concentration. The organic content varied from 7
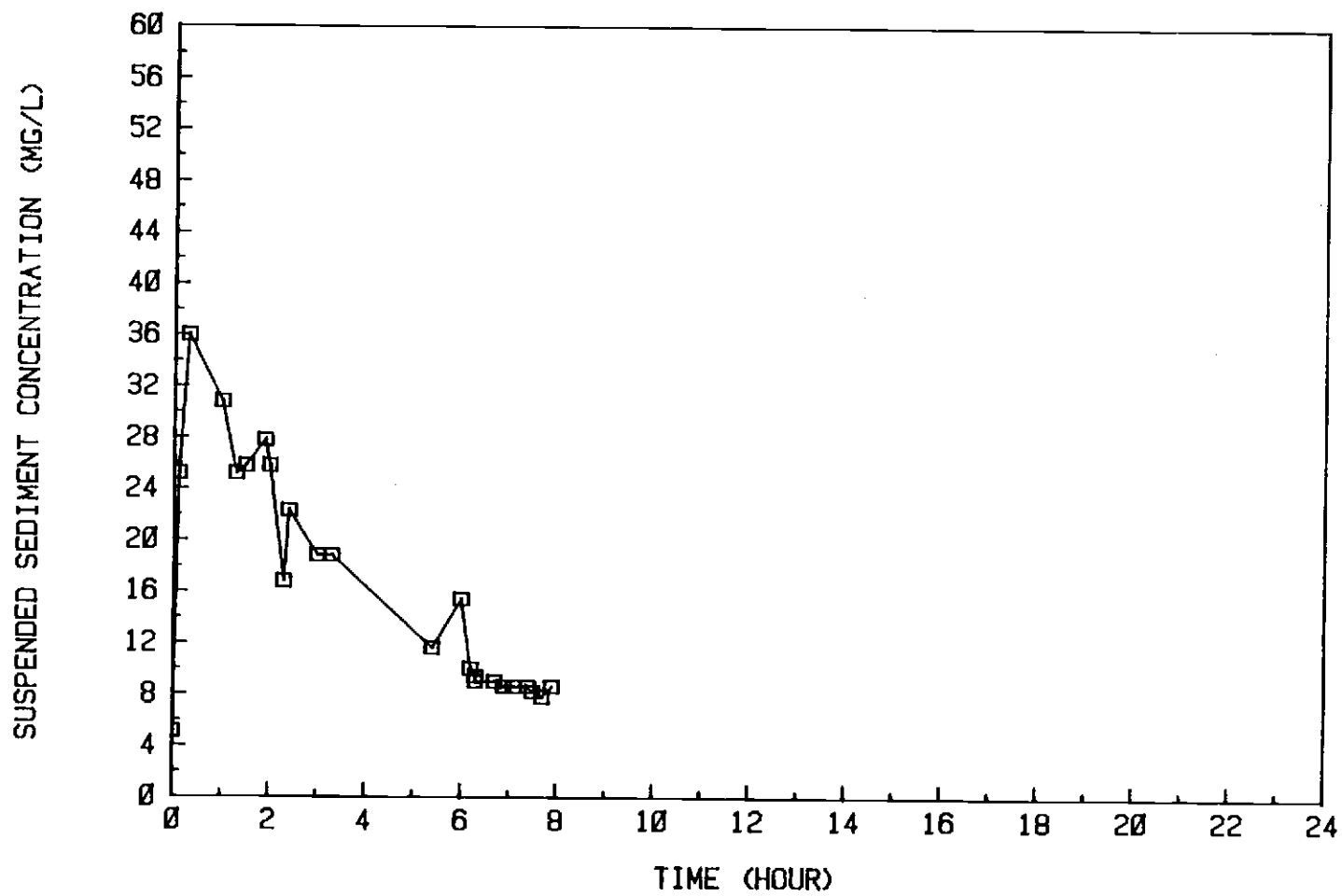
Figure 43. Suspended Sediment Concentrations For Runs 25 Through 34

to 38 percent of suspended sediment concentration.

6. Runs at Very Low Velocity and Shear Stress—Runs 30-34

For runs 30 through 34 (run 34 containing four phases), the maximum velocity and shear stress at the bed were systematically changed to cover all possible conditions available on the wave machine. The lowest values were 0.07 cm/sec and 0.03 dyne/cm^2, respectively. The orbital diameters varied from 0.01 cm to 1.5 cm. Visual observation showed that runs 30 through 33 were too weak to effect the particles at the bed. The suspended sediment concentrations versus time for runs 30 through 34 show a sudden decrease in concentration to an equilibrium value. The organic content of the suspended sedimet concentration varied from 23 to 30 percent.

At the end of the first category of runs, it was observed that the rough bed pattern consisted of many long deep scour streaks (45 cm long, 3 mm wide, and 5 mm deep), with evidence of coarse material in most of the deep scour streaks. Also, it was observed that the smooth bed surface pattern consisted of some long streaks (90-100 cm long, 2-3 mm wide, and 2-3 mm deep). The whole top skin layer was gone and 30 percent of the newly formed skin layer had been peeled off over the course of these runs. Many pit marks were evident.

7. Pattern of Eroded Bed Surface

The pattern of the bed surface was inspected and surveyed at the beginning of the experimental runs and several times during the first category of runs. The results showed that no significant changes occurred in the bed surface in terms of scour holes and

deposition areas. Many pit marks and scour streaks developed all along the bed surface. The following features were evident at both the smooth and rough bed: surface erosion, pit marks and streak lines, suspension of particles into the body of water, and a distinct color difference between the exposed layer and the original surface layer (effect of iron oxide). In addition, deep scour holes were evident at the rough bed.

The bed surface was photographed whenever significant changes were taking place, to aid in understanding and determining the incipient motion characteristics of the fine sediment under oscillatory flow. Figure 44 shows the bed surface before experimental runs. It shows the rough bed at the front of the test section and the smooth flat bed for the remaining test section. During experimental runs for initiation of sediment in the rough bed, the bed surface developed many pit marks and streak lines. Figures 45 shows such effects at the rough and smooth beds at the end of run 6 and during run 10. Figure 46 shows the suspension of sediment bed into the body of water during run 10.

Incipient motion of sediment particles at the smooth bed surface was characterized by the peeling off of the top skin layer. Figure 47 shows this bed pattern on the smooth bed and in the rough bed. Frequent suspension of sediment particles into the body of water was another facet of incipient motion characterizing the fine sediment bed. Figure 48 shows such suspension of sediment into the body of water during run 18.

The significance of irregularities in the incipient motion study
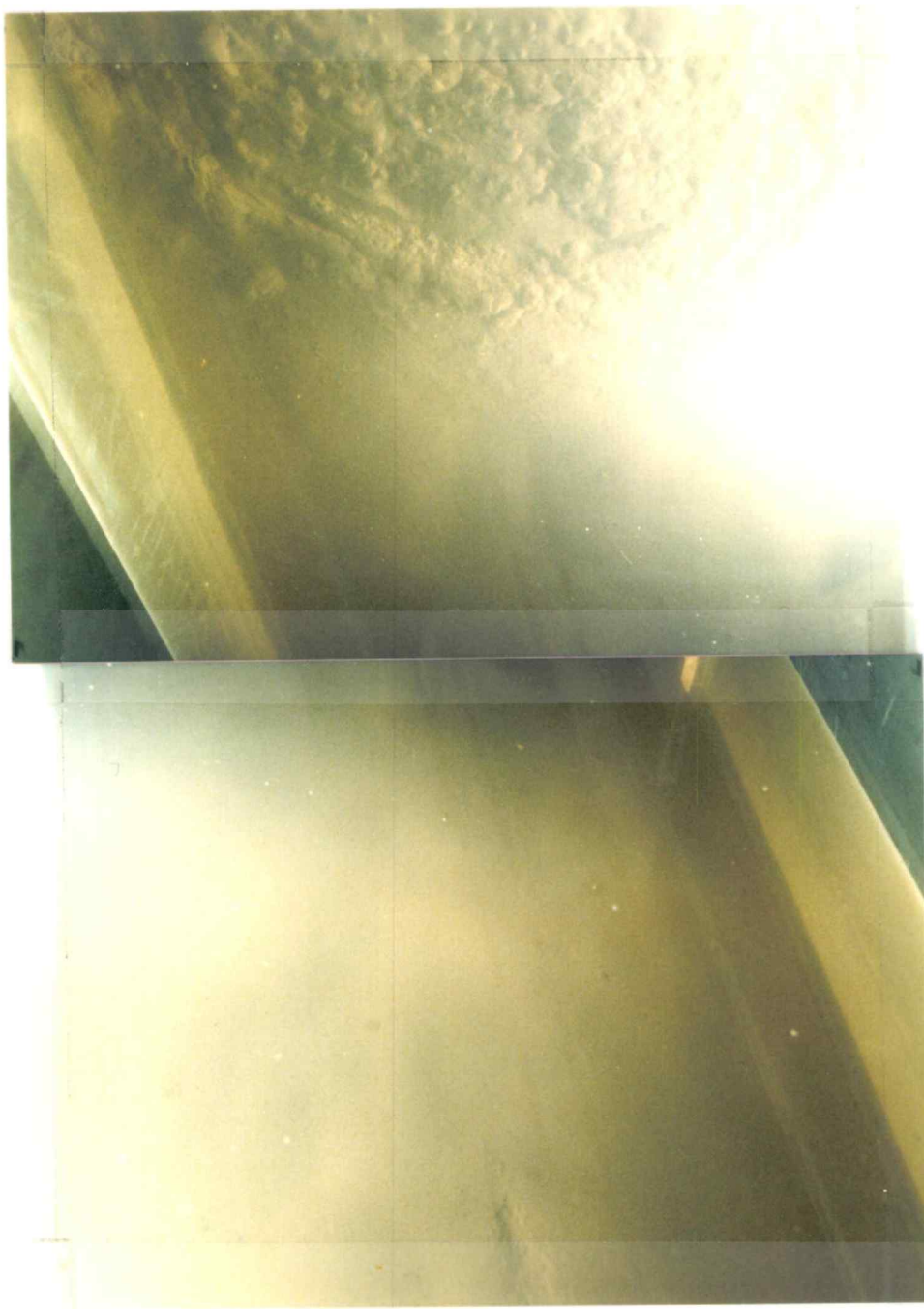
Figure 44.   Bed Surface Before Experimental Runs
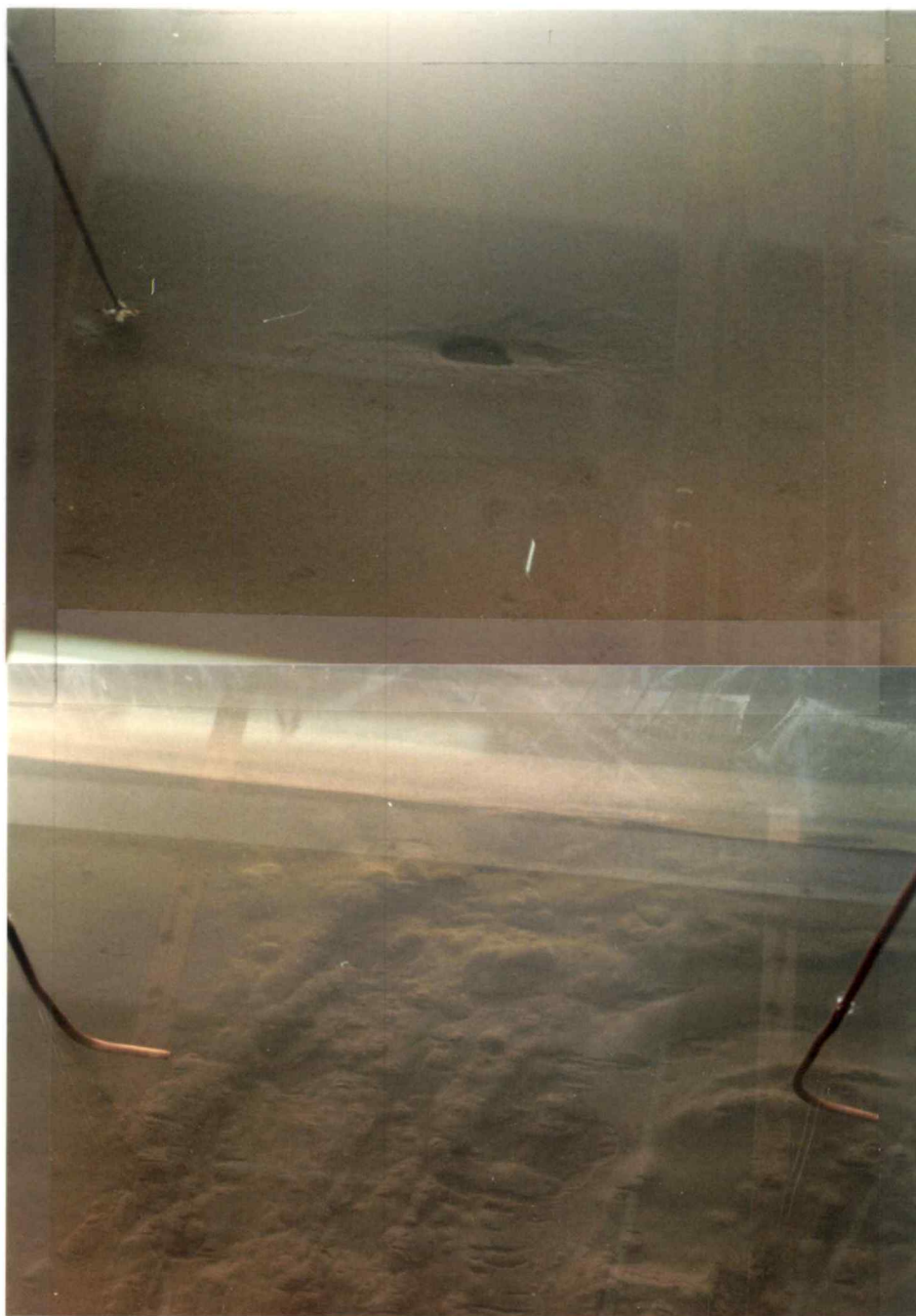
Figure 45.   Bed Surface for Smooth and Rough Beds

Figure 46.   Suspension of Bed Sediment Into Body of Water
During Run 10

Figure 47. Bed Patterns for the Smooth and Rough Beds

Figure 48.   Suspension of Sediment Into a Body of Water
During Run 18

fine sediment on sediment bed pattern is shown in Figure 49. The benthic worms and their effect on bed pattern are shown in Figure 50.

Runs 22 through 28 were characterized by shear stresses and velocities higher than required to initiate the sediment motion. Figure 51 shows the suspension of sediment into the body of water and Figure 52 shows the pit marks, streak lines and scour streaks developed during these experimental runs.

Results of Second Category of Runs (Runs 35-62)

The purpose of runs 35 to 46 was to determine the characteristics of incipient motion of compacted sediment bed for comparion with the incipient motion of freshly deposited sediment. The purpose of runs 47 to 62 was to determine the characteristics of incipient motion of a compacted sediment bed at two different water depth bed with varying wave height and wave period.

1. Incipient Motion at Rough Bed--Runs 35-38, 47-51, 58

The maximum velocities at the bed for runs 35 through 38, 47 through 51 and 58 varied from 5.5 cm/sec to 17.9 cm/sec. The maximum shear stresses at the bed ranged from 0.97 dyne/cm^2 to 4.82 dyne/cm^2. The orbital diameter ranged from 2.0 cm to 4.9 cm. In the rough bed and at the two irregular ends of the test section. These shear stresses were able to put particles into pivotal motion with downstream net transport.

After 71 days of settling, the bed surface looked very smooth. Upon initiation of wave movement, the same phenomena took place on

Figure 49. Streak Lines Due to Bed Irregularities
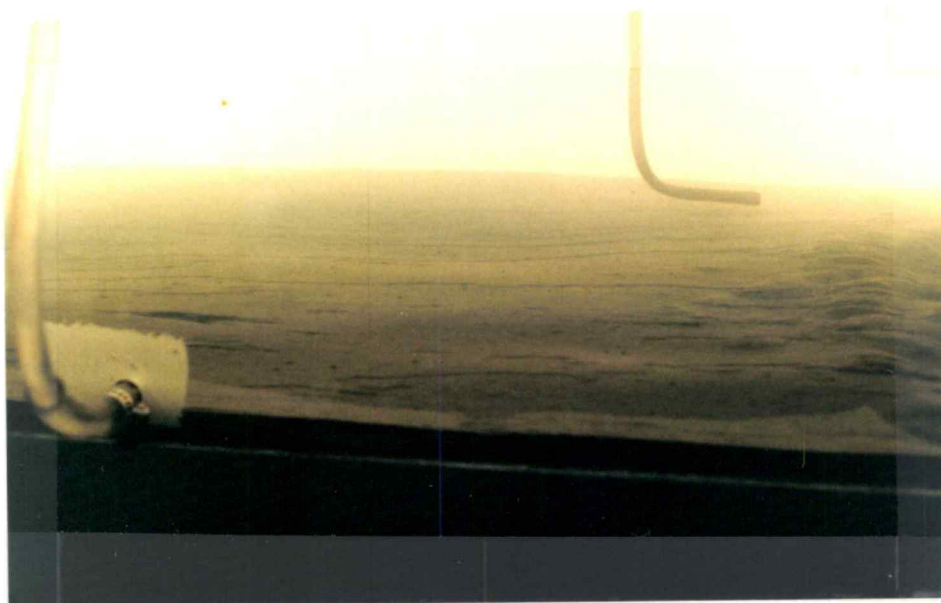
Figure 50. Benthic Worms and Their Effect on Bed Pattern
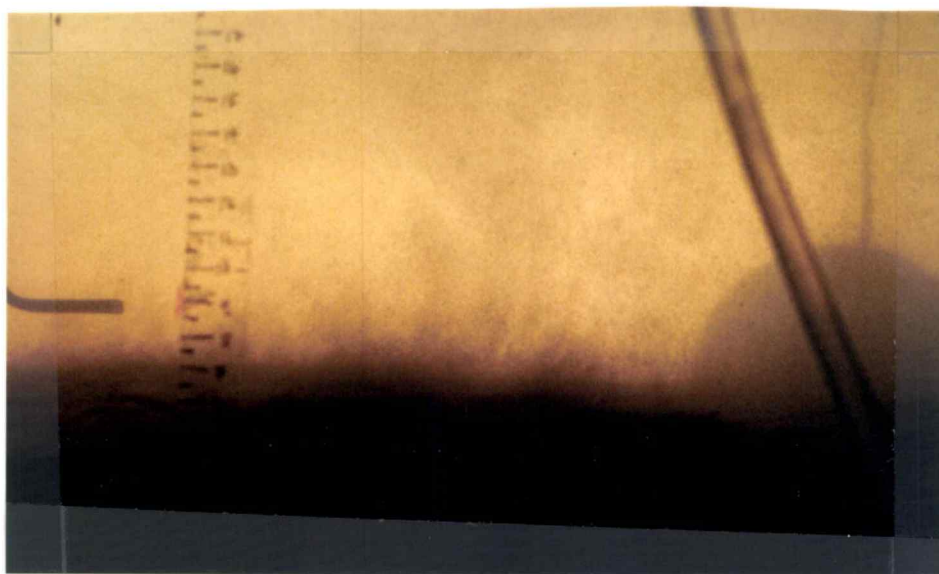
Figure 51. Typical Suspension of Sediment into Body of Water
During Runs 22 Through 28

Figure 52. Pit Marks, Streak Lines and Scour Streaks on Bed

the bed as in the first category of experimental runs. Bonded
particles started to peel off, with some immediately going into
motion in the rough bed. In the scour streaks, individual particles
moving in a back and forth motion formed a ripple-like formation.
Bonded particles in the rough bed moved back and forth and caused
more surface erosion of particles by abrasion.

Figures 53 and 54 show the suspended sediment concentrations
against time for runs 35 through 39 and for runs 47 through 51,
respectively. The concentration data show a steady increase in
concentration, but with a very sudden increase in run 47 and,
thereafter an abrupt decrease to the same level as in runs 35
through 38. This sudden increase was due to abrasion of the large
bonded particles on the surface of the bed at surface
irregularities, such as holes that had developed unintentionally
from current meter contact with the bed surface. The average
suspended sediment concentration values at the rough bed were higher
for this set of runs than for the corresponding set of runs for
incipient motion on a freshly deposited bed. This is due to the
higher velocities and shear stresses associated with these runs.

The maximum velocity and shear stress associated with these runs
were also higher than the runs for freshly deposited bed. This
brings two interesting results:

a) At the rough bed, as the sediment compacted or the
   shear strength of sediment increased, a higher shear
   stress was required for incipient motion; and

b) Even though a higher shear stress was required for
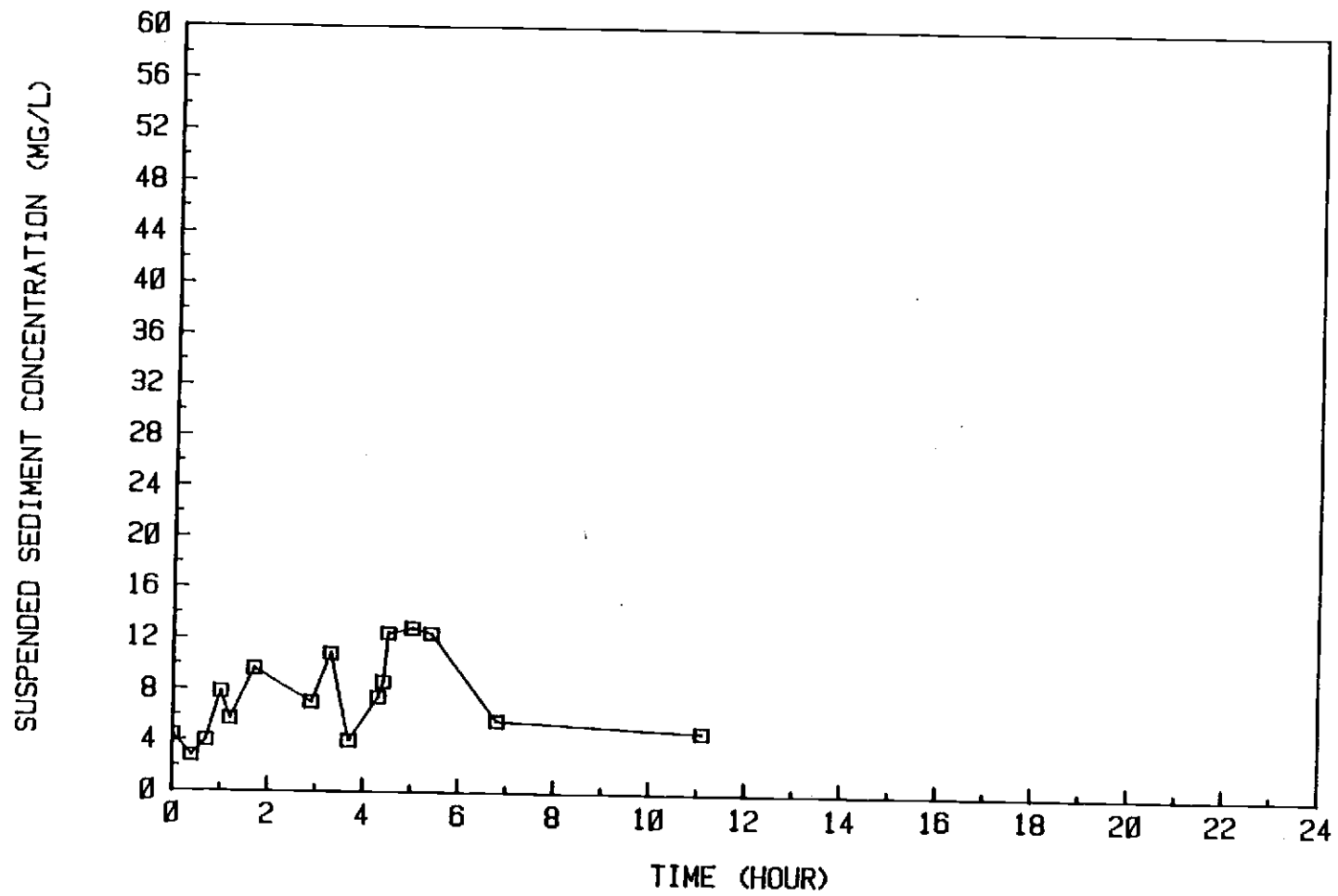
Figure 53. Suspended Sediment Concentrations For Runs 35 Through 39
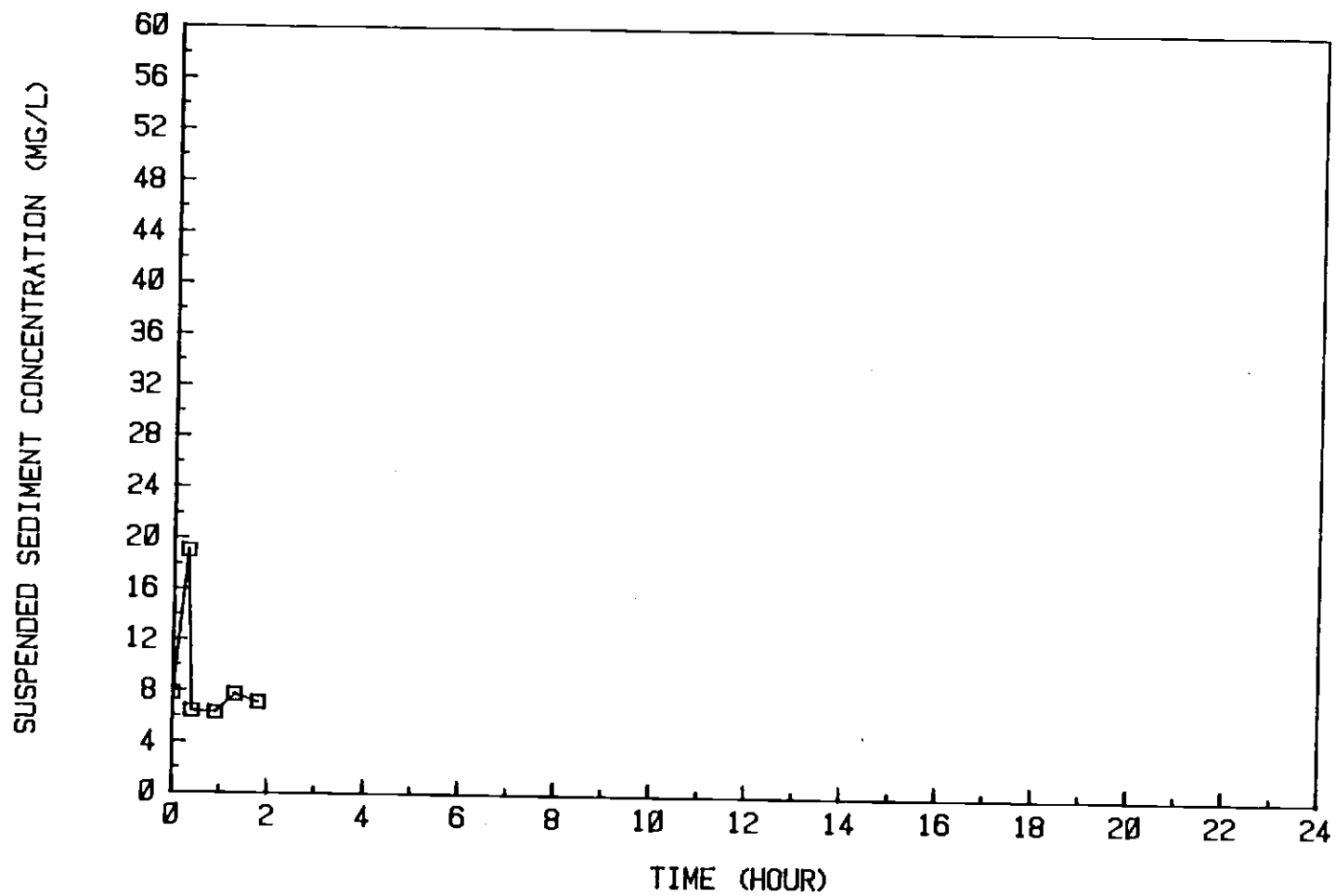
Figure 54. Suspended Sediment Concentrations For Runs 47 Through 51

Incipient motion in the compacted bed than in the freshly deposited bed, the resultant suspended sediment concentration was higher for the compacted sediment bed than for the freshly deposited bed. If suspended sediment concentration is used as a guide, this indicates that shear stress is not a function of shear strength for incipient motion.

2. Incipient Motion in Smooth Bed Surface--Runs 39-43, 52, 53

The incipient motion of smooth bed surface started with the conditions of run 39. The maximum velocity at the bed was 22.0 cm/s and the corresponding maximum shear stress at the bed was 5.39 dyne/cm^2. The orbital diameter was about 7.1 cm. The overall maximum velocities at the bed for incipient motion in experimental runs 39 through 43, 52, and 53 ranged from 20.0 cm/s to 25.0 cm/s. The maximum shear stresses ranged from 5.39 dyne/cm^2 to 6.00 dyne/cm^2 and the orbital diameters ranged from 4.8 cm to 7.2 cm.

Comparison of the maximum velocity, maximum shear stress, and the orbital diameter at the freshly deposited bed and the compacted sediment bed revealed that at the lower limit range, velocities and shear stresses for the freshly deposited bed were 32 percent lower than for the compacted bed and orbital diameter were 13 percent lower than for compacted beds. At the upper limit range, velocities were 14 percent lower, shear stresses were 8 percent lower, and orbital diameters were 13 percent shorter than for the compacted bed. That means for the incipient motion of fine sediment, shear stress is somewhat affected by compaction of sediment.

To determine whether the variations in velocity, shear stress and orbital diameter at conditions of incipient motion were due to the subjective determination of incipient motion or due to the effect of compaction, the analysis and comparison of suspended sediment concentration data is essential.

Figure 55 shows the suspension concentrations versus time for runs 40 through 46. The concentration data show an increase of concentration at the start of each run to a maximum of 16.5 mg/l. Comparison with freshly deposited concentration curves shows higher concentrations occurred for the compacted sediment bed. This reveals that due to higher shear stresses, more sediment is in suspension. Therefore, the shear stress for incipient motion is probably not a function of the compaction of the sediment. This conclusion requires more experiments for verification, with sediment beds of different shear strengths.

The erosion of particles took place in the same manner as already discussed in the first category of experimental runs. The data show a sudden increase in suspended sediment concentration at the beginning of the run and then the concentration decreased to a steady state around 5 mg/l. Most of the suspended particles deposited on the mats at the downsteam end of the wave flume; some deposition also occured near the ends of the test section.

The erosion pattern of the bed surface at the rough bed consisted of deep scour streaks. At the smooth bed surface, the erosion pattern consisted of pit marks and streak lines.
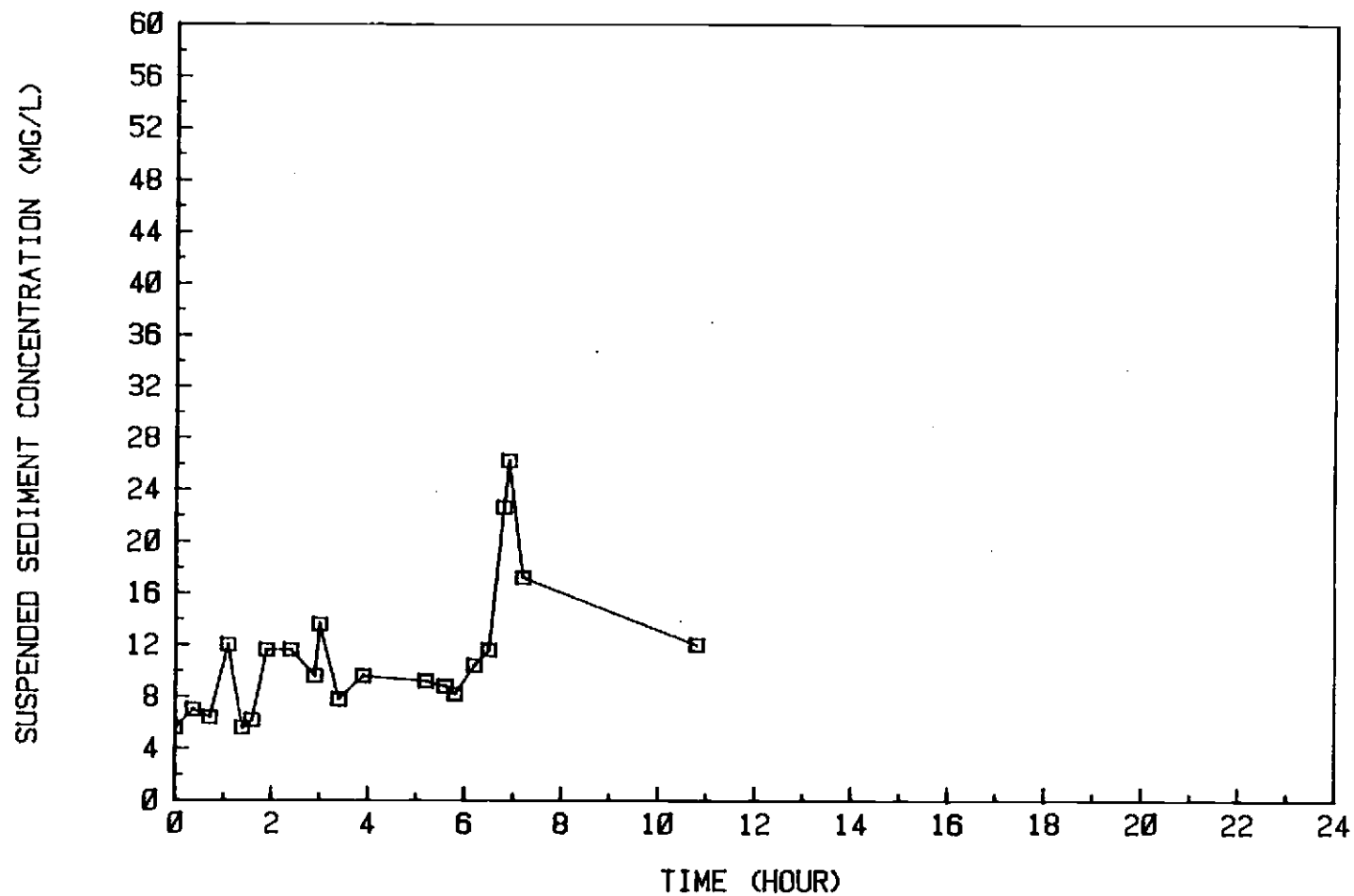
Figure 55.   Suspended Sediment Concentrations For Runs 40 Through 46

3. Motion Condition--Runs 44-46, 54, 59-62

Runs 44 through 46, 54, and 59 through 62 were characterized by many particles being in motion, continued peeling off of the sediment over the entire bed, higher concentrations of suspended sediment, and many streak lines and deep scour streaks. The same phenomena took place as for prior runs, except that the water was more turbid and full of individual and bonded particles in circular motion in the water body. There was a net downstream transport for particles close to the bed and a net upstream transport for particles near the water surface.

The suspended sediment concentration data for runs 52 through 62 are plotted in Figure 56. The suspended sediment concentrations reached a maximum of 34 mg/l. The concentration shows an increase at the start of each run and a gradual decrease with time, but with definitely higher concentrations than for all other runs. In comparison to the freshly deposited sediment bed, the concentrations for the compacted bed reached almost the same upper limit.

The maximum velocities at the bed ranged from 24.6 cm/sec to 42.0 cm/sec, the maximum shear stresses at the bed ranged from 6.7 dyne/cm^2 to 10 dyne/cm^2, and the orbital diameters ranged from 6.5 cm to 14.9 cm.
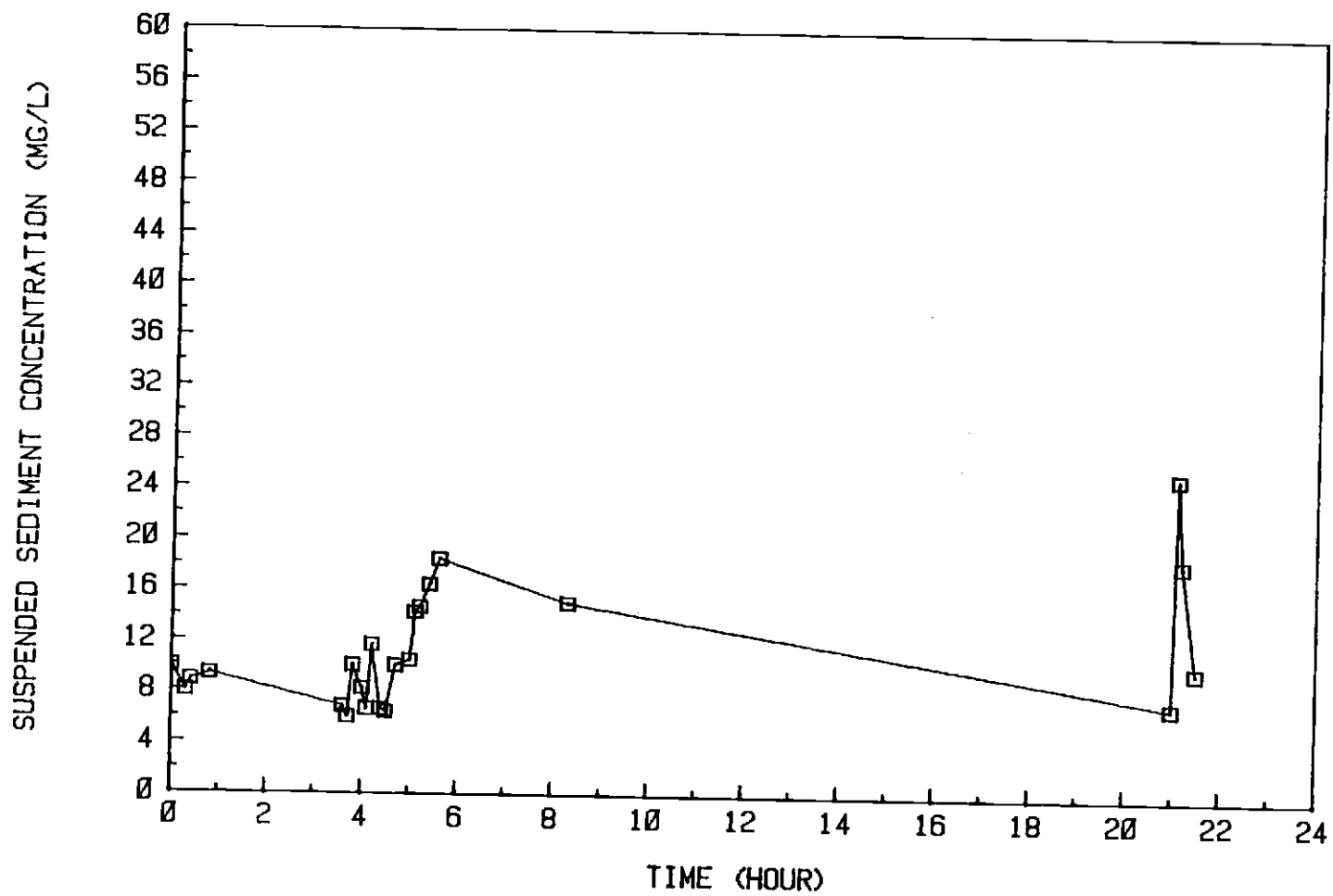
Figure 56. Suspended Sediment Concentrations For Runs 52 Through 62

Results of Third Category of Runs (Runs 63-67)

The third set of runs started with the addition of 800 grams of granulated sodium hexametaphosphate dispersing agent to the water in the flume. The effectiveness of dispersive agents on sediment depends upon the amount of dispersive agents, method of mixing, time of contact, type of sediment, and chemical characteristics of the water and sediment. In this case, time of contact was two days and dispersive agent was added to the middle of the water column at the smooth bed surface.

Several different wave heights and wave periods were used with a water depth of 12 inches. Visual observation was used to record the following phenomena:

a) With a bottom shear stress of 2.1 dyne/cm^2, a cloud of sediment was observed where the dispersive agent had been in contact with the bed surface;

b) with the shear stress increased to about 5.0 dyne/cm^2, a large amount of sediment went into suspension, starting at the irregular shaped end of the test section, then at the previously eroded middle of the smooth surface, and later in the rough bed zone;

c) over time, no additional particles went into suspension but the water remained turbid due to the breakdown of bonded particles of the top skin layer into clay and collidal particles by the dispersant. Clay and collidal particles contribute to turbidity and stay in suspension a long time; and

d) there was no evidence of peeling off of the sediment at

   places where the dispersing agent was added directly over

   the bed surface.

Figure 57 shows the suspension concentrations versus time for

runs 63 through 67. The concentration data show that in run 67

concentration increased to 64 mg/l, about twice greater than for any

runs in the two previous experimental series. Over time, the

concentration decreased to around 32 mg/l and stayed constant. This

final concentration was almost the same as the maximum concentration

that took place in the two previous experimental series. This

implies that the erosion of fine cohesive sediment took place layer

by layer, or as surface erosion.

   The concluding remarks from this set of runs are:

a) The surface bed of sediment under water containing a

   dispersant is more susceptible to erosion than the bed

   without the dispersive agents at comparable flow conditions;

   and

b) dispersive agents break down the skin layer.

Type of Boundary Layer Flow in Experimental Runs

Analysis of the experimental data shows that the flow regime or

boundary layer condition in all of the runs was either laminar or in

transition from laminar to smooth turbulent, based on evaluation

approaches discussed in the literature review (e.g., Li (1954),

Jonsson (1966) and Riedel (1972)). This also supports the
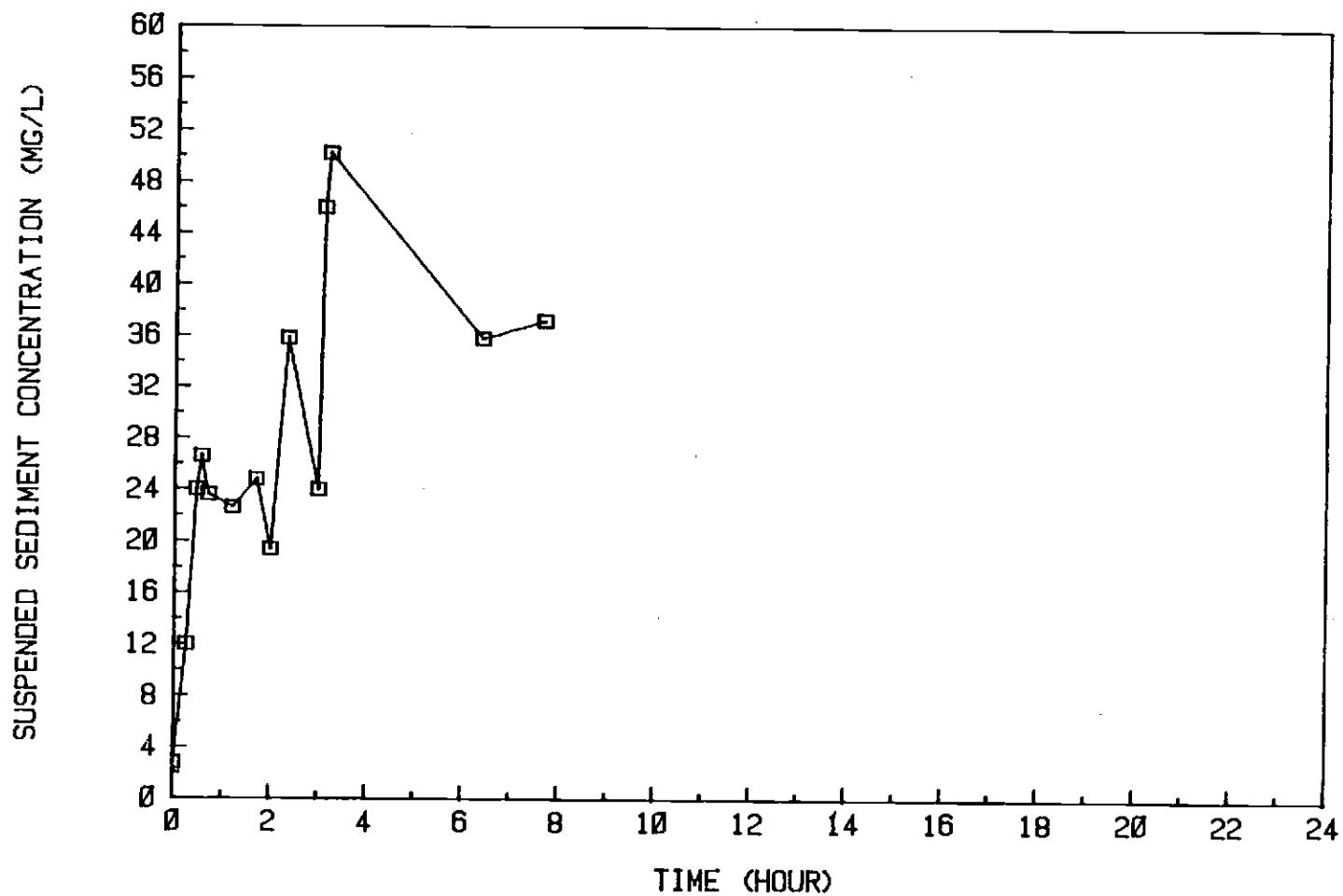
Figure 57. Suspended Sediment Concentrations For Runs 63 Through 67

dye-streak observation of Bagnold (1946) which concluded that the boundary layer was laminar in all of his experiments, even though quartz grains as large as 0.33 cm were used.

Three different approaches were used to identify the flow regime.

a) Whether δ/k is less than 18.5 or greater than 30 (Li, 1954 and others at Berkeley);

b) $RE = \dfrac{U_m \alpha}{\nu} \delta$ and $\dfrac{\alpha \delta}{K_s}$ in a graphical form (Jonsson, 1966); and

c) $RE = \dfrac{U_m \alpha}{\nu} \delta$ and $\dfrac{\alpha \delta}{K_s}$ in a graphical form (Riedel, 1972).

Jonsson's upper limit for the laminar flow regime is RE = 11,900; Riedel's upper limit is RE = 10,700. The results of these calculations are shown in Table 11. According to Li's concept, the flow regime was laminar for all experimental runs. But based on Jonsson's approach, there was a transition boundary layer (from laminar to smooth turbulent) for runs 27, 34c, 34d, 46, 56, and 60 through 62, all other runs having a laminar boundary layer. Reidel's approach gave similar results to Jonsson's approach: all of the runs were in laminar regime except runs 24, 27, 33, 34, 44, 46, 53, 56, and 59 thrugh 62, which were in transition of laminar to smooth turbulent regime.

Wave Height and Period Measurement and Calculation

The wave height under oscillatory flow was obtained for the majority of the first set of runs by measurement of the difference

Table 11. Flow Regime Determination For Oscillatory Flow

Run				Berkeley's Equation 1954	Riedel's Equation 1972	Jonsson's Equation 1966
1a	326	500	611	Laminar	Laminar	Laminar
1b	227	481	1,168	"	"	"
2	259	334	877	"	"	"
3	158	326	1,111	"	"	"
4a	149	297	1,030	"	"	"
4b	144	270	913	"	"	"
5	139	246	803	"	"	"
6	132	184	506	"	"	"
7	131	192	556	"	"	"
8	131	180	494	"	"	"
9	137	314	1,358	"	"	"
10	153	454	2,270	"	"	"
11	148	472	2,638	"	"	"
12	141	472	2,891	"	"	"
13	136	360	1,806	"	"	"
14	130	283	1,220	"	"	"
15	155	559	3,354	"	"	"
16	147	672	5,402	"	"	"
17	138	486	3,240	"	"	"
18	136	452	2,964	"	"	"
19	155	816	7,212	"	"	"
20	146	754	6,907	"	"	"
21	138	618	3,247	"	"	"
22	150	875	8,866	"	"	"
23	141	726	6,890	"	"	"
24	153	980	10,687	"	Transition to Turbulent	"
25	147	758	6,910	"	Laminar	"
26	140	454	2,704	"	"	"
27	161	1,088	11,888	"	Transition to Turbulent	Transition to Turbulent
28	135	924	9,686	"	Laminar	Laminar
29	136	401	2,253	"	"	"
30	128	165	426	"	"	"
31	124	110	204	"	"	"
32	121	75	100	"	"	"
33	110	17	6	"	Transition to Turbulent	"
34a	131	41	25	"	Laminar	"
34b	124	28	12	"	"	"
34c	107	2.3	0.15	"	"	"
34d	102	1.2	0.03	"	"	Transition to Turbulent
35	169	826	6,187	"	"	Laminar
36	132	532	4,196	"	"	"

Table 11. Flow Regime Determination for Oscillatory Flow (cont.)

Run				Berkeley's Equation 1954	Riedel's Equation 1972	Jonsson's Equation 1966
37	125	317	1,666	"	"	"
38	120	223	896	"	"	"
39	145	802	7,983	"	"	"
40	140	774	7,901	"	"	"
41	129	577	5,168	"	"	"
42	137	814	9,129	"	"	"
43	132	653	6,381	"	"	"
44	141	984	12,705	"	Transition to Turbulent laminar	"
45	132	737	8,089	"		"
46	146	1,281	19,831	"	Transition to Turbulent laminar	Transition to Tubulent laminar
47	205	399	983	"		
48	162	362	1,292	"	"	"
49	130	318	1,559	"	"	"
50	124	289	1,406	"	"	"
51	128	461	3,360	"	"	"
52	130	619	5,902	"	"	"
53	125	541	4,861	"	"	"
54	136	880	10,812	"	Transition to Turbulent laminar	"
55	170	590	3,101	"		"
56	142	1,783	12,961	"	Transition to Turbulent laminar	Transition to Turbulent laminar
57	128	268	1,135	"		
58	135	557	4,396	"	"	"
59	141	988	12,660	"	Transition to Turbulent	"
60	156	1,359	19,601	"	"	Transition to Turbulent
61	153	1,336	19,751	"	"	"
62	154	1,688	31,301	"	"	"

between crest and trough of successive waves. The wave period was obtained by measurement of the time required for successive wave crests to pass a fixed point. These measurements for wave height and period were repeated several times to obtain a representative average value. The wave envelope method was not used because the reflection coefficient was small.

The wave height and period were also obtained by analyzing the recorded waves by sonic wave profiler. The twenty wave cycles at the beginning and at the end of the runs were first eliminated; then an average value for wave height and wave period was obtained from the remainder of the record. Table 12 shows the wave height and period for these two different ways of making measurements.

The results show very good agreement between wave period measurements by two techniques. There was some discrepancy between two types of measurement of wave height, which was due to errors involved in visually measuring the wave height.

As a result of the good comparison of techniques the sonic wave profiler alone was used to determine wave height and period for all remaining runs.

Shear Stress Calculation

The maximum shear stress at the bed was calculated utilizing two relationships. These were:

a) $\tau_0 = 1/2 \, \rho \, f_w \, U_m^2$, where f_w was obtained from the

Jonsson friction factor and U_m was measured and calculated

by linear wave theory approximation; and

Table 12.   Wave Height and Period for First Set
of Runs by Two Different Techniques

Run	Wave Height Inch		Wave Period Second	
	S.W.P*	Meas.	S.W.P*	Meas.
5	2.38	2.25	0.86	0.82
6	2.60	2.48	0.77	0.78
7	2.88	2.91	0.76	0.71
8	3.20	3.15	0.73	0.69
9	3.76	--	0.81	--
10	2.88	2.91	1.01	1.01
11	3.48	2.95	0.95	0.95
12	4.48	3.54	0.87	0.87
15	3.20	2.95	1.06	1.06
17	5.28	4.92	0.83	0.83
18	5.28	4.65	0.82	0.82
19	4.40	3.94	1.09	1.10
21	6.00	4.72	0.86	0.86
22	5.44	4.72	1.02	1.09
23	6.24	4.72	0.90	0.91
24	5.60	4.57	1.06	1.07
26	4.80	4.72	0.84	0.84
27	5.76	4.53	1.10	1.09
28	6.48	5.31	0.97	0.96
29	5.20	4.33	0.79	0.79
31	3.28	3.15	0.66	0.66
32	3.04	2.76	0.62	0.61
33	2.56	2.36	0.52	0.54
34a	1.04	1.18	0.44	0.44

*S.W.P. = Sonic Wave Profiler

b) $\tau_o = \mu\dfrac{dU}{dy}$ where $\dfrac{dU}{dy}$ was calculated by differentiating

velocity from linear wave theory approximation.

Table 13 shows the maximum shear stress at the bed from the two

approaches for all experimental runs. The results show fairly close

agreement of values for both techniques. The differences are due to

the assumptions made in approach b that (a) waves in the generating

area are only sinusiodal waves and (b) laminar shear conditions

prevail. Therefore, technique a was used for analysis and discussion

in this study.

Velocity Measurement and Calculation

The continuous velocity at the boundary layer was measured with

the miniature current meter and recorded. The record was analyzed to

obtain the maximum horizontal velocity during the wave cycle for each

run during the first set of runs. The maximum horizontal velocity at

the bed was also calculated using the linear wave theory approach

with equation 22.

Table 14 shows the results for the measured and calculated

maximum velocity at the bed. The results show a very good agreement

between the measured and calculated velocity values. A few observed

differences are due to malfunction of the current meter or its

inability to function at very low velocities.

Table 13. Shear Stress Calculations for Oscillatory Flow

Run	$\frac{1}{2}f_w\rho U_m^2$	$\mu\frac{dU}{dy}$	Run	$\frac{1}{2}\rho f_w U_m^2$	$\mu\frac{du}{dy}$
1a	0.36	0.25	33	0.32	0.23
1b	1.02	0.72	34a	0.47	0.34
2	1.37	0.96	34b	0.37	0.26
3	2.05	1.48	34c	0.066	0.04
4a	2.22	1.56	34d	0.028	0.02
4b	2.23	1.57	35	3.53	2.50
5	2.19	1.57	36	4.73	3.33
6	1.95	1.40	37	3.33	2.35
7	1.06	1.47	38	2.66	1.87
8	2.10	1.50	39	3.39	3.80
9	3.11	2.18	40	5.70	4.03
10	3.22	2.28	41	5.52	3.89
11	3.67	2.61	42	6.32	4.62
12	4.18	2.92	43	5.91	4.18
13	3.56	2.49	44	7.41	5.25
14	3.20	2.22	45	6.71	4.74
15	3.67	2.58	46	8.53	6.04
16	5.20	3.70	47	0.97	0.69
17	4.60	3.30	48	1.78	1.24
18	4.49	3.14	49	3.06	2.16
19	5.03	3.54	50	3.19	2.25
20	5.53	3.89	51	4.61	3.26
21	5.44	3.89	52	5.96	4.20
22	5.97	4.28	53	5.84	4.13
23	5.99	4.18	54	7.33	5.17
24	6.30	4.43	55	2.50	1.77
25	6.24	4.43	56	2.34	2.93
26	4.27	2.98	57	2.68	1.88
27	6.84	4.85	58	4.82	3.62
28	7.04	4.94	59	7.49	5.29
29	4.15	2.94	60	7.61	5.38
30	2.04	1.46	61	8.01	5.66
31	1.49	1.05	62	9.97	7.05
32	1.11	0.80			

Table 14. Comparison of Calculated and Measured
Velocities for Oscillatory Flow

Run	Calculated Velocity cm/s	Measured Velocity cm/s
1a	2.97	0.00
1b	5.91	5.43
2	6.38	6.58
3	8.28	7.15
4a	8.45	8.02
4b	8.21	8.02
5	7.88	7.73
6	6.62	6.00
7	6.98	5.00
8	6.84	6.00
9	10.72	12.00
10	12.40	12.50
11	13.73	15.00
12	15.01	16.00
13	12.31	15.00
14	10.58	13.50
15	14.59	18.00
16	19.56	21.00
17	16.20	17.00
18	15.64	16.50
19	20.69	15.00
20	21.46	20.00
21	19.87	18.50
22	23.72	20.00
23	22.32	14.00
24	25.54	18.00
25	22.79	20.00
26	14.91	13.50
27	27.33	28.00
28	26.33	30.00
29	14.04	14.00
30	6.49	5.00
31	4.61	3.50
32	3.33	2.50
33	0.88	0.0
34a	1.54	0.0

Effect of Mass Transport Velocity

As already discussed, individual particles in a progressive, irrotational wave do not describe exactly closed paths but instead advance in the direction of wave propagation at a rate corresponding to the mass-transport velocity.

The flows for the experimental runs were laminar and the mass transport velocity was calculated with the Longuet-Higgins (1953) theory. The results are shown in Table 15. The results indicate that as maximum velocity at the bed increased the mass transport velocity also increased. The maximum mass transport velocity recorded was 15.8 cm/sec for run 62, which is 38 percent of the maximum velocity at the bed. The minimum mass transport velocity recorded was 0.0001 cm/sec for run 34d, which is less than 1 percent of the maximum velocity at the bed.

Orbital Diameter Calculation

The orbital diameter at the boundary layer was measured by visually observing the sediment particle movements along the bed. The orbital diameter also was calculated using the linear wave theory approach, with equation 45. Table 16 shows the results of orbital diameter measurements and calculations. The results show that there is some agreement for the measured and calculated values. However, there are extreme discrepancies in some cases due to several factors, particularly due to errors involved in visually measuring the loose sediment particles on the bed surface.

Table 15.   Maximum Velocity and Mass Transport Velocity
             Under Oscillatory Flow

Run	Maximum Velocity cm/s	Mass-Transport cm/s	Run	Maximum Velocity cm/s	Mass-Transport cm/s
1a	2.97	0.07	34b	1.13	0.02
1b	5.91	0.29	34c	0.16	0.004
2	6.38	0.36	34d	0.07	0.0001
3	8.28	0.68	35	16.68	2.48
4a	8.45	0.72	36	17.52	3.39
4b	8.21	0.70	37	11.67	1.63
5	7.88	0.68	38	8.93	1.03
6	6.62	0.53	39	21.96	4.79
7	6.98	0.58	40	22.53	5.19
8	6.84	0.58	41	19.94	4.55
9	10.72	1.29	42	24.99	6.63
10	12.40	1.53	43	21.75	5.26
11	13.73	1.94	44	28.93	8.62
12	15.01	2.39	45	24.58	6.71
13	12.31	1.70	46	34.70	11.88
14	10.58	1.33	47	5.52	0.29
15	14.59	2.05	48	8.01	0.63
16	19.56	3.95	49	11.01	1.45
17	16.20	2.96	50	10.95	1.52
18	15.06	2.75	51	16.37	3.32
19	20.69	4.07	52	21.42	5.50
20	21.46	4.62	53	20.20	5.14
21	19.87	4.33	54	27.63	8.72
22	23.72	5.64	55	11.82	1.15
23	22.32	5.16	56	16.34	2.60
24	25.54	6.28	57	9.51	1.02
25	22.79	4.33	58	17.89	3.36
26	14.91	2.42	59	29.05	8.33
27	27.33	7.18	60	32.68	9.40
28	26.33	6.95	61	33.59	10.13
29	14.04	2.29	62	42.03	15.82
30	6.49	0.54			
31	4.61	0.28			
32	3.33	0.16			
33	0.88	0.01			
34a	1.54	0.03			

Table 16.   Comparison of Calculated and Measured
Orbital Diameters

Run	Calculated do cm	Measured do cm	Run	Calculated do cm	Measured do cm
1a	4.40	0.50	34b	0.24	<1.0
1b	4.23	0.50	34c	0.02	0.0
2	2.94	--	34d	0.01	0.0
3	2.87	0.50	35	7.27	2.0
4a	2.61	--	36	4.68	1.5
4b	2.38	--	37	2.79	1.0
5	2.16	2.0	38	1.96	1.0
6	1.62	1.5	39	7.06	2.0
7	1.69	1.5	40	6.81	1.5
8	1.59	1.5	41	5.08	2.0
9	2.76	2.5	42	7.16	2.5
10	3.99	3.0	43	5.75	3.0
11	4.15	4.0	44	8.66	2.5
12	4.16	--	45	6.49	3.0
13	3.17	--	46	11.27	--
14	2.49	--	47	3.51	0.5
15	4.92	3.0	48	3.19	1.0
16	5.91	--	49	2.80	0.5
17	4.28	3.0	50	2.54	1.0
18	3.98	2.0	51	4.06	2.0
19	7.18	3.0	52	5.45	3.0
20	6.63	--	53	4.76	--
21	5.44	--	54	7.24	3.0
22	7.70	4.0	55	5.19	--
23	6.39	--	56	4.99	1.0
24	8.62	--	57	2.36	0.5
25	6.67	--	58	4.90	2.0
26	3.99	--	59	8.67	2.5
27	9.57	--	60	11.96	3.0
28	8.13	--	61	11.76	6.0
29	3.53	--	62	14.85	6.0
30	1.45	--	63	4.23	--
31	0.97	--	64	7.18	--
32	0.66	<1.0	65	5.44	--
33	0.15	<1.0	66	6.32	--
34a	0.36	<1.0	67	9.57	--

Therefore, the calculated values are used in analysis and discussion of the experimental results. In the future, using dye or some other buoyant particles on the bed surface or using some sophisticated electronic measuring devices could eliminate the possibilities of such errors.

Shear Strength of Fine-Grained Cohesive Sediment

Various methods for determining shear strength in the past included: (1) unconfined shear strength; (2) direct shear measurement; (3) vane shear measurement; (4) press-cell (compression); (5) penetrometer; (6) empirical approach; and (7) extrapolating or interpolating from field vane shear tests.

Unfortunately, most of these techniques are not suitable for measuring the shear strength of fine loosely deposited sediment only a few centimeters deep. Several attempts were made to use the vane shear and Torvane to measure the shear strength of the sediment in the flume, but it was not possible to obtain accurate data because the sediment was too loose, the depth of sediment was too small, and the instruments were not very sensitive. Application of empirical approaches was tried but failed due to the gross generalization involved in the available empirical techniques. Extrapolation of field shear strength measurements are not realistically close to the actual measurements because of scale effects, primarily due to thickness differences.

In general, the most viable approach to quantify the shear strength of the fine sediment in a flume is to use a penetration device similar to that used by Krone (1962) and Partheniades (1962). Because of differences in bed preparation between their studies and this study, it did not seem possible to accurately measure the actual shear strength with a device like theirs; hence, this approach was not pursued. Instead, only the sediment compaction with time was measured and quantified.

Boundary Layer Thickness

The laminar boundary layer thickness was calculated using the following equations:

a) $\delta_L = \sqrt{\frac{\nu T}{\pi}}$ which was used by Riedel (1972) and Dingler (1979);

b) $\delta_L = 6.5\sqrt{\frac{\nu T}{2\pi}}$ which Li (1955) used; and

c) $\delta_L = \frac{11.6\nu}{U_*}$ which Jonsson (1966) used.

Table 17 shows the boundary layer thickness values calculated using the three different approaches for two of the set of runs. The results show that the calculated laminar boundary layer thicknesses based on techniques a and b are reasonably close. Li's approach gives laminar boundary thickness at least 2.5 times higher than given by the two other techniques.

Shear Stress and Maximum Velocity

The velocity and shear stress data for the first and second series of experimental runs under oscillatory flow are plotted in Figures 58 and 59. The results show that there are linear relationships between shear stress and maximum velocity at the bed.

Table 17. Boundary Layer Thickness for Oscillatory Flow

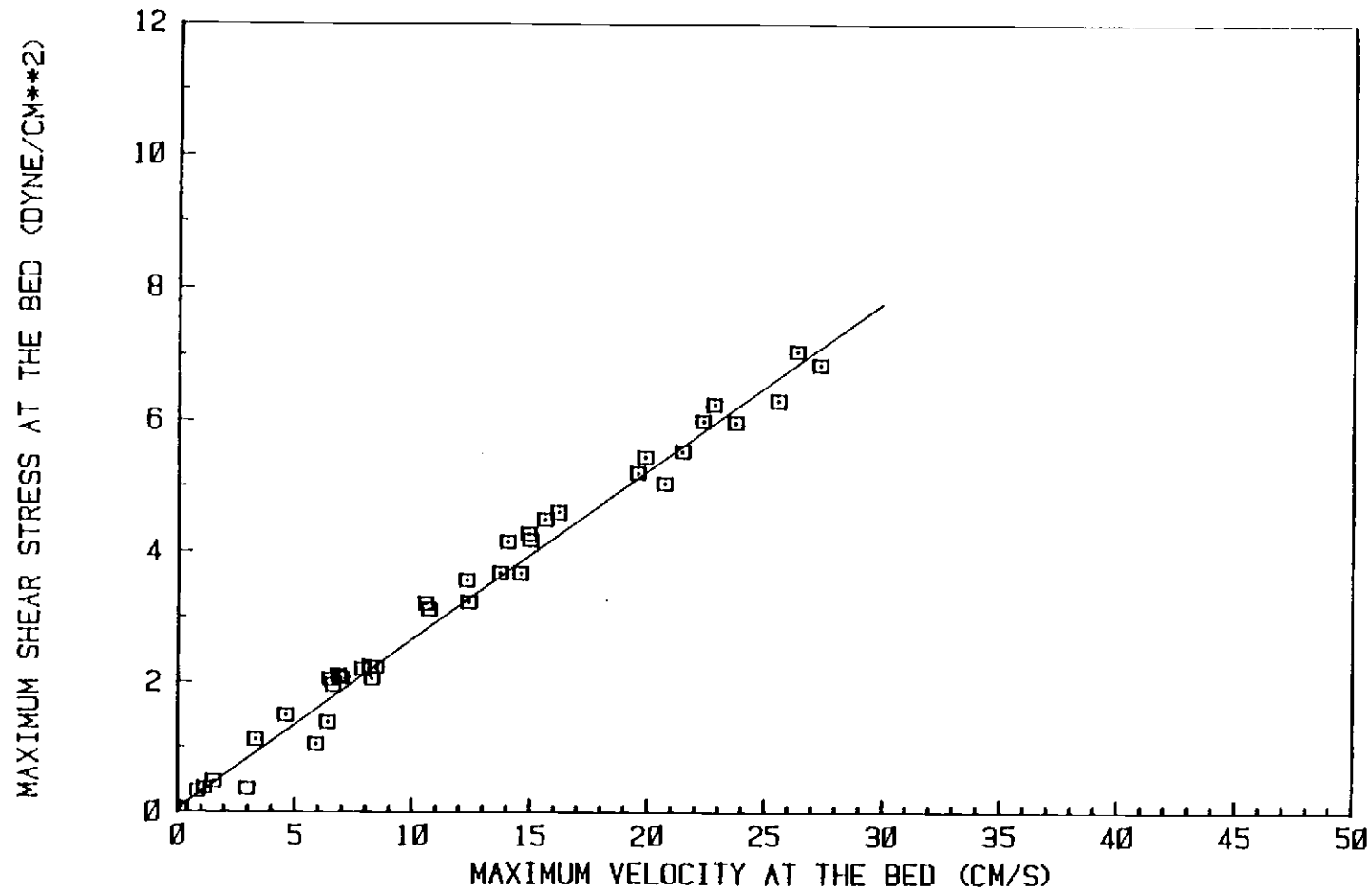| Run	$\delta = \sqrt{\frac{\nu t}{\pi}}$ cm	$=6.5\left(\frac{t}{2\pi}\right)$ cm	Jonsson's Graph cm	Run	$\delta = \sqrt{\frac{\nu t}{\pi}}$ cm	$\delta = 6.5\left(\frac{t}{2\pi}\right)$ cm	Jonsson's Graph cm
1a	0.13	0.58	0.20	32	0.05	0.21	0.10
1b	0.09	0.40	0.14	33	0.04	0.20	0.10
2	0.07	0.32	0.11	34a	0.05	0.23	0.10
3	0.06	0.28	0.10	34b	0.05	0.22	0.10
4a	0.06	0.26	0.09	34c	0.04	0.19	0.10
4b	0.06	0.26	0.09	34d	0.03	0.18	0.10
5	0.05	0.25	0.09	35	0.07	0.30	0.10
6	0.05	0.23	0.09	36	0.05	0.24	0.10
7	0.05	0.23	0.09	37	0.05	0.22	0.10
8	0.05	0.23	0.09	38	0.05	0.21	0.10
9	0.05	0.24	0.09	39	0.06	0.26	0.10
10	0.06	0.27	0.09	40	0.05	0.25	0.10
11	0.06	0.26	0.09	41	0.05	0.23	0.10
12	0.06	0.25	0.09	42	0.05	0.24	0.10
13	0.05	0.24	0.09	43	0.05	0.23	0.10
14	0.05	0.23	0.09	44	0.05	0.25	0.10
15	0.06	0.28	0.09	45	0.05	0.24	0.10
16	0.06	0.26	0.09	46	0.06	0.26	0.10
17	0.05	0.24	0.09	47	0.08	0.36	0.10
18	0.05	0.24	0.09	48	0.06	0.29	0.10
19	0.06	0.28	0.09	49	0.05	0.23	0.10
20	0.06	0.26	0.09	50	0.05	0.22	0.10
21	0.05	0.24	0.09	51	0.05	0.23	0.10
22	0.06	0.27	0.09	52	0.05	0.23	0.10
23	0.05	0.25	0.09	53	0.05	0.22	0.10
24	0.06	0.27	0.09	54	0.05	0.24	0.10
25	0.06	0.26	0.09	55	0.07	0.30	0.10
26	0.05	0.25	0.09	56	0.06	0.25	0.10
27	0.06	0.29	0.10	57	0.05	0.23	0.10
28	0.06	0.27	0.10	58	0.05	0.24	0.10
29	0.05	0.24	0.10	59	0.06	0.25	0.10
30	0.05	0.23	0.10	60	0.06	0.28	0.10
31	0.05	0.22	0.10	61	0.06	0.27	0.10
				62	0.06	0.27	0.10

Figure 58. Shear Stress Versus Maximum Velocity For Runs 1 Through 34
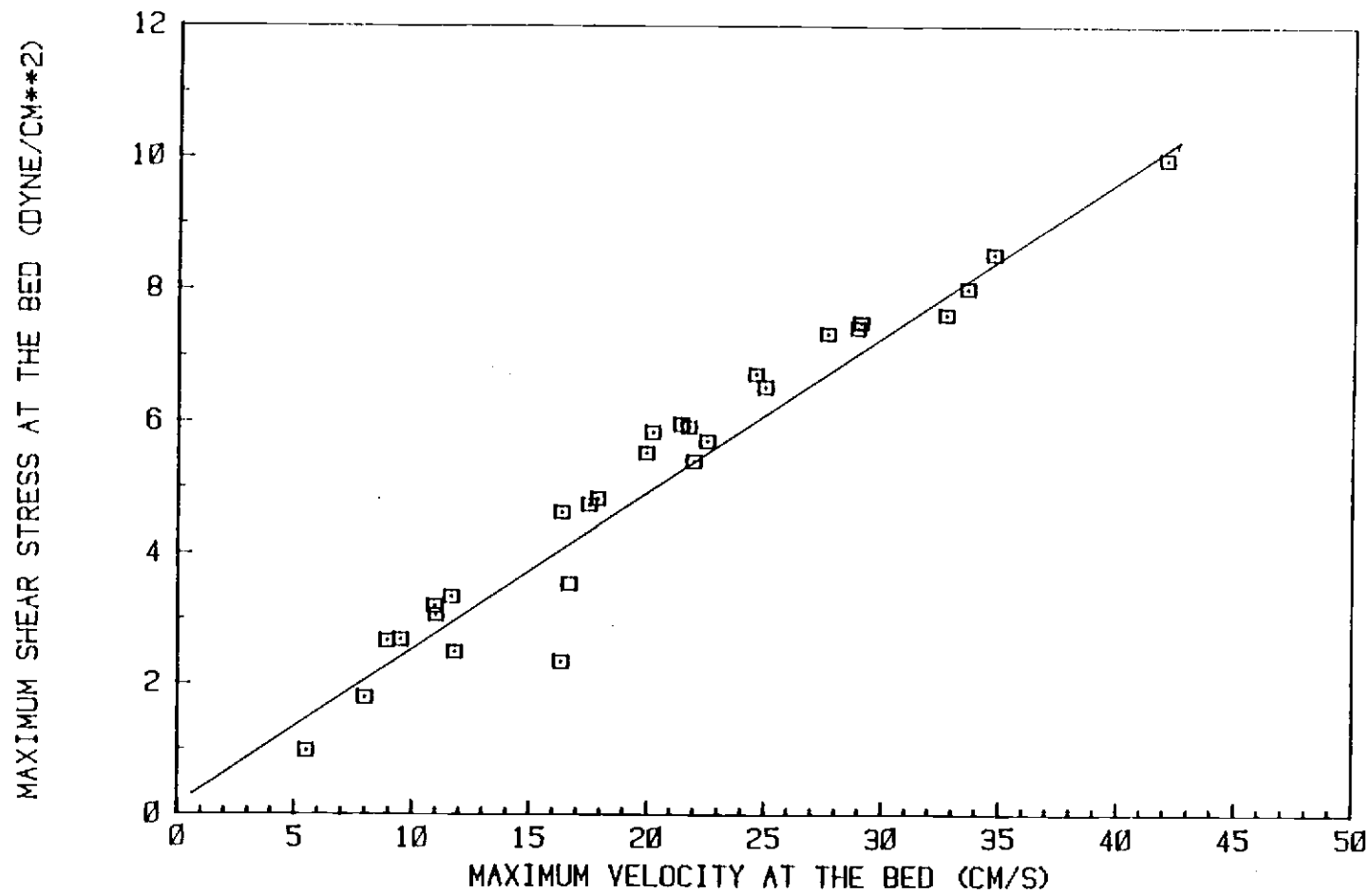
Figure 59. Shear Stress Versus Maximum Velocity For Runs 35 Through 62

Effect of Time on Suspended Sediment Concentration

Results of the suspended sediment concentration measurements for runs 6, 7 and 8 showed that when the shear stress or velocity at the bed was too weak to initiate erosion of the bed surface and cause suspension, time had no role in eroding and suspending material into the body of water. This means that with shear stress and velocity below the incipient motion condition the particles would not go into motion regardless of the duration of the experiment. If events did not happen near the start of an experimental run they did not happen at all. Experimental results for runs 18, 39 and 46 showed that at shear stress and velocity above the incipient motion condition many particles went into suspension and increased the suspended sediment concentration at the start of the run. As time progressed the suspended sediment concentration decreased and reached an equilibrium state.

Experiments With Unidirectional Flow

Outline of Experimental Runs

Twenty-one experimental runs were conducted to study the incipient motion of fine-grained sediment under unidirectional flow. These experimental runs were pursued to determine: (1) the effect of flow variables (water velocity and water depth) on incipient motion of fine-grained sediment; (2) the effect of suspended sediment concentration on incipient motion of fine-grained sediment; and

(3) the comparison of incipient motion at the rough bed with incipient motion at the smooth bed surface. Table 18 shows the detail data of each experimental run under unidirectional flow.

Technique used for Incipient Motion Determination

Measurements of incipient motion were accomplished by visual observation and velocity measurement. Suspended sediment samples were collected and analyzed. It was possible to observe, in real time, the initiation of sediment movement resulting from tractive forces exerted on the bed. Concurrently, photographs of the bed were taken.

Several procedures were used to estimate the threshold of sediment motion. The first was visual observation. A cloudy appearance within several millimeters of the bed and the changing configuration of the bed marked the time when significant movement occurred. Analysis of the photographs of the bed provided an alternative technique for estimating incipient motion.

Concurrently with photographic and visual observations, the velocity distribution was continually measured. From these data, estimates of mean velocity at the bed, shear stress, shear velocity and the Shield entrainment function were calculated for the observed conditions of incipient motion.

Table 18. Synopsis of Experimental Runs With Unidirectional Flows

Run	Time of run hr.	min.	sec.	State of Sediment Bed Fresh	Compacted	Fluid Tap Water	Turbid Water	Bed Flat	Duned	Water Depth cm	Type of Flow	Mean Velocity cm/sec	Shear Stress dyne/cm^2	Suspended Sediment Concentration Range mg/L	Water Temperature °C	pH
1	01	08	00	x		x		x		15.0	Turbulent	8.38	0.23	5.6-5.1	18.4	6.80
2	00	46	30	x		x		x		9.5	"	13.56	0.53	5.1	16.3	7.15
3	00	45	00	x		x		x		6.5	"	20.01	1.11	9.5-5.0	16.3	7.15
4a	00	32	30	x		x		x		11.0	"	25.57	--	5-17	17.8	6.80
4b	02	16	00	x		x		x		10.5	"	26.79	1.79	17-90-71	21.9	6.52
5	00	24	30	x		x		x		17.5	"	9.22	0.22	21.9-54.6	22.8	7.00
6	12	37	00	x		x		x		9.5	"	23.03	1.21	54.6-28.6	30.5	6.93
7	00	24	00	x		x		x		5.0	"	23.00	1.22	10.8-54.6	19.4	7.05
8	01	22	00	x		x		x		6.2	"	19.01	1.08	6.0-6.0	17.1	6.90
9	01	38	15	x		x		x		3.5	"	33.40	3.34	7.4-5.6	17.0	6.95
10	00	16	45	x		x		x		3.0	"	29.58	2.11	--	17.0	6.95
11	01	22	00	x		x		x		6.5	"	45.78	5.08	12.8-7.4	17.0	6.85
12	00	45	30	x		x		x		6.2	"	49.10	5.87	7.8	17.1	7.25
13	00	40	00	x		x		x		12.0	"	47.46	5.06	8.6	17.2	---
14	03	45	30	x		x		x		10.0	"	50.28	5.69	15.0-8.2	17.5	7.10
15	00	31	30	x		x		x		8.7	"	52.12	6.10	12.8	17.7	7.05
16	02	13	00	x		x		x		8.7	"	52.12	6.10	9.0-30.4	20.6	6.90
17	47	37	00	x			x	x		8.8	"	53.64	6.34	2300-276	21.1-33.8	7.30
18	01	32	00	x		x		x	x	7.8	"	46.49	6.42	230.0	22.8	6.60
19	01	34	00	x		x		x	x	9.2	"	51.64	6.05	49-211	20.2	7.10
20	02	14	30	x		x		x	x	8.9	"	54.79	6.62	217-216	25.2	7.30
21	05	53	45	x		x		x	x	8.3	"	57.24	7.19	236-979-620	20.9	7.20

<u>Results of Experimental Runs</u>

1. Initiation of Motion of Particles at Irregular

Test Section--Runs 1-3

Runs 1 through 3 were started with low pump speed, with a small

tailgate opening and deep water to determine the shear stress at

which motion of sediment particles just begins. Figure 60 shows the

suspension concentrations versus time for runs 1 through 4.

These experiments started with a very low mean velocity of 8.38

cm/sec and depth of 15 cm (run 1). No suspended sediment

concentration changes or evidence of any movement was observed

during these conditions. The velocity was then increased to 13.56

cm/sec by increasing the tailgate opening, with a resulting decrease

in water depth to 9.5 cm (run 2). Some small floating debris and

particles from the upstream end of the test section were moved and

transported downstream. The shear stress which was able to move the

particles at the irregular places of the sediment bed was 0.53

dyne/cm^2. The suspended sediment concentration did not change.

The tailgate opening was then increased to give mean water

velocity of 20.01 cm/sec and a water depth of 6.5 cm. These

conditions were able to scour more pieces of bonded particles from

the upstream end of the irregular zones of the test section. Some

of these particles then went into suspension and were trasported

downstream. Other pieces of sediment were dragged along the bed

surface while moving downstream and abraded additional particles

from the bed surface.

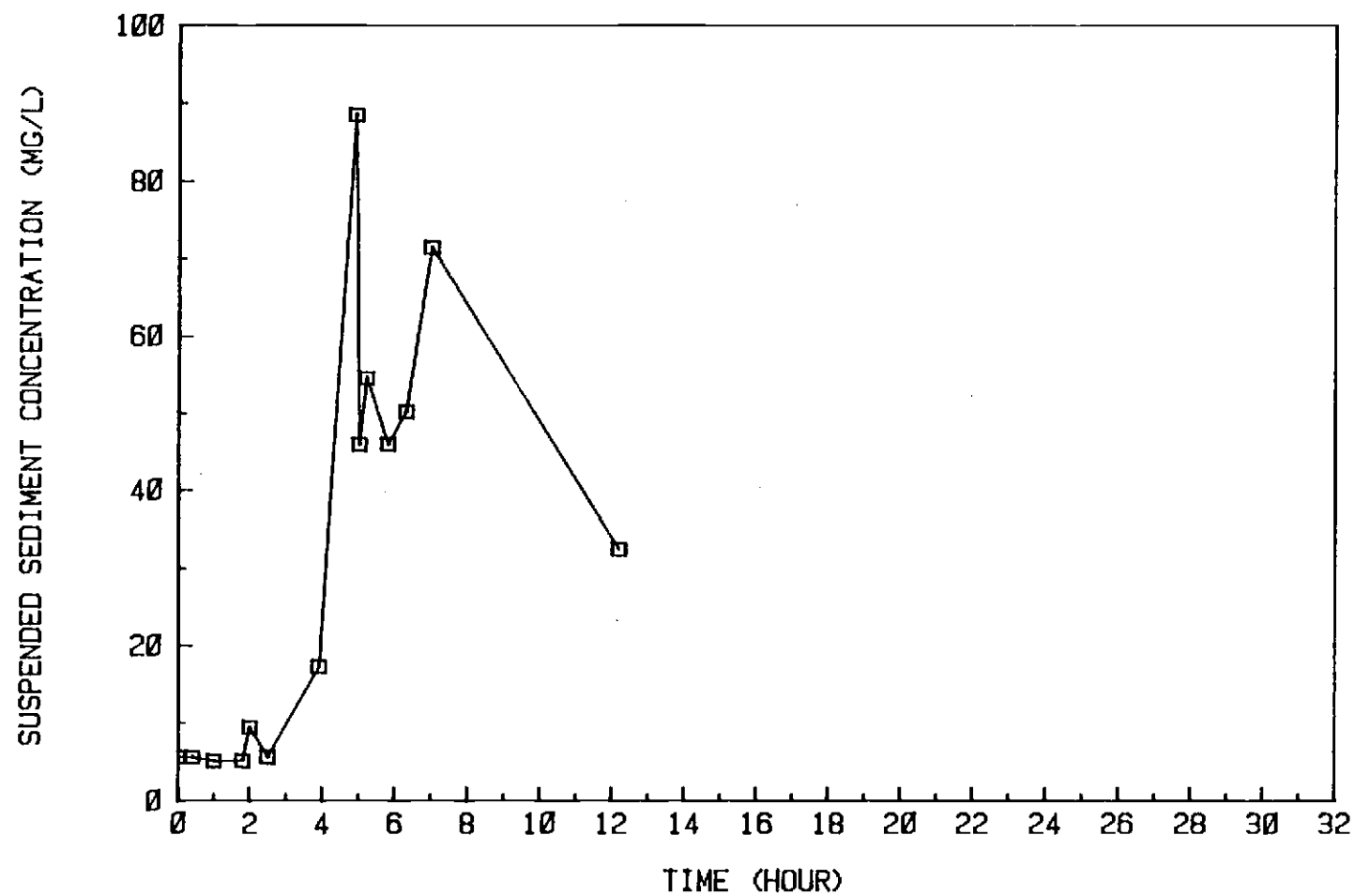Small individual particles moved downstream in a group, with

Figure 60.   Suspended Sediment Concentrations For Runs 1 Through 4

resultant abrasion of the bed surface, leaving small streaks on the surface of the bed. Figure 61 shows the pieces of bonded material eroded from the upstream end of the irregular zone. Figure 62 shows the pit marks left on the bed surface which were made by abrasion from moving pieces of bonded material. The shear stress for this run was calculated as 1.11 dyne/cm^2. The suspended sediment concentration data show an increase of concentration from 5 to 9.5 mg/l.

2. Transition to Incipient Motion--Runs 4 - 8

Runs 4 through 8 started from a low velocity, which was increased slowly by opening the tailgate. Figures 63 and 64 show the suspension concentrations versus time for runs 5 and 6, and 7 through 12, respectively.

In run 4, with an average velocity of 26.79 cm/sec and a water depth of 10.5 cm, particles again began to move from the irregular section at the upstream end of the test section. The pattern of particle movement downstream with continued abrasion of the bed surface, previously seen in run 3, was repeated. The concentration increased to more than 70 mg/l. Therefore, it was hard to visually observe the changes in the bed when the water was running. Worm lines and evidence of pit marks and streaks from large bonded pieces were observed.

In run 5, the tailgate was closed slightly to determine the effect of decreasing velocity on incipient motion. This condition produced a very low shear stress and particles started to deposit at irregular places.

Figure 61. Big Bonded Particles
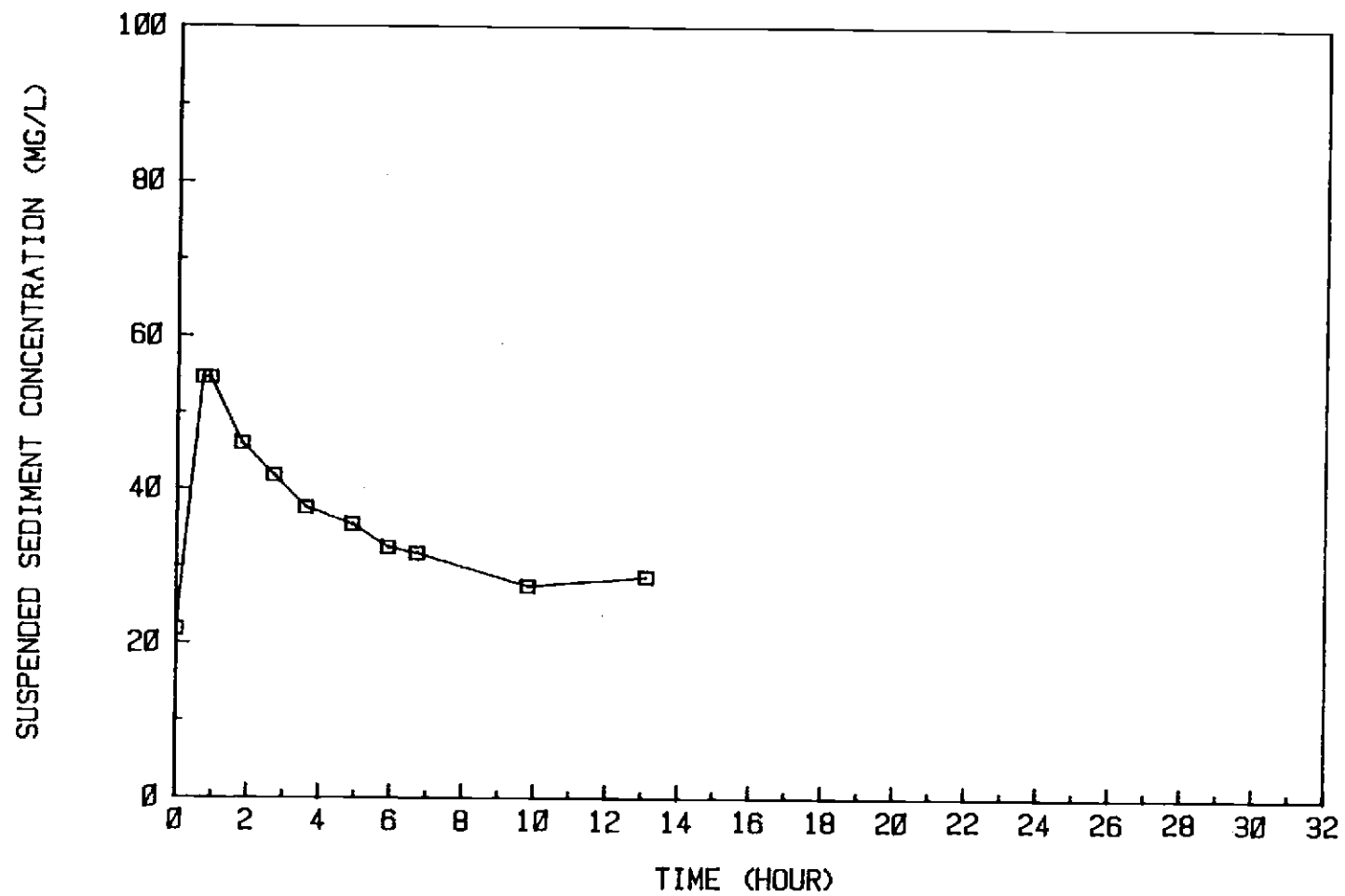
Figure 62.   Pit Marks and Streak Lines

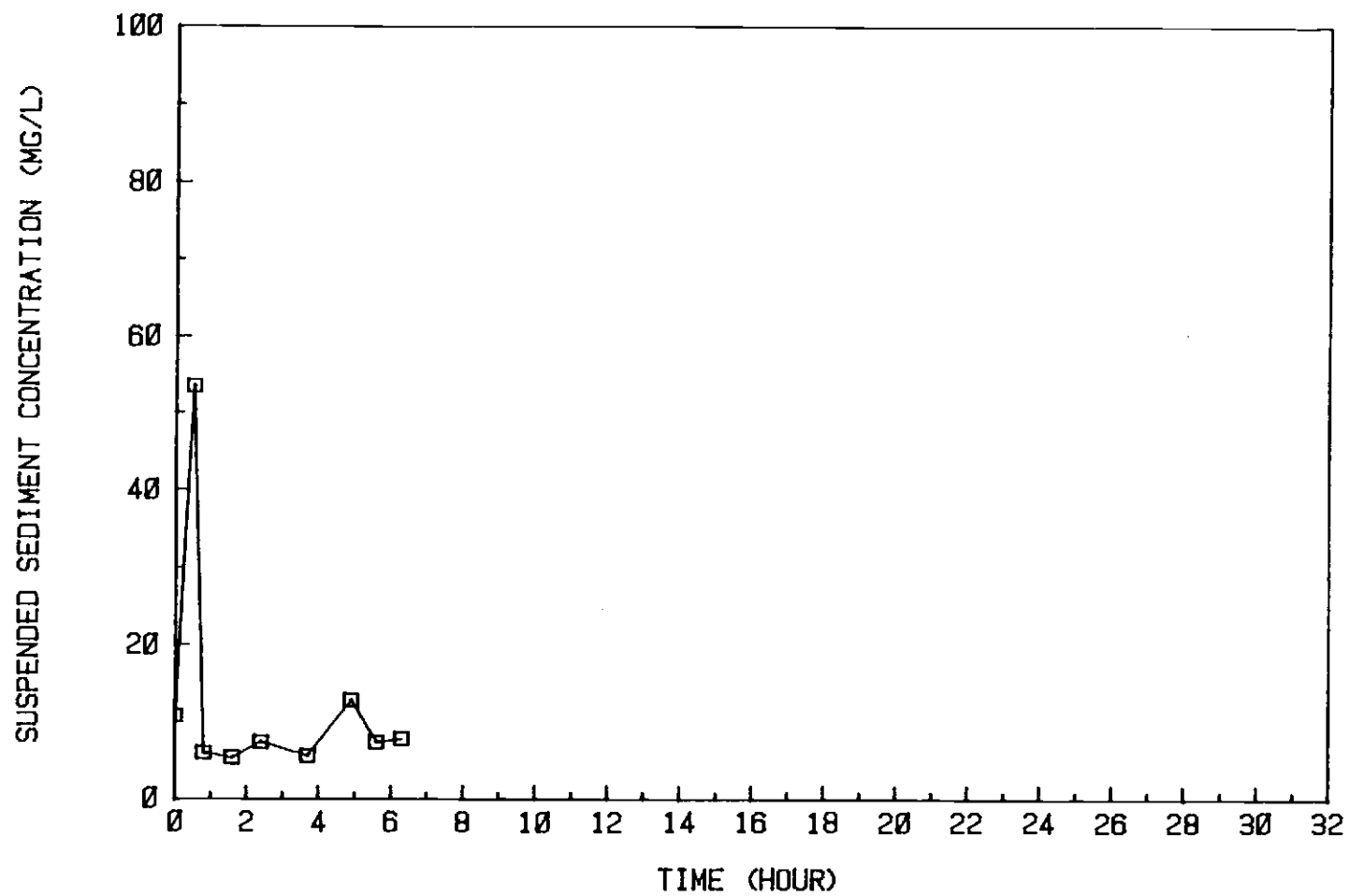Figure 63. Suspended Sediment Concentrations For Runs 5 and 8

Figure 64. Suspended Sediment Concentrations For Runs 7 Through 12

For run 6, the velocity was again increased to produce a higher shear stress, but the sediment concentration continued to decrease and finally reached an almost steady state at the end of the run. The decrease in sediment concentration with the increase in water velocity and shear stress in this run was due to:

a) The increased shear stress still is lower than run 4 to maintain the same suspended sediment concentration as run 4.

b) Most of the loose sediment or bonded particles from the irregular places were already in suspension, therefore leaving no sediment supply to contribute to an increase in concentration.

c) The eroded sediment particles were deposited elsewhere in the hydraulic system, which contributed to the decrease in the concentration.

d) When all of the particles that were able to deposit had done so, the concentration reached a steady state.

Runs 7 and 8 started at a lower water depth, but with the same shear stress as for run 6. Material which had deposited at the sump and in the pipelines during the runs 5 and 6 was now recirculated. The sudden increase in concentration was due to suspension of such particles in the system, and not from erosion of the bed material in the test section.

3. Start of the Peeling Off of the "Skin"--Runs 9 and 10

Runs 9 and 10 were run at conditions close to but below incipient motion. The average water velocity varied from 19.58 to 33.40 cm/sec and the shear stress varied from 2.11 to 3.34 dyne/cm^2

It was observed that the skin started to peel off in the same way as in the oscillatory flow. It was peeled off very slowly at low shear stresses and faster with increasing velocities and shear stresses. The bonded particles were removed from the bed by a peeling-off action and then transported downstream. In doing so, they dragged on the bed surface and, thus, caused more particle erosion.

The suspended sediment concentration versus time for runs 9 and 10 show a steady state condition.

It was found that at a shear stress of 2.11 dyne/cm^2, particles started to peel off very slowly and left pit marks on the bed surface. With an increase of shear stress to 3.34 dyne/cm^2, bonded particles peeled off at a little faster rate, but with no significant suspension of sediment. Therefore, it was concluded that the 2.11 to 3.34 dyne/cm^2 shear stress range at the bed and the 29.58 to 33.40 cm/sec average velocity range identify the minimum requirement to start the peeling of the sediment bed and formation of some minor pit marks; these occur without any streak formation or change in suspended sediment concentration. Therefore, higher velocity and shear stress are required to cause an incipient motion condition.

4. Incipient Motion--Runs 11-16

Runs 11 through 16 were associated with higher average velocities and higher shear stresses at the bed than for all previous runs. The average velocity ranged from 45.8 to 57.2 cm/sec

and the shear stress ranged from 5.08 to 6.10 dyne/cm^2.

The following observations were made during runs 11 to 16.

a) Bonded particles still continued to peel off and eroded particles were transported downstream beyond the test section before they deposited.

b) Small individual particles formed into a group and moved downstream with no significant ripple formation.

c) Sediment particles went into suspension, with some particles being transported downstream while in suspension and some particles settling back onto the bed.

d) The bed surface looked smooth after the end of a test run and overnight sedimentation or settling.

e) Benthic worms and bugs extracted sediment from within the bed and deposited it on the surface during the experimental runs. Figure 65 shows material extracted by benthic worms.

f) Most of the skin layer was eroded and started to move and dislodge the sediment particles from the layer below the skin layer. Over time, the skin was reformed in the exposed areas.

g) Just upstream of the test section, water penetrated through a tape seal in the floor of the approach channel and caused strong eddies to erode the bed materials and leaving a large scour hole at the upstream end of the bed. Figure 66 shows the resultant scour hole.
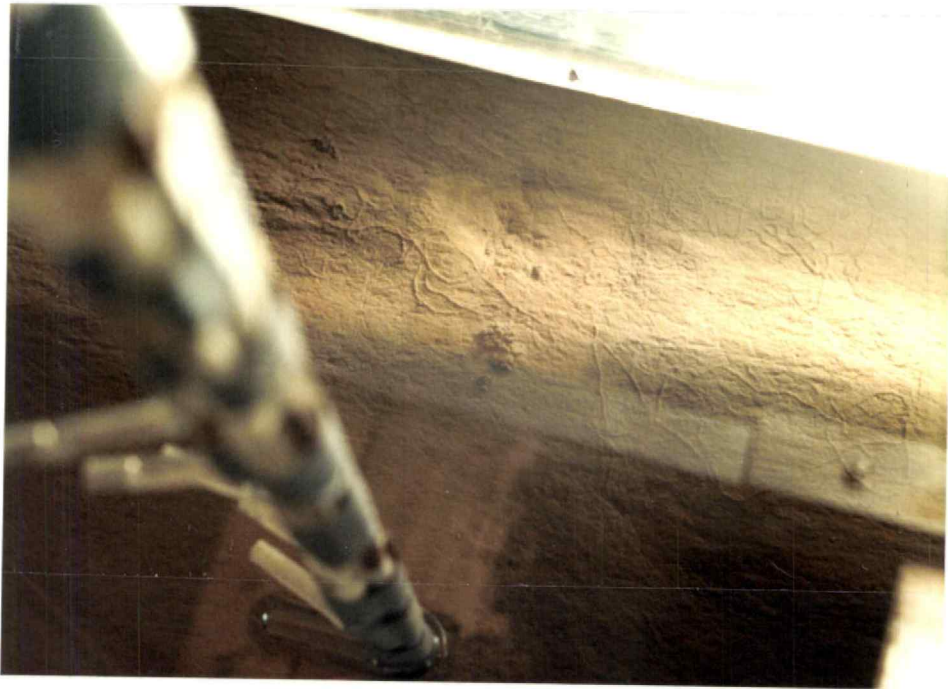
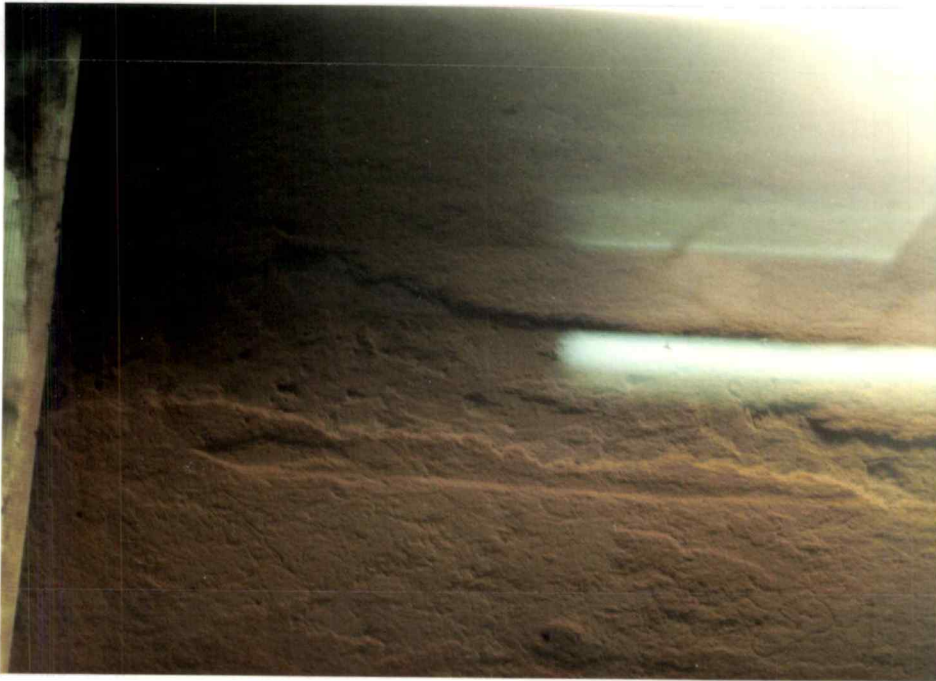Figure 65.   Material Extracted by Benthic Worms

Figure 66.   Scour Hole at Front of Test Section

The suspension of concentration versus time is shown in Figure 67 for runs 13 through 16. The data show fairly uniform suspended sediment concentrations for runs 11 through 15. At run 16, the concentration increased from 10 mg/l to 30 mg/l due to water penetration underneath the tape and resultant erosion as noted above.

5. Effect of Addition of Suspended Sediment on Incipient Motion--Run 17

Run 17 started with an addition of a slurry of the same sediment as present in the bed. The slurry was added in the sump of the recirculating pump system, where it mixed to give a concentration of almost 2,300 mg/l in the flume. The average water velocity and the shear stress at the bed during this run were 53.6 cm/sec and 6.3 dyne/cm^2, respectively.

The following phenomena were observed during this run:

a) Water turbidity was too high for observation of the bed during the experimental run. Therefore, all of the observations were made at the end of the run.

b) The final sediment bed surface appeared coarser than the initial surface, presumably due to abrasion of the bed by moving sediment particles.

c) The bed was not eroded, even at places of expected scour.

d) Survey of the bed surface before and after the run showed no changes in the bed surface profile.

Figure 68 shows the suspended sediment concentrations versus time for run 17. The results of the concentration and turbidity
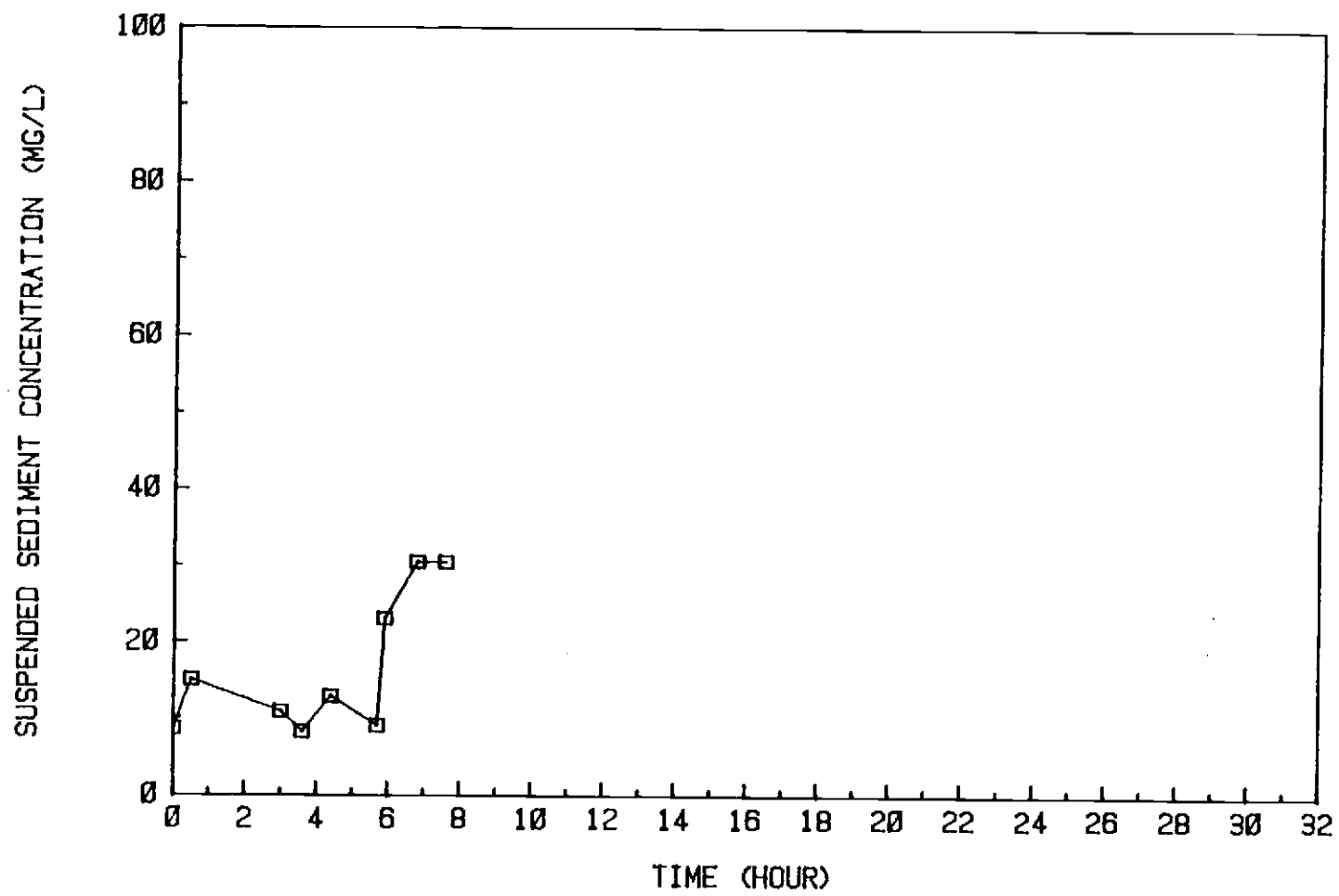
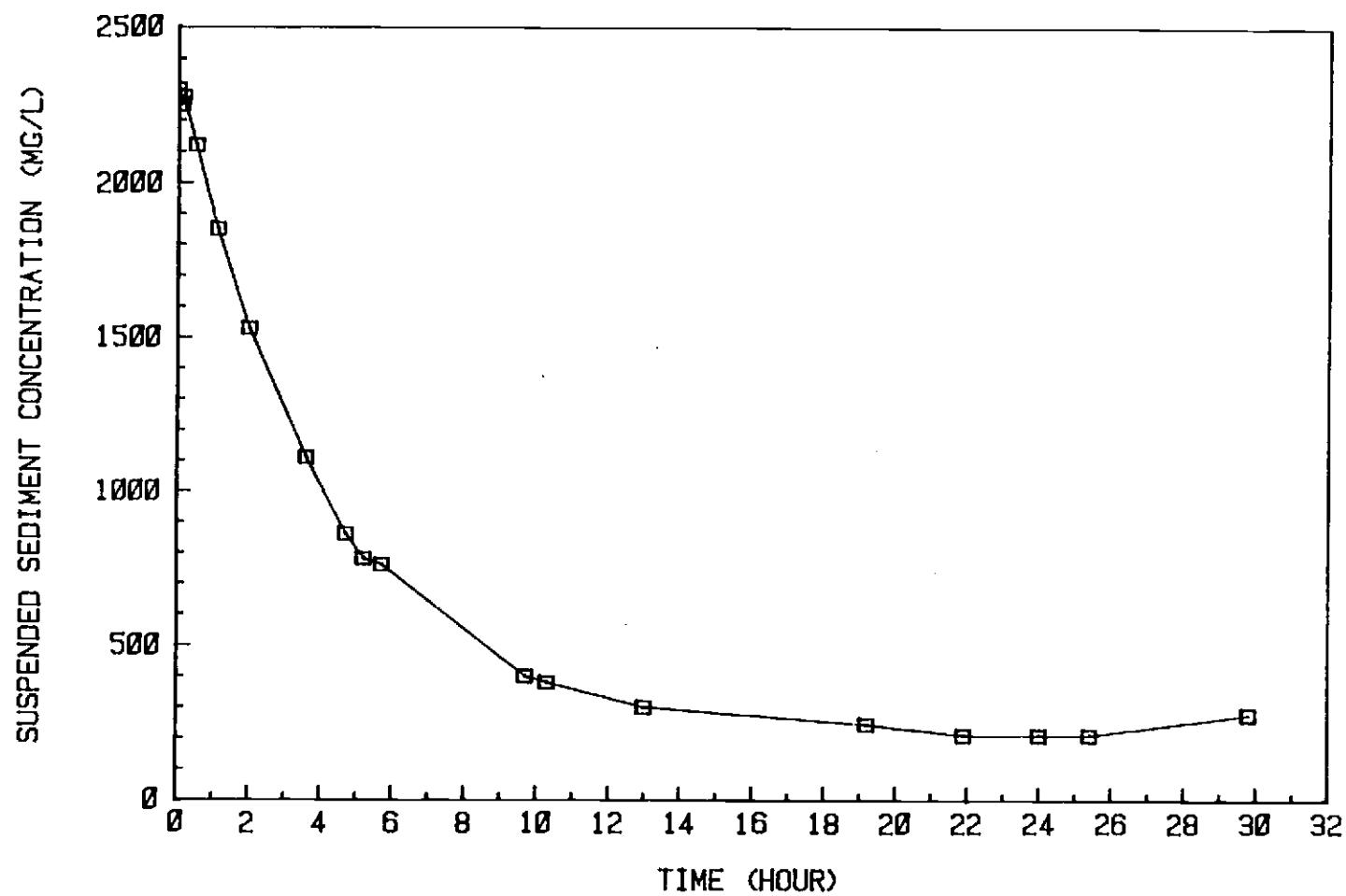Figure 67.   Suspended Sediment Concentrations For Runs 13 Through 16

Figure 68.   Suspended Sediment Concentrations For Run 17

data indicate that:

a) Suspended sediment concentration rapidly decreased and reached a steady condition of 260 mg/l.

b) The sand and silt particles added to the flume were deposited at places such as the sump, pipeline, or beyond irregularities in the flume floor beyond the ends of the test section.

c) The colloidal matter stayed in suspension and the equilibrium concentration is composed mostly of these collodial materials.

Figure 69 shows the bed surface at the end of this run.

6. Comparison of Incipient Motion of Rough Bed Versus Smooth Bed--Runs 18 and 19

Before run 18, the downstream half of the test section (290 cm to 410 cm) was remolded and made into a rough dune bed (20 cm length, 2 cm high), with a total of 5 dunes. The upstream half of the bed was left smooth. Figure 70 shows the bed surface with the dune field.

The average velocity and shear stress at the bed for runs 18 and 19 ranged from 46.49 to 51.64 cm/sec and 6.05 to 6.42 dyne/cm^2, respectively. These were almost the same flow velocity and shear stress as the previous run. The following phenomena was observed during these runs:

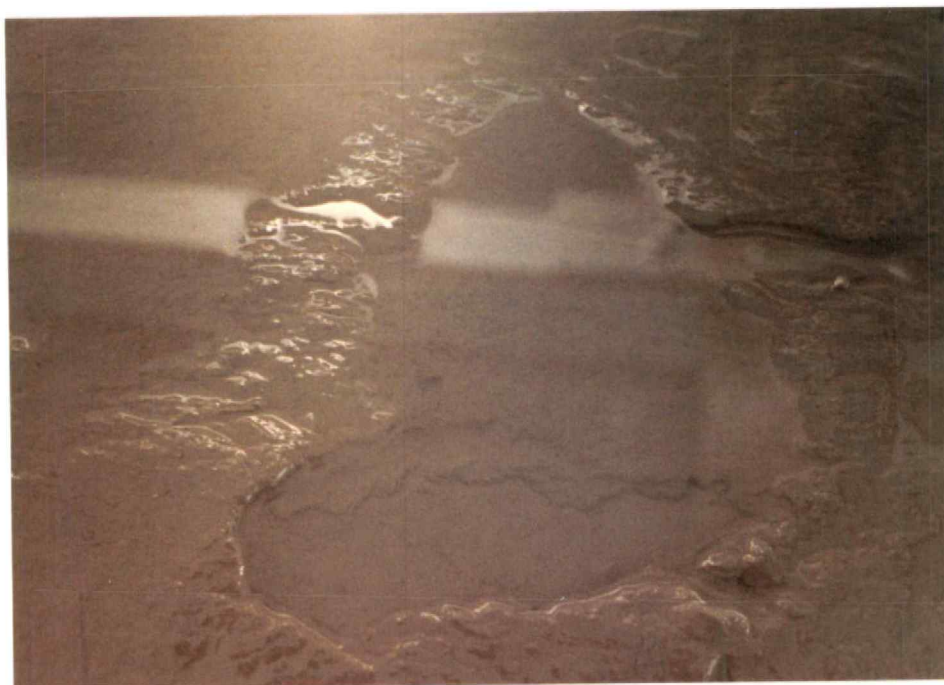a) Due to the high turbidity, direct observation of the bed was not possible during the runs.

Figure 69. Bed Surface After End of Run 17

Figure 70. Bed Surface at Dune Field

b) No noticeable changes were observed in the smooth part of
the bed. There was probably some peeling off of the
particles, as in previous runs.

c) In the dune field, the most-downstream dune was leveled off
to that of the surrounding bed surface and caused a scour
hole to the full depth of the sediment bed near the edge
of the test section.

d) The second dune from the end of the test section was reduced
in height almost 60 percent.

e) The smooth surface near the beginning of the dune field did
not change significantly, but streak lines developed there.

Figure 71 shows the suspended sediment concentrations versus
time for runs 18 and 19. The concentration data indicate a sudden
increase at the beginning of the run, followed by an abrupt sudden
decrease over time for run 18. This was followed by an increase in
concentration for run 19.

7. Scour Holes--Runs 20 and 21

The purpose of runs 20 and 21 was to determine the velocity and
shear stress required to erode the entire sediment bed. Following
the end of run 20, the slope of the channel was raised to increase
the shear stress at the bed surface. Observations during run 21
showed that even at a high induced shear stress, the sediment bed
eroded layer by layer, i.e., by surface erosion. The increase in
the slope caused a weak hydraulic jump at the upstream end of the
test section, which caused massive erosion there and development of
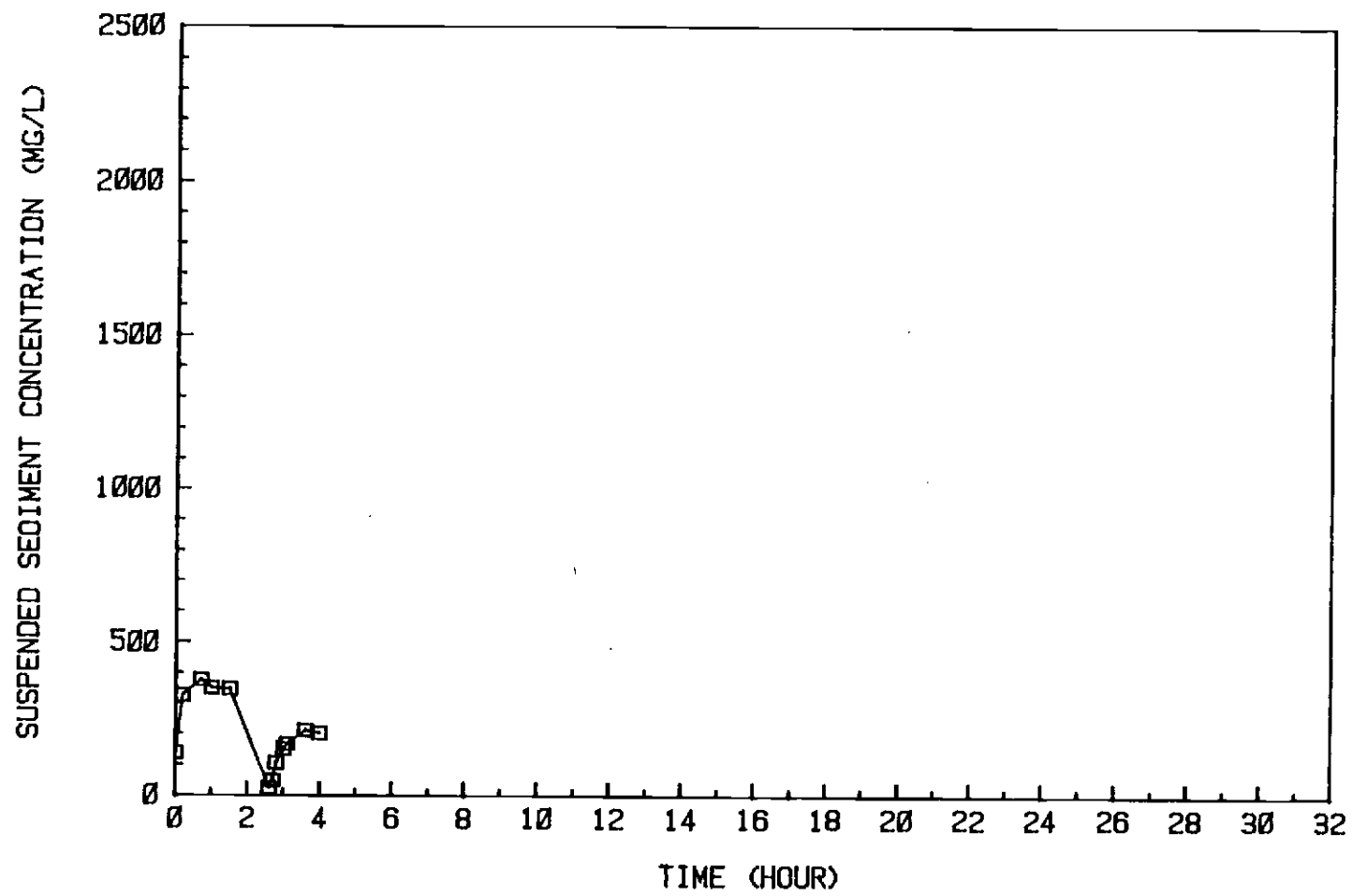
Figure 71.   Suspended Sediment Concentrations For Runs 18 and 19

a large scour hole for the full depth of the sediment bed. A velocity of 65.0 cm/sec was recorded at the downstream side of the hydraulic jump.

Figure 72 shows the suspension concentrations versus time for runs 20 and 21. The concentration data show an Increase of concentration to almost 1,000 mg/l due to the massive erosion of particles at the upstream end of the test section. This indicates that the type of eroding force is important in the erosion of cohesive bed sediment.

8. Bed Patterns

Figure 73 shows the bed surface between runs chronologically during the course of the tests. The erosion bed pattern was very uniform, with pit marks and streak lines developed on the bed. After overnight sedimentation, between runs, extracted sediment due to benthic worms and worm lines were evident on the smooth bed surface. Deep scour holes were observed at both ends of the test section, with depths corresponding to the depth of the sediment bed. The rest of the bed surface was very smooth with some fine sand and coarse silt forming ripple-like formations. The ripples were a few centimeters long in the direction of flow and had average heights of less than one-half millimeter.

Flow Conditions in the Flume

The average water velocity in the flume varied between about 8 and 57 cm/sec. The depth of flow varied bewtween 3 and 15 cm.
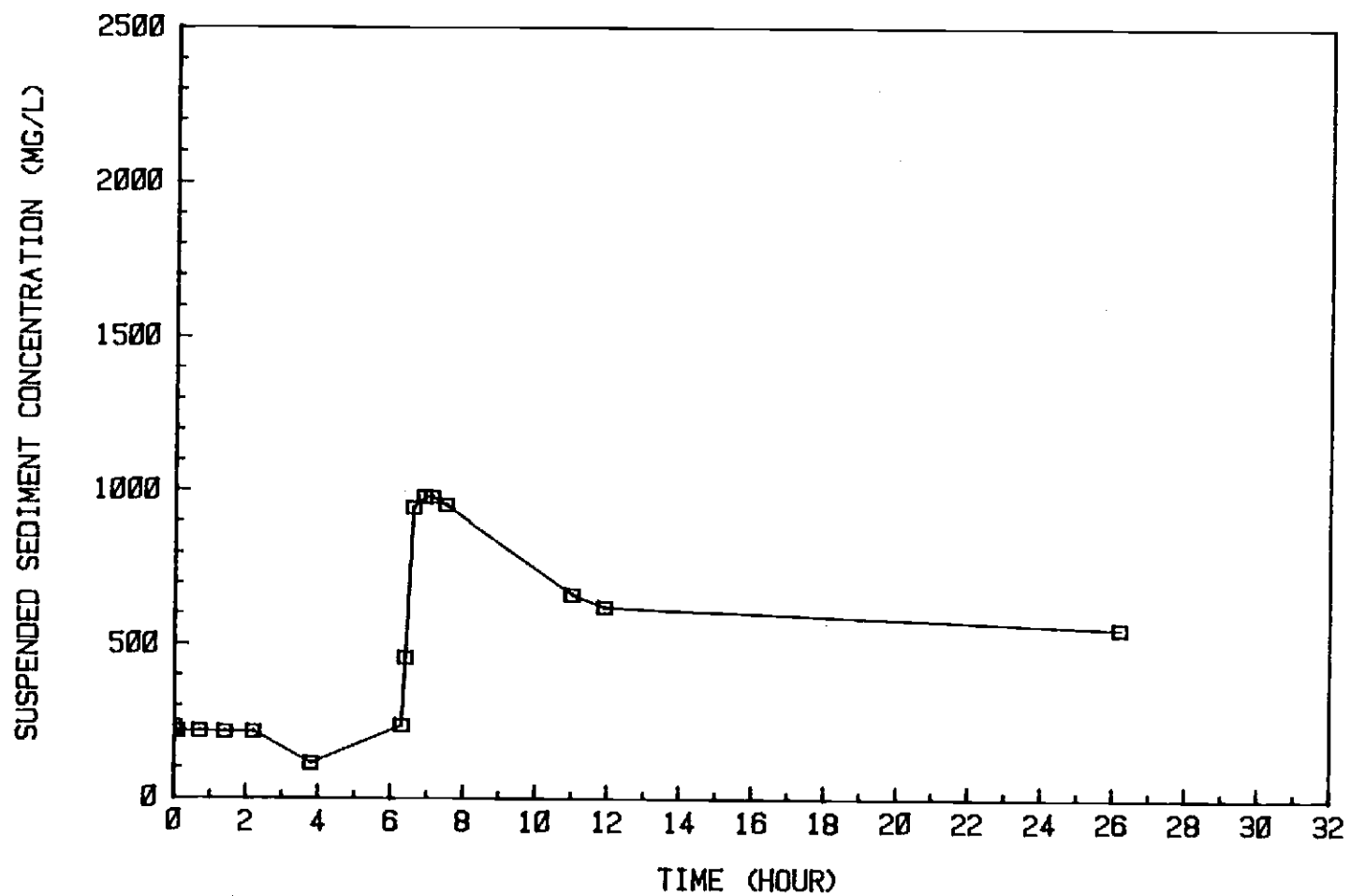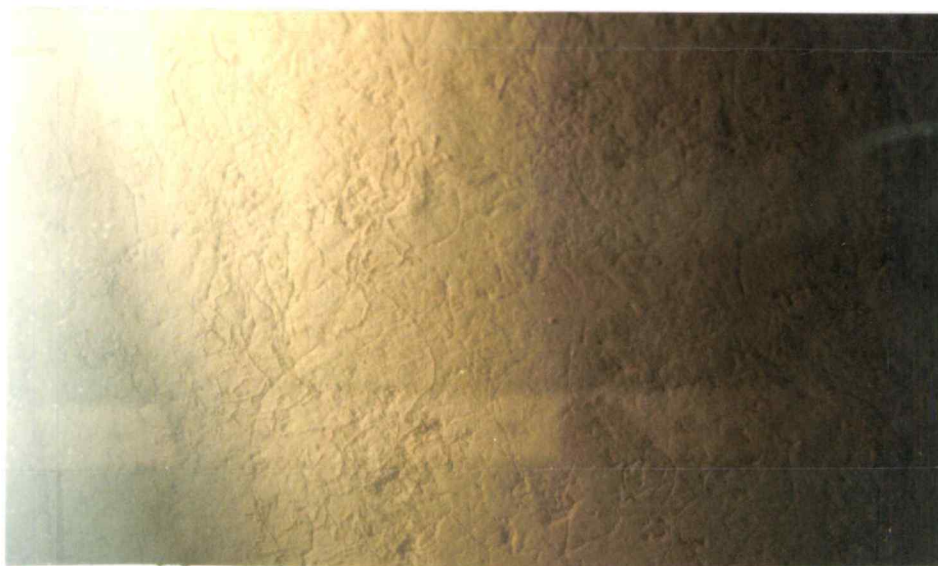
Figure 72.   Suspended Sediment Concentrations For Runs 20 and 21
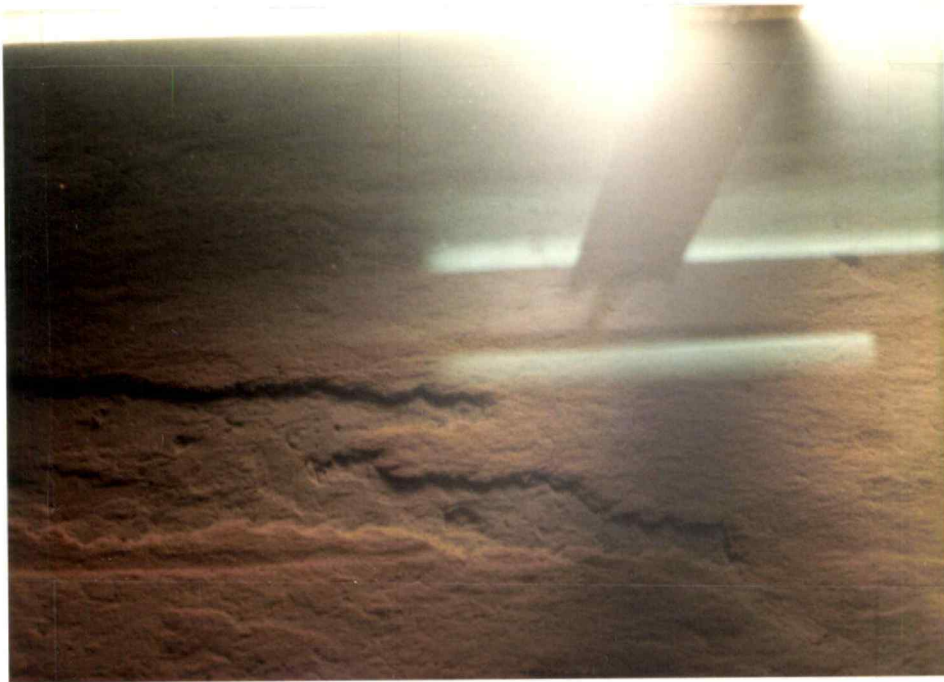
296

A. AFTER RUN 4

B. AFTER RUN 8

Figure 73. Bed Surface Chronologically After the Start
of the Runs

C. AFTER RUN 15

Figure 73 Cont. Bed Surface Chronologically After The Start
of the Runs

D. AFTER RUN 16

E. AFTER RUN 21

Figure 73 Cont. Bed Surface Chronologically After the Start
of the Runs

For these flow conditions the Reynolds numbers were in the range of 9,000 to 60,000. Hence, the flow was fully turbulent for all of the runs involving unidirectional flow.

Measured Velocity vs. Velocity Calculated From Logarithmic Velocity Equations

Because the flow was turbulent, the logrithmic velocity equation for turbulent flow conditions was used to calculate the average velocity at the test section for each run. Table 19 shows the velocity calculated with the logarithmic velocity equation for a smooth boundary condition. Also shown is the average velocity for each run based on volumetric discharge measurements. The results show good agreement between the measured and calculated values, with the calculated values being consistently larger.

Shear Stress and Mean Velocity

The velocity and shear stress data for the experimental runs under unidirectional flow are plotted in Figure 74. The results show that there is linear relationship between shear stress and mean velocity at the bed.

Effect of Bed Roughness on Flow Resistance

The energy gradient across the test section for run 16 was determined at an average velocity of 52.12 cm/sec and average depth

Table 19. Calculated and Measured Unidirectional Velocities

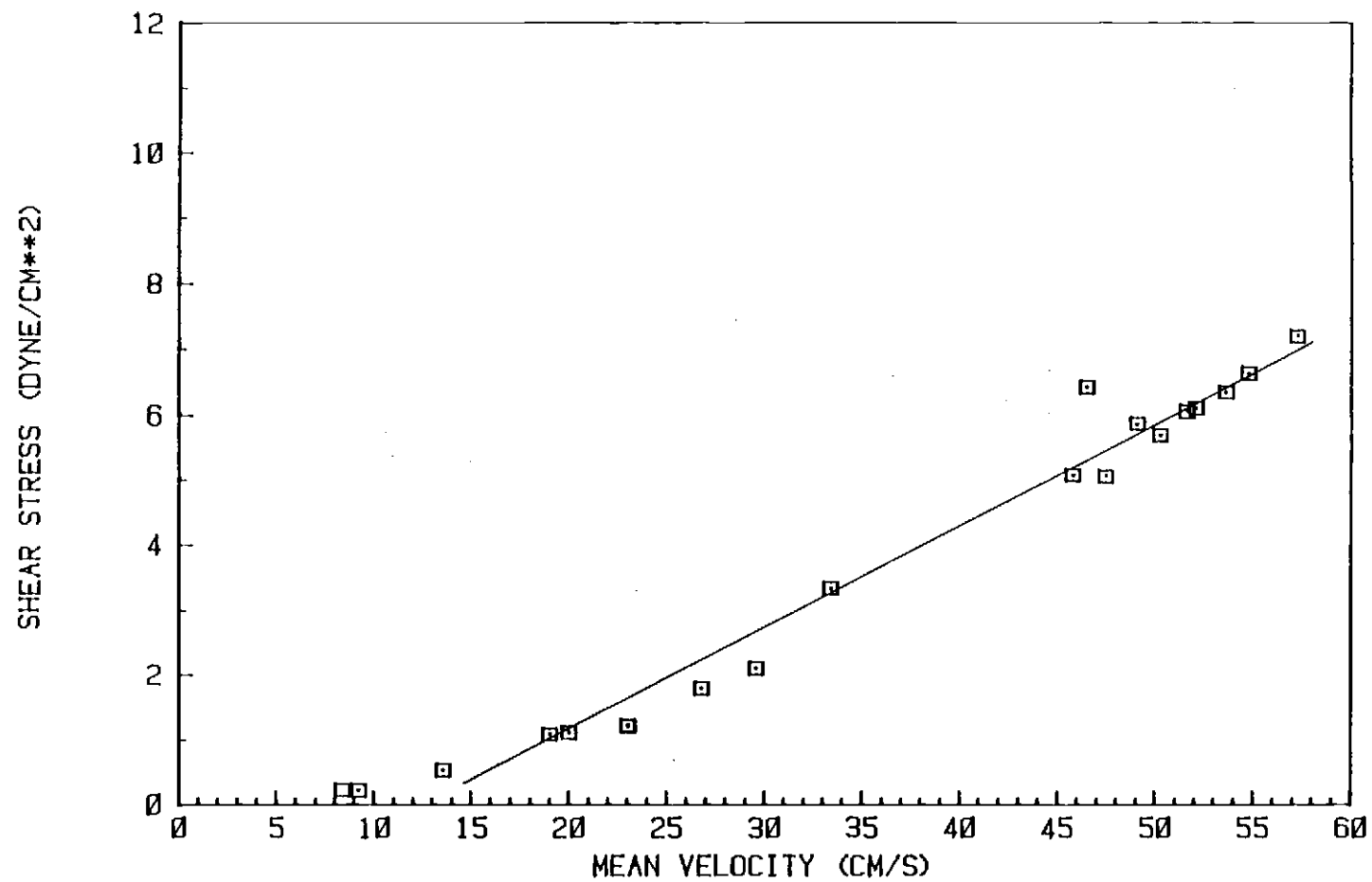| Run No.	Velocity, cm/sec	
	Logarithmic	Measured
1	10.56	8.38
2	15.69	13.56
3	22.64	20.01
4	31.43	26.79
5	10.51	9.22
6	26.02	23.03
7	23.57	23.00
8	22.30	19.01
9	39.24	33.40
10	29.69	29.58
11	52.89	45.78
12	56.99	49.10
13	56.34	47.46
14	67.34	57.20
15	77.48	65.10
16	60.97	52.12
17	63.36	53.64
18	62.24	49.49
19	60.98	51.64
20	64.51	54.79
21	67.18	57.24

Figure 74. Shear Stress Versus Mean Velocity For Unidirectional Flow

of 8.7 cm. It was found equal to 0.00011. During the latter part of the run, the suspended sediment concentration decreasd at a rate of 0.30 mg/l/min. Run 19, with an average velocity of 51.64 cm/sec and average depth of 9.2 cm had an energy gradient of 0.00015. The suspended sediment concentration increased at a rate of 1.82 mg/l/min. Comparing runs 16 and 19, the gradient were nearly the same, even though there were significant differences in the suspended sediment concentrations and rates of change of concentrations. Therefore, the eroding surface of run 19 did not cause any measureable increase of the frictional resistance of the bed compared to the depositing surface of run 16.

Run 17, with the addition of 2,300 mg/l of suspended sediment concentration at water depth of 8.8 cm and with an average velocity of 53.64 cm/sec after 32 minutes of experimental run, had an energy gradient of 0.0001 and a rate of suspended sediment concentration decrease of 71.88 mg/l/min. At 99 minutes after the state of run 17, the energy gradient was determined to be 0.000055. with the same water depth and velocity as before, but with the rate of suspended sediment concentration decrease of 12.02 mg/l/min. This means that with the decrease in suspended sediment concentration over time during the run, the energy gradient dropped to half its previous value. Hence, the addition of suspended sediment appeared to cause a change in the frictional resistance of the bed, such that it was greater at 32 minutes into the run than at 99 minutes. However, the coarse look of the bed surface at the end of the tests (almost 48 hours) indicated still further change in the frictional resistence of the bed.

Experiments With Sediment Consolidation and Density

Outline of Experiments

Three different sets of bench-type experiments were done to determine the consolidation and density charactersitics of the sediment. The first set of experiments allowed study of the consolidation behavior and density of the sediment in a long settling column. A well-mixed slurry of sediment was placed in the column, mixed, and allowed to settle, as described in the previous chapter. The height of the sediment was recorded periodically and samples of the sediment at several heights were extracted for density measurements. The second set of experiments involved study of the sediment consolidation behavior and density in eight one-liter graduated cylinders. The well-mixed slurry of sediment was placed in the cylinders, mixed, and allowed to settle, as already noted. The sediment depth and volume were recorded periodically. Density measurements were obtained by sujbecting the whole sample for oven-drying and weighing. The third set of experiments involved the consolidation behavior of the sediment in two 2-liter graduated cylinders. The well-mixed slurry of sediment was placed into columns, mixed and allowed to settle. Periodically, additional water was added which stirred up the upper part of the sediment column. Removal of equal volumes of water after several minutes of settling allowed extraction of the fine material suspended in the columns. Beyond these three experiments a simpler

experiment was carried out with a bucket of sediment. This was

subjected to air-drying and its compaction behavior was analyzed.

Results of Bench-Type Experiments

As already mentioned, these sets of tests attempted to determine

the consolidation and density characteristics of the sediment.

Sediment Behavior When Exposed to Air

The known amount of sediment from south Sturgeon Lake (the same

as used in the flumes) was left in the laboratory exposed to air to

dry out. As a result, there was a 56 percent reduction in volume

(from 4909 cm^3 to 2165 cm^3), a 38 percent reduction in depth (from

10 cm to 6.25 cm), and a 16 percent reduction in diameter (from 25

cm to 21 cm). Cracks were observed in the dried sediment,

indicative of the natural behavior of fine-grained cohesive

sediment.

Gravitational Settling Under Water

The Sturgeon Lake sediment that was poured into a long settling

column had an initial length of 36 inches. The inside diameter of

the column was 5.5 inches and water depth on top of the sediment was

5.0 inches. Measurement was obtained periodically to see the

settling characteristics of the mud. Table 20 shows the settling

data for the sediment.

The three feet column of sediment settled half a foot within the

first day. As time passed, the settling rate decreased until a

near-equilibrium state was reached. After 30 days, the height and

Table 20. Settling of Sturgeon Lake Sediment in a Long Column

Time	Day	Lag Time day hr min			Distance Lowered Inch	Mud Depth Inch
1515	5/11//82		0		0	36
1700	5/12/82	1	1'	45"	5.66	30.34
1306	5/13/82	1	21'	33"	6.91	29.09
2200	5/15/82	4	6	27	8.60	27.40
2000	5/17/82	6	4	45	8.91	27.09
2000	5/19/82	8	4	45	9.16	26.84
1400	5/24/82	12	20	45	9.66	26.34
1500	5/27/82	15	21	45	9.75	26.25
1500	6/11/82	29	23	45	10.88	25.12

volume reductions were 30 percent. Figure 75 shows the settling characteristics of this Sturgeon Lake sediment.

Consolidation and density characteristics were studied for short-column settling at two different times. Preliminary data was collected using two 1-liter graduated cylinders during initial field studies. The mixed-slurry sediment was poured into the graduated cylinders and left to settle down. More-detailed data was collected almost one year later when known amounts of mixed-slurry sediment were poured into eight 1-liter graduated cylinders with approximately 200 ml of distilled water. After thorough mixing, settling was allowed to occur and the changes in sediment volume were recorded. Also, the wet and dry densities were measured.

Tables 21 and 22 show the short column sediment settling characteristics for preliminary and detailed experiments. Table 23 shows the density characteristics of the sediment, based on the detailed study. Figures 76 and 77 show the gravitational settling versus time for the two studies. Figure 78 shows the dry density characteristics of the sediment over time.

The results indicate that almost a 12 percent reduction in volume of sediment occurred in the first day and that a 20 percent reduction in volume was experienced by the end of approximately 30 days. Also, the results indicate that sediment approached near-equilibrium settling conditions after 3 or 4 days. A 48 percent increase in bulk density was observed after approximately 30 days.
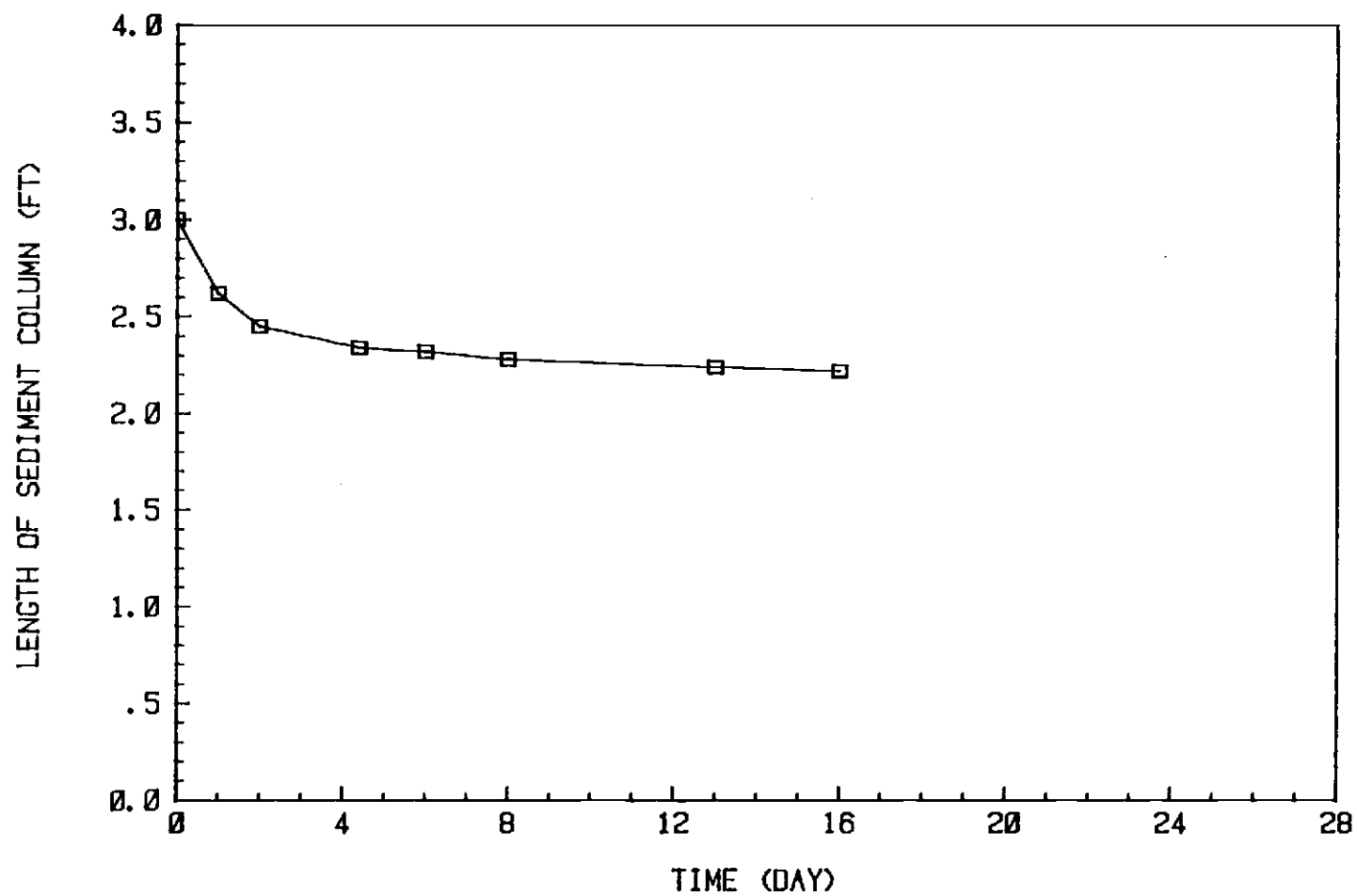
Figure 75. Settling Characteristics of Lake Sediment in Long Column

Table 21. Preliminary Study of Short-Column Settling of Sediment

Time	Date	Lag Time			Cylinder 1		Cylinder 2	
		Day	Hr.	Min.	Sed. Depth cm	Vol. ml	Sed. Depth cm	Vol. ml
11:00	5/11/82	0	0	0	32.90	940	35.82	975
15:15	5/11/82	0	4	05	32.38	925	35.53	967
17:00	5/12/82	1	6	-	29.75	850	33.62	910
13:00	5/13/82	2	2	-	28.70	820	32.70	890
22:00	5/15/82	4	11	-	28.00	800	31.60	860
20:00	5/17/82	6	9	-	27.83	795	31.41	855
20:00	5/19/82	8	9	-	27.65	790	31.23	850
15:00	5/24/82	13	4	-	27.65	790	31.28	850
14:00	5/17/82	16	3	-	27.48	785	30.86	840
15:00	6/11/82	30	4	-	27.30	780	30.52	830

Table 22.   Detailed Study of Short Column Settling of Sediment

Lag Time # of days	Cylinder No.	Volume Reduction Percent	Average Volume Reduction Percent
0.33	1	12	12
0.33	2	12	
1	3	14	
1	4	15	
1	5	16	15
1	6	14	
1	7	17	
1	8	14	
2	4	18	
2	5	19	18
2	6	18	
2	7	19	
2	8	16	
3	4	19	
3	5	20	
3	6	19	19
3	7	19	
3	8	17	
4	5	20	
4	6	19	19
4	7	20	
4	8	18	
5	6	20	
5	7	21	20
5	8	18	
12	6	20	
12	7	21	20
12	8	18	
33	6	23	23
33	7	23	
150	6	28	32
150	7	36	

Table 23. Average Density Characteristics of Sediments
In Short Column

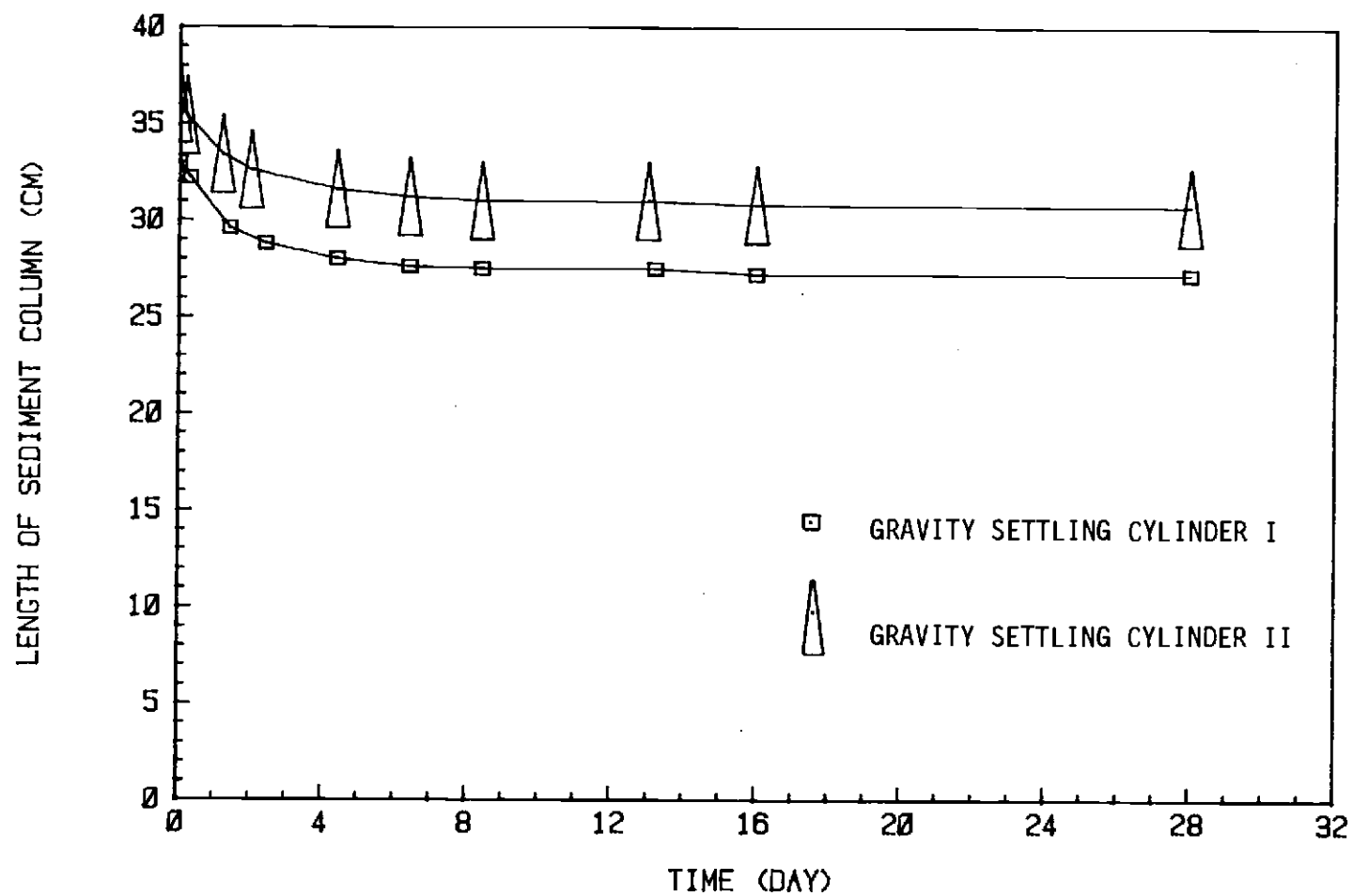| Elapsed-time (days)	Average dry density gram/cm
1/24	0.35
2/24	0.35
5/24	0.35
9.24	0.35
23/24	0.44
1.2	0.44
1.4	0.44
2	0.45
2.4	0.45
3	0.45
<4	0.48
5	0.49
33	0.50

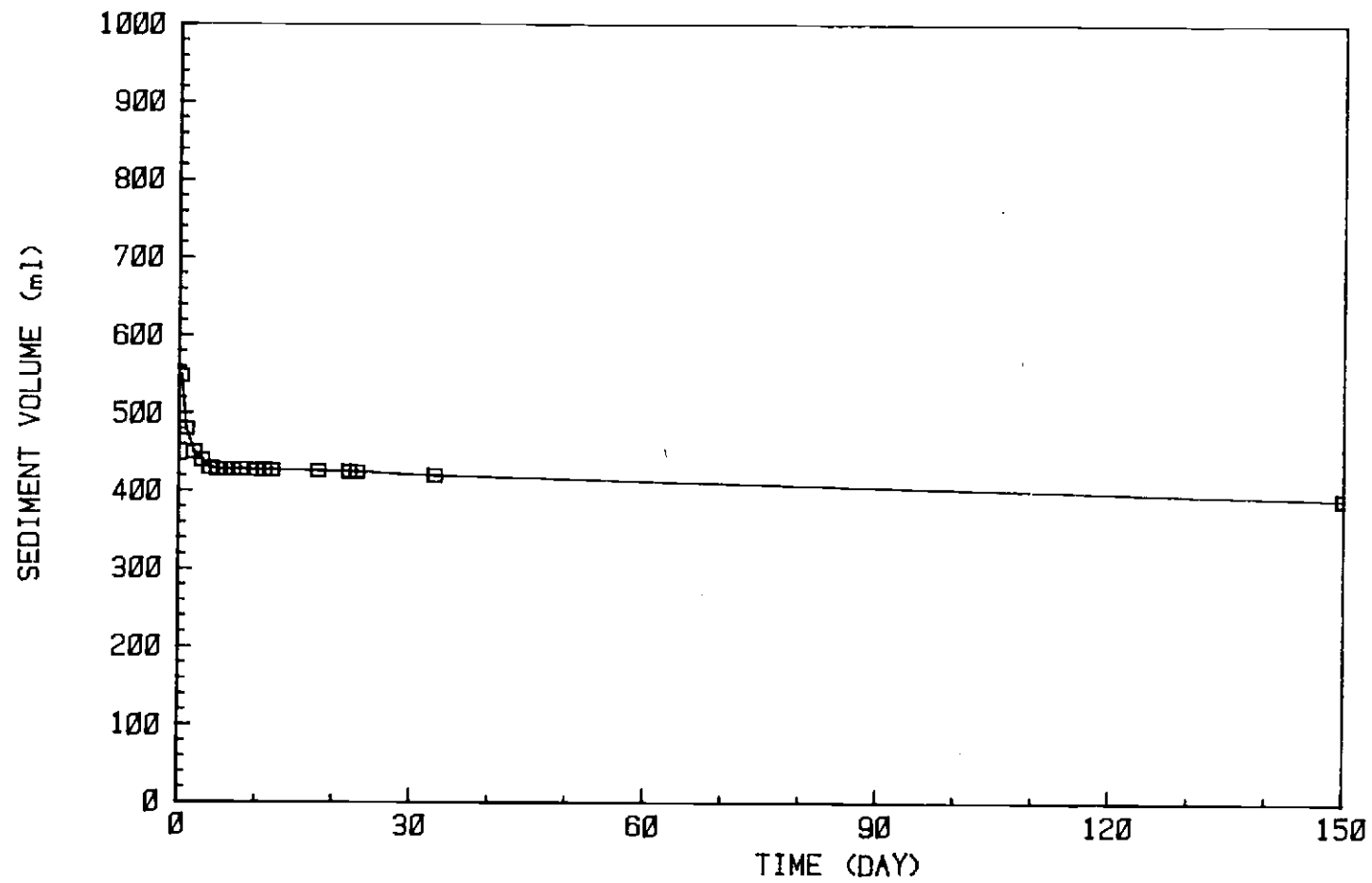Figure 76. Settling Characteristics for Sediment in 2-Liter Cylinders

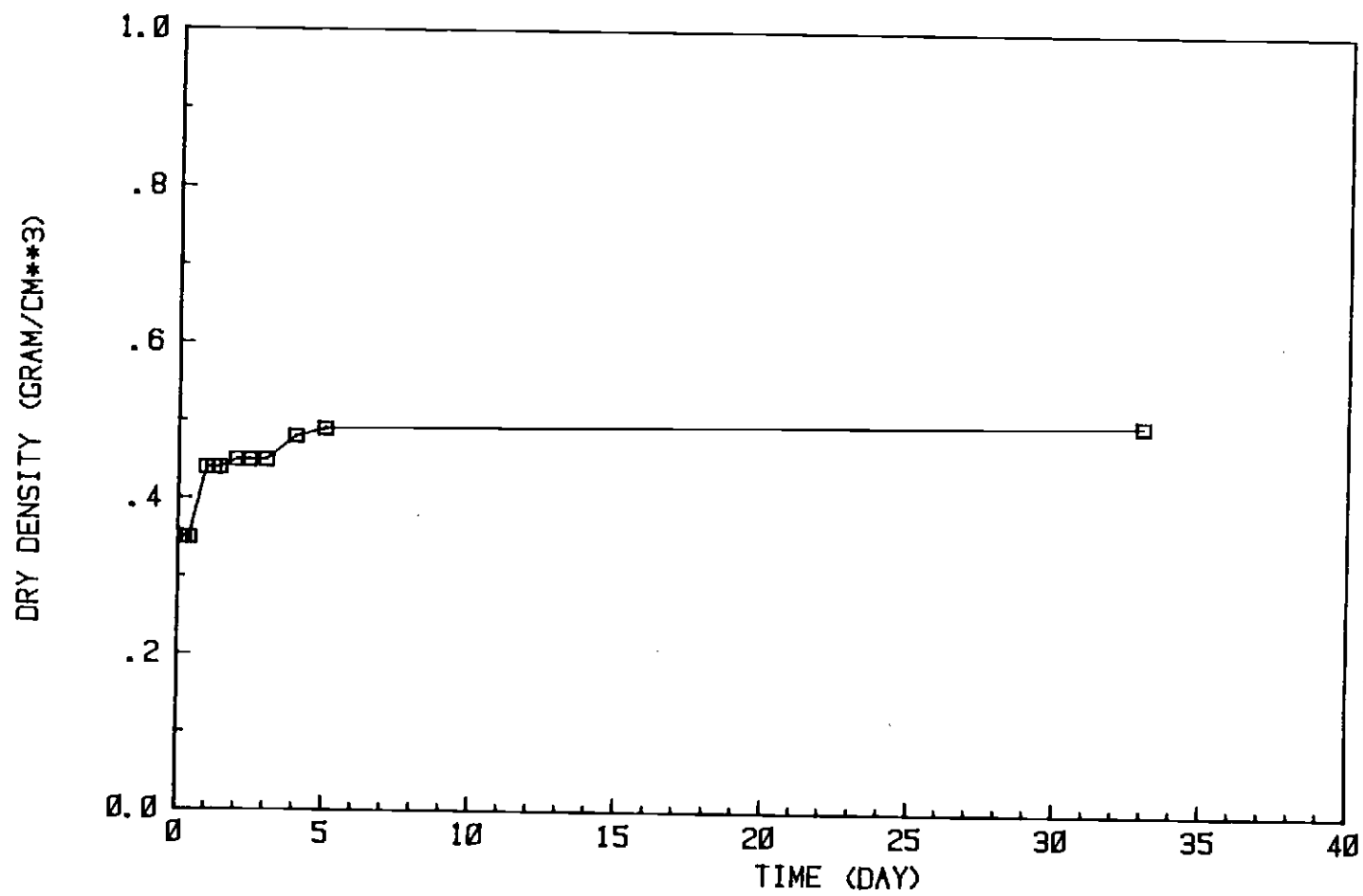Figure 77. Gravitational Settling Versus Time

Figure 78. Density Characteristics of Sediment in Settling Columns

Consolidation With Washing Out of Fine Sediment

In this experiment two 2-liter graduated cylinders were used. The mud was poured into the cylinders, then 500 ml of Sturgeon Lake water was added at once. After such addition of water, the suspended sediment was left to settle 10 minutes on 5/11/82 (the first day) and on 5/13/82 and for 2 1/2 minutes on 5/15/82 and 5/19/82, before extraction of supernatant.

Table 24 shows the consolidation characteristics of this flushed Sturgeon Lake sediment, the concentration of suspended sediment which was extracted, and the percent volatile solids of the extracted suspension.

Figure 79 shows the settling characteristics of the material remaining in the graduated cylinders.

The experiment results show that at the end of two days, the mud column had lowered 2.5 centimeters, and that a 22 percent compaction of the mud was experienced with 16 days of settling time. It was observed that upon water addition and the resultant agitation, suspended solids became coagulated and settled faster after 5/11/82 (i.e., on 5/13/82 and following this date) than on 5/11/82 (first day of experiment). Also, the suspended solids settled in a definite blanket.

Density Changes from Long-Column Settling

For the sediment in the long settling column, after 16 days of gravitational settling, sediment samples were withdrawn from the column at different depths with a syringe for density measurement. Table 25 shows the wet and bulk density, and percent moisture

Table 24. Consolidation Characteristics of Sediment After Washing Away Fine Material

			CYLINDER I					CYLINDER II			
Lag day	Time hr.	No. of Extraction	Total Volume ml	Sus.Sed. Conc. g/l	Volatile Solids Percent	Sediment Height cm	No. of Extractions	Total Volume ml	Sus.Sed. Conc. g/l	Volatile Solids Percent	Sediment Height cm
0	0	7	3,400	2.98	6.0	23.53	6	2,975	2.42	6.9	23.58
2	2	8	4,200	2.3	6.0	21.00	8	4,030	1.78	6.5	21.46
4	11	10	5,350	4.3	6.0	19.84	10	5,073	3.90	6.4	20.65
8	9	9	4,000	6.1	6.0	19.06	9	3,850	6.10	6.2	20.84
13	3	0	--	--	--	18.67	0	--	--	--	19.43
16	4	0	--	--	--	18.28	0	--	--	--	19.03
30	4	0	--	--	--	16.72	0	--	--	--	17.41

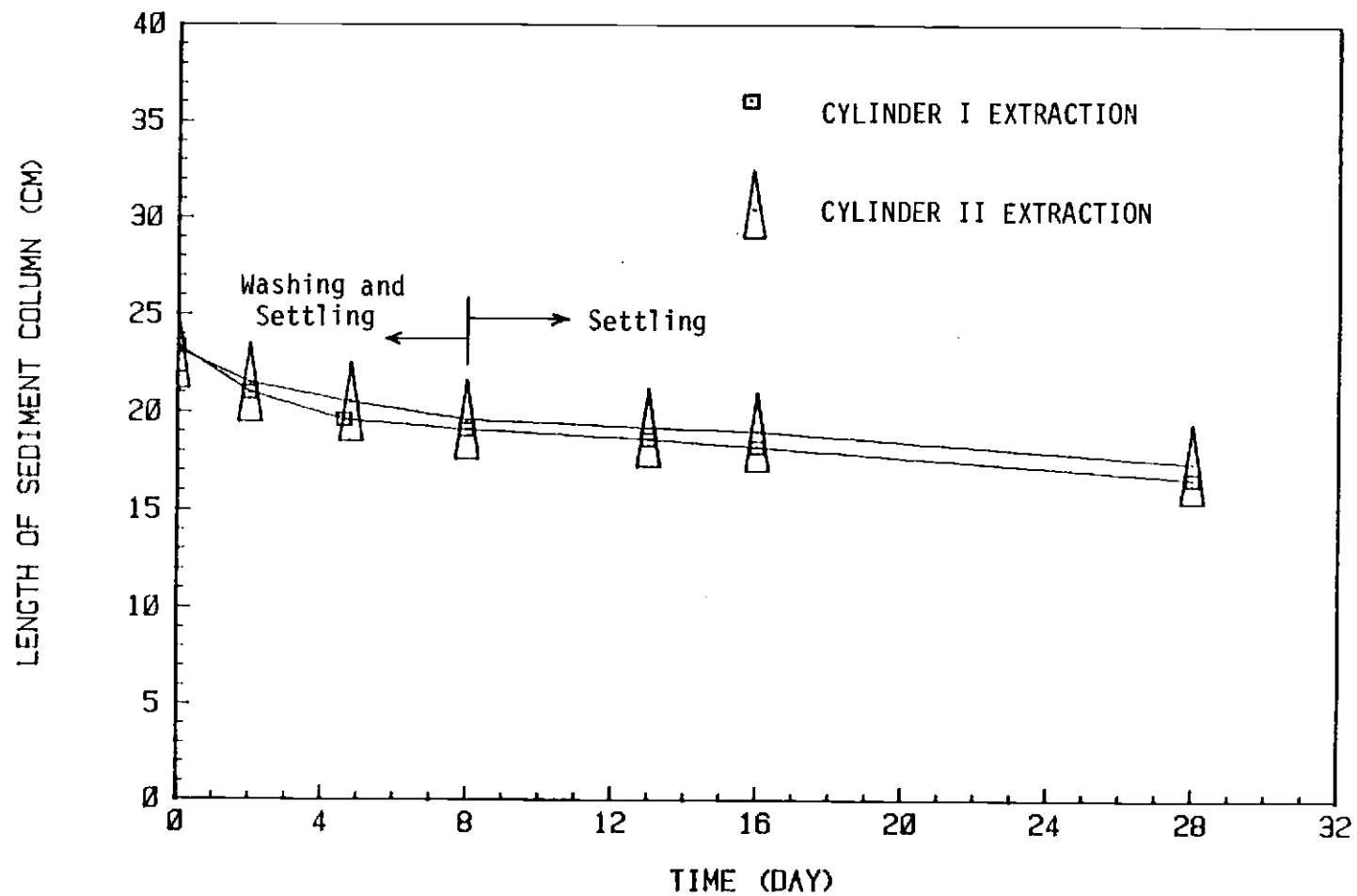Figure 79.   Settling Characteristics Due to Washing Away Fine Particles

Table 25. Density Measurements in Long Column

Distance from Bottom	Wet Density gram/cm^3	Water Content Percent	Bulk Density gram/cm^3
(at bottom)			
0"	1.33	56.2	0.60
6"	1.33	56.7	0.57
12"	1.31	60.0	0.53
18"	1.01	96.7	0.03

Sediment Height = 18"
Water on top = 6"

adetermined at different locations of the column. The density
measurement results show a 24 percent increase in density in the top
18 inches of sediment.

VI. DISCUSSION OF EXPERIMENTAL RESULTS

Sediment Characteristics Applicable to Incipient Motion and Transport

The bottom sediment in a lake or ocean environment serves as the interface between the active hydraulic environment above and the sedimentary environment below. This benthic boundary layer experiences much biological, chemical, and physical activity. The physical features which influence this benthic boundary layer include: grain size distribution, consolidation and density characteristics, clay content, and type of clay in the sediment, and hydrodynamic behavior of overlying water.

The sediment for laboratory experimentation was collected from Sturgeon Lake. The Sturgeon Lake sediment is exposed to a variety of disturbances and loading conditions. Disturbances may be caused by natural hydraulic erosion and deposition, bioturbation, or man-induced activities such as boat traffic. The net effect of each disturbance is that the sediment matrix is dilated, pore volume is increased and strength is reduced. Between disturbances, the sediment bed is at rest and may be loaded due to its own weight or due to the surcharge imposed by newly deposited sediments. Loading tends to compress the sediment structure, forcing out pore water so that more of the load may be carried by intergranular contact of sediment particles.

The process of change in sediment pore volume resulting from an applied load is referred to as consolidation. Consolidation tends to reduce the pore volume and increase sediment strength.

Consolidation and density characteristics of the sediment could reveal the strength and resistance of fine-grained sediment to hydraulic erosion and transportation. The lake sediment was observed to be fluffy and loose, without much strength. The active hydraulic environment of the lake, due to tide-induced unidirectional flow and wind-induced oscillatory flow, tends to promote selective removal of fine sediment and organic matter, flushing of pore water, and reduction in strength. The presence of fine-grained sediment and organic matter, together with poor lake circulation and flushing, produces turbid conditions throughout the water column. Those areas of the lake which experience only minor net through-flow are hydraulically inactive and the corresponding sediment structure contains more fine sediment and higher amounts of organic matter.

The laboratory data on consolidation and density of the sediment indicate that if the submerged sediment was under no active hydraulic disturbances, it consolidated substantially. Total consolidation increased with depth in the sediment column. Data also indicate that the density of the sediment increased with depth in the sediment column. The consolidation and density of the top bed layer, at the interface of sediment and water, were much smaller than for the underlying sediment. Therefore, the shear strength at the surface would not be very effective in resisting erosion.

In Sturgeon Lake, the sediment bed is continously exposed to a variety of disturbances. Thus, the surface sediment does not have a chance to consolidate in the manner of the quiescent laboratory cylinders. To see the effects of a disturbed environment, the

experimental washing out of fine sediment gave results which indicated that the loss of fine sediment and organic matter from the sediment surface caused the remaining, coarser sediment to consolidate at a higher rate. From this it can be surmised that the fluffy and loose surface sediment in Sturgeon Lake in areas of poor flushing hinders consolidation and that if flushing of fine sediment were improved, a greater consolidation might occur.

To simulate the natural deposition of sediment in the laboratory flumes, a well mixed slurry of sediment was poured into still water at a designated location (refer to Chaper 4) to naturally deposit and form a sediment bed. The mode of deposition and time history of deposited material affect the incipient motion characteristics of the sediment.

During the deposition period, the clay particles in general exhibit a non-salt cohesion (Krone, 1962) resulting from the contact of positive mineral edges of particles with negative mineral faces of other particles. As more sediment particles deposit, crowding reduces the freedom of orientation and fewer particles experience edge-to-face cohesion; as a result, a number of particles are forced into a more parallel arangement. The crowding corresponds to a weak bonding of the particles. Particle bonding depends on mineral shapes and sizes as well as the total surface area.

As time progresses, some clay particles can come together through Brownian moton, fluid shear, and differential settling and form a particle aggregate. These aggregates settle down and crush the previously settled material. The crushed material forms a bed that

is more resistant than the surface sediment. This process of aggregation, settling, and crushing continues as long as sediment particles are in the water column. If, during settling, the aggregated particles join the bed without breaking up, the bed surface is more resistant than if the aggregates break up.

The material which comprises the top bed surface is a mixture of fine inorganic sediment, and organic matter. Organic determinations for the top layer revealed 13 percent organic matter there in comparison with 5 percent in the sediment bed below the surface. The top bed surface was called a skin layer because of its hydraulic behavior. The top skin layer formation depends on the time history of sediment particle deposition. The top skin layer formed overnight.

Unidirectional Flow

The experimental objective addressed here was to study the incipient motion of fine-grained cohesive sediment under unidirectional flow. The mean flow velocity, the shear stress at the bed, and changes in suspended sediment concentration were used as the principal criteria to quantify the incipient motion. From experimental observations, the incipient motion of fine-grained sediment is defined on the basis of the appearance of pit marks, the peeling off of bonded particles, and the development of streaks on the bed surface. These processes were associated with increase in suspension concentration from initial background conditions. The hydraulic conditions for incipient motion are given by the corresponding average flow velocity and shear stress at the bed.

Effect of Flow Depth, Velocity and Shear Stress on Incipient Motion

The incipient motion of fine-grained sediment under
unidirectional flow can be defined as the condition at which
individual or bonded particles start to peel off, leaving pit marks
which lead to streak formation, together with an obvious increase in
suspended sediment concentration. This condition can be defined in
terms of hydraulic parameters.

I attempted to relate maximum instantaneous velocity near the
bed, water depth, mean flow velocity, and shear stress to incipient
motion. The results of the experiments show that maximum
instantaneous velocity at a given location near the bed is not a
good indicator of incipient motion of fine-grained sediment under
unidirectional flow, because the instantaneous value does not
represent any particular mean value. The mean water velocity in the
flume is a better index for incipient motion. However, many
researchers argue that the water depth should also be used in
conjunction with the mean water velocity. Water depth alone is a
very poor criteria for incipient motion because it does not reflect
the eroding conditions. Similarily, mean velocity alone is
inadequate because the corresponding depth will affect the shear
stress exerted at the bed.

Figure 80 shows the water depth histogram for all of the
experimental runs. Those runs for which incipient motion occurred
are indicated. The graph shows that water depth does not represent
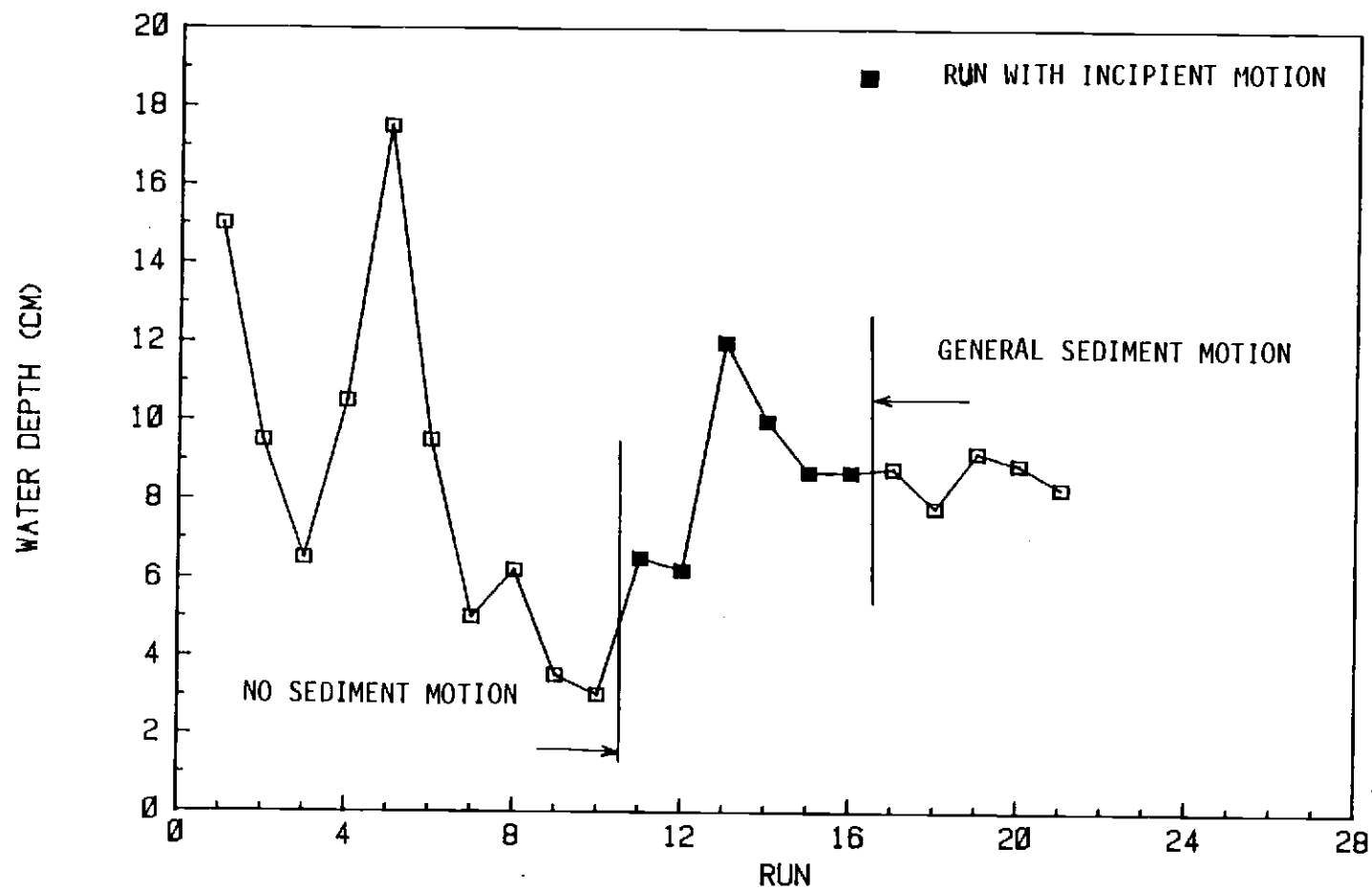a reliable index for the incipient motion condition.

Figure 80. Water Depth Histogram for Runs With Unidirectional Flow

Figure 81 shows the mean water velocity histogram for all of the experimental runs. Those runs for which incipient motion occurred are indicated.The results show that mean water velocity can be used as a good index for incipient motion.

Shear stress was found to be the most reliable index for incipient motion. Figure 82 shows the shear stress histogram for all of the experimental runs. Those runs for which incipient motion occurred are indicated. The results show that incipient motion of fine-grained sediment under unidirectional flow occurs in the range of 5.08 to 6.10 dyne/cm^2.

Several published empirical formulas were used to determine the incipient motion of fine-grained sediment and compared to my experimetal results. Table 26 provides the critical velocities and the critical shear stresses required for incipient motion of fine-grained sediment in the flume (D_{mean} = 0.0178 mm and D_{50} = 0.0085 mm) based on the equations of various investigators. The results show that the range of critical velocity required for incipient motion in Sturgeon Lake sediment is about 20 to 170 cm/sec and that the range for critical shear stress required for incipient motion in Sturgeon Lake sediment is even wider, about 1 to 125 dyne/cm^2.

The Fortier and Scobey criteria for incipient motion can be eliminated because their field study results are for canals. The remaining investigators, with the exception of Abdel-Rahman, are in good agreement with my experimental results.
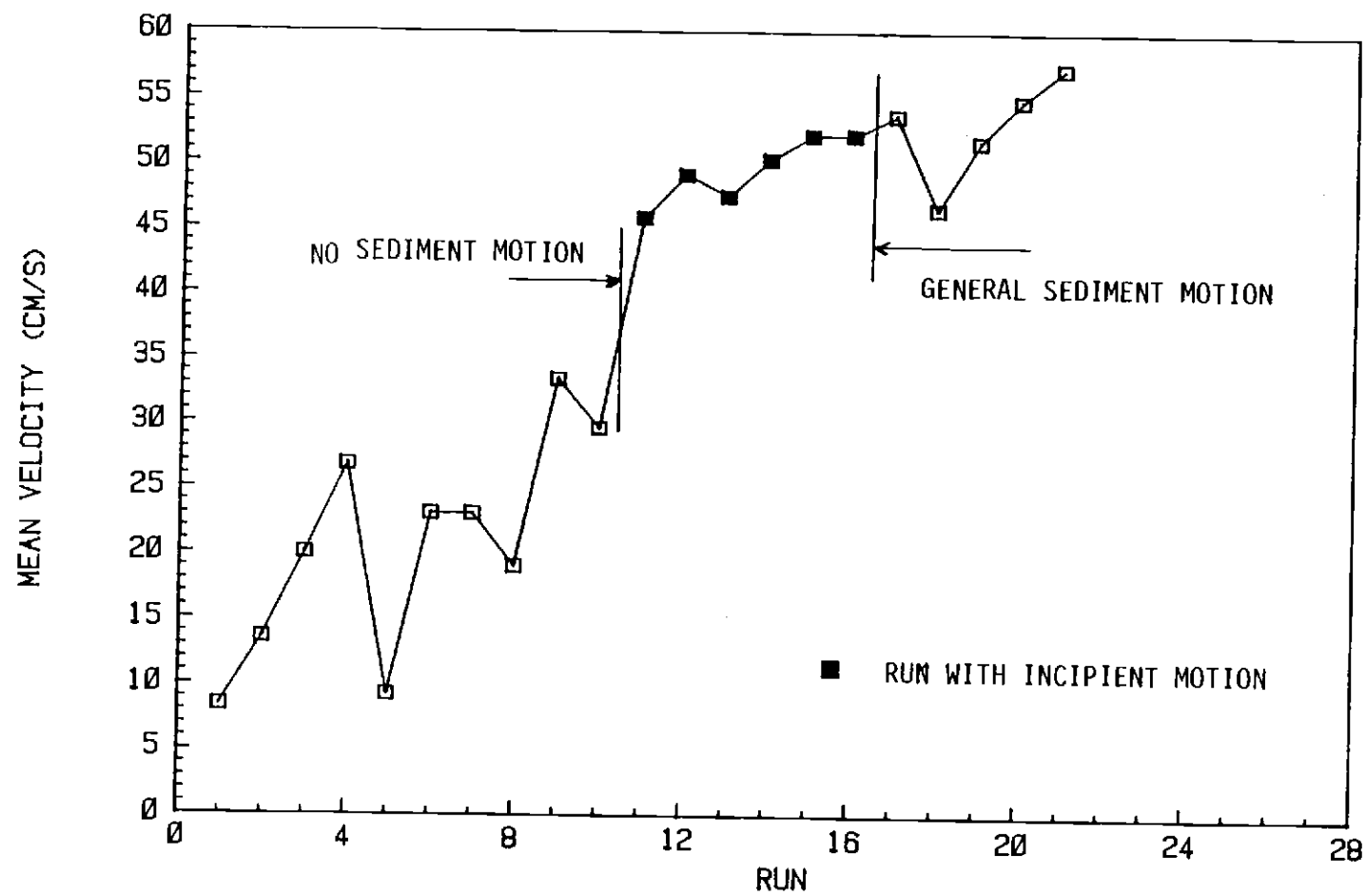
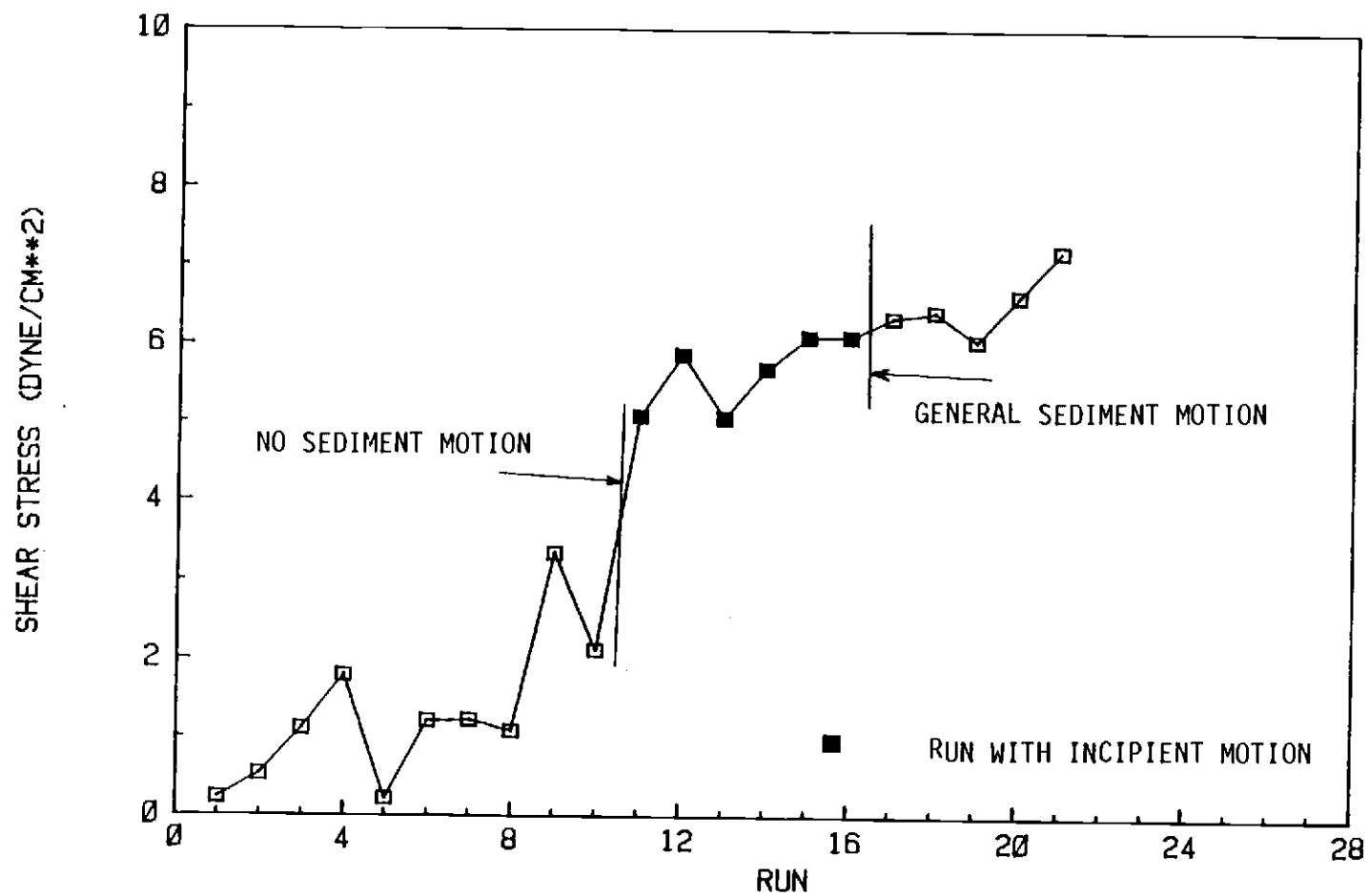Figure 81. Mean Velocity for Runs With Unidirectional Flow

Figure 82. Shear Stress for Runs With Unidirectional Flow

Table 26. Critical Velocity and Shear Stress for Incipient Motion
of Fine-Grained Sediment Under Unidirectional Flow,
Based on Empirical Formulas

Investigator	Critical Velocity cm/s		Critical Shear Stress dyne/cm^2		Runs In Motion
Shields (1936)					4b and 10 critical 9 to 21 motion
Inman (1949)			1.10[a]	1.77[b]	4, 6-21, 3, 8 critical
Hjulstrom (1936)	32-64[a]	53.3-96[b]			4-21
Lane (1955)	61-91		1.5[a]	1.0[b]	3, 4, 6 to 21
Neill (1967)					all except run 1
Sundborg (1956)	20-110[a]	20-170[b]			11 to 21
Smerdon & Beasley (1961)			4 to 24		11 to 21
Abdel-Rahman (1964)			7 to 43		21
Fortier & Scobey (1926)	61-114		23 to 125		None based on shear stress, based on velocity 14 to 21
Miller (1973)			0.98 - 1.53		3, 4, 6 to 21
Yalin (1972)			0.83 - 0.95		3, 4, 6 to 21
Hall (1982)					All in motion
Partheniades (1962)			0.96 minimum shear stress		3, 4, 6 to 21

[a]Based on D_{mean} of particle

[b]Based on D_{50} of particle

Effect of Suspended Sediment Concentration on Incipient Motion

The suspended sediment concentration was measured to aid in evaluating incipient motion. Figure 83 shows the suspended sediment concentrations versus time for all of the experiment runs. The suspended sediment concentration results show that at the incipient motion shear stresses just given (runs 11-16), the suspension concentration increased from 10 mg/l to 30 mg/l and continued to stay steady at 30 mg/l at the end of run 16. The higher suspended sediment concentration at lower shear stresses (runs 1-10) was associated with loose particles and bonded particles from the bed margins which went into suspension and moved downstream, causing additional abrasion of the sediment bed and, consequently, more suspension.

The results of experimental run 17 shows that fluid flow with 2,300 mg/l of suspended sediment concentration at shear stress of 6.34 dyne/cm^2, slightly above incipient conditions, did not erode the bed surface, but that instead the bed surface coarsened. Thus, the fluid flow with large suspended sediment concentration did not have any noticable effect on the erosion of the bed. One obvious conclusion is that the incipient motion of fine-grained bed sediment is independent of the suspended sediment concentration in the overlying water. The reasons for this are:

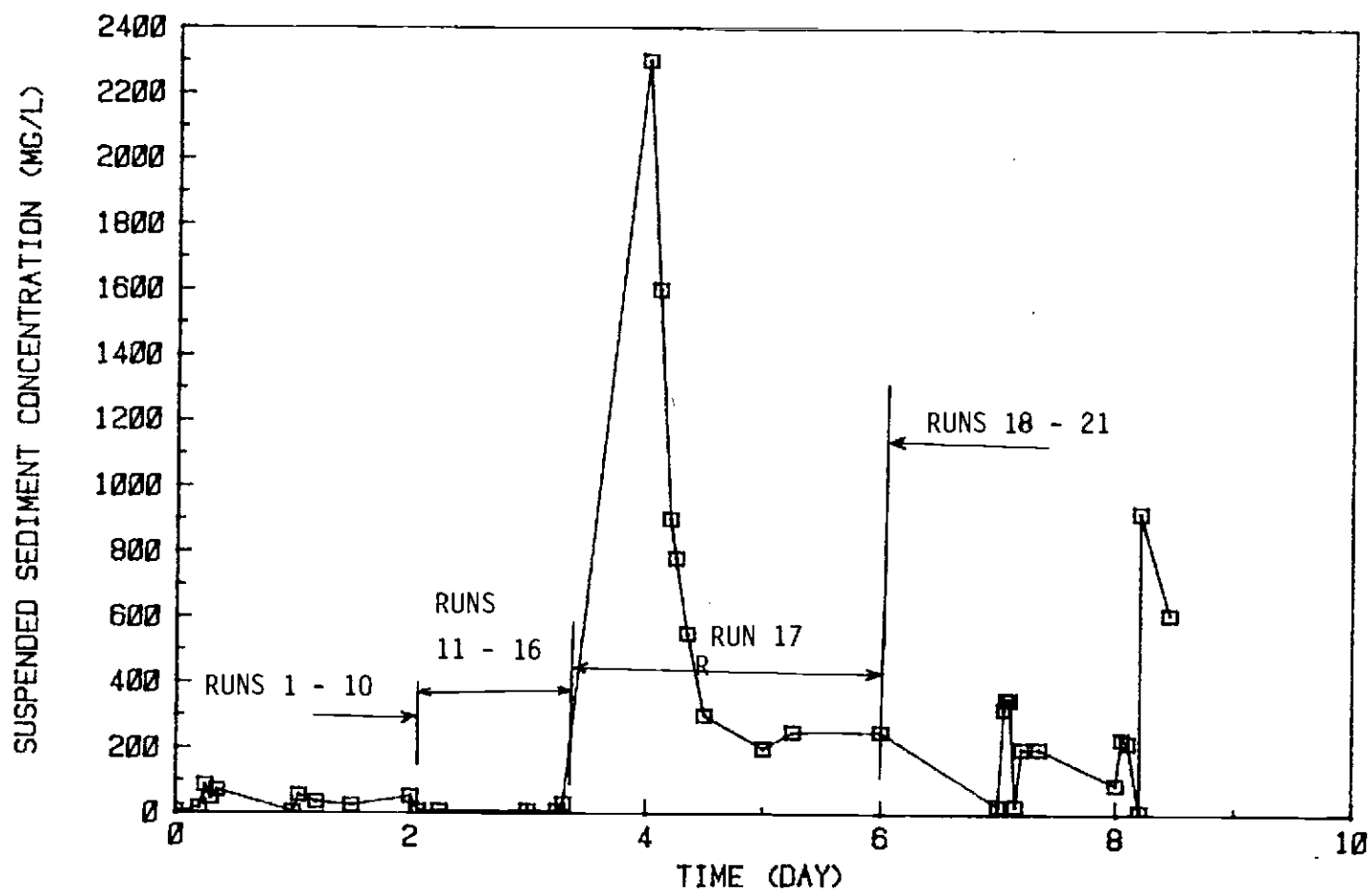a) The coarser sand and silt particles in the body of water abraded the smooth bed surface, giving it a coarse look;

Figure 83.   Suspended Sediment Concentrations Versus Time for Unidirectioal Flow

b) The turbulent structure at the bed, which is responsible for

removing and transporting sediment particles, is not changed

by the increase in suspended sediment concentration; and

c) The shearing force at the bed is probably retarded by the

presence of fine suspended sediment particles at the

boundary layer.

Effect of Dunes on Incipient Motion

The results regarding shear stress, velocity, and suspended

sediment concentration show that the rough bed field is susceptible

to erosion at lower shear stresses than for the smooth bed surface.

In general, bed surfaces with any kind of irregularities start to

erode or go into suspension at lower velocities and shear stresses

than do smooth beds. Besides the turbulent structure near the bed,

which is responsible for removing and picking up of the fine

particles on a smooth bed, eddies and secondary currents are present

in the rough bed. Thus, particles are eroded and put into

suspension in the rough bed at lower shear stresses than are

required to initiate erosion in a smooth bed.

Bed Patterns

Some of the bed features and related phenomena observed during

the experimental runs under unidirectional flow are:

a) Average bed erosion of 6.6 millimeter occurred from entire

surface of the bed during runs 1 through 16.

b) During experimental run 17, the suspended sediment
    concentration decreased abruptly and reached an equilibrium
    state.

c) Almost 10 millimeters of erosion took place from entire
    surface of the bed during run 17.

d) The minimum bed shear stress at which incipient motion was
    first observed was 5.08 dyne/cm^2 and the corresponding mean
    flow velocity was 45.78 cm/sec.

e) The incipient motion of the bed depended on the bed shear
    stress, increasing rapidly for shear stresses above a
    threshold value.

f) The rough bed was less resistant to erosion than the smooth
    bed.

g) Incipient motion started by a peeling off of the bonded
    particles from the skin layer.

h) The bed pattern, after incipient motion started, was formed
    by many pit marks, leading to streak formation.

Oscillatory Flow

Incipient motion of non-cohesive sediment under various flow
conditions has been studied extensively by many investigators.
Several empirical formulas have been developed to identify the
incipient motion characteristics. In nearly all previous studies,
as discussed in the literature review chapter, the determination of
incipient motion was based on subjective criteria.

The experimental objective was to study the incipient motion of fine-grained cohesive sediment under oscillatory and unidirectional flow. The maximum shear stress at the bed, maximum velocity at the bed, orbital diameter at the bed, and changes in suspended sediment concentration were used as the principal hydraulic criteria to quantify the incipient motion. From experimental observations, the incipient motion of fine grain sediment is defined as the appearance of pit marks, the peeling off of bonded particles, and the development of streaks on the bed surface.

The peeling off of the bonded sediment particles occurred from the top skin layer. The top skin layer in the flume was formed on the bed surface by bonding sediment particles and by organic and microbial matter. When the induced flow strength exceeds the bonding strength of the top skin layer, the particles start to peel off. The behavior of this top skin layer is discussed later in this chapter.

Effect of Wave Parameters on Incipient Motion

Wave parameters are the principal variables which define the flow conditions and flow forces that erode the sediment particles from the bed. Three wave parameters were varied in laboratory experiments: water depth, wave height, and wave period. Wave length was not used because the wave length can be defined in terms of wave period. A variety of values for each individual wave

parameter was used to attempt to define the incipient motion
condition.

Water depths of 9 inches, 12 inches, and 15 inches were used in
the experimental runs. For each water depth, all possible
combinations of wave height and wave period were tested, subject to
the limitations of the wave-making machine. The results show that,
at a given water depth, when wave height and wave period change
simultaneously, the wave period alone is not a good parameter for
identifying incipient motion. Also, wave height alone does not
provide a good criterion for identifying incipient motion, even
though at a given water depth, the suspended sediment concentration
increases with increasing wave height. Water depth is another wave
parameter which contributes to suspension and incipient motion, but
it alone is not suitable for defining incipient motion. Therefore,
it was found that each wave parameter has some effect on incipient
motion; i.e., when wave height gets larger for fixed water depth and
wave period or when wave period gets longer for fixed water depth
and wave period or when water depth gets smaller for fixed wave
height and wave period, greater suspension of sediment occurs. But
these effects do not directly allow the defining of incipient
motion. Therefore, no single wave parameter alone is an adequate
indicator of incipient motion.

A combination of the wave parameters could be used as an
indirect measure of the likelihood of incipient motion. But, the
combination of wave parameters must be used to define or calculate
some other flow parameters which are more directly involved in

Incipient motion, such as the velocity and shear stress at the bed. These flow parameters are directly associated with fluid forces that interact with the resisting sediment particles. This suggests that to determine incipient motion, the wave parameters must be used to obtain fluid force parameters, which then must be compared with sediment parameters that describe the sediment's resisting ability. Therefore, while the wave parameters are important to incipient motion, they must be used as the starting parameters of oscillatory flow with an important intermediate sequence of steps before incipient conditions can be defined. Therefore, I used the velocity and shear stress, instead of wave parameters alone, as an appropriate index of incipient motion.

Effect of Boundary Layer Flow Parameters on Incipient Motion

The three main flow parameters under oscillatory flow are: maximum horizontal velocity, maximum shear stress, and orbital diameter. These parameters, as mentioned earlier, can be determined from wave parameters. Some of these flow parameters were directly measured in the laboratory for comparison with calculated values. From the available wave theories, it was found that use of linear wave theory is appropriate for the computations made of flow parameters from wave parameter measurements.

Results of all three sets of runs show that the maximum velocity at the bed or the maximum shear stress at the bed can be used in determining the incipient motion of fine sediment. The orbital

diameter is another good indicator for inciplent motion, but due to the potentially large differences between visual measurement and calculation of the orbital diameter, it is recommended for limited use only in the range where observed and calculated values of the orbital diameter are in good agreement.

The three parameters were separately analyzed to determine which was best to use in studying inciplent motion.

1. Maximum Velocity at the Bed

There are some shortcomings of using the maximum velocity at the bed for determining inciplent motion of fine-grained sediment under oscillatory flow. These shortcomings include: accuracy of velocity measurement, nature of wave flow, and mass transport.

As already discussed, a miniature propeller current meter was used to measure the maximum velocity at the bed and this involved some problems. Other, more sophisticated techniques, give better results.

The wave flow is not always oscillatory in nature. Therefore, applying linear wave theory to calculate maximum velocity at the bed does not give accurate results. Utilizing a higher order of wave theory gives better results but involves more time and difficulty.

The individual particles in a progressive, irrotational wave do not exactly describe closed paths: besides their orbital motion they also possess a second-order mean velocity, called mass transport velocity, in the direction of wave propagation. Therefore, mass transport velocity should be accounted for in using velocity as a criterion for inciplent motion under oscillatory flow.

Due to these constraints, the maximum velocity at the bed should be measured as accurately as possible. If velocity can be determined exactly at the boundary layer, it is a good index to use in determining incipient motion.

The maximum velocities at the bed for all three sets of runs are plotted in Figure 84. The range of maximum velocity for incipient motion is shown on the graph. For the experimental runs within this range, incipient motion occurred. Those below the range experienced no motion and those above the range exceeded incipient motion.

The maximum velocity range for incipient motion with oscillatory flow is plotted on the Hjulstrom and Sundborg curves for incipient motion with unidirectional flow (Figure 85). The results show that the observed critical velocities are below the critical erosion range of the Hjulstrom curve (hence, stable if initially at rest), but within the critical erosion zone for unconsolidated clay according to the Sundborg curve.

2. Shear Stress at the Bed

The maximum strear stress at the bed was found to be the best criterion for incipient motion of fine-grained sediment under oscillatory flow. Surface erosion occurs particle by particle or for a group of small bonded particles. Such removal of particles occurs when the induced shear stress overcomes interparticle bonding. Maximum shear stress at the bed is an index to measure the incipient motion of fine sediment. It is the shear stress at which particle bonding breaks and particles start to move back and forth and are transported downsteam. However, most of problems associated
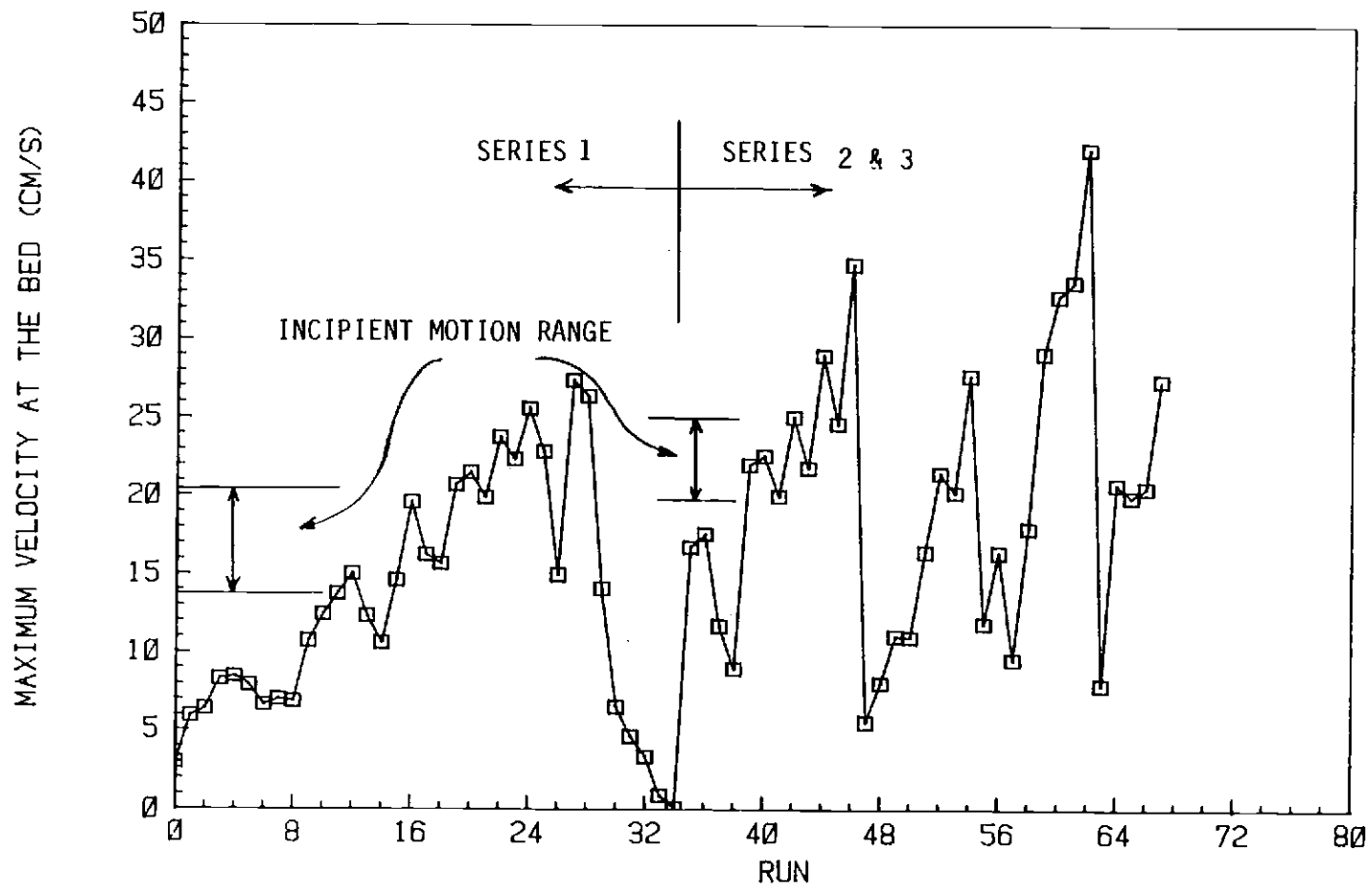
Figure 84. Maximum Velocity at the Bed for the Experimental Runs
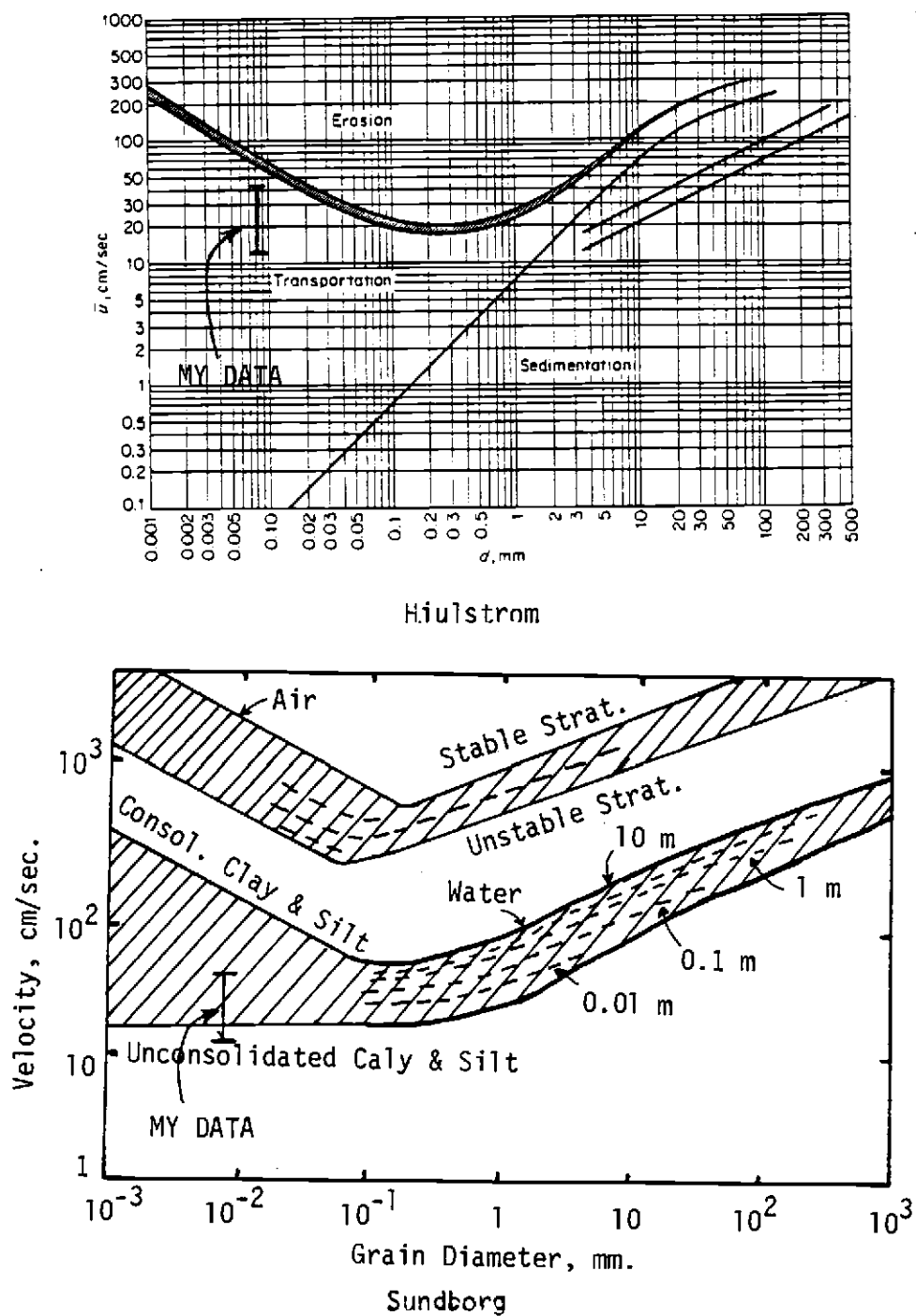
Hjulstrom

Sundborg

Figure 85. Maximum Velocity Range for Incipient Motion
on Hjulstrom and Sundborg Curves

with using velocity are reflected in attempts to use the shear stress in the same manner, because the shear stress equations are dependent on the velocity measurement data.

Figure 86 shows the maximum shear stresses at the bed for all experimental runs. The maximum shear stress steadily increased with increasing wave height and wave period. It was also attempted to relate the maximum observed suspended sediment concentration to maximum shear stress at the bed. Figure 87 shows the maximum suspended sediment concentrations measured for all of the experimental runs.

Figure 88 shows the maximum suspended sediment concentrations versus maximum shear stress at the bed for all of the experimental runs. There is considerable scatter to the correlation. Those data for the runs at which incipient motion and suspension occurred are replotted in Figure 89. The series of runs in which the chemical dispersant was used are also eliminated from Figure 89. The results show that there is a closer relationship between suspended sediment concentration and shear stress for each of the two sediment beds: the recently formed bed of the first series of runs and the more-compacted bed of the second series. As maximum shear stress at the bed increased the suspended sediment concentration increased. The relationships for the two beds are convergent toward the lower limits of incipient motion, at small shear stress. This supports the argument that bed shear strength has relatively little or no effect on incipient motion of fine cohesive sediment.

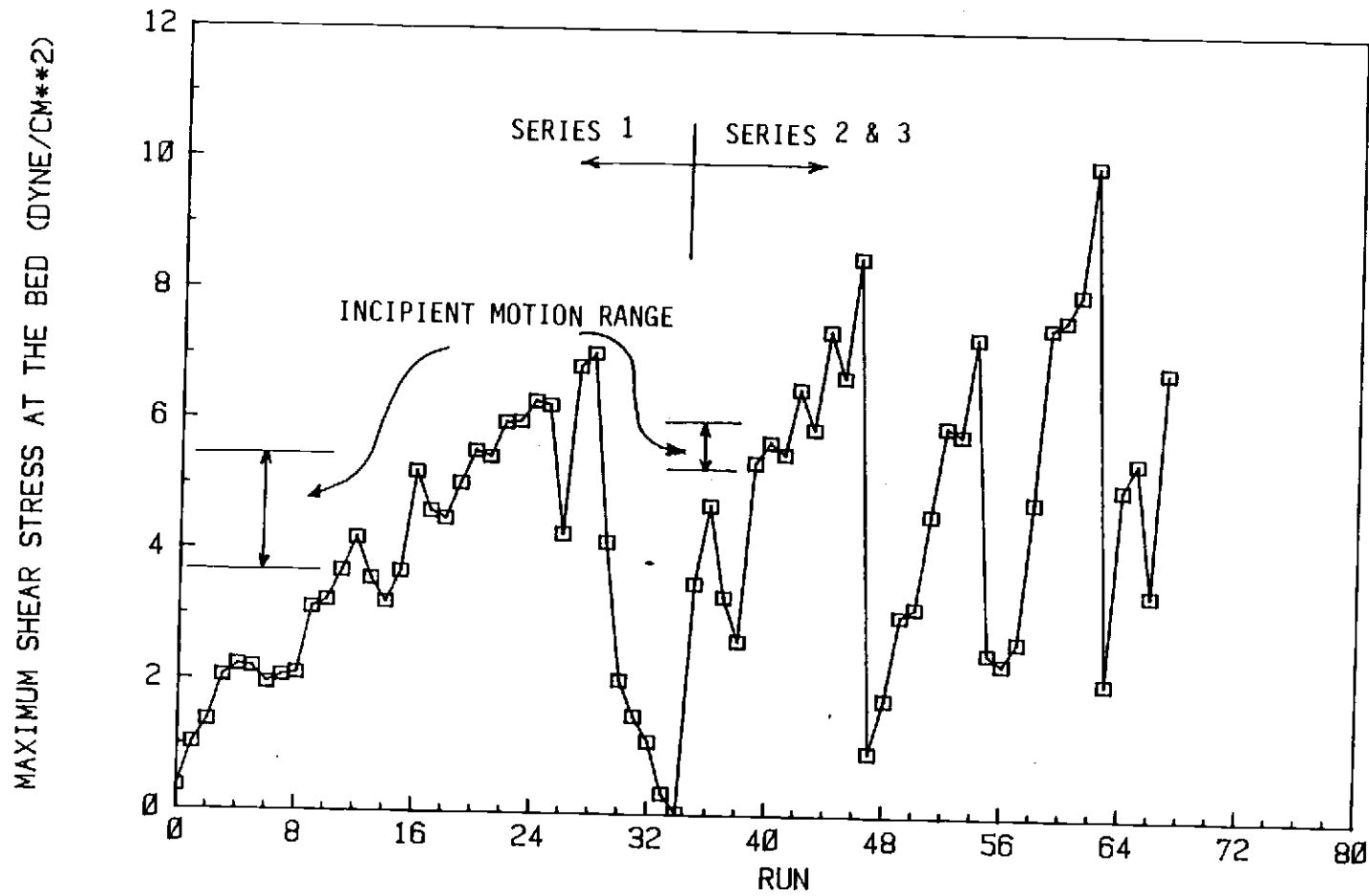The experimental results of Figure 88 show that once the shear

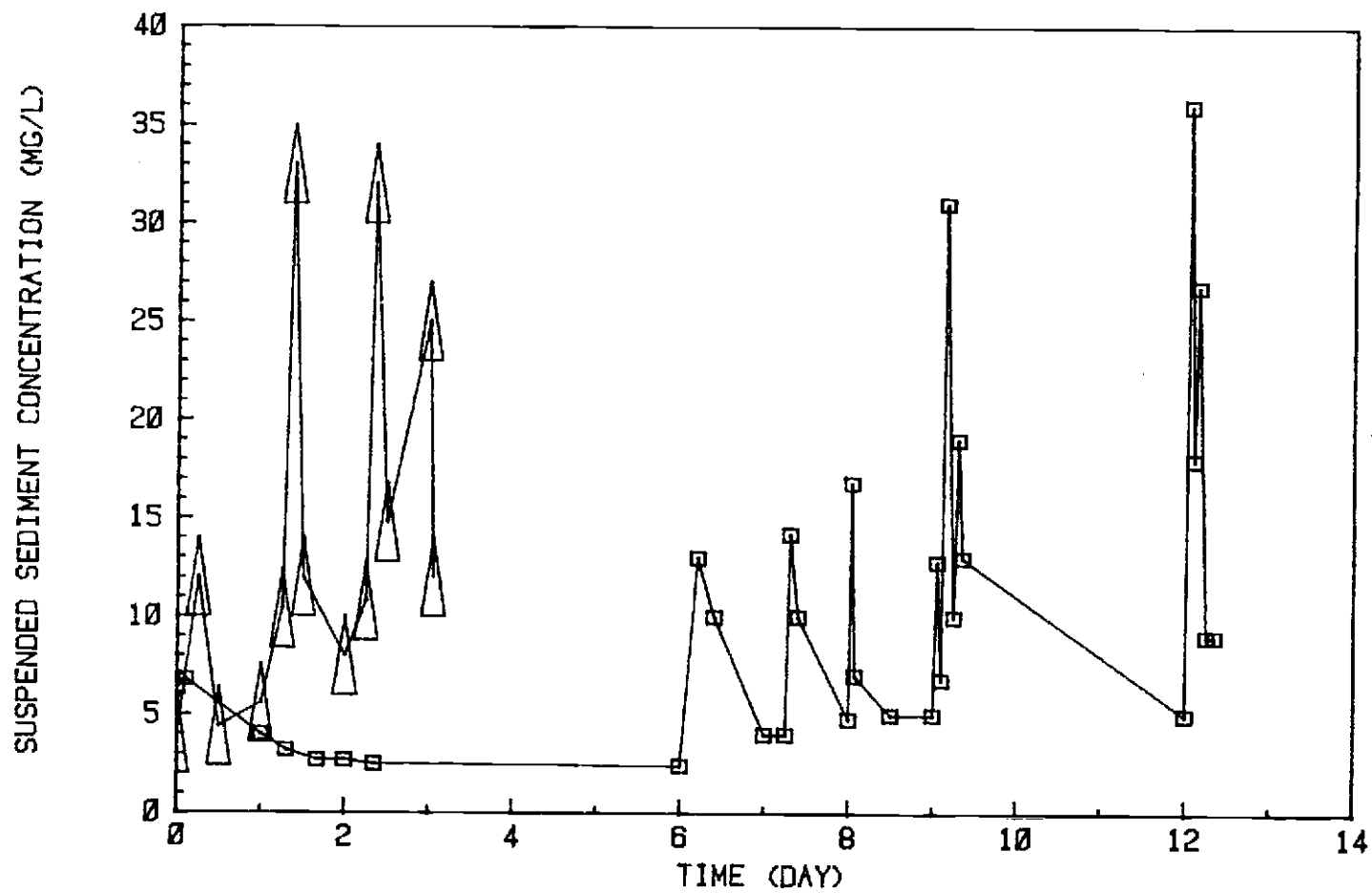Figure 86.   Maximum Shear Stress at the Bed for the Experimental Runs

Figure 87. Maximum Suspended Sediment Concentration for all of the Runs
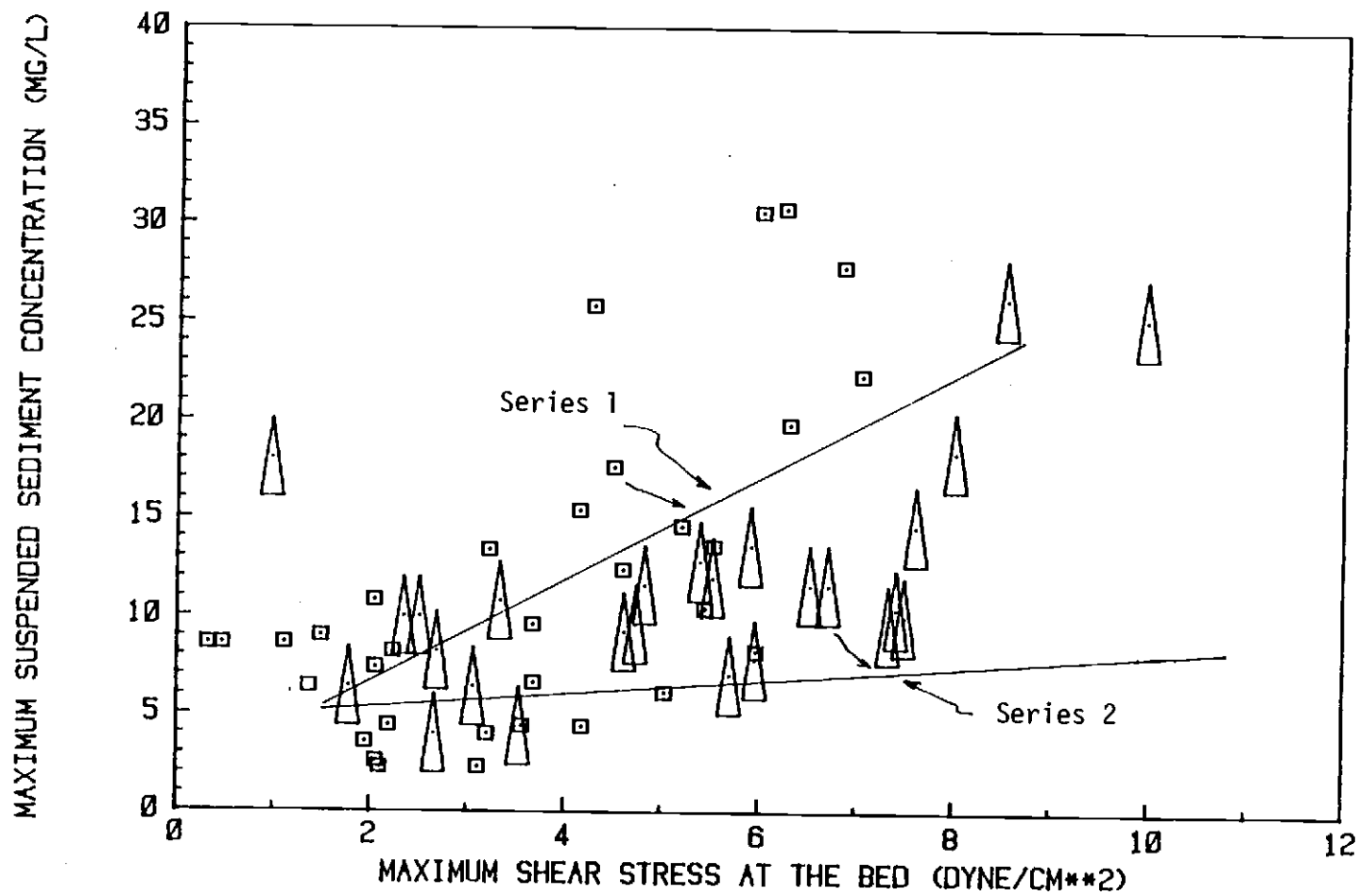
Figure 88.   Suspended Sediment Concentration Versus Maximum Shear Stress
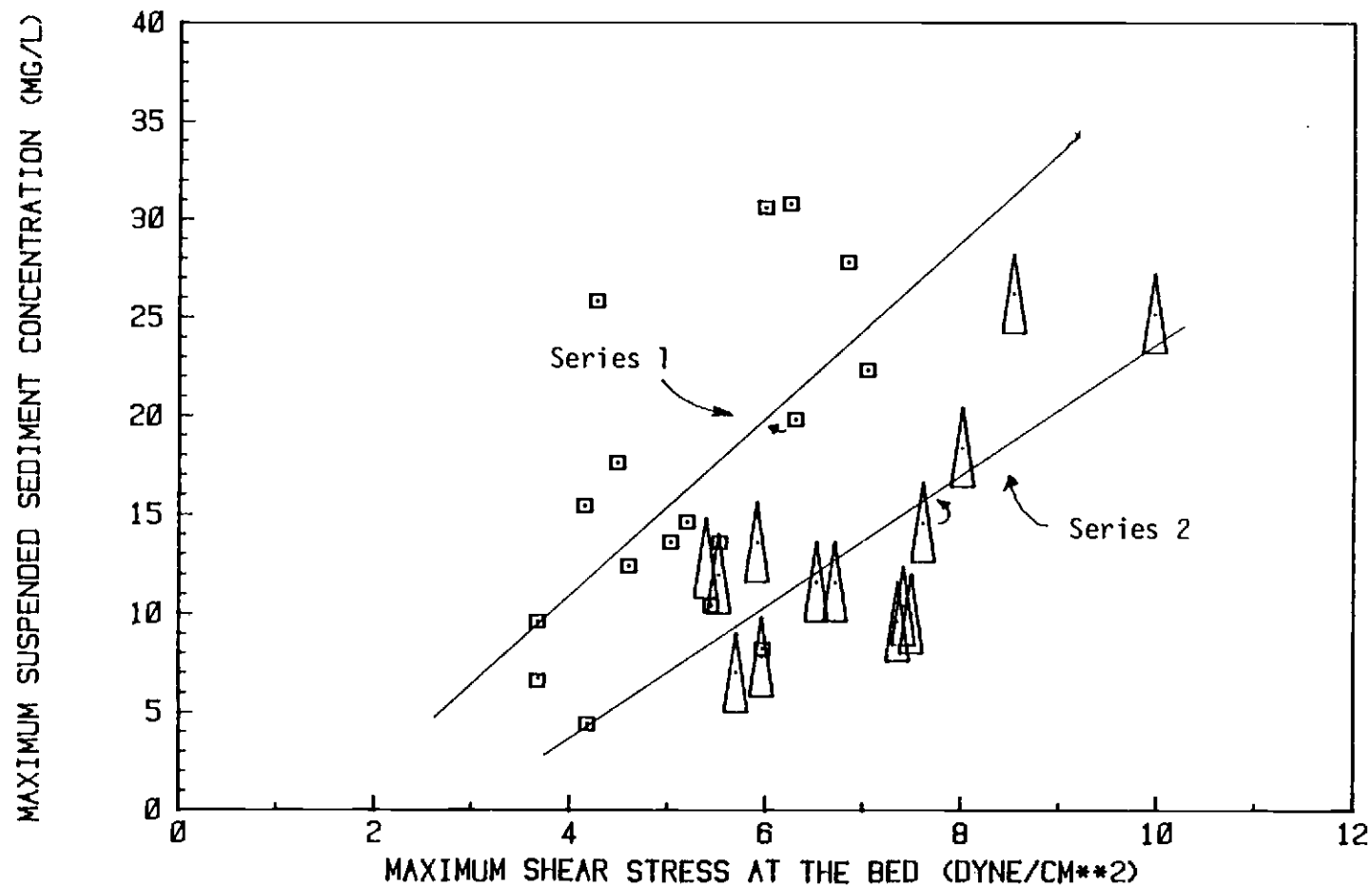for all of the Runs

Figure 89. Suspended Sediment Concentration Versus Maximum Shear Stress for Runs at Incipient Motion and Motion Conditions

stress reached the range that produced incipient motion conditions, the suspended sediment concentration increased more rapidly with increasing shear stress. Perhaps this could be considered to be an upper limit to incipient motion conditions. This critical value was found to be 5.7 dyne/cm^2 for the first experimental series with a recently deposited bed and 7.5 dyne/cm^2 for the second experimental series with an older bed. Thus, it could be argued that bed shear strength does have an effect on the beginning of general sediment motion of fine sediment once the initial bed disturbance has occurred.

The shear stresses and suspended sediment concentrations for those experimental runs at which incipient motion occurred are plotted on logarithmic paper in Figure 90. It is seen that the points for each series of runs can be fitted with straight lines. This weakens the argument just raised for a critical shear stress value at the beginning of general sediment motion, and supports the earlier argument that bed shear strength has little or no effect on the lower limit of incipient motion. However, bed shear strength does seem to have some effect, because two separate lines, rather than one, can reasonably be fitted to the data of Figure 90.

The structure of beds formed by deposition of suspended sediment depends on the mode of deposition and on time after deposition. Sediment beds formed in still water are considered to be stronger than those formed from flowing, relatively stable suspensions. Sediment bed changes with time are reportedly greatest shortly after deposition. However, the consolidated sediment bed, after 91 days,
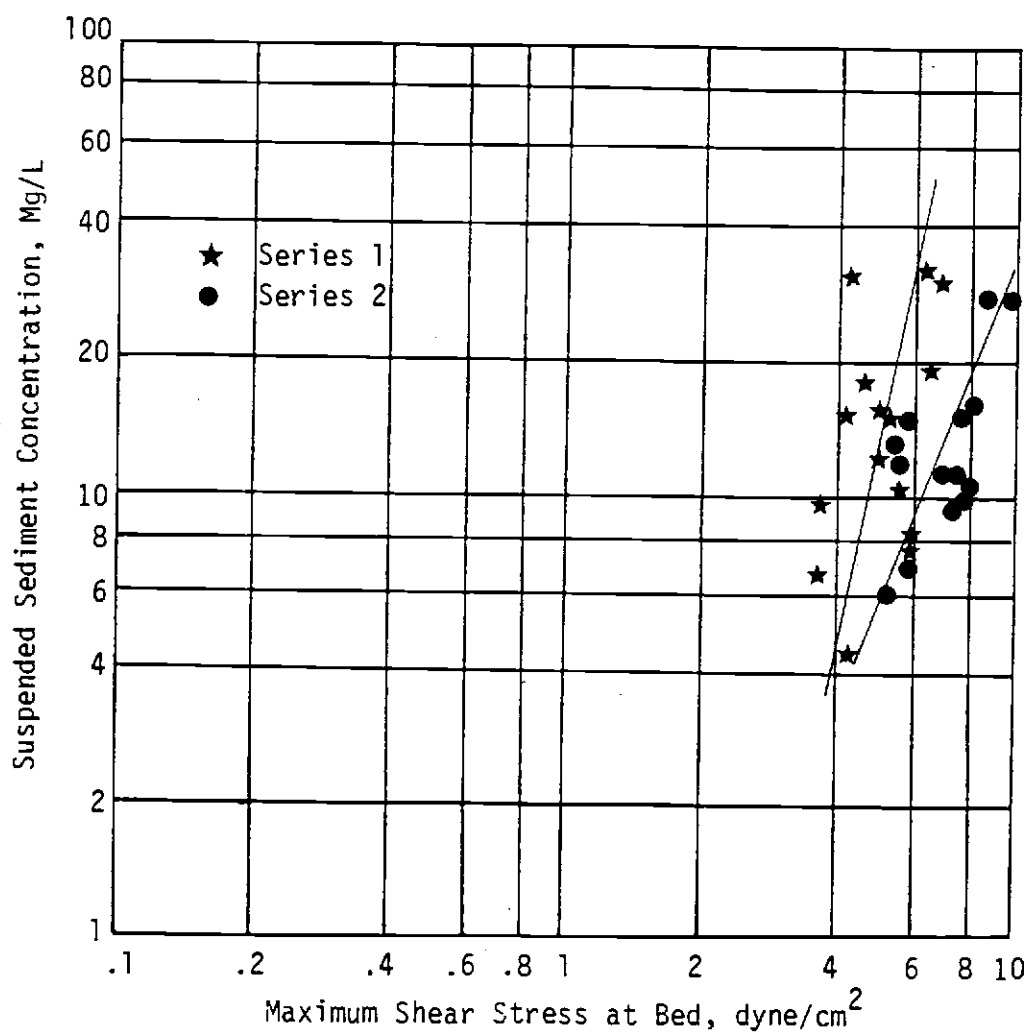
Figure 90.   Suspended Sediment Concentration Versus
              Maximum Shear Stress on Logarithmic Paper

had not experienced a significant increase of bonding strength.

The validity of the first research hypothesis was tested by applying the principles governing the incipient motion under unidirectional flow for oscillatory flow. The incipient motion characteristics of fine cohesive sediment under oscillatory flow were determined by observing and recording the changes taking place on the bed surface as was done under unidirectional flow. Then, flow parameters such as velocity and shear stress were used to quantify the incipient motion. The results show that, even though there are differences in the boundary layer flow and velocity behavior between the two types of flow, the incipient motion can be defined in terms of velocity or shear stress. For oscillatory flow, the instantaneous maximum values were chosen to represent these flow parameters.

In Oscillatory flow, the peak velocity under the crest of a passing wave acts for only a short time. The bed experiences a range of velocities with peaks in both directions during passage of waves. The boundary layer flow also varies due to flow reversals. It also varies with the variation of wave parameters. Experimental results for the conditions tested show that laminar flow dominates under oscillatory flow, whereas under unidirectional flow for the same velocities, turbulent flow dominates.

The maximum velocity for incipient motion was plotted against well known curves giving incipient motion for unidirectional flow as already shown. It was found that the results of incipient motion under oscillatory flow can be defined in terms of velocity or shear

stress as was done under unidirectional flow.

3. Orbital Diameter at the Bed

Figure 91 shows the orbital diameters calculated for the experimental runs. The orbital diameter at the bed at incipient motion of the fine-grained sediment under oscillatory flow was used for comparison purposes but was not considered a sole criterion of incipient motion. There were some shortcomings associated with using linear wave theory to calculate the orbital diameter. The orbital diameter was also determined visually by measuring particle movement on the bed. This involved subjective errors. By measuring several times and using average values, these errors are reduced; but better techniques are still needed.

Several investigators, such as Vincent (1958), tried to relate the orbital diameter of incipient motion to wave period. I tried to relate the orbital diameter of a particle in the vicinity of the bed to the wave period. Figure 92 shows Vincent's results for sand particles, with D_{50} ranging from 0.024 cm to 0.063 cm, and my experimental results for fine particles, with D_{50} = 0.00085 cm. Both sets of results show that as wave period increases, the orbital diameter at incipient motion increases. My curve for fine particles has a greater slope than Vincent's curves for sand particles, indicating that for slight increases of wave period, the smaller particles experience larger increases in orbital diameter.

Figure 93 shows wave period versus do^2/D_{50} for the incipient motion conditions of my experimental runs, together with incipient
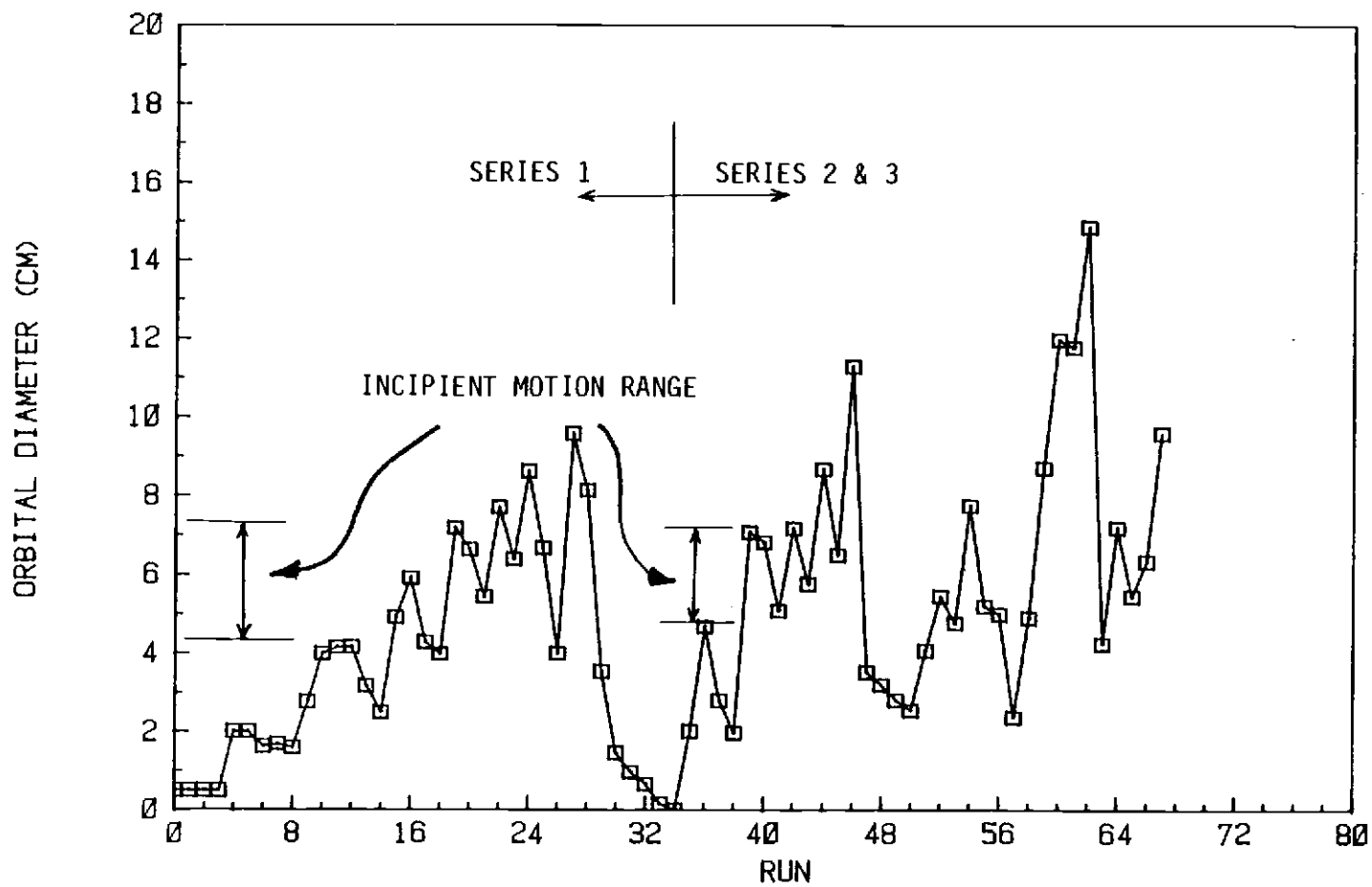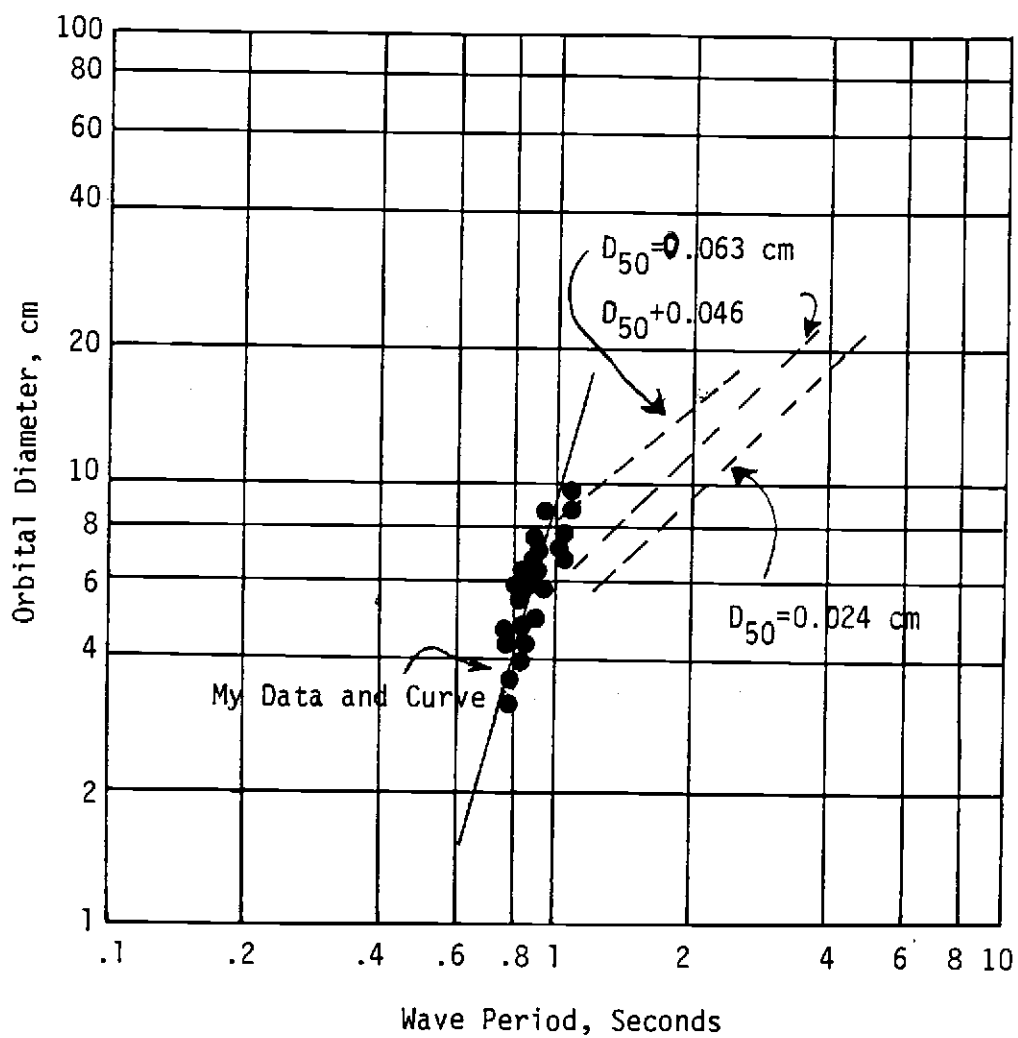
Figure 91. The Orbital Diameter for all Runs

Figure 92.   Orbital Diameter Versus Wave Period for
             Incipient Motion Runs
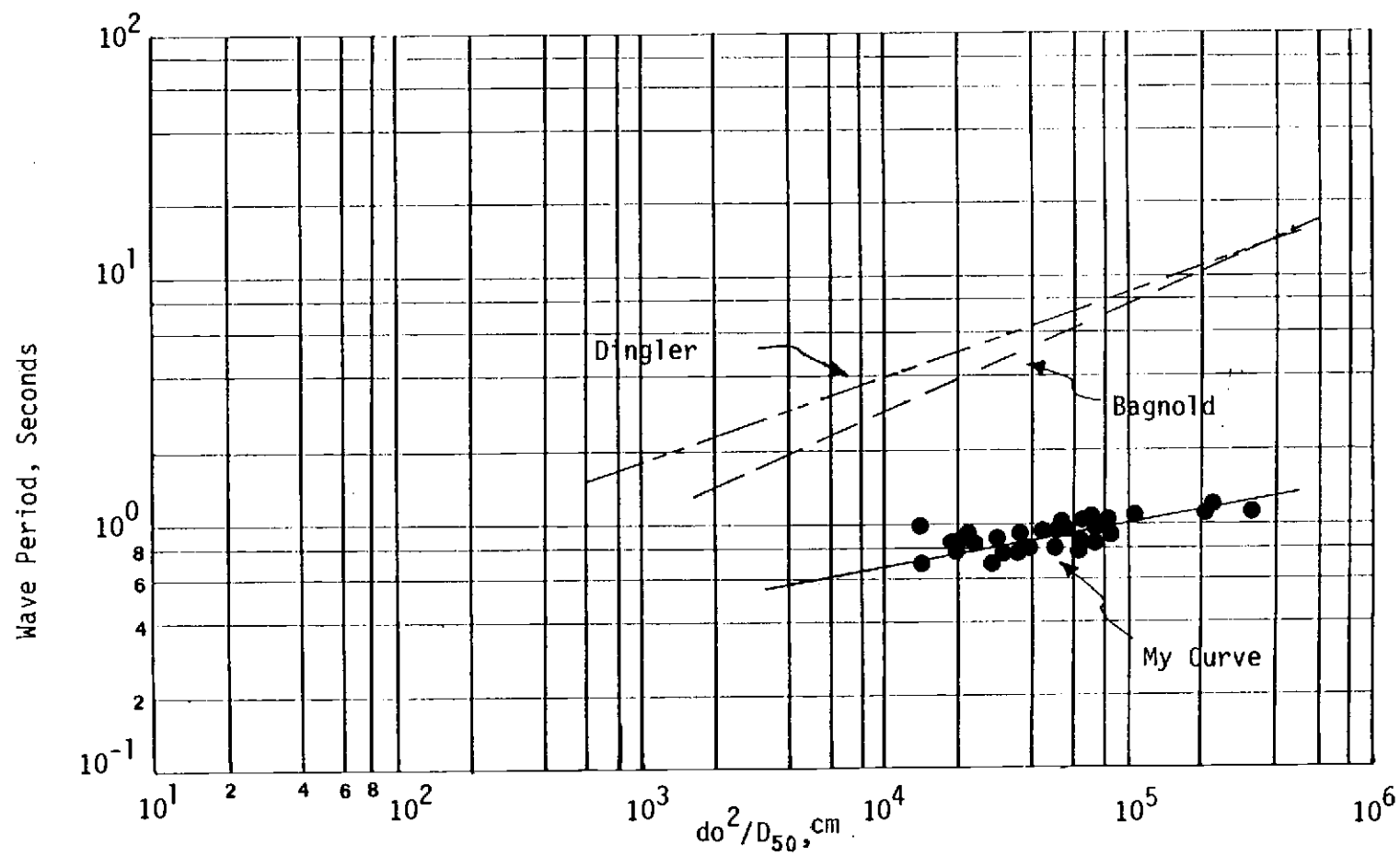
Figure 93. Wave Period Versus do^2/D$_{50}$

motion relations from Dingler and Bagnold. The results show a better
agreement with other investigators than found with wave period and
orbital diameter only (see Figure 92). Therefore, orbital diameter
in conjunction with the wave period could be used as an index for
incipient motion. Again, my data for fine sediment are displaced
from those of others for sand.

Applicability of Published Empirical Formulas for Incipient Motion

A number of researchers studied the incipient motion of sand
particles under wave action. Silvester and Mogridge (1970) put the
empirical formula into a common dimensionless form for incipient
motion of sand particles on a flat bed under oscillatory flow. Those
for laminar flow are shown in Table 27, together with equations by
Komar and Miller (1973) and Chan et al. (1972).

The equations were used to calculate the maximum velocity
required to initiate motion of the laboratory sediment. Table 28
shows the maximum velocity required to initiate motion for each
experimental run, based on the laminar flow equations given by
Bagnold and by Bonnefille and Pernecker. Table 29 shows that the
other equations applied to higher-than-incipient motion.

Comparison of measured maximum velocity at the bed with the
empirically determined threshold maximum velocity at the bed provides
the following results: the formulas of Bagnold and Bonnefille and
Pernecker for sand particles provide good agreement with my incipient
motion velocity criterion. The remaining empirical formulas

Table 27. Selected Empirical Equations for Incipient Motion of Sand Particles Under Oscillatory Flow

Investigators	Flow Conditions	Dimensionless Equation
Bagnold	laminar	$\dfrac{U_{max}}{(s-1)^{2/3} g^{2/3} D^{1/3} D^{0.1} T^{1/3}} = 3.18$
Bonnefille and Pernecker	laminar	$\dfrac{U_{max} \nu^{1/6}}{(s-1)^{5/6} g^{5/6} D^{1/2} T^{1/2}} = 0.072$
Eagleson and Dean	laminar	$\dfrac{U_{max} \nu^{1/2}}{(s-1)\ g\ D\ T^{1/2}} = 0.131$
Manohar	laminar	$\dfrac{U_{max} \nu^{1/3}}{(s-1)^{2/3} g^{2/3} D^{2/3}} = 0.159$
Silvester and Mogridge	flat bed	$\dfrac{U_{max} \nu^{1/18}}{(s-1)^{7/9} g^{7/9} D^{1/3} T^{1/2}} = 0.034$
Rance and Warren	sand	$\dfrac{U_{max}}{(s-1)^{3/5} g^{3/5} D^{2/5} T^{1/5}} = 0.69$
Komar and Miller	---	$\dfrac{U^2_{max}}{(\rho_s - \rho) g D (do/D)^{1/2}} = 0.30$
Chan et al	---	$\dfrac{\tau_Q}{(\rho \mu)^{0.5} (sg-1)^{0.75} D^{0.25}} = 0.37$

Table 28.   Calculated and Measured Maximum Velocities Required to
            Initiate Motion

Run No.	Bagnold Velocity cm/s	Bonnefille & Perneckar Velocity cm/s	Measured Velocity cm/s	Run No.	Bagnold Velocity cm/s	Bonnefille & Perneckar Velocity cm/s	Measured Velocity cm/s
1a	34.18	38.31	2.97	33	16.47	12.81	0.88
1b	26.83	26.65	5.91	34a	18.44	15.18	1.54
2	23.18	21.33	6.38	34b	17.83	14.43	1.13
3	21.07	18.55	8.28	34c	16.14	12.44	0.16
4a	20.27	17.50	8.45	34d	15.58	11.78	0.07
4b	19.84	16.95	8.21	35	22.74	20.79	16.68
5	19.4/	16.48	7.88	36	19.32	16.28	17.52
6	18.77	15.59	6.62	37	18.61	15.39	11.67
7	18.69	15.49	6.98	38	18.10	14.76	8.93
8	18.44	15.18	6.84	39	20.55	17.85	21.96
9	19.09	15.99	10.72	40	20.13	17.32	22.53
10	20.55	17.85	12.40	41	19.01	15.89	19.94
11	20.13	17.32	13.73	42	19.77	16.85	24.99
12	19.55	16.57	15.01	43	19.24	16.19	21.75
13	19.09	15.99	12.31	44	20.06	17.22	28.93
14	18.52	15.28	10.58	45	19.24	16.19	24.58
15	20.88	18.29	14.59	46	20.61	17.94	34.70
16	20.13	17.32	19.56	47	25.80	25.12	5.52
17	19.24	16.19	16.20	48	22.06	19.86	8.01
18	19.17	16.09	15.64	49	19.01	15.89	11.01
19	21.07	18.56	20.69	50	18.44	15.18	10.95
20	20.27	17.50	21.46	51	18.85	15.69	16.37
21	19.4/	16.48	19.87	52	19.01	15.89	21.42
22	20.61	17.94	23.72	53	18.52	15.28	20.20
23	19.77	16.85	22.32	54	19.62	16.67	27.63
24	20.88	18.29	25.54	55	22.80	20.87	11.82
25	19.92	17.04	22.79	56	20.20	17.41	16.34
26	19.32	16.28	14.91	57	18.85	15.69	9.51
27	21.14	18.63	27.33	58	19.47	16.48	17.89
28	20.27	17.50	26.33	59	20.06	17.22	29.05
29	18.93	15.79	14.04	60	21.45	19.05	32.68
30	18.18	14.86	6.49	61	21.14	18.63	33.59
31	17.83	14.43	4.61	62	21.20	18.72	42.03
32	17.46	13.99	3.33				

Table 29. Experimental Data In Comparison to Published Equations

Investigator	Flow Regime	Incipient Motion Runs	Higher Than Incipient Motion
Bagnold	Laminar	16, 19	20 to 25 and 27, 28 39 to 46, 52 to 54 59 to 62
Bonnefille and Pernecker	Laminar	16, 26, 29 36, 58	16, 17, 19 to 25 27, 28, 39 to 46, 52 to 54, 59 to 62
Eagleson and Dean	Laminar	----	all of runs except 1, 33, 34b, c, d
Manohar	Laminar	----	all of runs except 33, 34c, d
Silvester and Mogridge	Flat Bed	----	all of runs except 33, 34c, d
Rance and Warren	----	----	all of runs except 1, 33 34a, b, c, d
Komar and Miller	----	----	all of runs except 1a, 33, 34
Chan et al.	----	----	all of runs except 1, 2 31-34, 47 and 48

do not represent the Incipient motion for fine-grained sediment, possibly due to factors such as: type of material used, type of apparatus, different wave parameters, and subjective nature of incipient motion determination.

Dingler (1979) provided a non-dimensional empirical formula for incipient motion of sand particles 0.0177 to 0.1454 cm in size with wave periods ranging from 2 to 20 seconds under oscillatory flow. Dingler's equation (equation 62) was used for my experimental data. Figure 94 shows the results for my incipient motion data, together with the Bagnold and Dingler relations. My data closely parallel but are displaced from the Bagnold and Dingler lines because of the use of fine-grained sediment instead of sand particles.

Shield Criterion For Incipient Motion

The threshold at which sediment particles are disturbed and set in motion can be subjectively observed visually or defined by the critical shear stress exerted by the fluid flow on the bed surface. Following the work of Shields (1936) under unidirectional flow, the incipient motion criterion is defined as the ratio of the critical shear stress to the immersed weight of the topmost grain layer of the bed. This has the nature of a generalized friction coefficient which takes into account both grain size and grain density for cohesionless bed grains under unidirectional flow. This relation was given as equation 12.
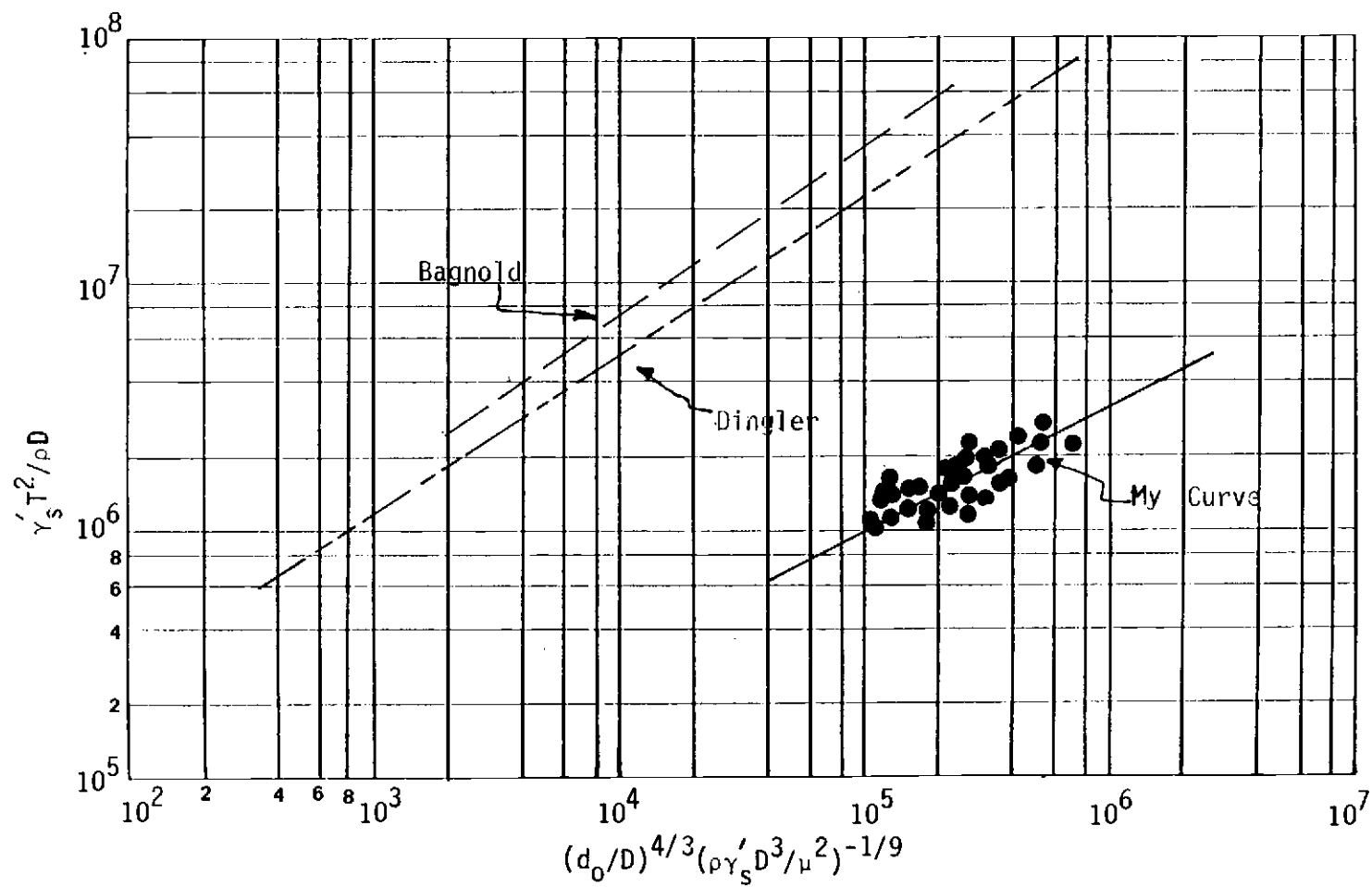
Figure 94. $\gamma_s'T^2/\rho D$ Versus $(d_0/D)^{4/3}(\rho\gamma_s'D^3/\mu^2)^{-1/9}$

The Shields criterion has been used extensively in the study of incipient motion of non-cohesive sediment in undirectional flow. Recently, many investigators such as Komar and Miller (1973, 1975), Madsen and Grant (1975) and Dingler (1979) used the Shields criterion for non-cohesive sediment under oscillatory flow and concluded that the Shields function, with all of its shortcomings, may serve as a relatively reliable and quite general criterion for the threshold of sediment movement under oscillatory flow.

I attempted to use the same Shields criterion for fine-grained sediment under oscillatory flow. Figure 95 shows the Shields curve in the form given by Bagnold (1963). One curve is given for a flat bed, another curve applies to a rippled bed, crosses represent Dyer's data for fine sand on the sea floor, and the range of my experimental data is given. The results show that the Dyer field data are about one order of magnitude higher than the Bagnold laboratory curves. My data are similarly displaced from Bagnold's curves. The reason lies in the cohesion strength of fine-grained sediment, which requires higher shear stress for incipient motion than does cohesionless material.

My shear stress data for incipient motion were also plotted on the graph developed by Miller et al. (1977) from published data of threshold shear stress versus grain size diameter. The range of my data is shown in Figure 96. Dyer's (1980) fine-sand incipient motion data range is also added to the graph for comparison with my laboratory experimental results of fine sediment. The results indicate that the critical shear stress for incipient motion for
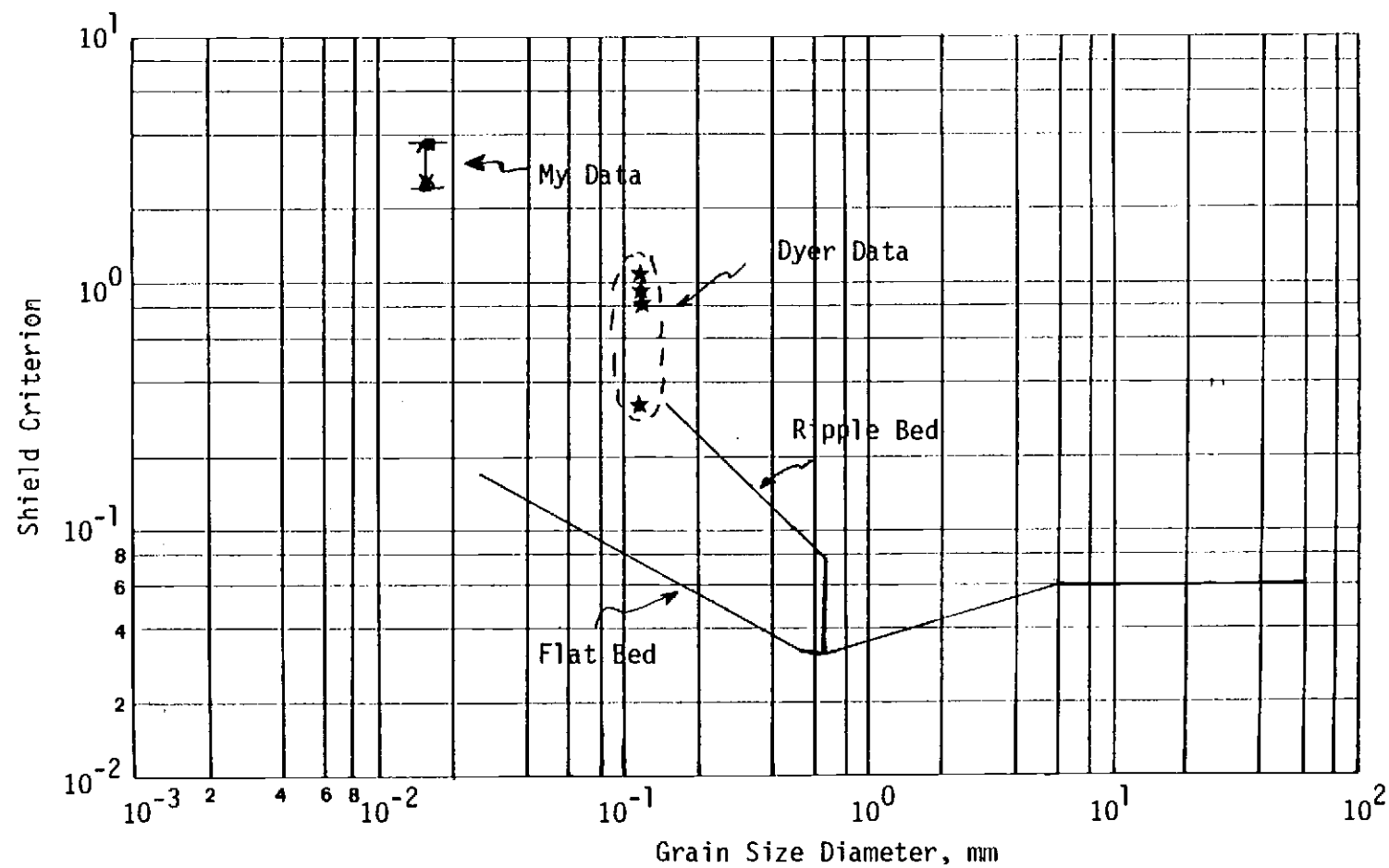
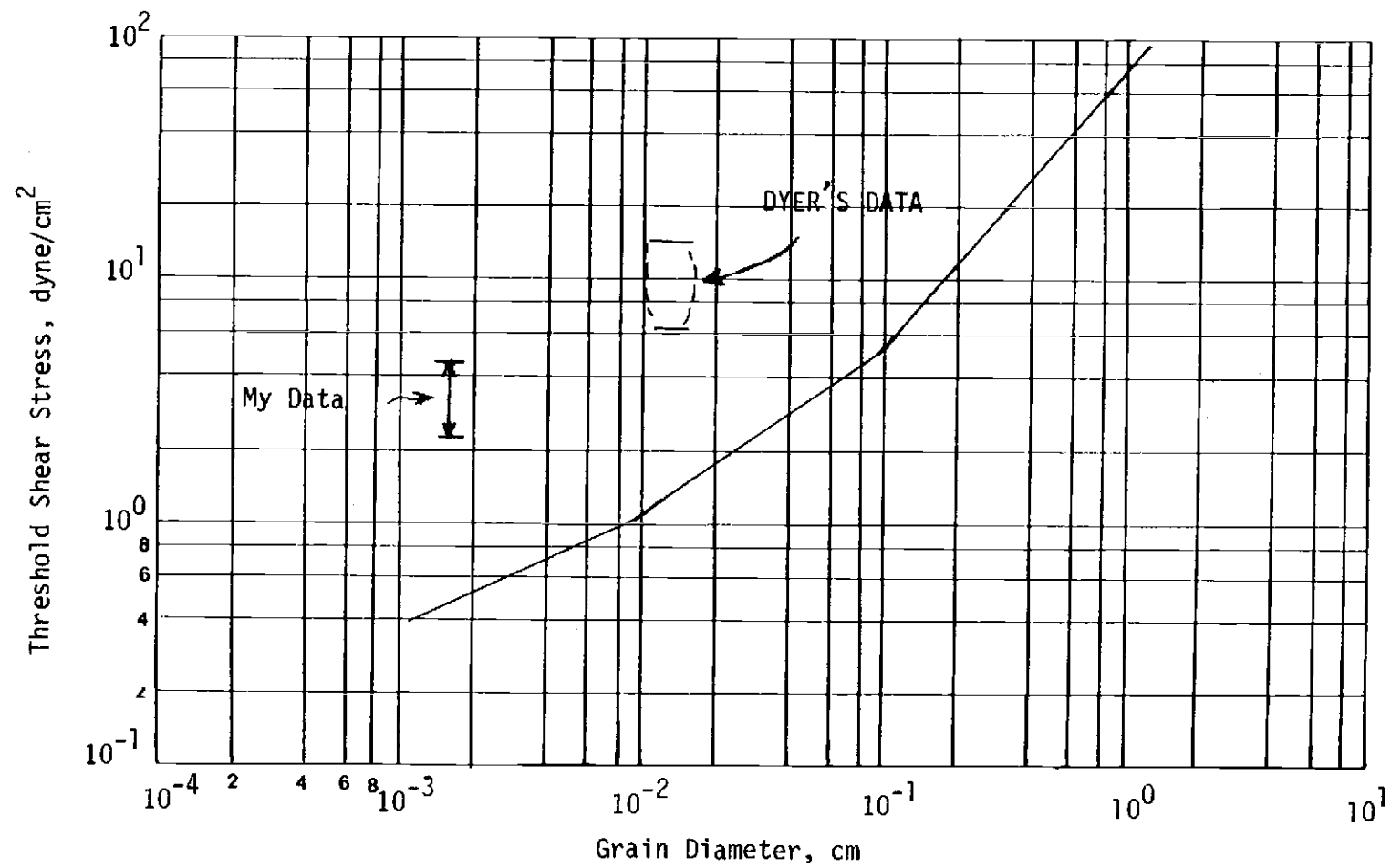Figure 95. Shields Criterion Versus Grain Size Diameter

Figure 96.   Threshold Shear Stress Versus Grain Diameter

Dyer's fine sand and my experimental data are both one order of magnitude higher than the published threshold curve. My data did not differ from Dyer's data in departure from the Miller curve as much as was the case with Shields curve (Figure 96). Therefore, for better comparison, the incipient motion conditions were plotted on a variation of the Shields curve given by Miller et al. (1977), which is shown in Figure 97. Two straight lines on Figure 97 are shown, based on the data of Bagnold (1946) and Manohar (1955) for sand particles. My data are one order of magnitude higher than the others. This is because the effect of fine cohesive particles already mentioned.

Effect of Bed Roughness on Incipient Motion

Results of the first and second categories of experimental runs showed that particles from the rough bed surface went into suspension at lower maximum velocities and shear stresses than those from the smooth bed surface. This is mainly due to the shearing force of the water near the boundary layer. The height of the viscous sublayer that developed at the rough bed was less than the height of the dunes and ripples in the rough bed surface. The imposed shear force was in close contact with the sediment surface and started to erode the particles from the layer below the top skin layer. The maximum calculated boundary layer thickness at incipient motion was 0.062 cm, which is less than the dune height.
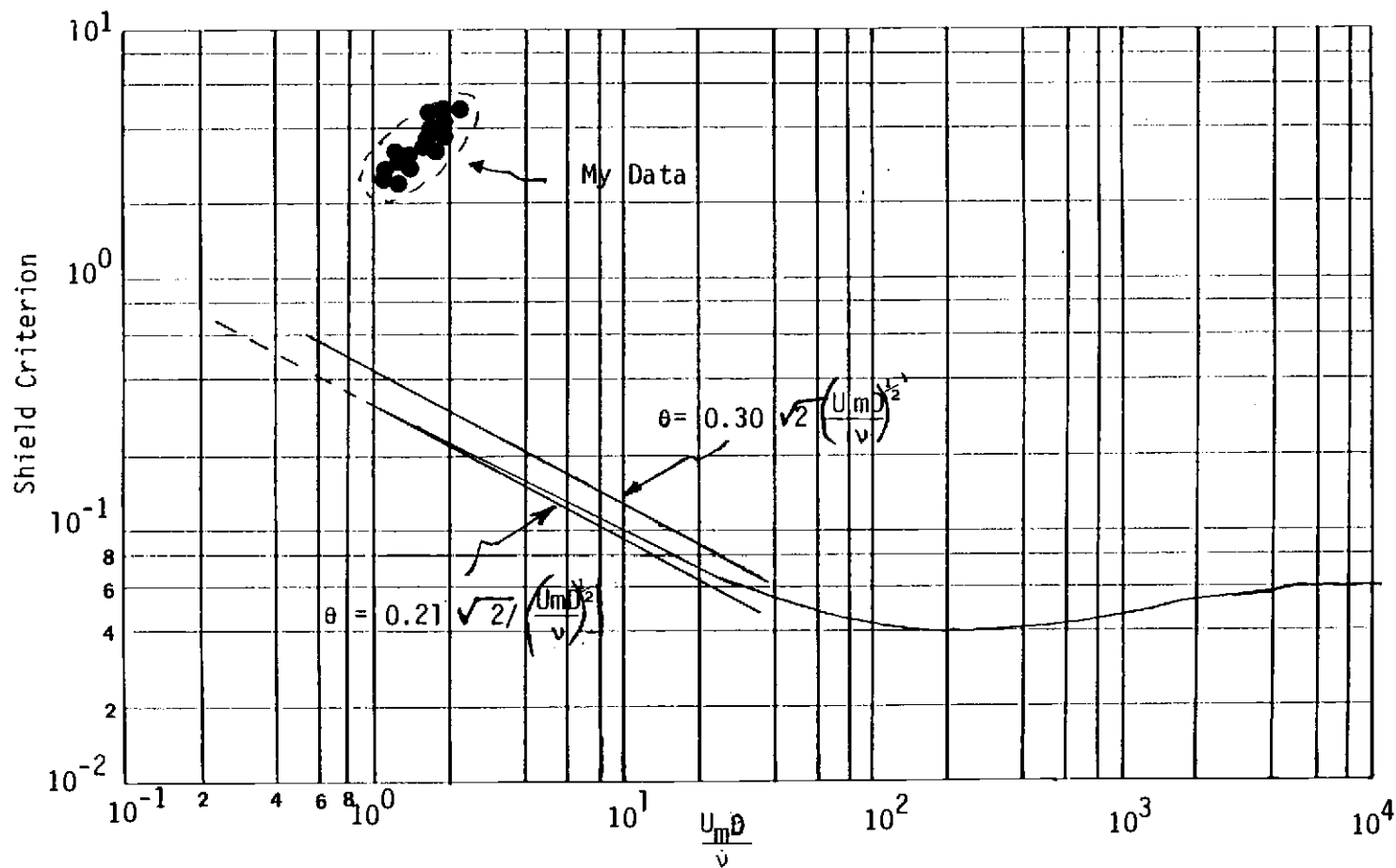
Figure 97. Shields Criterion Versus $\dfrac{U_m D}{\nu}$

The fine sediment particles are believed to have been subject to incipient motion at lower maximum velocity and shear stress for the rough bed than for the smooth bed. This is because of the formation of eddies, turbulence and secondary forces at the boundary layer of the rough bed. The eddies that developed on the rough bed added to the flow strength to cause incipient motion at lower fluid force than required to bring incipient motion on a smooth surface.

Effect of Consolidation on Incipient Motion

I was unable to measure the shear strength of the sediment bed by standard techniques. Instead, I assumed that the natural densification or compaction of the sediment bed with time increased the shear strength of the bed. The incipient motion of the recently deposited sediment bed (10 days old) was compared to that for a more recently compacted bed (91 days old).

Many investigators of incipient motion of fine-grained sediment found that cohesive sediment shear stress, not shear strength of the sediment bed, is the dominant factor. Prthenaides (1962, 1977) concluded that the erosion of fine cohesive sediment by action of water is independent of the shear strength. Kandiah (1974) found that interparticle cohesion is a primary factor in determining the resistance to erosion of clay soils. He indicated that the cation exchange capacity is related to te interparticle cohesion and is a basic parameter governing the erodibility of a clay soil. Metha (1973) also used shear stress, not shear strength, as the most important variable in his depositional study of fine cohesive

sediment.

It was found from my experiments that the incipient motion of the fine-grained sediment is independent of shear strength of the bed. In other words, the recently deposited sediment bed has the same resistance to the shearing action of water due to waves as the more compacted sediment bed.

The following observations provides supporting evidence for this conclusion. In the first set of runs, for the recently deposited sediment, the range of maximum velocity for the incipient motion of the smooth bed was 13.7 to 21.5 cm/s and the range of maximum shear stress was 3.67 to 5.53 dyne/cm^2. In the second set of runs, for an older deposit age, the range of maximum velocity for the incipient motion of smooth bed was 20.0 to 25.0 cm/sec and the range of maximum shear stress was 5.39 to 6.00 dyne/cm^2. The differences, although consistent, may be due to the subjective nature of determination of incipient motion. Suspended sediment concentration data for the two sets of runs showed that more sediment particles went into suspension with the older, more compaced sediment bed and is relatable to the consistenly higher stress and velocity just mentioned.

Logically, it seems that the more compacted the sediment bed, the more resistance there should be to the shearing force of the water. But this may not be the case for fine-grained sediment. Beside the above supportive evidence, the mechanism of fine cohsieve sediment erosion must be considered. The fine-grained sediment was eroded layer by layer (surface erosion). The compaction and consequent

increase In density of the sediment did not significantly increase
the resistance of the skin layer. The skin layer thickness is on the
order of a few millimeters. Other factors, such as cohesion, organic
matter, type of clay, and chemical characteristics of water and
sediment, are the influencing parameters. The weakest bond of the
bed surface determines when the particles go into motion.
Consolidation and density changes would not seem to influence the
particle bonding at the water-sediment interface.

Bed Patterns

The most striking phenomenon of the bed erosion pattern was the
persistent peeling off of the bonded particles from the top skin
layer. The peeling off of the skin layer was distributed uniformly
all over the bed surface (rough bed and smooth surface). An average
bed erosion of 5.6 millimeters occurred from the surface of the bed.
The top skin layer formation was due to the cementing of clay and
silt particles with dust from the laboratory environment and iron
oxides from within the sediment bed. The peeling off started when
the maximum shear stress at the bed was able to break this bond in
the weakest plane. That is why the individual or bonded particles
started to peel off from the rough bed first and then from places
with fine irregularities in the bed surface. Local turbulence and
eddies at the irregularities in the bed surface caused the incipient
motion to occur at a lower shear stress than would normally be
required.

The short deep scour streaks in the rough bed were a result of the structure and intensity of turbulence and the shear stress at the bed. In comparison, the long scour streaks in the smooth plane surface developed primarily as a result of shear stresses due to weaker local turbulence. The bonded particles, upon becoming detached in the rough bed field, moved back and forth over a long period of time and caused further abrasion and eddies, resulting in deeper scour streaks.

The distinct colors of the surface and exposed layers of the sediment bed were an indication of iron and manganese oxide (see Chapter III) as cementing agents in the top skin layer.

Combined Effect of Oscillatory and Unidirectional Flows on Incipient Motion

Comparison of Effects

Due to a lack of appropriate facilities for testing the combined effects of oscillatory and unidirectional flow on incipient motion of fine-grained sediment, the analyses of this combined effect relied on the results of the independent studies of incipient motion in oscillatory flow and unidirectional flow. The results were compared and integrated with my research on the separate flow to understand what is happening in the case of combined flow.

Table 30 shows the conditions for incipient motion of fine-grained sediments under the separate oscillatory and

Table 30. Conditions for Incipient Motion of Fine-Grained Sediment
Under Oscillatory and Unidirectional Flow

Parameter	Oscillatory Flow		Unidirectional Flow	
	Smooth	Rough	Smooth	Dune
Velocity for Incipient Motion* cm/sec	13.7 to 21.5	5.9 to 8.5	45.8 to 52.1	46.5 to 51.6
Bed Shear Stress for Incipient Motion dyne/cm	3.70 to 5.53	2.0 to 2.2	5.1 to 6.1	6.0 to 6.4
Suspended Sediment Concentration Near the Bed mg/L	up to 18	5.1 to 7.4	up to 30	49

*Maximum value at boundary layer is given for oscillatory flow;
mean value in flume is given for unidirectional flow.

unidirectional flows in terms of velocity, shear stress, and the suspended sediment concentration. The results show that for a given sediment bed (the same material and the same bed preparation) a lower velocity was required to initiate erosion in the oscillatory flow than in the unidirectional flow. However, the velocity locations with respect to the bed differed for the two flow cases. Current meter velocity measurements were made at the bed in unidirectional flow a few times for each run and gave velocities comparable to the mean velocity in the flume. Therefore, use of the mean value is considered acceptable here, as it gives a more reliable average than the point measurements. The shear stress data also show a similar trend, but not as markedly as do the velocity data.

The difference in shear stress and velocity for the two different flows can be explained as follows:

> Flow near the bed is laminar in the oscillatory case, while the flow near the bed in the unidirectional case is turbulent. The viscous forces are the dominant forces in both cases, but the effects of possible pressure differences and mass-transport currents must be considered in the oscillatory flow. Velocity at the bed is orbital in the oscillatory flow and is affected by mass-transport velocity.

Figure 98 shows the suspended sediment concentration versus critical shear stress at the bed for incipient motion conditions under unidirectional and oscillatory flows. The results show that at a given shear stress, larger suspended sedient concentrations are associated with unidirectional flow than with oscillatory flow.
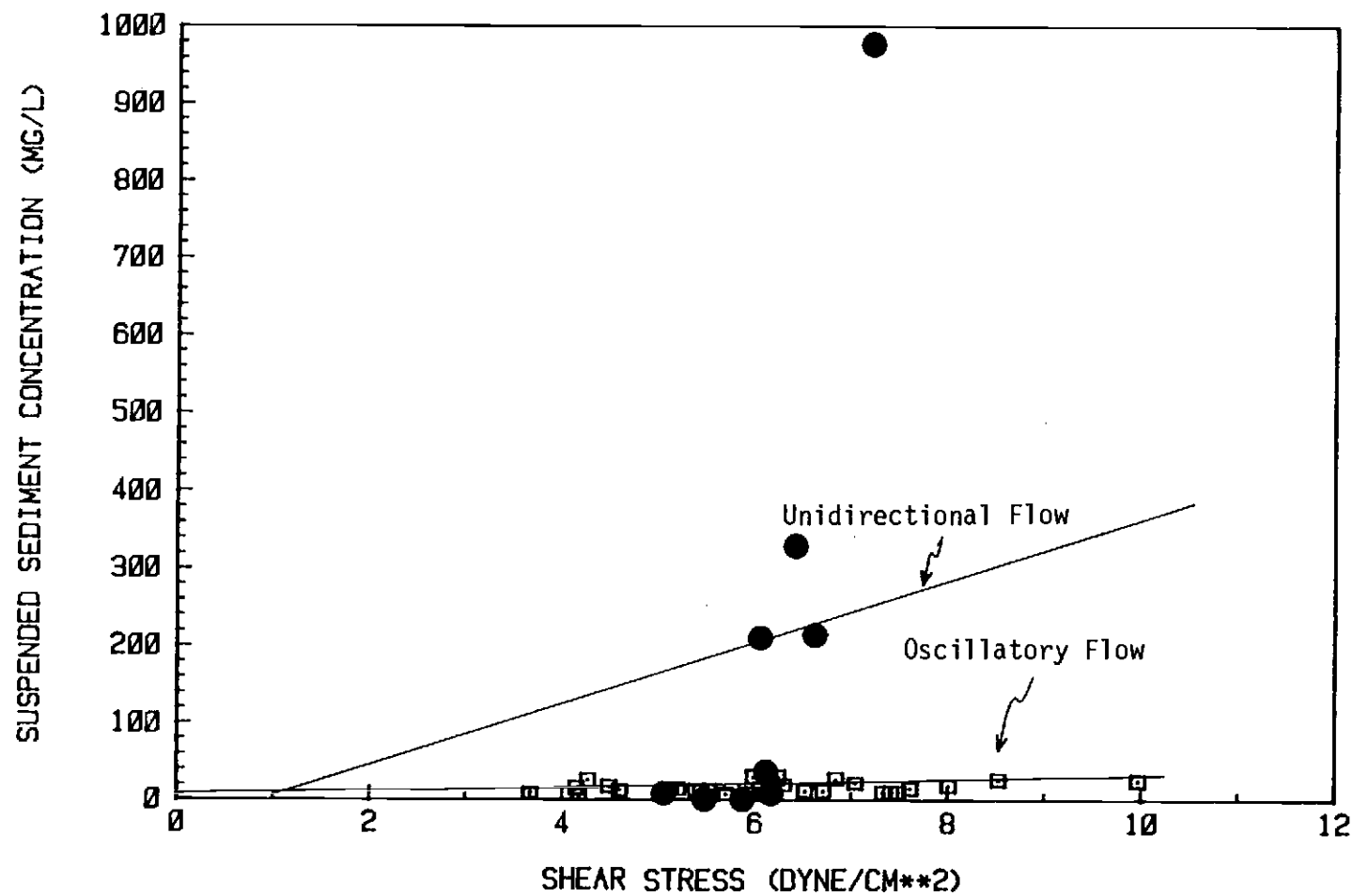
Figure 98. Suspended Sediment Concentration Versus Shear Stress for Incipient Motion, Comparing Oscillatory and Unidirectional Flows

Also, the changes of suspended sediment concentration over the range of incipient motion show that higher suspended sediment concentrations are associated with unidirectional flow. Under the oscillatory flow, most of the eroded material traveled back and forth and was gradually transported downstream at the bed; some of the eroded material went into suspension with a circular motion and traveled upstream to the waveboard. Under unidirectional flow, the sediment particles eroded at higher velocities and shear stresses, went into motion faster, and were soon transported downstream. The higher suspended sediment concentrations under the unidirectional flow were due to more suspension of sediment occurring in irregular-shaped zones at the upstream end of the test section.

The hypothesis regarding linear summation of the incipient motion of unidirectional flow and oscillatory flow for the combined flows was rejected at the early stage of literature review and laboratory experimentation. The boundary layer flow varies depending on the wave parameters under oscillatory flow. Turbulent structure at the boundary layer under unidirectional flow will be dominant. It is not known whether the superposition of the oscillatory flow on the unidirectional flow aids the spread of the turbulent boundary layer or inhibits it or if the behavior of the system depends on which type of flow is generated first. Therefore, due to the complex situation under the combined flows, linear summation of the results of individual flows is not recommended and does not give good results.

The revised hypothesis was that from consistent measurements of the separate effects of unidirectional flow and oscillatory flow on the incipient motion of fine cohesive sediment bed, it is possible to estimate the effects of combined unidirectional and oscillatory flows on the incipient motion of such cohesive sediment.

Through detailed analysis of velocity, shear stress, and suspended sediment concentration for incipient motion under separate flows, it was found that lower velocity and shear stress for incipient motion was associated with oscillatory flow. Then the results were compared with limited published results for sand particles and found to be in good agreement.

Expected Combined Effects

The following statements can be made about the incipient motion behavior of fine sediment under combined oscillatory and unidirectional flow:

1. Incipient motion of fine sediment occurr at lower velocities and shear stresses with oscillatory flow than with the unidirectional flow. Therefore, oscillatory flow is expected to be responsible for the incipient motion of the sediment bed subject to combined flows. Unidirectional flow is expected to then carry the suspended sediment in a downstream direction.

2. The flow conditions under unidirectional flow for all of the experimental runs were fully turbulent but under oscillatory flow most of the experimental runs had laminar flow

conditions and some were in the transition from laminar
to smooth turbulent flow. It is speculated that the flow
will be turbulent in superimposing unidirectional flow
on oscillatory flow.

3. The turbulence structure near the bed from unidirectional
    flow is expected to dominate when oscillatory flow is
    superimposed, as long as the waves do not break.

4. Incipient motion of fine-grained sediment under oscillatory
    flow, when unidirectional flow is superimposed, is expected
    to occur at lower shear stresses than without the
    unidirectional flow.

5. Under a combined effect, oscillatory flow is expected to be
    more responsible for removing and peeling off the sediment
    and unidirectional flow for bringing the sediment into
    suspension.

6. The turbulence intensities at the bed under the combined
    oscillatory and unidirectional flow are expected to be higher
    than for either flow alone. Thus, a greater number of
    particles will go into suspension.

7. The net shear stress at the bed under the combined
    oscillatory and unidirectional flow is expected to be
    almost the same magnitude as for waves alone, but the
    vortex-dominated layer will extend above the bed and
    the only means of particle suspension will be a weak
    wave-induced vortex layer (see Tunstall and Inman, 1975).

8. More suspended particles are expected to be transported downstream for a given time interval than before.

9. The net velocity near the bed for combined oscillatory and unidirectional flow is expected to be in the same direction as the wave propagation direction for flow producing incipient motion. This should be analyzed in the future, for wave and current in the same direction as well as in the opposite direction.

A Model for the Mechanism of Incipient Motion of Fine-Grained Sediment

The Occurence of Incipient Motion

The sediment particles must be detached from the bed surface before they can be carried back and forth at the bed. The threshold condition of incipient motion of sediment particles at the bed is very important to understand. A model for the mechanism of incipient motion of fine-grained sediment under oscillatory flow is developed here which explains the observed phenomena and possibly the relationship between the shear stress and the wave parameters at incipent motion.

The shearing force acting on the bed surface due to waves and unidirectional flow is responsible for removing individual or bonded particles from the bed surface. For a hydraulically smooth bed, the particles are completely immersed within the laminar sublayer and the forces acting on them are due to viscous stresses.

Incipient motion for fine-grained sediment is defined as the

conditions which the individual or bonded particles on the bed surface begin to move. The initial movement of sediment particles is started by the peeling off of the top skin layer of bonded particles, leaving pit marks on the bed surface which develop into streak lines. Suspension of sediment is a part of this incipient motion process.

Factors Controlling the Incipient Motion

Surface Layer Cohesion

Particles in the sediment matrix can be formed in several different ways, such as:

1) silt with silt system
2) silt with sand system
3) silt with clay system
4) silt with sand and clay
5) silt with a lot of clay
6) silt with organic matter
7) silt with sand and organic matter
8) silt with clay and organic matter
9) silt with clay and sand and organic matter
10) silt with a lot of clay and organic matter
11) clay with sand system
12) clay with clay system
13) sand with sand system.

Figure 99 shows these possibilities for sediment matrix formation. In cases 3, 4 and 11, if enough clay particles fill the spaces
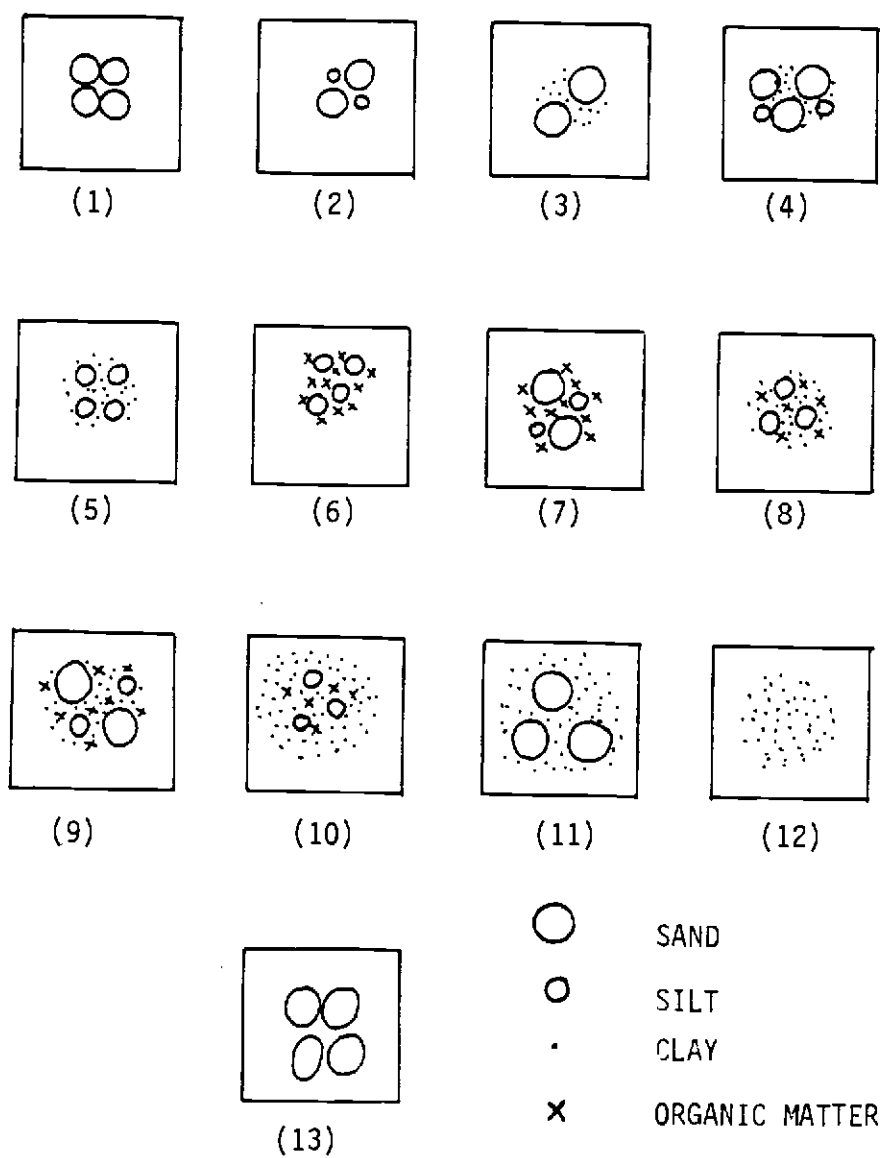
Figure 99. Sediment Matrix Formation Possibilities

between the silt and sand particles, the clay acts as a cementing agent. This situation represents the cohesive sediment matrix case. I call this a cohesive system. If insufficient clay material is available to fill the spaces between the silt and sand particles and, thus, to act as a cementing agent, a situation like cases 1 and 2 is represented. I call this as a non-cohesive system. Case 13 is also non-cohesive. Cases like 5 or 12 represent more than enough clay (for a cohesive system) in the sediment matrix system. I call this a clay system. The rest of the cases deal with interactions of particles with organic matter. It is evident that organic matter with cohesive sediment adds more cohesion to the system. The effect of organic matter on a non-cohesive sediment, whether it gives some cohesion to the particles or acts in a neutral manner, is beyond the scope of this research.

The Sturgeon Lake sediment contains approximately 80 percent silt with 18 percent clay and a trace of fine sand. With a liquid limit of 55 percent and plasticity index of 15 percent, based on standard techniques, the sediment is classified as cohesive sediment. X-ray diffraction analysis showed that illite was the dominant type of clay.

The sediment also includes organic matter and iron. Organic matter exists in many forms, ranging from plant roots and organisms to decomposed organic residues. The organic content of sediment was above five percent which is indicative of a high percentage of

organic in the sediment.

The well-mixed sediment particles were settled in the flume under quiescent water conditions. The mode of deposition and time history of sediment bed formation have some effects on the resisting behavior of the sediment bed. In prototype situations, the suspended sediment particles experience deposition and resuspension under various shear flow conditions.

Many field studies on erosion control have demonstrated that sediment with organic matter resists erosion more effectively than sediment without organic matter. The organic matter forms bonds with the surface of two or more clay particles or stabilizes the sediment bed against water entry by the presence of hydrophobic organic material, such as fats and waxes. Therefore, organic matter adds cohesive strength to the sediment bed, but the extent of this addition depends upon how much organic matter is involved with what type of sediment (clay content, gradation). These are questions on which future research can shed some light.

In a cohesive system, silt-clay or silt-clay-sand bonding takes place and gives more cohesive strength than the clay-clay bond in a clay system. The surface layer of the bed in the flume was probably formed by a combination of silt-clay-silt, silt-clay-sand, clay-clay, and silt-silt. Organic matter probably attached to all of the above bondings. Besides organic matter, dust and other impurities were attached to the sediment particles. This attachment of organic and other matter to sediment particles formed a skin layer. The skin

layer had 13 percent organic matter compared to 5 percent of organic matter in the sediment bed. The high amount of organic matter in the skin layer gave bonding characteristics to the sediment particles.

The effect of iron oxide in strengthening the skin layer was not studied in the laboratory, but from the literature it is evident that sediment with a high quantity of iron contributes to an increase in the bonding strength of the sediment particles. Even though the iron concentration in the skin layer was not determined, the overall sediment mixture contains 22.8 mg/gram of iron. Iron could oxidize to iron oxides, which in turn increase the resistance of the bed to erosion. This can be accomplished by bonding the clay particles in the bed itself. To determine quantitatively the effect of iron oxide on bonding of sediment particles and the degree of increasing or decreasing cohesion, controlled laboratory tests and chemical analysis of the sediment and water are essential.

Breaking of Bonds and Incipient Motion

Incipient motion was defined as the condition when the maximum shear stress acting at the bed caused the bonded particles to start to peel off, leaving many pit marks which led to streak formation. Suspension of the removed particles from the bed took place in many situations simultaneously with the peeling off of the skin layer.

The incipient motion of this top skin layer started when the induced shearing force of a wave exceeded the cohesion or bonding strength of the skin layer of the bed surface particles. That is why the bonded particles (which are a matrix involving some combination

of silt, clay, sand and organic matter) start to peel off at places with the weakest bonds. The weakest bonds probably included silt-silt with organic matter, silt-clay systems (clay structures bonded to silt), or clay-clay system bonds.

The peeling off of the skin continued to progress as long as the induced shear force was not reduced below the bonding strength of the sediment layer. The erosion of an exposed layer began promptly after peeling off of the top skin layer. This erosion of an exposed layer started with the removal of individual particles, with no evidence of a skin formation. As time progressed, the skin was reestablished due to overnight settling of suspended impurities, sediment extractions from benthic worms or bugs, and oxidation of iron at the sediment bed surface.

Another possible explanation for why the skin layer would peel off at some places on the bed surface may be that the movement of eroding fluid into the soil pores at non-bonded (non-cemented) places, these being the weakest possible places, caused weakening of the interparticle bonding.

With the aid of the Parthenlades (1962) mechanism of erosion of clay particles, another facet of the mechanism of particle removal from the bed can be explained. At the bed surface, the edges of each particle will be attached to the surface irregularities of some other particles. Therefore, a joint will be formed which will be possibly wrapped in a thin layer of highly viscous absorbed water. The two particles could have two possible conditions; either in contact or

separated by a few water molecules. If the clay particle is attached
to only one other particle but is free to move, then a movement could
break the joint. Such particles will be removed from the bed surface
by shear forces. If a particle is instead bonded at more than one
point, the failure could take place by bending stresses at some
weakest plane of the particle itself, rather than at a joint.

A dispersive agent was added to the water to disperse the
sediment particles at the bed surface to their original sizes by
breaking down the aggregations of clay-to-clay, clay-to-silt,
clay-to-sand, and clay-to-organic matter particles to individual clay
or silt particles. This broke down the cohesion between surface
particles, which then went into suspension at lower velocities and
shear stresses than required for deposited sediment without a
dispersive agent. The suspended sediment concentrations associated
with this run were the highest recorded concentrations among all
runs. Moreover, the maximum values of velocity and shear stress
responsible for this incipient motion of the smooth bed surface with
dispersent added were 7.9 cm/sec and 2.1 dyne/cm^2, respectively, well
below those for recently deposited or compacted sediment beds.

Effects of Bed Consolidation on Incipient Motion

Sediment compaction with time, due to natural densification,
increases the shear strength of the sediment bed. The particles are
in closer contact to each other.

The resultant effect at the bed surface is of greater interest
with respect to incipient motion. The following situations could

take place there as a result of bed consolidation:

1st. A surface skin forms as time progresses;

2nd. Water is pushed out of the underlying sediment bed through the weakest plane of bonded surface particles (joints, particles itself) or at the edge of the sediment bed;

3rd. Upon removal of most of the water from the bed,

    a) the particles may be in contact without water molecule separation, or

    b) the surface skin may be more cohesive than before due to stronger bonding, or

    c) there is no change in surface skin cohesiveness.

Figure 100 shows the original sediment matrix and that which results when water is pushed out of the bed. Condition (c) prevails based on laboratory experiments, because no major changes took place in the top skin layer.

During consolidation processes, the clay particles and their assciated cloud of hydrated irons tend to rearrange themselves to a configuration having the lowest energy (Krone, 1962). This configuration reduces interparticle spacing and increases the fraction of interparticle water that is influenced by the particles. Therefore, water has an active part in determining the structural character of consolidated sediment.

The fine material in the sediment matrix also has an active role in the structure of consolidated sediment. The experimental results of washing away fine particles from the sediment matrix showed that
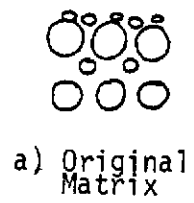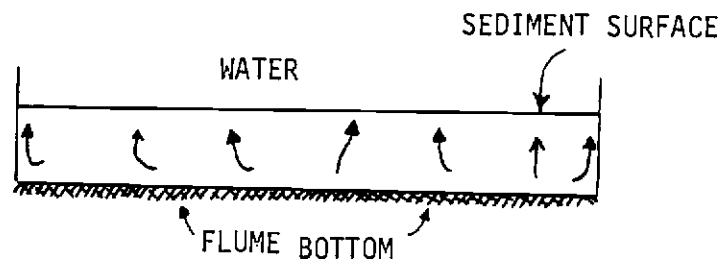
Figure 100.   Sediment Matrix due to Densification

sediment particles consolidate at a higher rate without the fine particles present.

The experimental results showed that the shear strength of the bed surface skin layer do not change with compaction of the sediment bed. The mechanism of failure of skin layer, already discussed, is a surface phenomenon. The behavior of a sediment bed in a flowing body of water was shown to depend strongly on the shear applied by the flow to the bed. Therefore, the incipient motion, at least for the top skin layer, is independent of shear strength of the sediment bed.

The results showed that as long as the induced shear stress is above the bonding strength of the top skin layer, the peeling off of the bonded particles will continue. The newly exposed layer, when the top skin layer is removed, breaks in individual particles. As time prgresses (e.g., overnight) a new skin layer will be formed.

Sediment below the top layer is initially dense and compacted. But, as the top layer is removed, the exposed sediment is again in contact with water molecules; therefore, water molecules can then enter the bonded particles through joints and decrease their cohesiveness. As the new skin layer is formed, the mechanism of failure will be the same as for the previous skin layer.

VII. SUMMARY AND CONCLUSIONS

General

Sediment transport processes can be affected by a combination of wind-induced oscillatory flow and runoff- or tide-induced unidirectional flow. Theoretical understanding of boundary layer flow when the two flow conditions are superimposed is still in the developing stages. Therefore, the best available alternative to understanding the processes of incipient motion of fine-grained sediment at this time is the application of results from laboratory and field studies of unidirectional and oscillatory flows.

In a turbulent flow field, such as Sturgeon Lake, the incipient motion of fine-grained sediment depends on the flow variables as well as on the physicochemical properties of the deposited sediment. Using a given type of fine sediment (Sturgeon Lake sediment) with filtered river water, the physicochemical properties of the sediment can be kept constant, so that the incipient motion of the sediment can be related to flow variables. Thus, the complex hydrodynamic interaction of tide-induced unidirectional flow and wind-wave induced oscillatory flow can be studied under controlled sediment conditions.

Field study and observation of sediment and water characteristics, as well as the hydrodynamic characteristics of the Sturgeon Lake. revealed the relevant processes involved. It was then possible to simulate these processes in the laboratory. This permitted testing of research hypotheses applicable to the research objectives.

The laboratory experiments were performed in bench-type settling columns, to determine the consolidation and density changes of sediment, and in recirculating and wave flumes, to simulate the tide-induced unidirectional and wind-wave induced oscillatory flows, respectively. Due to the lack of special equipment, the superposition of oscillatory flow on unidirectional flow was not experimentally feasible. However, the combined effect could be evaluated by inference from the results for separate flows.

Validity of Research Hypotheses

First Hypothesis

The first research hypothesis was that the incipient motion of silt-clay sediment under oscillatory flow can be determined and described in a manner similar to that used for unidirectional flow.

In oscillatory flow, the peak velocities on the bed surface will act only for a very short time and the boundary layer is not as well developed as for unidirectional flow. The boundary layer varies depending on the ratio of water depth to wave parameters. In spite of these added difficulties, it was possible to define and quantify the incipient motion characteristics of fine-grained sediment in terms of flow parameters for oscillatory flow in a manner analogous to unidirectional flow. It was found that for fine cohesive sediment particles, the principles governing the incipient motion under unidirectional flow were applicable for oscillatory flow. Even though the water motion near the bed at the boundary layer was oscillatory, the incipient motion of the sediment could be related to

critical shear stress and critical maximum velocity at the bed in the
same way as for unidirectional flow. The laboratory results were
compared wih established curves of past investigators and found to be
in good agreement for the range of flow and sediment conditions
studied.

Second Hypothesis

It was initially hypothesized that the combined effects of
unidirectional flow and oscillatory flow were additive and could be
treated by linearly summing the separate effects. After the review
of literature, and while the flume studies of separate flows
progressed, however, it became evident that linear summation was not
appropriate and that a more fundamental hypothesis was needed. It
also became clear that the available laboratory apparatus would limit
certain aspects of experimentation.

The second research hypothesis, thus, was that from consistent
measurements of the separate effects of unidirectional flow and
oscillatory flow on the incipient motion of a silt-clay sediment bed,
it is possible to reasonably estimate the effects of combined
unidirectional and oscillatory flows on the incipient motion of such
cohesive sediment.

The laboratory flume results of incipient motion of fine-grained
sediment under the separate effects of unidirectional flow and
oscillatory flow were analyzed and tested against a limited available
literature regarding sand particles. It was found that the boundary
layer oscillatory flow tends to remain laminar at velocities which,

In unidirectional flow, are turbulent. The combined boundary layer
flow for the two flow conditions can not be linearly summed and would
be complex. Nevertheless, consistent measurements of the separate
effects of unidirectional flow and oscillatory flow on the incipient
motion of a fine-grained sediment bed, showed that the effects of
combined unidirectional and oscillatory flows on the incipient motion
of such cohesive sediment could be estimated. How this estimate can
be made is summarized in the following section in this chapter.

<div align="center">Incipient Sediment Transport Processes</div>

General Features of Incipient Motion

It is found that the action of flowing water causes the initial
movement of sediment to take place layer by layer (surface erosion).
The movement of sediment takes place in a boundary layer that is
developed at the sediment-water interface from the effects of
viscosity of the fluid. The initial motion of sediment occurs in a
laminar sublayer and is caused by turbulent shear exerted by the
flow.

The importance of surface erosion (skin erosion) of cohesive
sediment under the action of flow indicates that a more detailed
exploration of the chemistry of the bonding particles in the surface
layer (skin layer) is essential. Such an extensive study was not
undertaken, however, because it was beyond the objectives of this
hydraulic research.

Incipient motion was defined as the condition at which the
individual particles or bonded particles begin to move, leaving pit

marks on the bed surface which develop into streak lines. Suspension

of sediment is a part of this incipient motion process. The initial

movement of particles was started by the peeling off of the top skin

layer of bonded particles. The sediment particles are bonded by

organic matter, microbial activities and iron oxide within the

sediment.

Surface Skin Layer Aspects

One of the most significant findings of the research is that the

top surface of the fine-grained research sediment exhibited a skin

layer which governs the erosion process associated with incipient

motion.

The top skin layer was formed by sediment particles bonded by

benthic worms, organic matter, dust, and/or iron oxide. A

mechanistic model of sediment cohesion and incipient motion was

developed. Cohesion of silt-clay-silt, with organic matter and iron

oxide as cementing agents, contributed to strong cohesion at the

surface layer of the bed. Other forms of cohesion have lower bonding

strength and erode at the weakest plane of the bond, with lower shear

stress or velocity than silt-clay-silt cohesion. Removal of the top

skin layer by the peeling off of the bonded particles exposed the

material below the top skin layer. The exposed material eroded by

removal of individual particles. The exposed material formed a new

skin layer overnight.

In general, the bed was eroded by removal of either individual

particles or of small bonded particles. No removal of chunks of

sediment (mass failure) was observed on the bed surface. It is
believed that for a homogenous sediment bed, the erosion takes place
by removal of individual particles and small numbers of bonded
particles; i.e., erosion of fine-grained sediment is a surface
phenomenon.

Bed Patterns

In all experimental runs under unidirectional and oscillatory
flow. the bed pattern was developed by the peeling off of the
individual and bonded particles from the top skin layer, leaving many
pit marks which later developed into streak lines. The streak lines
in a rough bed were short and deep and the streak lines in a smooth
bed surface were long with very small depth. A distinct vertical
color variation was observed in the exposed bed.

Bed Consolidation Aspects

Benthic worm activity was evident all over the bed surface. This
was shown by the mounded sediment, worm trails, and other marks due
to worm movement.

The bench-type laboratory experiment results on the consolidation
and density of the sediment indicate that if the submerged sediment
was under no active hydraulic disturbances, it consolidated
substantially. Active hydraulic disturbance of the sediment was
simulated and it was found that removal of fine sediment and organic
matter from the sediment surface caused the remaining coarser
sediment to experience a greater degree of consolidation than if no

such removal occurred. This has importance to prototype situations where the relative degree of flushing and mixing can be manipulated.

The following summary of experimental results may contribute to understanding the behaviour of fine-grained sediment under unidirectional flow, oscillatory flow, and both flows combined.

Specific Features for Unidirectional Flow

The following conclusions were made regarding the incipient motion of fine cohesive sediment under unidirectional flow:

1. Flow conditions in the boundary layer at the sediment-water interface were calculated and found to represent turbulent flow for all of the experimental runs.

2. Incipient motion was related to average velocity of the flow and shear stress at the bed surface. It was found that the shear stress at the bed is an accurate index for incipient motion. The average flow velocity is also a usable index but with a lesser degree of accuracy.

3. Incipient motion of freshly deposited sediment bed occurred at shear stress of 5.1 dyne/cm^2 (.51 N/m^2) to 6.1 dyne/cm^2(.61 N/m)^2. Corresponding average flow velocities was recorded as 45.8 cm/sec to 52.1 cm/sec.

4. A change of suspended sediment concentration by the addition of 2,300 mg/l of the same material as in the bed to the recirculation pump system did not change the shear stress needed to cause incipient motion. The suspended sediment concentration decreased abruptly at the beginning of the experimental run and reached an equilibrium

level over time. The bed surface looked coarser after the experimental run.

5. A duned bed or a bed with a rough surface was more susceptible to incipient motion than a smooth flat bed. Any irregularities on the surface of the bed caused sediment to move at lower shear stress or velocity than for a smooth bed.

Specific Features for Oscillatory Flow

The following conclusions were made regarding the incipient motion of fine cohesive sediment under oscillatory flow:

1. Incipient motion was related to the maximum shear stress, the maximum velocity, and the orbital diameter at the bed surface. It was found that the maximum shear stress is an accurate index of incipient motion of fine-grained sediment. It was also found that the maximum velocity is another good index of incipient motion of fine-grained sediment. Orbital diameter, by itself, has not found to be a good index.

2. Incipient motion of the recently deposited sediment occurred at shear stresses of 3.67 dyne/cm^2 (0.37 N/m^2) to 5.53 dyne/cm^2 (0.55 N/m^2). Corresponding maximum velocities were recorded as 13.7 cm/sec to 21.5 cm/sec. The orbital diameters of 4.2 cm to 7.2 cm were also recorded. The results show that incipient motion occurred over a range of values rather than for a single value.

3. The suspended sediment concentration changes during experimental runs showed that after a critical shear stress value of 5.7 dyne/cm^2 (.57 N/m^2) for a recently deposited bed and 7.5 dyne/cm^2

$(.75 \text{ N/m}^2)$ for a consolidated bed had been reached, the suspended sediment concentration increased much more rapidly with increasing shear stress.

4. Incipient motion for the consolidated bed (densification of sediment bed for 91 days) occurred at shear stresses of 5.39 dyne/cm^2 $(.54 \text{ N/m}^2)$ to 6.52 dyne/cm^2 $(.65 \text{ N/m}^2)$. Corresponding maximum velocities were recorded at 19.9 cm/s to 25.0 cm/s. Comparison of shear stresses, velocities and suspended sediment concentrations for the recently deposited sediment bed and the densified bed showed that the densified sediment bed did not appear to be more resistant to erosion than recently deposited sediment bed.

5. A duned bed or a bed with a rough surface was more susceptible to incipient motion than a smooth flat bed for given values of the wave characteristics. Any irregularities on the surface of the bed caused greater exposure and higher susceptibility to movement, resulting in movement at lower shear stress or velocity than for a smooth bed. Bioturbation had a considerable effect on incipient motion of fine-grained sediment by roughening the bed surface.

6. Time has no role in the removal of particles from the bed at shear stresses below the incipient motion condition. At incipient motion conditions, however, a sudden increase in suspended sediment concentration was observed at the beginning of each run, after which the suspended sediment concentration decreased and reached an equilibrium steady rate as time progressed.

Likely Effects for Combined Unidirectional and Oscillatory Flows

The incipient motion of fine-grained sediment was not studied experimentally under the combined effect of oscillatory and unidirectional flows. The following statements are based on comparison of incipient motion under oscillatory and unidirectional flows and on analyses and speculation about the combined effect:

1.   Incipient motion of fine-grained sediment occurred at lower velocities and shear stresses for oscillatory flow than for unidirectional flow. Therefore, it can be said that oscillatory flow will be responsible for incipient motion of the sediment bed when both flows are combined. The role of unidirectional flow will be not only to add to the shear stress caused by oscillatory flow, thus serving to intensify the rate of erosion, but also to carry away the freshly suspended material.

2.   Oscillatory flow tends to remain laminar at velocities which would correspond to unidirectional turbulent flow.

3.   The flow condition would be expected to be turbulent when superimposing oscillatory flow on unidirectional flow. However, the structure of turbulence near the bed will be slightly changed when the flows are superimposed.

Application of Research

Study of sediment suspension by wave action, apart from contributing to the understanding of the dynamic sedimentary processes as a whole, has implications for the prediction of the rate and direction of spreading of dumped dredge spoils and other sediment

within reach of waves. Also, it has relevance to understanding the movement of solids in a beach profile, estuary, tidal lake, tidal channel, and the general shoaling of estuarine channels and lakes.

Recommendations for Future Research

Unidirectional Flow

1. A shear plate should be developed which overcomes the difficulties mentioned in this study.
2. Incipient motion should be studied for a wide range of shear strength and density of the bed sediment.
3. The effect of bioturbation should be studied.
4. More sophisticated collection and measurement of suspended sediment concentration is needed.

Oscillatory Flow

1. The incipient motion of cohesive sediment beds, in terms of orbital velocity and shear stress, must be studied for varying clay content and clay type and with varying amounts of organic matter.
2. The incipient motion of pure silt beds, in terms of the orbital velocity and shear stress, must be studied to eliminate the effect of clay cohesion.
3. The incipient motion of fine-grained sediment beds must be studied for varying shear strength, degree of consolidation, and density of the bed.

4. This study has been done with filtered river water.
    However, the effect of salinity should also be studied
    so as to provide information applicable to estuary and
    marine environments.

5. The suspended sediment concentration was measured at
    different locations of the test sections at regular
    intervals. More sophisticated sampling is needed to
    give more detailed information as a function of time
    in order to better define the incipient motion in terms
    of the suspended sediment concentration.

6. The effect of bioturbation should be studied in more detail.

7. The effects of temperature and sediment chemical properties,
    such as CEC, pH. and pore fluid composition, on incipient
    motion should be studied.

8. The effect of iron oxide on cohesion of sediment particles
    should be studied in more detail.

Combined Oscillatory and Unidirectional Flows

Very little practical work has been done on the interaction
between oscillatory and unidirectional flow, in bringing the
fine-grained sediment into suspension. It is not known whether the
superposition of the oscillatory flow on the unidirectional flow aids
the spread of the turbulent boundary layer or inhibits it; or if the
behavior of the system depends on whether the oscillatory or
unidirectional flow are generated first. It would be helpful to have
the vertical velocity profile of the combined system. The net

direction of velocity should be determined under varying conditions of wave and currents. Thus, understanding the turbulent structure near the bed under the combined effect of both oscillatory and unidirectional flow is essential.

VIII.   REFERENCES

Abdel-Rahman, N.H., "The Effect of Flowing Water on Cohesive Beds," thesis presented to Laboratory of Hydraulic Research and Soil Mechanics, Swiss Federal Institute of Technology, Zurich, 1964.

Abou-Seida, M.M., "Sediment Transport by Waves and Currents," Technical Report HEL-2-7, Hydraulic Engineering Laboratory, College of Engineering, University of California, Berkeley, 1964.

Alishahi, M.R., and Krone, R.B., "Suspension of Cohesive Sediment by Wind-Generated Waves," Hydraulic Engineering Laboratory, University of California, Berkeley, 1964.

Bagnold, R.A., "Motion of Waves in Shallow Water-Interaction Between Waves and Sand Bottom," Proceedings of the Royal Society, London, Series A, Vol. 187, 1946, pp. 1-15.

Bagnold, R.A., "Mechanics of Marine Sedimentation,"The Sea, Vol. 3, Interscience Publishers, New York, N.Y., 1963, pp. 507-528.

Bhattacharya, P.K., "Sediment Suspension in Shoaling Waves," A Thesis Submitted to University of Iowa, in partial fulfillment of the requirements for the Doctor of Philosophy, 1971.

Bijker, E.W., "The Inverse of Bed Shear in a Current Due to Wave Motion," Publication No. 46, Delft Hydraulics Laboratory, The Netherlands, February 1967.

Bijker, E.W., and Vellingu,P., "Sand Transport by Waves," Proceedings of 15th International Coastal Engineering Conference, Hawaii, 1976, pp. 1149-1167.

Blinco, P.H., and Partheniades, E., "Turbulance Characteristics in Free Surface Flows Over Smooth and Rough Boundaries," Journal of Hydraulic Research, Vol. 9, No. 1, 1971, pp. 43-69.

Blinco, P.H., and Simons, D.B., "Measurement of Instantaneous Boundary Shear Stress," Hydraulic Engineering and the Environment, Proceedings of the 21st Annual Hydraulic Division Specialty Conference, ASCE, Bozeman, Montana, 1973, pp. 43-54.

Bonnefille, R., and Pernecker, L., "Debut d" Entrainment des Sediments Per La Houle Proceedings of the 11th Congress IAHR, Vol.V, 1965, pp. 207-208.

Bowden, K .F., and Fairbairn, L.A., "Measurement of Turbulant
    Fluctuations and Reynolds Stresses in a Tidal Current,"
    Proceedings of the Royal Society of London, Vol. 237, 1956,
    pp. 422-438.

Brown, K.C., and Joubert, P.N., "The Measurement of Skin Friction in
    Turbulent Boundary Layers With Adverse Pressure Gradients,"
    Journal of Fluid Mechanics, Vol. 35, Part 4, 1969 pp. 737-757.

Bursall, T.S., "Bottom Shear Measurement in an Open Channel Flow,"
    Proceedings of the 12th Congress IAHR, Vol. 1, 1967,
    pp. 194-201.

Caldwell, D.R., and Chriss, T.M., "The Viscous Sublayer at the
    Sea Floor," Science, 205, 1979, pp. 1131-1132.

Carstens, M.R., and Neilson, F.M., "Evolution of a Duned Bed Under
    Oscillatory Flow." Journal of Geophsical Research, Vol. 72,
    1967, pp. 3053-3059.

Carstens, M.R., and Neilson, F.M., and Altinbilek, H.D., "Bed Forms
    Generated in the Laboratory Under an Oscillatory Flow:
    Analytical and Experimental Study," Technical Memorandum
    No. 28, U.S. Army Engineers Coastal Engineering Research
    Center, Washington, D.C., 1969.

Chan, K.W., Baird, M.H.I., and Round, G.F., "Behaviour of Beds of
    Dense Particles in a Horizontally Oscillating Liquid,"
    Proceedings of the Royal Society of London, A.330, 1972,
    pp. 537-559.

Chepil, W.S., "Equilibrium of Soil Grains at the Threshold of
    Movement by Wind," Proceedings of the Soil Science Society
    of America, Vol. 23, Madison, WI., 1959, pp. 422-428.

Chien, N., "The Present Status of Research on Sediment Transport,"
    Proceedings of the American Society of Civil Engineers, Vol. 80,
    1954.

Clyde, C.G., and Cheng, E.D.H., "A dynamometer for Measuring Force
    Components on Large Roughened Elements in Open Channel Flow,"
    Proceedings of the 17th Annual Specialty Conference, Hydraulic
    Division, ASCE, Logan, Utah, 1969.

Coleman, N.L., "A New Examination of Sediment Suspension in Open
    Channels," Journal of Hydraulic Research, Vol. 7, No.1, 1969,
    pp. 67-82.

Coleman, N.L., "Velocity. Profile With Suspended Sediment," Journal
    of Hydraulic Research, Vol. 19, No. 3, 1981, pp. 211-229.

Collins, J.I., "Inception of Turbulence at the Bed Under Periodic Gravity Waves," Journal of Geophysical Research, Vol. 68, No. 21, 1963, pp. 6007-6014.

Das. M.M., "Mechanics of Sediment Suspension Due to Oscillatory Waves." Hydraulic Engineering Laboratory, College of Engineering, University of California, Berkeley, HELZ-32, June, 1971.

Davies. A.G., and Wilkinson, R.H., "Sediment Motion Caused by Surface Water Waves," Proceedings of the Sixteenth Conference on Coastal Engineering, Hambarg, Germany, 1978, pp. 1577-1595.

Dean, R.G., "Evaluation and Development of Water Wave Theories for Engineering Applications," U.S. Army Corps of Engineers Coastal Engineering Research Center, Special Report No. 1, Vol. 1, 1974, p. 121.

Dedow, H.R.A., "A Pulsating Water Tunnel for Research in Reversing Flow," La Houille Blanche, No. 7, 1966, p. 837.

Dingler, J.R., "The Threshold of Grain Motion Under Oscillatory Flows in a Laboratory Wave Channel," Journal of Sedimentary Petrology, Vol. 49, No. 1, 1979, pp. 287-294.

Dracos, T., "Some Field and Laboratory Measurements Concerning the Mechanics of Sediment Transport," International Symposium on River Sedimentation, March, 1980.

Dunn, I.S., "Tractive Resistance of Cohesive Channel," Journal of Hydraulics Division, ASCE, Vol. 85, No. SM3, 1959, pp. 1-24.

Dyer, K.R., "Velocity Profile Over a Rippled Bed and the Threshold of Movement of Sand," Estuarine Coastal Marine Science, Vol. 10, 1980, pp. 181-199.

Eagleson, P.S., "Laminar Damping of Oscillatory Waves," Journal of Hydraulic Division, ASCE, Vol. 88, No. HY3, 1962, pp. 155-181.

Eagleson, P.S., and Dean, R.G., "Wave-Induced Motion of Bottom Sediment Particles," Journal of Hydraulic Division, ASCE, Vol. 85, No. HY10, 1959, pp. 53-79.

Eagleson, P.S., Dean, R.G., and Peralta, L.A., "The Mechanics of the Motion of Discrete Spherical Bottom Sediment Particles Due to Shoaling Waves," Beach Erosion Board, TM No. 104, 1958.

Einstein, H.A., "Formulas for the Transportation of Bed Load," Transactions, ASCE, Vol. 107, Paper No. 2140, 1942, pp. 561-573.

Einstein, H.A., and El-Samni, E.S.A., "Hydrodynamic Forces on a Rough Wall," Reviews of Modern Physics, Vol. 21, 1949, pp. 520-524.

Einstein, H.A., "Needs in Sedimentation," Journal of Hydraulic Division, ASCE, Vol 87, No. HY2, 1961, pp. 1-6.

Einstein, H.A., "Sediment Transport by Wave Action," Proceedings of the 13th Coastal Engineering Conference, Vancouver, B.C., Canada, Vol. II, 1972, pp. 933-952.

Einstein, H.A., and Barbarossa, N.L., "River Channel Roughness," Transactions, ASCE, Vol. 117, 1952, pp. 1121-1146.

Eliasson, J., Jonson, I.G., and Skongaard, C., "A New Way of Measuring the Wave Friction Factor in a Wave Flume," Basic Research Program Report No. 5, 5-8 Coastal Engineering Laboratory, Technical University of Denmark, 1964.

Flaxman, E.M., "Channel Stability in Undisturbed Cohesive Soils," Journal of Hydraulic Division, ASCE, Vol. 89, No. HY2, 1963, pp. 87-96.

Fortier, S., and Scobey, F.C., "Permissible Canal Velocities," Transactions, ASCE, Vol. 89, Paper No. 1588, 1926, pp. 940-984.

Fredsoe, J., "Turbulent Boundary Layer in Wave-Current Motion," Journal of Hydraulic Engineering, ASCE, Vol. 110, No. 8, 1984, pp. 1103-1120.

Gessler, J., "The Beginning of Bed Load Movement of Mixtures Investigated as Natural Armoring in Channels," Laboratory of Hydraulic Research and Soil Mechanics, Swiss Federal Institute of Technology, Zurich, Switzerland, Report No. 69, 1965.

Ghosh, S.N., and Rory, N., "Boundary Shear Distribution in Open Channel Flow," Journal of Hydraulic Division, ASCE, Vol. 96, No. HY4, 1970, pp. 967-994.

Goda, Y., "Wave Forces on a Vertical Cylinder: Experiments and a Proposed Method of Wave Force Compensation," Report of Port and Harbour Technical Research Institute, Report No. 8, 1964, p. 74.

Graf, W.H., Hydraulic of Sediment Transport, McGraw-Hill Book Co. Inc., New York, N.Y., 1971.

Grant, W.D., and Madsen, O.S., "Combined Wave and Current Interaction With a Rough Bottom," Journal Of Geophysical Research, Vol. 84, No. C4, 1979, pp. 1797-1808.

Grass, A.J., "Initial Instability of a Fine Bed Sand," Journal of the Hydraulic Division, ASCE, Vol. 96, No. HY3, 1970, pp. 619-632.

Griffith, O.F. III, and Grimwood, M., "Turbulence and Measurement Study," Journal of Hydraulic Division, ASCE, Vol. 107, No. HY3, 1981, pp. 311-326.

Grim, R.E., "Clay Mineralogy," McGraw-Hill Book Co., 1968.

Grissinger, E.H., "Resistance of Selected Clay Systems to Erosion by Water," Water Resources Research, Vol. 2, No. 1, 1966, pp. 131-138.

Grissinger, E.H., "Bank Erosion of Cohesive Materials," Gravel-Bed Rivers, edited by Hey, R.D., Bathurst, J.C., and Thorne, C.R., John Wiley and Sons, 1982, pp. 273-287.

Hall, R.K., "Initiation of Erosion of Consolidated Clays By Unidirectional Flow," A Thesis Submitted to Queen's University In Partial Fullfilment of Requirement for a Masters of Science Degree, 1981.

Hallermeier, R.J., "Sand Motion Initiation by Water Waves: Two Asymptotes," Journal of Waterways, Ports and Harbors, ASCE, Vol. 106, No. WW3, 1980, pp. 299-318.

Hattori, M., "The Mechanics of Suspended Sediment Due to Wave Action," Coastal Engineering In Japan, Vol. XII, Dec. 1969.

Hjulstrom, F., "Studies of the Morphological Activity of Rivers as Illustrated by the River Fyris," Bulletin, Geological Institute of Upsale, Vol. XXV, Upsale, Sweden, 1935.

Hjulstrom, F., "Transportation of Detritus by Moving Water," In: Recent Marine Sediments, A symposium (Edited by P.D. Trask), Spec. Publis. Soc. Econ. Paleont. Miner., Tulsa, 4, 1939, pp. 5-31.

Hom-ma, M., and Horikawa, K., "Suspended Sediment Due to Wave Action," Proceedings of the 8th Conference on Coastal Engineering, 1962.

Hom-ma, M., Horikama, K., Kiyoshi,and Kajima, R., "A Study on Suspended Sediment Due to Wave Action," Proceedings of the 10th Congress of IAHR, London, 1963.

Hwang, L.S., and Laursen, E.M., "Shear Measurement Technique for Rough Surfaces," Journal of Hydraulic Division, ASCE, Vol. 89, No. HY2, 1963, pp. 19-37.

Inman, D.L., "Sorting of Sediment in the Light of Fluid Mechanics," Journal of Sediment Petrology, Vol. 19, 1949, pp. 51-70.

Inman, D.L., "Wave-Generated Ripples in Nearshore Sands," U.S. Army Corps of Engineers, Beach Erosion Board, Washington, D.C., TM-100, Oct. 1957.

Inman, D.L., and Bowen, A.J., "Flume Experiments on Sand Transport by Waves and Currents," Proceedings of the 8th Conference on Coastal Engineering, American Society of Civil Engineers, 1962, pp. 137-150.

Ippen, A.T., and Drinker, P.A., "Boundary Shear Strength in Curved Trapezoidal Channels," Journal of Hydraulic Division, ASCE, Vol. 88, No. HY5, 1962, pp. 143-179.

Ippen, A.T., and Eagleson, P.S., "A Study of Sediment Sorting by Waves Shoaling of a Plane Beach," Beach Erosion Board, TM No. 63, 1955.

Iwagaki, Y., and Asano, T., "Water Particle Velocity in Wave-Current Systems," Coastal Engineering in Japan, Tokyo, Vol. 23, 1980, pp. 1-14.

Iwagaki, Y., Tsuchiya, Y., and Sakai, M., "Basic Studies on the Wave Damping Due to Bottom Friction," Coastal Engineering in Japan, Vol. 8. 1965, p. 37.

Jonsson, I.J., "Measurements in the Turbulent Wave Boundary Layer," Proceedings of the 10th Congress of IAHR, London, Vol. I, 1963.

Jonsson, I.J., "Wave Boundary Layers and Friction Factors," Proceedings of the 10th Conference of Coastal Engineering, Tokyo, 1966, pp. 127-148.

Jonsson, I.J., "A New Approach to Oscillatory Rough Turbulent Boundary Layer," Institute of Hydrodynamics and Hydraulic Engineering, Technical University of Denmark, Lyngby, Denmark, Series Paper 17, 1978.

Jonsson, I.J., and Carlson, N.A., "Experimental and Theoretical Investigations in an Oscillatory Turbulent Boundary Layer," Journal of Hydraulic Research, Vol. 14, No. 1, 1976, pp. 45-60.

Kajiura, K., "A Model of the Bottom Boundary Layer in Water Waves," Bull. Earthquake Research Institute, Vol. 46, 1968, p. 75.

Kalkanis, G., "Turbulent Flow Near an Oscillating Wall," Beach Erosion Board, Corps of Engineers, Tech. Memo. No. 97, 1957.

Kalkanis, G., "Transportation of Bed Material Due to Wave Action," U.S. Army, Coastal Engineering Research Center, Tech. Memo. No. 2., Feb., 1964.

Kamphuis, J.W., "Determination of Sand Roughness for Fixed Beds," Journal of Hydraulic Research, Vol. 12, No. 2, 1974, pp. 193-203.

Kamphuis, J.W., "Friction Factor Under Oscillatory Waves," Journal of the Waterways, Harbors and Coastal Engineering Division, ASCE, Vol. 101, No. WW2, 1975, pp. 135-144.

Kamphuis, N.J., and Hall, K.R., "Cohesive Material Erosion by Unidirectional Current," Journal of Hydraulic Engineering, ASCE, Vol. 109, No. 1, 1983, pp. 49-61.

Kandiah, A., "Fundamental Aspects of Surface Erosion of Cohesive Soils," A Thesis Submitted to the University of California, Davis, In Partial Fulfillment of the Requirements for the Doctor of Philosophy Degree, 1974.

Kemp, P.H., and Simons, R.R., "The Interaction Between Waves and a Turbulent Current," Journal of Fluid Mechanics, Vol. 116, March 1982, pp. 227-250.

Kennedy, J.F., and Falcon, M., "Wave-Generated Sediment Ripples," Massachusetts Institute of Technology, Cambridge, Massachusetts, Hydrodynamics Laboratory Report, No. 86, Aug. 1965.

Klingeman, P.C., et al., "Physical, Chemical, and Biological Description of Sturgeon Lake," Water Resources Research Institute, Oregon State University, Corvallis, Oregon, 1982a.

Klingeman, P.C., et al., "Sturgeon Lake Problem Diagnosis, Options for Restoration, and Recommendations," Water Resources Research Institute, Oregon State University, Corvallis, Oregon, 1982b.

Kobune, K., "Random Wind Velocity Field for Periodic Theo4ry," A Thesis Submitted to Oregon State University, Corvallis, In Partial Fulfillment of the Requirements for the Degree of Civil Engineering, 1978.

Komar, P.D., and Miller, M.C., "The Threshold of Sediment Movement Under Oscillatory Water Waves," Journal of Sediment Petrology, Vol. 43, No. 4, 1973, pp. 1101-1110.

Komar, P.D., and Miller, M.C., "Reply: On the Comparison Between the Threshold of Sediment Motion Under Waves and Unidirectional Currents With a Discussion of the Practical Evaluation of the Threshold," Journal of Sediment Petrology, Vol. 45, 1975, pp. 362-367.

Kramer, H., "Sand Mixtures and Sand Movement in Fluvial Models," Transactions, ASCE, Vol. 100, Paper No. 1909, 1935, pp. 798-878.

Krone, R.B., "Flume Studies of the Transport of Sediment in Esturarial Shoaling Processes," Report of the Hydraulic Engineering Laboratory, University of California, Berkeley, 1962.

Krone, R.B., "Silt Transport Studies Utilizing Radioisotopes," Second Annual Report, Institute of Engineering Research, University of California, Berkeley, 1957.

Kuiti, E.G., and Yen, C., "Scouring of Cohesive Soils," Journal of Hydraulic Research, Vol. 14, No. 3, 1976, p. 1951.

Lamb, S.H., Hydrodynamic, 6th Edition, 1932, pp. 619-621.

Lane, E.W., "Progress Report on Studies on the Design of Stable Channels of the Bureau of Reclamation," Proceedings of the American Society of Civil Engineers, Vol. 79, 1953.

Lane, E.W., "Design of Stable Channels," Transactions, ASCE, Vol. 120, Paper No. 2776, 1955, pp. 1234-1279.

Leipmann, H.W., and Dhawan, S., "Direct Measurement of Local Skin Friction in Low Speed and High Speed Flow," Proceedings of the National Institute of Applied Mechanics, 1952, p. 869.

L"Hermitte, P., "Movement des Materiaux de Fond so l'action de La Houle," Annales des Pents et Chauss, 1961, p. 357.

Li, H., "Stability of Oscillatory Laminar Flow Along A Wall," Beach Erosion Board, Corps of Engineers, Tech. Memo. No. 47, 1954.

Lofquist, K.E.B., "Sand Ripple Growth in an Oscillatory-Flow Water Tunnel," Technical Paper No. 78-5, U.S. Army Engineers Coastal Engineering Research Center, Fort Belvoir, Va., 1978.

Longuet-Higgins, M.S., "Mass Transport in Water Waves," Philosophical Transactions of the Royal Society of London, Series A, Vol. 245, 1953, pp. 535-581.

Longuet-Higgins, M.S., "Oscillatory Flow Over Steep Sand Ripples," Journal of Fluid Mechanics, Vol. 107, 1981, pp. 1-35.

Ludwieg, H., and Tillman, W., Investigation of the Wall Shearing Stress in Turbulent Boundary Layers," Transactions, NACA TM No. 1285, 1950.

Madson, O.S., "Wave Climate of the Continental Margin: Elements of Its Mathematical Description," Marine Sediment Transport and Environmental Management, John Wiley and Sons, Inc., New York, N.Y., 1976.

Madsen, O.S., and Grant, W.D., "The Threshold of Sediment Movement Under Oscillatory Waves: A Discussion," Journal of Sedimentary Petrology, Vol. 45, 1975, pp. 360-361.

Manohar, M., "Mechanics of Bottom Sediment Movement Due to Wave Action," Beach Erosion Board, Corps of Engineers, Tech. Memo. No. 75, 1955.

Mehta, A.J., "Depositional Behavior of Cohesive Sediments," thesis submitted to the University of Florida, in Partial fulfillment of the requirements for the Doctor of Philosophy Degree, 1973.

Mehta, A.J., and Partheniades, E., "An Investigation of the Depositional Properties of Flocculated Fine Sediments," Journal of Hydraulic Research, Vol. 13, No. 4, 1975, pp. 361-381.

Miller, M.C., "Laboratory Field Investigations on the Movement of Sand Tracers Under the Influence of Water Waves: Ripple Development and Longitudinal Spreading of Tracer Material," A Thesis Submitted to the Department of Oceanography in Partial Fulfillment of the requirements for a Doctor of Philosophy Degree, Oregon State University, Corvallis, Oregon, 1978.

Miller, M.C., McCave, I.N., and Komar, P.D., "Threshold of Sediment Motion Under Unidirectional Currents," Sedimentology, Vol. 24, 1977, pp. 507-527.

Mogridge, G.R., "Testing Sediment Movement due to Wave Action," Journal of Hydraulic Division, ASCE, Vol. 96, No. HY7, 1970, pp. 1587-1604.

Mogridge, G.R., and Kamphius, J.W., "Experiments on Bed Form Generation by Wave Action," Proceedings of the 13th Conference on Coastal Engineering, Vancouver, B.C., Canada, 1972, pp. 1123-1142.

Nakato, T., Locher, F.A., Glover, J.R., and Kennedy, J.F., "Wave Entrainment of Sediment From Rippled Beds," Journal of Waterways, Ports and Harbors, ASCE, Vol. 103, No. WW1, 1977, pp. 83-99.

Nece, R.E., and Smith, J.D., "Boundary Shear Stress in Rivers and Estuaries," Journal of the Waterways, Harbors and Coastal Engineering Division, ASCE, Vol. 100, No. WW2, Proceedings Paper 10512, 1970, pp. 105-122.

Neill, C.R., "Mean Velocity Criterion for Scour of Coarse Uniform Bed-Material," International Association of Hydraulic Research, 12th Congress, Fort Collins, Colorado, Vol. 3, 1967, pp. 46-54.

Neill, C.R., "Note on Initial Movement of Coarse Uniform Bed Material," Journal of Hydraulic Research, Vol. 6, 1968, pp. 173-176.

Nielsen, P., "Some Basic Concepts of Wave Sediment transport," Institute of Hydrodynamics and Hydraulic Engineering (ISVA), Technical University of Denmark, Lyngby, Denmark, Series Paper No. 20, Jan., 1979.

O'Melia, C.R., "Aquasols: The Behavior of Small Particles in Aquatic Systems," ES&T, Feature Article, Vol. 14, No. 9., Sept., 1980, pp. 1052-1060.

Paintal, A.E., "Concept of Critical Shear Stress in Loose Boundary Open Channels," Journal of Hydraulic Research, 9(1), 1971, pp. 91-107.

Partheniades, E., "A Study of Erosion and Deposition of Cohesive Soils in Salt Water," A Thesis submitted to the Department of Civil Engineering in Partial fulfillment of Requirements for the Doctor of Philosophy Degree, University of California, Berkeley, 1962.

Partheniades, E., "Erosion and Deposition of Cohesive Soils," Journal of Hydraulic Division, ASCE, Vol. 91, No. HY1, 1965, pp. 105-139.

Partheniades, E., "Results of Recent Investigations on Erosion and Deposition of Cohesive Sediments," Sedimentation edited by H.W. Shen, Fort Collins, Colorado, 1972.

Peregrine, D.H., and Jonsson, I.G., "Interaction of Waves and Currents," Miscellaneous Report No. 83-86, U.S. Army, Corps of Engineers, Coastal Engineering Research Center, March, 1983.

Raichlen, F., "Some Turbulent Measurements in Water," Journal of the Engineering Mechanics Division, ASCE, Vol. 93, No. EM2, 1967, pp. 73-97.

Rance, P.J., and Warren, N.F., "The Threshold of Movement of Coarse Material in Oscillatory Flow," Proceedings of the 11th Conference on Coastal Engineering, London, England, 1968, pp. 487-491.

Rathum, R.E., and Guy, H.P., "Measurement of Hydraulic and Sediment Transport Variables in a Small Recirculating Flume," Water Resources Research, 3, 1967, pp. 107-122.

Raudkivi, A.J., Loose Boundary Hydraulic, Pergamon Press,
2nd Edition, 1976.

Richardson, E.G., "The Suspension of Solids in a Turbulent Stream,"
Proceedings of the Royal Society of London, Series A, Vol. 162,
1937, pp. 583-597.

Riedel, H.P., "Direct Measurement of Bed Shear Stress Under Waves,"
A Thesis Presented to the Queen's University at Kingston,
Ontario, Department of Civil Engineering in Partial Fulfillment
of the Requirements for the Doctor of Philosophy Degree, 1972.

Rouse, H., "Modern Conceptions of the Mechanics of Fluid
Turbulence," Transactions, ASCE, Vol. 102, Paper No. 1965,
1937, pp. 463-543.

Sarpkaya, T., and Isaacson, M., "Mechanics of Wave Forces on
Offshore Structures," Van Nostrand Reinhold Company, 1981,
p.160.

Schuster, J.C., "Measuring Water Velocity by Ultrasonic Flow Meter,"
Journal of Hydraulic Division, ASCE, Vol. 101, No. HY12, 1975,
pp. 1503-1517.

Scott, T., "Sand Movement by Waves," Beach Erosion Board, Tech.
Memo. No. 48, 1954.

Shields, A., "Anwendung der Aenlichkeitsmechanik und der Turbvlen-
zforschung auf die Geschiebebewegung," Mitteilungen der Preussi-
schen versuchsanstalt fur Wasserhaw und Schiffbau, Berlin,
Germany, Translated to English by W.P Ott and J.C. Van Uchelen,
California Institute of Technology, Pasadena, Calif., 1936.

Silvester, R., "Modeling of Sediment Motions Offshore," Journal of
Hydraulic Research, Vol. 8, No. 2, 1970, pp. 229-259.

Silvester, R., and Mogridge, G.R., "Research of Waves to the Bed of
the Continental Shelf," Proceedings of the 12th Conference of
Coastal Engineering, Vol. II, 1970, pp. 651-667.

Sleath, J.F.A., "Transition in Oscillatory Flow Over Rippled Beds,"
Proceeding, Institution of Civil Engineers, London, England,
Part 2, Vol. 59, 1975, pp. 309-322.

Smerdon, E.T., and Beasley, R.P., "Critical Tractive Forces in
Cohesive Soils," Agricultural Engineering, St. Joseph,
Michigan, Jan., 1961, pp. 26-29.

Smoluchowski, M. "Versuch einer Mathematichen Theorie der
Koagulations Kinetiks Kolloider Losungen," Z. Physik,
Chem. 1917, 92, pp. 129-168.

Sternberg, R.W., "Friction Factors In Tidal Channels With Differing Bed Roughness," Marine Geology, Vol. 6, 1968, pp. 243-260.

Strenberg, R.W., "Measurements of Incipient Motion of Sediment Particles In the Marine Environment," Marine Geology, Vol. 10, 1971, pp. 113-119.

Sundborg, A., "The River Klaralven, A Study of Fluvial Processes," Geografiska Annaler, 1956, pp. 127-316.

Task Committee on preparation of Sedimentation Manual, "Sediment Transportation Mechanics: Erosion of Sediment," Journal of Hydraulic Division, ASCE, Vol. 88, No. HY4, 1962, pp. 109-127.

Task Committee on Preparation of Sedimentation Manual, "Friction Factors In Open Channels," Journal of the Hydraulic Division, ASCE, Vol. 89, No. HY2, March, 1963A, pp. 97-143.

Task Committee on Preparation of Sedimentation Manual, "Sediment Transportation Mechanics: Introduction and Properties of Sediment," Journal of Hydraulic Division, ASCE, Vol. 88, No. HY4, 1963, pp. 77-107.

Task Committee on Preparation of Sedimentation Manual, "Sediment Transportation Mechanics: Suspension of Sediment," Journal of Hydraulic Division, ASCE, Vol. 89, No. HY5, 1963C, pp. 45-76.

Task Committee on Preparation of Sedimentation Manual, "Initiation of Motion," Special Report, Journal of Hydraulic Division, ASCE, Vol. 92, No. HY2, 1966, p. 291.

Task Committee on Preparation of Sedimentation Manual, "Erosion of Cohesive Sediments, Proceedings, ASCE, Vol. 94, No. HY4, 1968, pp. 1017-1049.

Taylor, F.R.S., "Note on R.S. Bagnold's Empirical Formula For the Critical Water Motion Corresponding With the First Disturbance of Grains on a Flat Surface," Proceedings of the Royal Society of London, Series A, 1946, Vol. 187, pp. 16-18.

Teleki, P.G., and Anderson, M.W., "Bottom Boundary Shear Stresses on a Model Beach," Proceedings of the 12th Coastal Engineering Conference, Washington D.C., Vol. 1, 1970, pp. 269-288.

Tunstall, E.B., and Inman, D.L., "Vortex generation by Oscillatory Flow Over Rippled Surfaces," Journal of Geophysical Research, Vol. 80, No. 24, 1975, pp. 3475-3484.

U.S. Army Corps of Engineers, "Shore Protection Manual," U.S. Army Coastal Engineering Research Center, Vol. I, 1977.

U.S. Bureau of Reclamation, "Interim Report on Channel Stability of Natural and Artificial Drainageways in Republican, Loup, and Little Sioux River Areas, Nebraska and Iowa," Hydrology Branch, Project Planning Division, Sept., 1953.

Vanoni, V.A., "Transportation of Suspended Sediment by Water," Transactions, ASCE, Vol. 3, 1946, pp. 67-133.

Vanoni, V.A., "Measurements of Critical Shear Stress," California Institute of Technology, Report No. KH-R-7, 1964.

Vincent, G.E., "Contribution to the Study of Sediment Transport on a Horizontal Bed Due to Wave Action," Proceedings of the 6th Conference on Coastal Engineering, Gainesville, Fla., 1958, pp. 326-355.

Vongvisessomjai, S., "Oscillatory Ripple Geometry," Journal of Hydraulic Engineering, ASCE, Vol. 110, No. 3, 1984, pp. 247-266.

Vongvisessomjai, S., "Oscillatory Boundary Layer and Eddy Viscosity," Journal of Hydraulic Engineering, ASCE, Vol. 110, No. 4, 1984, pp. 387-404.

Wang, H. and Liang, S.S., "Mechanics of Suspended Sediment in Random Waves," Journal of Geophysical Research, Vol. 80, No. 24, 1975, pp. 3488-3494.

Ward, P.R.B., and Chikwanha, R., "Laboratory Measurement of Sediment by Turbidity," Journal of Hydraulic Division, ASCE, Vol. 106, No. HY6, 1980, pp. 1041-1053.

White, C.M., "The Equilibrium of Grains on the Bed of a Stream," Proceedings, Royal Society of London, series A, No. 958, Vol. 174, Feb. 1940, pp. 322-338.

Yalin, M.S., "Mechanics of Sediment Transport," Pergamon Press, 1972.

Yalin, M.S., and Russell, R.C.H., "Shear Stresses Due to Long Waves," Journal of Hydraulic Research, Vol. 4, No. 2, 1977, pp. 55-98.

Yang, C.T., "Incipient Motion and Sediment Transport," Journal of Hydraulic Division, ASCE, Vol. 99, No. Hy10, 1973, pp. 1679-1704.

Yucel, O., and Graf, W.H., "Wall Shear Stress Measurements With Hot-Film Sensors," Hydraulic Engineering and the Environment Proceedings of the 21st Annual Hydraulic Divisions Specialty Conference, ASCE, Bozeman, Montana, 1973, pp. 55-72.